PŘÍLOHA I

Hošek, J. – Hambach, U. – Lisá, L. – Matys Grygar, T. – Horáček, I. – Meszner, S. – Knésl, I. (2015): An integrated rock-magnetic and geochemical approach to loess/paleosol sequences from Bohemia and Moravia (Czech Republic): implications for the Upper Pleistocene paleoenvironment in central Europe. – Palaeogeography, Palaeoclimatology, Palaeoecology 418, 344-358.

Palaeogeography, Palaeoclimatology, Palaeoecology 418 (2015) 344–358

Contents lists available at ScienceDirect

Palaeogeography, Palaeoclimatology, Palaeoecology

journal homepage: www.elsevier.com/locate/palaeo

An integrated rock-magnetic and geochemical approach to loess/paleosol sequences from Bohemia and Moravia (Czech Republic): Implications for the Upper Pleistocene paleoenvironment in central Europe

Jan Hošek [a,g,*], Ulrich Hambach [b], Lenka Lisá [c], Tomáš Matys Grygar [d], Ivan Horáček [e], Sascha Meszner [f], Ilja Knésl [a]

[a] Czech Geological Survey, Klárov 3, Prague 1, Czech Republic
[b] BayCEER & Chair of Geomorphology, University of Bayreuth, D-95440 Bayreuth, Germany
[c] Institute of Geology of Czech Academy of Science, Rozvojová 269, Prague 6, Czech Republic
[d] Institute of Inorganic Chemistry of Czech Academy of Science, Řež 1001, Czech Republic
[e] Department of Zoology, Faculty of Science, Charles University, Viničná 7, Prague 2, Czech Republic
[f] Dresden University of Technology, Institute of Geography, Mommsenstrasse 7, Dresden, Germany
[g] Institute of Geology and Paleontology, Faculty of Science, Charles University in Prague, Albertov 6, Prague 2, Czech Republic

ARTICLE INFO

Article history:
Received 18 June 2014
Received in revised form 27 November 2014
Accepted 30 November 2014
Available online 9 December 2014

Keywords:
Loess/paleosols sequences
Rock-magnetism
Geochemical proxies
Upper Pleistocene
Paleoclimate
Central Europe

ABSTRACT

Two central European loess/paleosol sequences (MIS 6-2), from central Bohemia (Zeměchy) and southern Moravia (Dobšice), situated in the important climatic transition zone between the oceanic (Atlantic) and continental climate regimes, were investigated for rock magnetism, geochemistry, grain size and micromorphology. In both sites the magnetic profile shows good agreement with the standard model of magnetic enhancement in paleosols as established in the Chinese loess. The magnetic signal is dominated by the presence of fine-grained magnetite and maghemite, formed in-situ and controlled by the intensity of soil formation. Magnetic proxies corresponded to proxies of chemical weathering and leaching intensity such as the Chemical Index of Alteration (CIA), the Cation Exchange Capacity (CEC) and the Rb/Sr ratio (correlation coefficient r = ~0.6–0.93) during the whole Lower Weichselian (MIS 5d–5a) and, in general, also during the Pleniglacial (MIS 4-2). Nevertheless, for the Eemian period (MIS 5e) this relationship was not always valid, either due to weak magnetic enhancement (at Dobšice) or even weak depletion of the magnetic minerals with soil formation (at Zeměchy). The presented data demonstrate that magnetic signals can be overprinted more easily than chemical proxies during later diagenetic events, and are hence not in all cases reliable for deciphering paleoclimate changes during all periods of the studied time interval. Rock-magnetic, geochemical and micromorphological results suggest drier conditions in southern Moravia compared to central Bohemia during the Weichselian Glacial, probably due to the more continental climate in southern Moravia.

1. Introduction

Loess/paleosols sequences (LPSs) of the last climate cycle kaleidoscopically cover wide areas of the European continent and provide a valuable archive of the Upper Pleistocene paleoenvironment there. Yet, as indicated by many large scale geographic comparisons (e.g. Kukla 1977; Pye, 1987; Derbyshire et al, 1988; Bronger and Heinkele, 1989; Pécsi, 1990; Haesaerts and Mestdagh, 2000; Marković et al., 2008; Jary and Ciszek, 2013), European LPSs are marked by regional differences and pronounced facies variability in their pedosedimentary records that complicate finer super-regional correlations (Kemp, 2001). Such complications are especially evident in a transect from suboceanic (Atlantic) regions towards more continental areas, apparently due to the influence of the different climate regimes. Detailed studies of geographic and environmental variation in regional responses to general climate trends during the Upper Pleistocene are therefore of high priority for Quaternary science in Europe. A dense network of reliably-dated, high-resolution records from different geographic locations is a basic prerequisite for such spatial analyses (Frechen, 2011; Muhs, 2013).

For a particular LPS, a detailed history of the paleoenvironmental circumstances responsible for the pedogenetic and diagenetic processes (Zhang et al., 2007; Bloemendal et al., 2008) can be reliably reconstructed using instrumental mineral-magnetic and geochemical analyses

* Corresponding author at: Czech Geological Survey, Klárov 3, Prague 1, 118 00; Czech Republic. Tel.: +420 731 905 752.
E-mail addresses: johan.hosek@gmail.com (J. Hošek), ulrich.hambach@uni-bayreuth.de (U. Hambach), lisa@gli.cas.cz (L. Lisá), grygar@iic.cas.cz (T.M. Grygar), ivan.horacek@natur.cuni.cz (I. Horáček), sascha.meszner@tu-dresden.de (S. Meszner).

http://dx.doi.org/10.1016/j.palaeo.2014.11.024
0031-0182/

(Wang et al., 2012). However, in order to reflect the different ways of mineral-magnetic enhancement in sediments and soils (the Chinese vs. Alaskan-Siberian scenario), or the post-depositional loss of ferromagnetic particles (e.g. Begét et al., 1990; Bogucki et al., 1995; Vodyanitskii et al., 2007; Liu et al., 2007; Bábek et al., 2011; Baumgart et al., 2013; Buggle et al., 2013a; Gocke et al., 2014), combining the magnetic and geochemical analyses is quite important. Thus the direct paleoclimatic interpretation of the rock-magnetic record can be corrected and/or improved (Evans and Heller, 2003; Maher et al., 2003).

In European loess research, a large number of studies combining geochemical, rock magnetic and sedimentological approaches have appeared during the last decade. These provide a relatively dense network of continuous LPS records that cover the area of north-western Germany, southern and eastern Poland, western Ukraine and the Danube catchment (e.g., Antoine et al., 2010; Panaiotu et al., 2001; Marković et al., 2006; Kravchinsky et al., 2008; Jordanova et al., 2011; Buggle et al., 2009; Bokhorst et al., 2009; Fitzsimmons et al., 2012; Fischer et al., 2012; Jary and Ciszek, 2013; Baumgart et al., 2013; Vandenberghe, 2013; Rolf et al., 2014; Schatz et al., 2014; Gocke et al., 2014; Újvári et al., 2014). Together, these studies provide a reliable platform for transregional comparisons of climate development during the Upper Pleistocene.

Within the territory of the Czech Republic a range of key loess sites have been investigated (e.g. Dolní Věstonice, Prague-Sedlec, Kutná Hora or Červený Kopec in Brno). These sites have provided detailed paleoclimatic and pedoecological records based on mollusk and vertebrate assemblages (Ložek, 1964; Horáček and Ložek, 1988); pollen data (Urban, 1984); paleopedological analyses (Smolíková, 1982); and archeological findings (e.g. Klíma et al., 1962; Svoboda et al., 1996). Nevertheless, except from the extensive multi-proxy studies of the profile at Dolní Věstonice (Oches and Banerjee, 1996; Bábek et al., 2011; Fuchs et al., 2013; Antoine et al., 2013; Lisá et al., 2014), and the multi-parameter magnetic characterization of the profile at Znojmo (Zhu et al., 2001), representative analytical paleoenvironmental data are still not available for the vast majority of loess series in the Czech Republic.

The present paper reports rock magnetic, geochemical, grain size and micromorphology data for two, until now, poorly-studied Upper Pleistocene series located in the Bohemian and Moravian parts of the Czech Republic more than 200 km apart. The study sites are situated in a relatively dry loess area, in the important transitional zone between Atlantic and continental macro-climatic settings. Regarding their geographical location and the methodological approach, this study helps to fill a gap in European loess research and, furthermore, helps towards a better understanding of the relationship between loess magnetism, chemical weathering and pedogenic intensity.

2. Geological settings

Both study sites are located within a dry loess zone, between north European and Alpine glaciations during glacial periods (Fig. 1). From a paleopedological point of view, both series conform to the standard succession of Upper Pleistocene soil development that is characteristic for this central European zone, as has been established for the area of former Czechoslovakia (Ložek, 1968; Demek and Kukla, 1969) and Upper Austria (Fink and Kukla, 1977; Zöller et al, 1994; Frechen, 2011). The indexing components of the succession, termed pedocomplexes (PK) by Kukla (1961), reveal specific sequences of paleosols, loess and loess derivates that form obvious lithostratigraphic units representing particular stages of climate development. In short, there is a good correlation between particular lithostratigraphic units of loess sequences (PKs) and units of the global climatostratigraphic scale (Marine and Oxygen Isotopic Stages — MIS/OIS). In the region under study, this is also well supported by their numerical dating in many sites throughout central Europe using different means: luminescence techniques (e.g. Musson and Wintle, 1994; Zöller et al., 1994; Frechen et al., 1999; Fuchs et al., 2013); amino-acid racemization chronology (Oches et al., 1996); and radiocarbon dating (e.g. Klíma et al., 1962; Hatté et al., 2001; Lang et al., 2003; Antoine et al., 2013; Kadereit et al., 2013; Újvári et al., 2014). The Upper Pleistocene sequence covers the pedocomplexes: PK III (corresponding to MIS 5e), represented usually by a Bt (zone of clay accumulation in the middle part of a soil) and BC horizons of the Eemian forest brown soil (parabraunerde, luvisol), and an overlying steppe chernozem; PK II (corresponding to MIS 5a and 5c) — two horizons of chernozem separated by colluvial loess sediments (pellet sands sensu Kukla, 1961) (MIS 5b); and PK I (a pedogenetic unit representing MIS 3), which is typically a weak brownish truncated soil of cambisol type .

The descriptions of soils and sediments of the studied sections are based on field observations and micromorphological studies. An overview scheme of the sections and sampled profiles are shown in Figs. 2 and 3.

2.1. Zeměchy

The Zeměchy-section outcrops in a loess gully situated 30 km north of Prague, near the Vltava River. Although the site has become a popular stop of many international field excursions, it has never been studied in detail. Beyond some basic lithological descriptions published as part of excursion guides (Tyráček, 1995; Hošek et al., 2012), or as regional geological reports (Cílek, 1996; Ložek, 1995), only the magnetic susceptibility of the Lower Weichselian part was previously measured (Forster et al., 1996), and five OSL dates were acquired from the Pleniglacial part of the sedimentary record (Zander et al., 2000). The gully is a result of recent erosion; it is 350 m long and 10–15 m wide, incised up to 19 m into a W–E oriented loess “dune” (greda). The pre-Quaternary geological bedrock is composed of weathered carboniferous arkoses. The fluvial gravels and sands accumulated by the Knovíz stream on the bedrock are overlaid by sandy loess corresponding to the Saalian (Riss) glacial (MIS 6, unit number Z 15 in Fig. 3).

A reddish-brown prismatic $Bt_{1(2)}$-horizon and BC horizon of a forest luvisol (parabraunerde) (layer Z14 in Fig. 3) represents the Eemian Interglacial. This horizon, together with brownish pellet sands sensu Kukla (1961) (Z13) and the overlaying chernozem horizon (Z12), represents the 170-cm-thick pedocomplex PK III. A thin layer of coarse sandy loess (Z11) on the surface of PK III may be correlated with the loess marker sensu Kukla (1975). This layer probably represents a phase of strong storm events and has been reported elsewhere in central, western and eastern Europe (Kukla, 1975; Kukla and Cílek, 1996; Antoine et al., 2010; Rousseau et al., 2013). The PK III is overlain by a 90-cm-thick layer of pellet sands (sensu Kukla, 1961) (Z10) and an initial weak brown soil (Z9) developed on colluvial sediment. The 160-cm-thick PK II is composed of a lower dark-gray chernozem (Z8) penetrated by frost wedges and an upper dark to black chernozem (Z6) rich in charcoal. The chernozem soils are separated by brownish pellet sands (Z7) with krotovinas in the uppermost part. The top of PK II is covered by a thin layer of coarse sandy loess (Z5) (marker II) and disturbed by biogenic activity. The described pedocomplexes are overlain by a 6-m-thick accumulation of sandy loess corresponding to the Pleniglacial period (Z4, Z2). The PK I pedocomplex (Z3) from the Middle Pleniglacial (part of MIS 3) is difficult to recognize in the field. It has developed only as a thin, light-brownish layer with a whitish (Ca) horizon below. A gravel layer on the surface of the soil horizon suggests erosional events that may have removed the upper part of the paleosol and, potentially, also some of the overlaying loess. The erosion events probably occurred during warming phases of the MIS 3 interstadial that enhanced the seasonal degradation of the permafrost active layer leading to solifluction-related deformation and alteration of the thin gley horizon (Z2b) preserved above the interstadial soil. The assumption of intensive erosion is also supported by OSL dating (Zander et al., 2000; see Fig. 2). Samples for OSL dating, taken at a distance of 110 cm from the loess above and below the gravel layer (original sample names ZE14 and ZE15, respectively) suggest a considerable hiatus in relatively continuous sedimentation (see OSL ages 51 ky and 22.1 ky). Above the

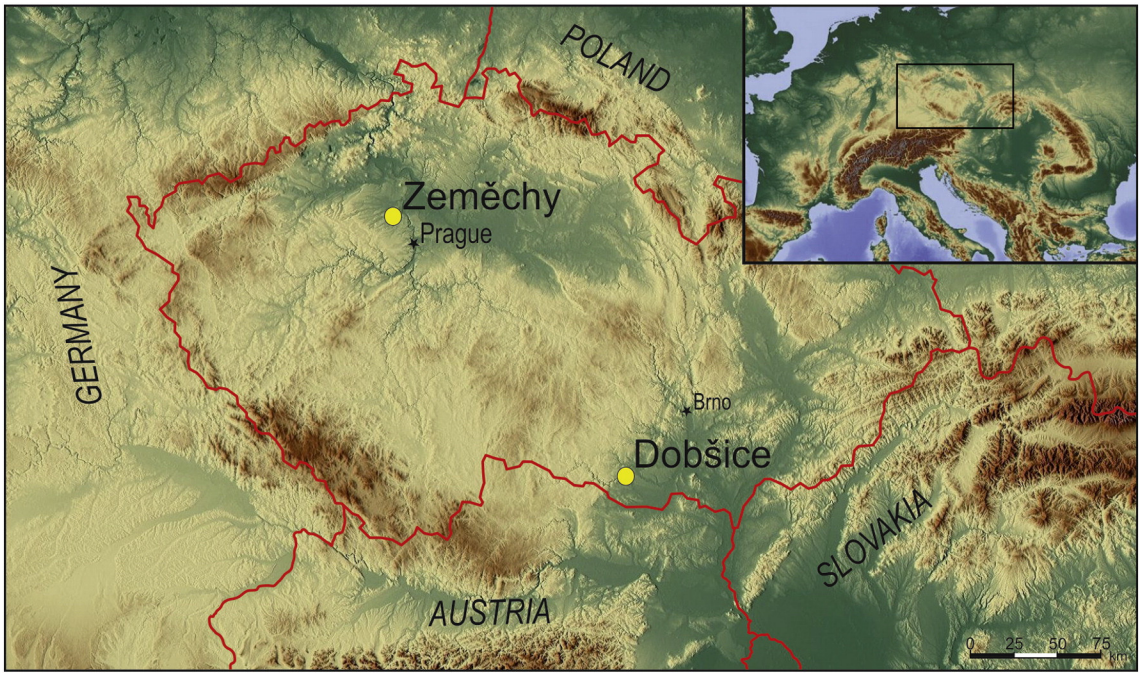

Fig. 1. Location of sites.

position of PK I, Late Pleniglacial loess has accumulated, showing intercalations of several thin gley horizons. The Holocene soil (Z1) is represented by a thin horizon of dark gray, agriculturally-influenced, chernozem soil with a Ca horizon.

2.2. Dobšice

The Dobšice section is situated on the north-western edge of the Pannonian Basin, in the area of surficial contact between the Bohemian Massif and the Carpathian foredeep (Fig. 1). Besides a malacological study of selected horizons (Ložek, 1968), so far only a lithological description, including a micromorphological study, has been published (Havlíček and Smolíková, 1995). The 15-m-thick loess/paleosol sequence has become exposed in the industrial complex of a former brickyard. The sequence overlays a Middle Pleistocene terrace of the Dyje River. The geological bedrock of the area consists of metamorphic rocks of the Bohemian Massif and of Neogene sediments of the Vienna Basin (mainly clay and sands). In general, the pedosedimentary record shows many similarities with the above-described record of Zeměchy. Markers sensu Kukla (1975) are present (unit numbers D12, D7 in Fig. 3) covering both PK III and PK II. The Eemian soil (D14) is developed as a full mature Bt horizon and BC horizon of a luvisol, which is covered by a chernozem horizon (D13). Based on micromorphological analysis (Havlíček and Smolíková, 1995), both soils of the Eemian complex were found to be genetically independent. In comparison with Zeměchy, the chernozems of PK II (D8, D11) are more brownish (in soil taxonomy close to the chernozem/kastanozem transition) and contain higher amounts of silt. In the pellet sands (D9), separating the chernozems of PK II, and also in the Pleniglacial loess (D6), the mollusk *Chondrula tridens* was identified by Ložek (1968). The Dobšice site mostly differs from Zeměchy in its development and preservation of the PK I soil (D5), which corresponds here more to a pararendzina (with cambic features). In the underlying loess (D6), numerous krotovinas are present. In the unit D3, signs of an initial pseudogley process were found. The Holocene soil, similar to that in Zeměchy, is represented by a gray, anthropogenically-influenced soil (D1).

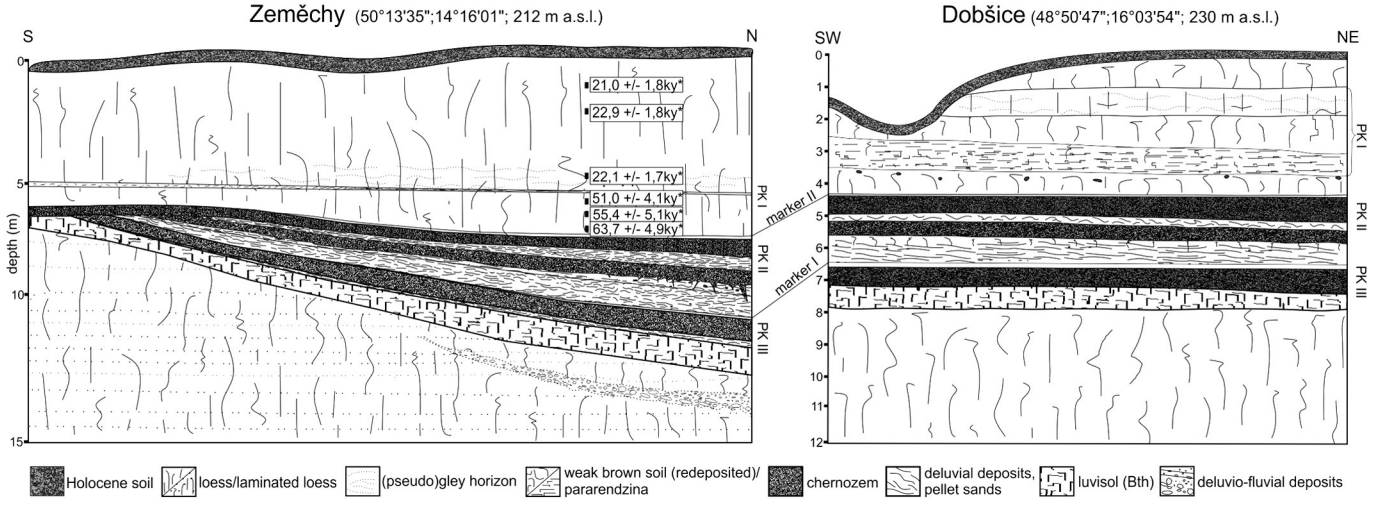

Fig. 2. Lithostratigraphical scheme of the studied sites. *OSL dates (Zander et al., 2000).

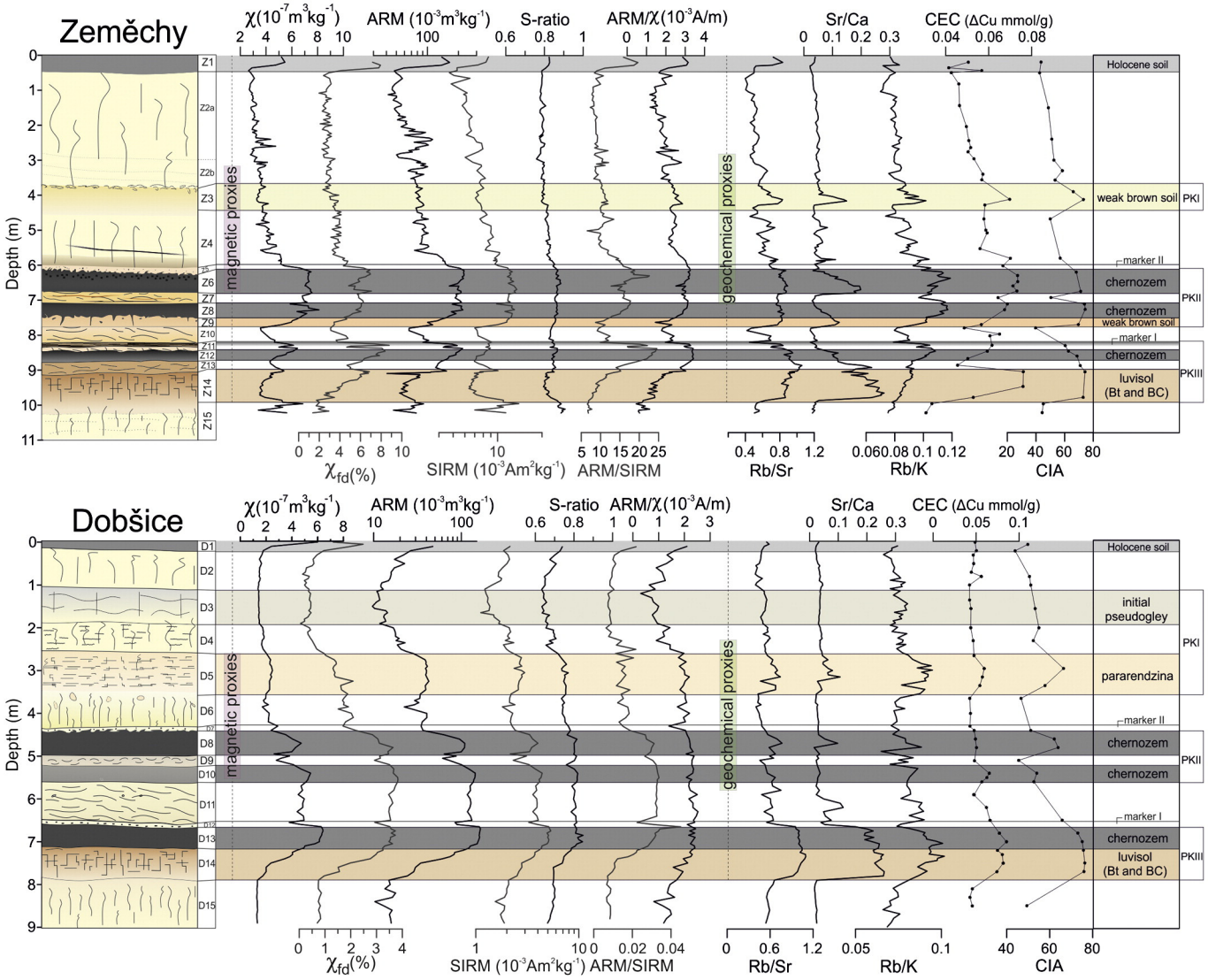

Fig. 3. Magnetic and geochemical proxies of the studied sites together with the lithostratigraphy of the sampled profiles.

3. Methods

3.1. Rock magnetic measurements

Unoriented samples were collected at 3–5 cm intervals from cleaned profiles. The low frequency magnetic susceptibility (χlf, here referred to as χ) was measured at 0.976 kHz, and high frequency magnetic susceptibility (χhf) at 3.904 kHz, using kappabridges MFK1 and KLY-4 (AGICO, Brno). The difference between the two measurements gives the frequency-dependent susceptibility expressed here as a percentage of χfd: $\chi fd\% = (\chi lf - \chi hf) / (\chi lf) \times 100$. The anhysteretic remanent magnetization (ARM) was measured using a LDA-3 demagnetizer with a peak alternating field of 100 mT and a DC biasing field of 0.5 mT.

Values of saturated isothermal remanent magnetization (SIRM) were imparted with a MMPM 10 pulse magnetizer using a field of 2.5 T, and back field remanence measurements were made at 200 mT. The S-ratio was calculated as IRM_0.2 T/IRM 2.5T.

All remanence measurements were made using a JR6-A spinner magnetometer with a noise level of 0.1×10^{-8} A m^2.

The temperature-dependence of the susceptibility (TDS, $\chi - T$) from room temperature up to 700 °C and back to room temperature was measured continuously with a furnace-equipped KLY-3 Kappa-bridge. The powdered whole-material specimens for both loess and paleosol were heated and cooled in an argon atmosphere to prevent possible oxidation.

Frequency dependent susceptibility measurements were carried out at the laboratory of AGICO, s.r.o. in Brno. Magnetic susceptibility of samples from the Dolní Věstonice brickyard (taken in 5 cm intervals) was acquired using a KLY-2 Kappa-bridge (AGICO, Brno) in the Paleomagnetic laboratory of Cologne University within the framework of a project led by one of us in the mid-1990s. Additional rock magnetic measurements were carried out at the Laboratory for Palaeo- and Enviromagnetism of the University of Bayreuth.

3.2. Geochemical and grain size analyses

Element analyses were performed on an X-ray fluorescence (XRF) spectrometer MiniPal4.0 with an Rh tube, maximal primary X-ray energy of 30 keV and a Peltier-cooled ED detector. The XRF signals of some 20 elements were determined, but only the results for Ca, Sr, Rb and K are discussed in this paper.

For selected samples (n = 25 in Zěměchy; n = 22 in Dobšice) conventional silicate analyses after wet decomposition were also carried out. Selected components were used for calculation of the Chemical Index of Alteration (CIA) and as verification of the accuracy of XRF data. The CIA was calculated as $CIA = [Al_2O_3 / (Al_2O_3 + Na_2O + CaO^* + K_2O)]$

× 100. CaO*, referring to silicatic Ca (after Nesbitt and Young, 1982), was obtained by subtracting acid-soluble Ca (in $CaCO_3$) from total Ca content. The cation exchange capacity (CEC) was determined using a procedure proposed by Meier and Kahr (1999) for pure clay mineral specimens and then optimized for sediments and soils (Grygar et al., 2009). $[Cu(trien)]^{2+}$ solution was obtained from $CuSO_4 \cdot 5H_2O$ (Penta, Czech Republic) and trien, triethylenetetramine (1,4,7,10-tetraazadekane, Sigma-Aldrich), and then to the final concentration 0.01 M with potentiometric control of the constant ligand-to-metal ratio.

The solutions were analyzed by Atomic absorption spectroscopy — AAS (Cu and Mg) and Atomic emission spectroscopy — AES (Ca and Na). The sample weight for analysis was adjusted depending on its actual Cation Exchange Capacity (CEC) in order to consume about 50% of $[Cu(trien)]^{2+}$ using the routine described by Grygar et al. (2009).

After removal of carbonate and organic matter by H_2O_2 and HCl respectively, the particle size distribution was measured using a laser granulometer CILAS 1190 LD that provides a measurement range from 0.04 to 2500 μm. For the correlation of magnetic and geochemical parameters the Pearson's correlation coefficient r was used.

3.3. Micromorphology

Oriented soil samples were taken in small Kubiena boxes (dimensions 3 × 5 cm) from each lithological layer. Upon slow drying followed by impregnation with resin, thin sections were produced from samples in the laboratory of the Czech Geological Survey (equivalent to Bullock et al., 1985; Stoops, 2003). The thin sections were studied under polarizing and binocular microscopes in the Institute of Geology ASCR, v. v. i., in Prague at a magnification of 16–800× and interpreted according to Stoops et al. (2010).

4. Results and interpretation

4.1. Magnetic properties

4.1.1. Concentration related magnetic parameters

The rock magnetic records correlate well with the lithology and show many similarities in both sections (Fig. 3). In general, the paleosols are characterized by an enhancement of the magnetic signal compared to loess units and pellet sands.

The values of χ (in 10^{-7} m^3 kg^{-1}) vary from 2.6 to 8.1 in Zeměchy (Z) and from 1.2 to 6.4 in Dobšice (D). In Zeměchy, maximum χ values (8.1) occur in the lower chernozem of PKII (layer Z9), whereas in Dobšice these occur in the chernozem of PKIII (6.4, D13). In both sections, minimum values occur in Saalian and Weichselian-Pleniglacial loess (χ about 1–5 in Z; 1–2 in D), chernozems showing higher values of χ than luvisols, where the magnetic enhancement occurs just in the upper part (Bt-horizon), whereas the underlying BC horizon is characterized by lower values of χ. This is very likely caused by the following process: in a Bt horizon the precipitation of iron oxides occur and consequently a higher amount of pedogenetic magnetite in comparison with the BC horizon can be observed (e.g. Rivas et al., 2006; Torrent et al., 2006; Jordanova et al., 2013). The χ-values of the lower and middle part of luvisols range between 4 and 5 in Zeměchy and 2 and 6 in Dobšice, representing approximately intermediate values between unweathered loess and chernozem paleosols. Pellet sands have higher χ values than loess, probably depending on the amount of top-soil particles in the reworked sediment. The pleniglacial parts of the records exhibit continually-decreasing χ values on the way up to the Holocene soil at both sites. The pararendzina of PK I in Dobšice (D5) show slightly higher values than the over- and underlying loess units (D2, 5) and the pseudogley horizon (D3), whereas the horizon corresponding to the weak brown soil in Zeměchy (Z3) did not show any differences to the loess itself.

The values of SIRM, ARM and χ often represent concentration and grain size-dependent parameters (Evans and Heller, 2003). *SIRM* gives information about the total (ferro-) magnetic mineral concentration with grain size larger than the superparamagnetic (SP)/single domain (SD) threshold (~0.02 μm). Unlike χ, SIRM is not influenced by the presence of para- and dia-magnetic minerals such as phyllosilicates, carbonates or quartz (Thompson and Oldfield, 1986). χfd indicates the proportion of fine viscous magnetic grains just below the SP/SD boundary (~0.02 μm; Thompson and Oldfield, 1986), while *ARM* is sensitive to single domain (SD, ~0.02–0.06 μm) grains of magnetically "soft" minerals like magnetite and maghemite (Maher et al., 1986). Both grain size fractions are preferably formed during pedogenesis (Heller and Evans, 1995).

Generally, ARM and SIRM values, as well as the χfd, follow the χ signal pattern in both sections. Again, values are uniformly low in loess, and enhancement can be observed in chernozems and the upper part of luvisols. Intermediate values are observed in reworked sediments derived from loess and soils. The correlation between χ and remanence parameters (see the highest correlation coefficients between χ and ARM in Table 1) strongly suggests that the magnetic signal of both sections is mainly controlled by the presence of single domain magnetic minerals. In contrast to Zeměchy, the Dobšice section shows less differences of χfd-values between pellet sands and chernozems, suggesting a higher content of SP/SD (pedogenetic) magnetic grains in the sediment.

The plot of χfd and χ is shown in Fig. 4. The increasing χfd and χ values follow the model of magnetic enhancement (i.e. the neoformation of ultrafine magnetite during pedogenesis) proposed, for example, by Heller et al. (1993), whereas decreasing χ with increasing χfd values point to magnetic depletion during low-temperature oxidation of magnetite, likewise leading to a shift of the magnetic domain assemblage towards SP domains. in Zeměchy magnetic enhancement was obvious in all horizons; however, in the upper (Pleniglacial) part of Dobšice signs of depletion of primary MD and SD grains relative to SP particles were found, probably due to the effect of water-logging (initial pseudogley horizons). Similar processes in the Pleniglacial loess have been observed elsewhere, for example in Saxony (eastern Germany) (Baumgart et al., 2013) in the Kraichgau area (western Germany) (Taylor et al., 2014), in Poland, and Western Ukraine (Nawrocki et al., 1996).

In Zeměchy, much higher absolute amounts of ferrimagnetic minerals are present than in Dobšice, resulting in higher ARM and SIRM values (Z: 37.7–227.1 10^{-3} A/m; 4.7–13.9 10^{-3} A/m; D: 9.6–165.2 10^{-3} A/m; 1.2–5.3 10^{-3} A/m). Similarly, χfd is much lower in Dobšice (~0.3–3.5%) than that in Zeměchy (~1.3–8.8%), suggesting that SP grains in chernozems of Bohemian sections are more common than in the equivalent/corresponding Moravian horizons.

4.1.2. Magnetic mineralogy and particle size

The S-ratio is, like the χfd, a concentration-independent proxy indicative of the relative abundance of ferrimagnetic to antiferromagnetic minerals (Maher, 1986; Wang et al., 2012). Elevated values reflect the dominance of magnetite (or maghemite), while lower values represent

Table 1
The correlation of magnetic and geochemical parameters.

		χ	ARM	χ_{fd}	SIRM	Rb/Sr	Rb/K	CEC	CIA
Dobšice	χ		0.99	0.89	0.97	0.5	0.63	0.63	0.53
	ARM	0.99		0.87	0.98	0.58	0.56	0.62	0.52
	χ_{fd}	0.89	0.87		0.84	0.56	0.61	0.56	0.51
	SIRM	0.97	0.98	0.84		0.62	0.67	0.6	0.5
	Rb/Sr	0.5	0.58	0.56	0.62		0.78	0.89	0.76
	Rb/K	0.63	0.56	0.61	0.67	0.78		0.74	0.76
	CEC	0.63	0.62	0.56	0.6	0.89	0.74		0.85
	CIA	0.53	0.52	0.51	0.5	0.93	0.76	0.85	
Zeměchy	χ		0.92	0.7	0.9	0.59	0.77	0.7	0.49
	ARM	0.92		0.78	0.79	0.57	0.79	0.63	0.48
	χ_{fd}	0.7	0.78		0.42	0.78	0.63	0.44	0.48
	SIRM	0.9	0.79	0.42		0.43	0.67	0.79	0.43
	Rb/Sr	0.59	0.57	0.78	0.43		0.65	0.65	0.78
	Rb/K	0.77	0.79	0.63	0.67	0.65		0.74	0.71
	CEC	0.7	0.63	0.44	0.79	0.65	0.74		0.73
	CIA	0.49	0.48	0.48	0.43	0.78	0.71	0.73	

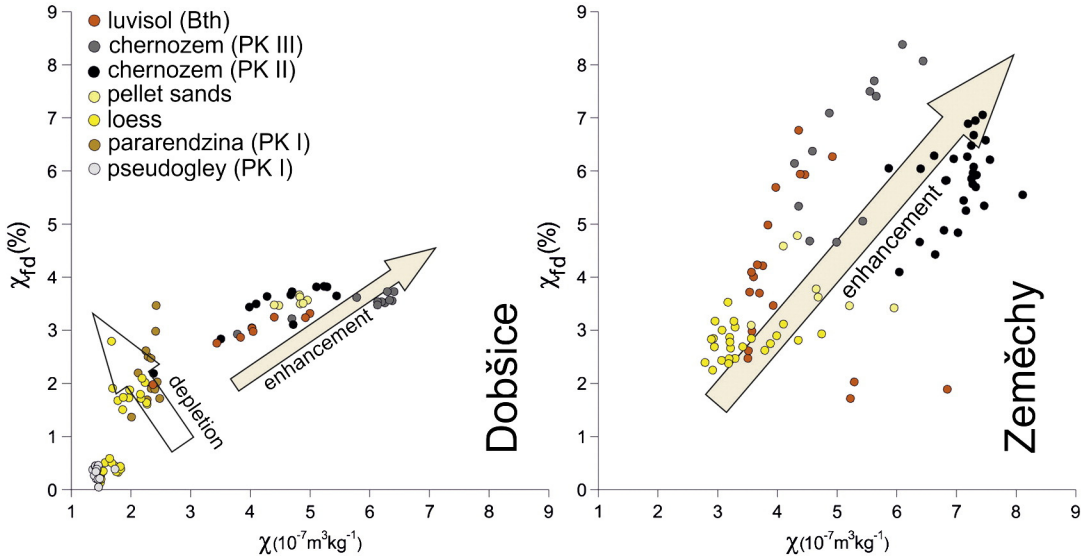

Fig. 4. Scatter plots of χ versus χ_{FD}.

increasing contributions from antiferromagnetic minerals, i.e. hematite or goethite. In both sites the S-ratio ranges between 0.85 and 0.9 in chernozem soils and in the upper part of luvisols, thus reflecting the high concentration of ferrimagnetics in the soil horizons. In both sections, the pleniglacial part of the record typically shows lower values of the S-ratio (0.62–0.8 in Zeměchy, 0.65–0.75 in Dobšice) and a descending trend (more visible in Dobšice) mainly in the loess between PK II and PK I soils. Nevertheless, the relatively uniform values close to 1 through both profiles suggest the dominance of ferrimagnetic minerals and little mineralogical variation. This interpretation is supported by temperature-dependent susceptibility (χ–T; Fig. 6).

Typical χ–T curves for the lower part of chernozems, the middle part of luvisols and Pleniglacial loess are shown in Fig. 6. In chernozems, as well as in loess, there are two major peaks for heating curves around 300 and 510–520 °C, while in luvisols only one peak occurs around 300 °C. The 'rise' in the heating curves at about 300 °C possibly indicates the transition of weakly-magnetic Fe-hydroxides (e.g., lepidocrocite) to maghemite (Oches and Banerjee, 1996). The increase of susceptibility

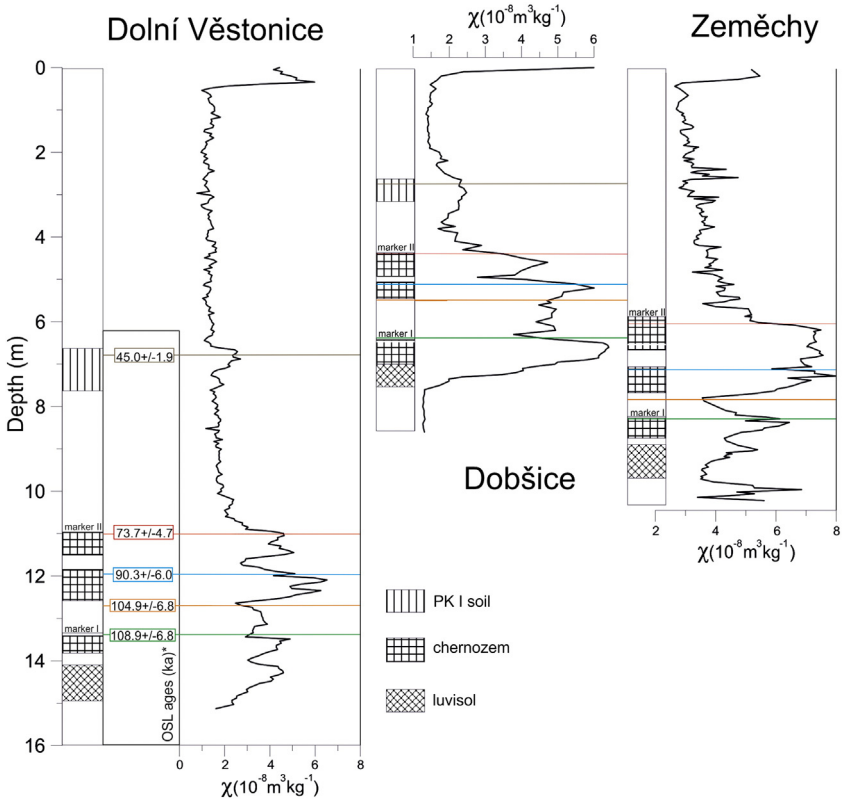

Fig. 5. Correlation of the Dolní Věstonice profile and the studied sections, based on the magnetic susceptibility.
*OSL dates adopted from Fuchs et al. (2013).

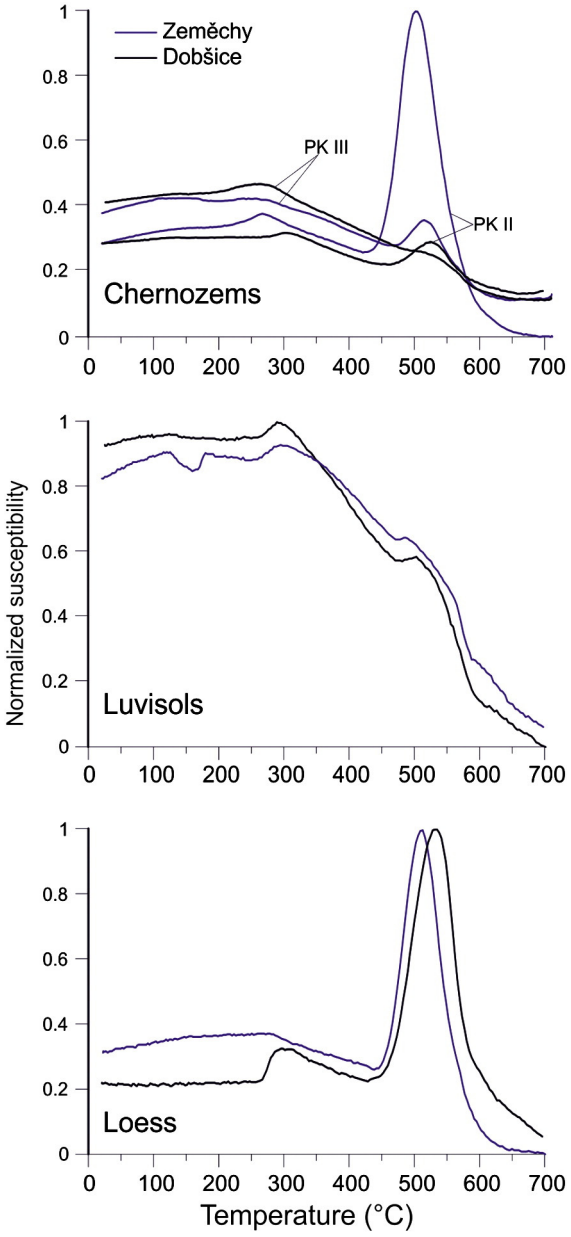

Fig. 6. Temperature dependent magnetic susceptibility of selected horizons. The values were standardized to a variation between zero and one.

between 250 and 300 °C (found in luvisols and loess) was interpreted by Liu et al. (2005) as a result of the gradual unblocking of fine-grained SD particles, which are *multidomain* (MD) at room temperature. The susceptibility drop between ~ 300–450 °C (almost absent for loess samples) has been interpreted as the inversion of *maghemite* to hematite (Sun et al., 1995; Oches and Banerjee, 1996; Liu et al., 2005). Liu et al. (2005) suggest that only the *fine-grained pedogenic particles* can efficiently be converted to hematite between 300 and 400 °C during heating. The rapid increase of susceptibility within the temperature interval of 450–520 °C (absent for luvisols) shows the formation of a new ferromagnetic mineral. This observation can be caused by the reduction of low susceptibility *hematite* to high susceptibility magnetite in an oxygen-free environment (Hunt et al., 1995). The sharp loss of susceptibility of all samples above 520 °C indicates the presence of *magnetite*, with its Curie point of 585 °C, being apparently a major magnetic mineral of the loess/paleosol sequences. A Curie temperature of about 580–585 °C can be observed in all samples. Unlike the warming curves, the cooling curves (not shown here) are dominated by newly-formed magnetite at ~500–400 °C.

In the luvisol of Zeměchy, we found a minor peak of susceptibility at 120 °C and a sharp loss between 120 and 180 °C, which may indicate the presence of *goethite* with a Curie temperature of around 120 °C (Liu et al., 2012).

In general, χ–T experiments suggest magnetite and maghemite enhancement of chernozem horizons as well as partially of pellet sands, while in the middle part of luvisols the enhancement only occurred to a limited extent — and by maghemite rather than magnetite formation. The higher concentrations of hematite in chernozems than in brown soils, and the presence of goethite in brown soils, is in accordance with previous results obtained by diffuse reflectance spectroscopy measured in Dolní Věstonice (Bábek et al., 2011).

Because the SIRM values had no contribution from SP grains, the low values of ARM/SIRM suggest a higher proportion of soft MD or SD magnetic grains, while high values correspond to the presence of stable single domain (SSD) magnetic grains (Evans and Heller, 2003). In Zeměchy, the course of ARM/SIRM with depth suggests the presence of SSD magnetic grains mainly in the upper part of the chernozems, whereas in luvisols, pellet sands and loess horizons larger grains dominated. This is in accordance with the results of the χ–T measurements. In Dobšice, however, the differences between paleosols and loess horizons are not very pronounced; the generally higher amount of SSD grains having been induced by the colluvial sediments. Hence, one almost continuous increase of magnetic parameters can be observed throughout the whole Lower Weichselian. In the Pleniglacial loess (including the weak interstadial soils), a stagnant trend is apparent at both sites. The ARM/χ ratio has been used to investigate the relative contributions of SP and SD grains to the bulk signal (e.g. Zeeden et al., 2010). In general, this record follows the pattern of χfd, proving the contributions of SP/SD grains to the magnetic signal.

The analyses presented above show that the samples contain mainly ferrimagnetic minerals (magnetite and maghemite) and partially antiferromagnetic minerals (goethite, hematite). The chernozem soil horizons are characterized by more fine-grained ferrimagnetic minerals in contrast to loess and luvisols. All these characteristics are, in general, consistent with previous studies of loess/paleosols sequences situated in central Europe (Oches and Banerjee, 1996; Forster et al., 1996; Zhu et al., 2001) and neighboring areas (Süttö, Hungary — Rolf et al., 2014; Lower Austria — Hambach, 2010).

4.2. Chronology of studied sections

The trends of χ with stratigraphy for both investigated sites correspond well to the litho-/pedo-stratigraphical and magnetic susceptibility record obtained from the Dolní Věstonice (DV) brickyard (Fig. 5). We employed the magnetic susceptibility data from DV as a tool to transfer the numerical ages (Fuchs et al., 2013) from DV to the sections under investigation (Fig. 5). For the Pleniglacial part of the record in Zeměchy, OSL dates by Zander et al. (2000) (Fig. 2) were also used to constrain the chronology. As a result, we obtained a composite chronology of all sections, based on OSL and correlation of the χ signals, which was corroborated by direct correlation of the Rb/Sr-weathering index to the global $\delta^{18}O$ record on its time scale (Lisiecki and Raymo, 2005).

4.3. Results of geochemical investigations

The results of geochemical analyses are summarized in Fig. 3. During chemical weathering, dissolved ions are transported through the sequences with percolating rainwater, depending mainly on their solubility and ability to be retained by clay (Perel'man, 1977). The weathering process can be divided into the early Ca and Sr removal stage, the intermediate K removal stage and the last Si removal stage (Nesbitt et al., 1980). Therefore, simple ratios of mobile (such as Sr and Ca) to relatively stable (such as Rb, Ti, and K) elements are used. This approach has

been widely adopted as an appropriate measure for the degree of chemical weathering and leaching intensity in sediments (Gallet et al., 1996; Nesbitt et al., 1996; Chen et al., 1999; Ding et al., 2001; Muhs et al., 2001; Bokhorst et al., 2009). For the evaluation of the weathering intensity of the silicate component, we used the Chemical Index of Alteration (CIA) (Nesbitt et al., 1980). The interpretation syllogism of the geochemical results is included.

The Rb/Sr ratio of both sections shows maximum values in luvisols and chernozems, being only slightly increased in Middle Pleniglacial weak soils (PK I) and with minimum values in loess. In Dobšice, much less pronounced peaks in the chernozems of PK II occurs compared to Zeměchy. In both sections, a moderate/good correlation was found between Rb/Sr and magnetic parameters (Table 1); however, this did not hold for the luvisol horizons (see Table 1). Rb is usually enriched in K-rich minerals such as muscovite, biotite, K-feldspar and K-rich micas and illite. Furthermore, this element is unaffected by sediment diagenesis and by precipitation and concentrations of Fe and Mn oxihydroxides. It is strongly retained in the weathering zone due to its adsorption or exchange onto clay minerals (Nesbitt et al., 1980). Rubidium fixation in soils is a tracer of the transformation process affecting the 2:1 clay minerals in the acid brown earth-pod's (Herbauts, 1982) weathering sequence: kaolinite, illite, chlorite, vermiculite and smectite. Unlike Rb, Sr is a mobile element bound in Ca-feldspars and primary carbonates; it is easily soluble during leaching and chemical weathering processes. Because Rb is bounded to the clay particles, the resulting ratio is grain-size dependent. Nevertheless the clay in the LPS is mostly a product of the pedogenesis and weathering of the primary (silty) material and hence the Rb/Sr ratio is a sound indicator of loess chemical weathering (Gallet et al., 1996; Chen et al., 1999; Bloemendal et al., 2008; Bábek et al., 2011). It also seems to be a valuable indicator of the Late Glacial paleoenvironmental changes in a lake catchment, as was proved by analysis of non-calcareous lake sediments in Southern Bohemia (Hošek et al., 2014).

Unlike the Rb/Sr ratio, Rb/K shows lower values in the luvisols in both sites, whereas in the upper parts of the profiles the ratio increases again in paleosols and decreases in loess, clearly independent of the dilution by carbonates. This behavior indicates secondary clay enrichment, because Rb substitutes for K in K-feldspars and mica and becomes enriched during weathering, whereas K is more mobile and preferentially leached under moderate/strong chemical weathering (Nesbitt et al., 1980; Zech et al., 2008). The variability of K in the investigated profiles is in agreement with the various correlations between CEC and the elemental signatures that are discussed below. Further, a surprisingly high correlation coefficient between the Rb/K ratio and χfd was found throughout the profiles (see Table 1), suggesting that SD/SP magnetic grain enhancement/depletion in the sediment and soils throughout the profiles, and potassium mobility, may be both driven by related processes.

The highest Sr/Ca ratio is found in the interglacial luvisols in both sections. In Zeměchy, an increase of this ratio also occurs in the lower part of the PK II chernozems, whereas these events are not present in Dobšice. Slightly higher values of the ratio are recorded in the PK I soils of both sites. Ca, as well as Sr, is mainly present in primary carbonates and in relatively soluble carbonate minerals and is hence depleted in the weathering zone (Gallet et al., 1996; Bloemendal et al., 2008). Nevertheless, due to its size, Ca is adsorbed less strongly to clay structures than Sr, and more Ca reprecipitates as secondary carbonates relative to Sr. The vegetation may also play a role in the retention of Ca from wash-out, as the biogenic coefficient of Ca is much higher (0.17) than of Sr (0.06) (Perel'man, 1977). The ratio of Sr/Ca primarily reflects carbonate dissolution and hence mostly increases with increased leaching intensity, during more humid conditions (Bloemendal et al., 2008; Bokhorst et al., 2009). The low correlation between the CIA with Sr/Ca (Pearson correlation coefficient $r = 0.2$ and 0.4, data not shown in Table 1) in both sites suggests that carbonate dissolution was not necessarily accompanied by silicate and feldspar weathering. At Zeměchy, a strong negative correlation ($r = -0.78$) was found between the Sr/Ca ratio and ARM in soil horizons, suggesting that the leaching process also affected fine-grained (0.02–0.06 μm) magnetic particles.

The Chemical Index of Alteration (CIA) gives information about feldspar weathering by relating Al, which is enriched in weathering residues, to Na, Ca and K. Na and K are assumed to be removed from a soil profile in the course of plagioclase and K-feldspar weathering (Nesbitt and Young, 1982). In recent years, this proxy has been relatively frequently used as a suitable tool for the quantitative expression of chemical weathering in loess (e.g. Chen et al., 1999; Buggle et al., 2008; Újvári et al., 2008). The index is referred to as an "Na type" of weathering, whereas the above-described Rb/Sr ratio is considered as a "Sr-type" weathering index (Buggle et al., 2011).

4.4. Cation exchange capacity (CEC)

During the chemical weathering of loess, there occurs an ion exchange and transformation of clay minerals. The $[Cu(trien)]^{2+}$ ion is selectively adsorbed to expandable clay minerals. Increased CEC values obtained by $[Cu(trien)]^{2+}$ can thus be mainly attributed to a higher concentration of the most common expandable clay structure, i.e. smectite (Grygar et al., 2009; Bábek et al., 2011). Expandable clay minerals are characterized by the presence of loosely-bound cations and layers of water-bearing, polarized, organic molecules between the structural sheets. This type of structure is thus typical for more humid environments and their relatively low presence in the sediment suggests that conditions in these sections were most likely arid (and acidic), as they have been largely depleted or at least altered. Illite-type clays are formed under high pH conditions, mostly from weathering of K- and Al-rich minerals such as muscovite and feldspar. The illite/smectite ratio in the loess series thus provides a promising proxy strongly related to soil humidity and its seasonality (Li et al., 2007; Varga et al., 2011; Újvári et al., 2014)

Although CEC has rarely been used for loess/paleosol sequences, several studies have suggested that CEC can be correlated with other indicators of weathering intensity related to precipitation, indicators such as magnetic susceptibility, diffuse reflectance spectroscopy and element ratios of Rb, Ca and Sr (Maher, 1998; Bokhorst et al., 2009; Bábek et al., 2011).

At both sites, the CEC follows the proxies of weathering/pedogenesis intensity; elevated values (interpreted as higher amounts of smectite) coincide with soils, and the highest values correspond with luvisol horizons, for which the most intensive chemical weathering can be expected. In Dobšice, in comparison with Zeměchy, lower values are recorded in chernozems of PK II, especially in the upper one. The middle Pleniglacial soils (PK I) of both sites shows relatively high values, whereas in the overlying loess a gradual decrease occurs. CEC was positively correlated with the Rb/K ratio ($r = 0.74$), which can indicate the conversion of illite to expandable clay minerals (a process accompanied by a partial loss of K^+ ions) and this suggests the presence of K in muscovite and feldspar. The highest correlation between CEC and magnetic parameters was found in the case of χ and SIRM.

4.5. Grain-size analyses

Fig. 7 shows selected grain size distribution parameters of the sediment. Both sites are characterized by a higher content of the clay fraction (<4 μm) in soil horizons (~20%) compared to pellet sands and loess (~10%). The highest enrichment of clay is recorded in the upper parts of the luvisol (Bt horizons) and the overlaying chernozem (PK III) in both sites. A relatively high clay content is also recorded in the middle Pleniglacial part (PK I) of both sites. In general, the amount of clay in the sediment shows a similar pattern to that of the magnetic susceptibility record and proxies of chemical weathering such as Rb/Sr and Rb/K ratios (see Fig. 3), probably due to the pedogenic modification that has changed the grain size composition of the non-quartz component of

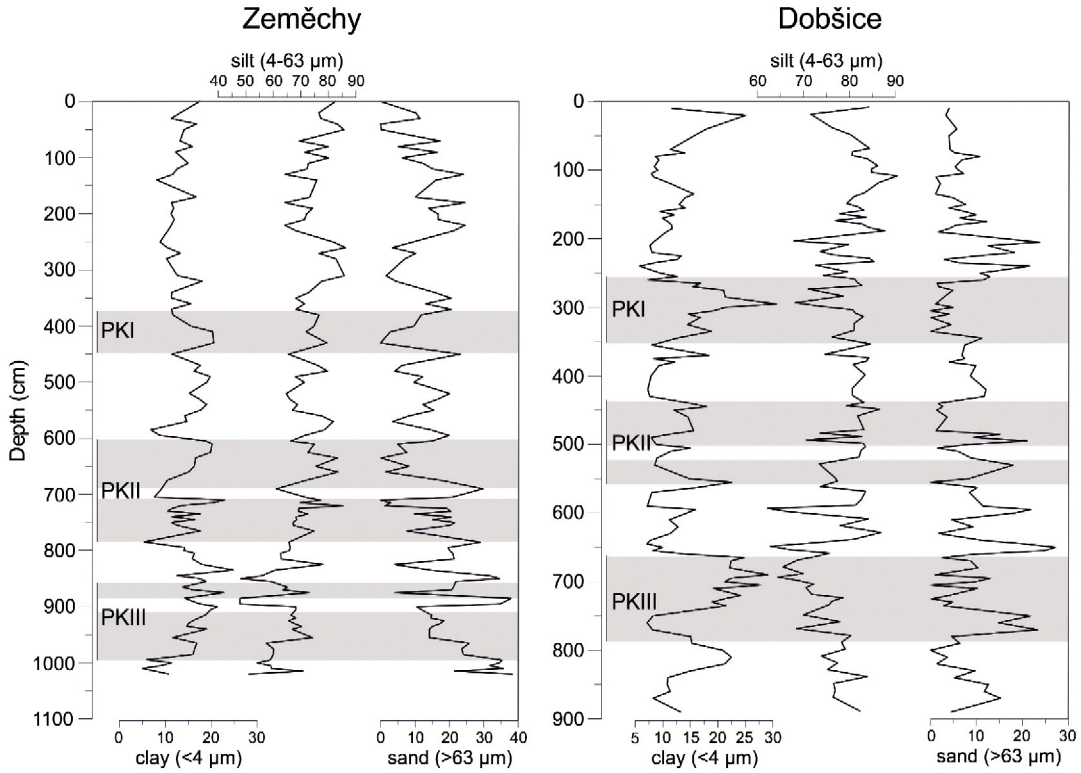

Fig. 7. Results of grain size analyses of the discussed sites.

the original dust. This is in accordance with the correlation between clayey humic soil horizons, magnetic susceptibility or organic carbon content that has been observed in Upper Pleistocene soil complexes from many European sites (e.g. Antoine et al., 1999, 2009, 2013).

The silt fraction (4–63 μm) dominate throughout both profiles (~60–90%). Maxima are typical for upper Pleniglacial loess (above PK I). The sand concentration (>63 μm) ranges from ~1–30%; higher amounts of sand are typical for colluvial sediments (pellet sands) and the upper Pleniglacial loess, as well as for marker horizons (marker I). In general, the amount of sand in Zeměchy is higher than in Dobšice, probably due to a nearby outcrop of carboniferous arkoses, whereas At Dobšice sand originates from Pleistocene fluvial terraces of the Dyje River.

4.6. Micromorphology

Micromorphological features of the main horizons are summarized in Table 2, the characteristics reflecting the local soil and environmental development. While the horizon representing the interglacial luvisol is preserved only by the Bt horizon, with the A horizon missing, the chernozem-like pedo-horizons are characterized by well-developed humified A horizons. During the development of chernozem-type soils, the accumulation of organic matter by humification is the dominant pedogenetic process. For luvisols, besides the strong in-situ weathering, the main pedogenetic process is the translocation of clays down the section. Thus the characteristic feature of such soils is the clay-enriched Bt horizon. The thickness of such horizons usually reflects the intensity and/or temporal duration of the pedogenetic processes. Higher humidity and/or water-logging might be causes for the pedogenetical processes connected with gley formation. Pronounced differences between the sections were found in some horizons, especially in the Lower Weichselian part of profiles (PK II); however, in this respect Dobšice differed from Zeměchy by having a markedly lower level of polygenesis. Secondary redoximorphic features (pseudogley processes) are here present just in the horizon of PK I (D3). Dobšice is also interesting from a pedozoological point of view because, besides the activity of earthworms (Lumbricidae) occurring throughout, the activity of Enchytraeidae (potworms) occurred, or even dominated (D10), in all the paleosols including the pararendzina of PK I.

5. Discussion

5.1. Rock-magnetic and geochemical results and their predictive value as paleoclimate indicators

The rock-magnetic investigation results (Fig. 3) suggest that the magnetic signal at both sites is mostly influenced by fine-grained (SP and SD) magnetite and partially also by maghemite. These components are typically formed during loess weathering and pedogenesis in a relatively warm and humid climate with a pronounced dry season (Fontes and Weed, 1991; Maher, 1998; van Velzen and Dekkers, 1999; Oldfield, 2007; Torrent et al., 2006; Zhang et al., 2007; Buggle et al., 2013a).

The good correlation between magnetic and geochemical proxies through the Weichselian parts of the studied profiles (Fig. 3) suggests that fine-grained magnetite/maghemite formation was accompanied by a more intensive weathering of minerogenic components, and a higher element mobility and clay mineral (trans)formation. For example, the formation of magnetic grains close to the SP/SD boundary (ARM/ χ) clearly correlated with the feldspar weathering and consequently with potassium mobility (Rb/K ratio, CEC). This is probably because, similar to that in pedogenetic bacteria activity, K mobility in soils and sediments (and its availability and diffuse flux for plant uptake) is strongly influenced by soil moisture (Zeng and Brown, 2000). On the other hand, the dissolution and leaching of Sr-rich carbonate minerals (Rb/Sr ratio) did not show such a direct link to magnetic enhancement.

Table 2
Micromorphological characterization of the significant lithological horizons.

Layer	Micromorphological features	Interpretation
Dobšice		
D3	Crack microstructure, sandy loam, crystalitic B fabric, decomposed organic matter — rare, bioturbation, $CaCO_3$ coating — rare, FeOH nodules (pseudogley concretions).	Weakly developed pseudogley (PK I)
D5	Granular to crack microstructure, sandy loam, crystalitic B fabric, $CaCO_3$ coating and infillings, Mn coating and nodules	Weakly developed pararendzina with A and $CaCO_3$ horizon (PK I)
D8	Spongy to granular microstructure, sandy loam, crystalitic B fabric, decomposed organic matter, bioturbation, $CaCO_3$ coating and infillings, excrements, phytoliths.	Upper chernozem (A and $CaCO_3$hor) of PK II
D9	Subangular blocky microstructure, sandy loam, crystalitic B fabric, humous concentratios — aggregates, $CaCO_3$ coating and infilling.	Loess/reworked loess
D10	Spongy to granular microstructure, sandy loam, crystalitic B fabric, decomposed organic matter, partly decomposed wood fragments, bioturbation, $CaCO_3$ and Mn coating and infillings, excrements.	Lower calcareous chernozem (A and $CaCO_3$hor) of PK II
D12	Subangular blocky microstructure, crystalitic B fabric, sandy loam (quartz and feldspar, fragments of granite and quartzite up to 2 mm; obvious positive gradation), $CaCO_3$ and Mn coating and infillings.	Marker loess sensu Kukla (1975)
D14	Spongy to granular microstructure, sandy loam, porostriatic B fabric, partly decomposed wood fragments, charcoal, bioturbation, $CaCO_3$ and Mn coating and infillings, humic concretions — common, excrements.	Luvisol (Parabraunerde) (Bt and $CaCO_3$ horizon) of PK III
Zeměchy		
Z3	Spongy microstructure, enaulic related distribution, 30% micro and mesovoids, vughs and compound packing voids, moderately sorted silt, crystallitic B fabric, light brown matrix, very fine grained black opaque decomposed organic matter (up to 10%), FeOH nodules present (up to 3%).	Weak brown soil (PK I)
Z8	Inter grain vesicular pore microstructure, enaulic related distribution, 30–50% micro and mesovoids, vughs and compound packing voids, moderately sorted silt, crystalitic B fabric, dark brown, fine grained black opaque decomposed organic matter (up to 30–50%),	Lower chernozem of PK II
Z11	Channel microstructure, enaulicrelated distribution, 50% micro and mesovoids, channels, vughs and compound packing voids, moderately sorted silt, crystallitic B fabric, brown, fine grained black opaque decomposed organic matter (up to 10%), charcoal fragments, three phases of calcium carbonate pedofeatures origin: 1.) crystallic pseudomorphoses of root cells due to bioturbation; 2.) hypocoating of channels; 3.) infillings of channels by crystallitic carbonates.	marker loess sensu Kukla (1975)
Z14	Intergrain channel microstructure, enaulic related distribution, 30% micro and mesovoids, channels and vughs, moderately sorted silt to fine sand, porostriatic B fabric, light brown to orange, very fine grained black opaque decomposed organic matter (up to 30%).	Luvisol (Parabraunerde) (Bt and $CaCO_3$ horizon) of PK III

On the contrary, the strong carbonate dissolution may have lead to the loss of fine-grained magnetic particles during the leaching processes.

In contrast to the interstadial chernozem soils, interglacial luvisols showed lower values of magnetic concentration-dependent parameters, as well as weaker magnetite/maghemite enhancement as shown by the χ–T measurements (Fig. 6). This is in contrast to the LPSs from the Pannonian Basin, where a strong magnetic enhancement also occurred within the lower part of the paleosol-complex (S1) corresponding to the Last Interglacial, and where magnetic concentrations were more than twice as high than that for the loess horizons (Marković et al., 2008, 2009; Buggle et al., 2013a). In both sites the Interstadial soils of PK I also exhibited a pronounced maxima of CEC and clay content, and a minima of calcite concentration, that are clear signs of a relatively intensive pedogenesis. However, in the case of Zeměchy, the PK I horizon was not detected by its magnetic measurements (see Fig. 3).

For the last interglacial in central Europe, the malacological, palynological and pedological data generally indicated more humid and warmer conditions (even compared to the Holocene). This favorable climate was replaced during the Lower Weichselian by rather cold and arid conditions with three interstadial oscillations characterized by a warmer, but still relatively dry, climate (Ložek, 1964; Smolíková, 1982; Urban, 1984; Caspers and Freund, 2001). The clear discrepancy between these statements and the above-mentioned surveyed rock magnetic record suggests a non-linear relationship of magnetic parameters with climatic change. This finding should constitute a point of special interest and is further discussed here in more detail.

The influence of climate on a magnetic signal (particularly the magnetic susceptibility) in LPSs and modern soils has already been extensively discussed in many studies (e.g. Heller et al., 1993; Maher et al., 2003; Liu et al, 2007; Buggle et al., 2013a). Nevertheless, the relationships between the state of magnetic variables and the course of the Pleistocene climate are far from being interpreted as linear (Han et al., 1996). This means that some climate changes, clearly documented by well understood proxies – such as pedological or geochemical indicators (Liu et al., 1995; Guo et al., 2001) and malacology (Rousseau and Wu, 1997) – are not necessarily reflected by expected changes in the magnetic susceptibility.

The above-mentioned magnetic enhancement of the studied sequences is mostly the influence of pedogenetic processes (i.e. a China scenario). Thus, it could be expected that the non-linearity of the record with climatic (pedogenetic) development has been probably caused by a post-sedimentary loss of the magnetic signal. We suggest two main reasons for the observed bias between the predicted paleoclimatic development and the recorded magnetic parameters:

(1) Erosion of the humic Ah horizon in the case of PK III
According to the micromorphological studies (see Table 2), the luvisol and overlaying chernozem (PK III) are genetically-independent soils at both sites (proved by the absence of braunlehm plasma in the chernozem horizons). In the case of Zeměchy, they are separated by a thin layer of colluvial sediments (Figs. 2 and 3). These colluvial and/or aeolian sediments are typically present in the PK III of many sites. This documents the higher erosion rate immediately after the climate deterioration at the end of the interglacial. In the case of Zeměchy, the colluvial layer (Z13) contains a small amount (up to 3%) of weak decomposed organic detritus, which might represent the rest of the reworked humic topsoil. Rock-magnetic studies of the Holocene luvisol from the loess area (e.g. Jordanova et al., 2013; Huang et al., 2011) suggest a high concentration of pedogenetic ferrimagnets, as in the humic Ah horizon and in the upper part of the Bt horizon, whereas middle and lower parts of the Bt horizon show significant lower magnetic enhancement. In contrast, geochemical parameters (such as CEC or the ratio of immobile/mobile elements) yield relatively comparable values in both the

Bt and Ah horizons (Duan et al., 2002). Having an Ah horizon missing would therefore be more relevant for an interpretation based on magnetic rather than geochemical proxies.

(2) Leaching and transformation of ferrimagnets in the Bt horizon
As mentioned above, an increase of percolating water could have a major impact on the concentration of ultrafine magnetic particles. Direct leaching can influence magnetic particles, mostly fine-grained, as is suggested by the negative correlation between ARM and the Sr/Ca ratio. Another reason for the χ decrease could be excessive moisture during the Interglacial (as supported by geochemical proxies) that could have caused a transformation of magnetite/maghemite into goethite/limonite (Liu et al., 2007, 2012). This interpretation is supported by the occurrence of goethite in the luvisol as proven by χ–T measurements.

The proxies of chemical weathering (particularly Rb/Sr ratio, CIA and CEC) of the studied profiles (Fig. 3) show the highest values in interglacial soil and they are also enriched in the interstadial paleosol layers relative to the loess (including the PK I soil in Zeměchy which did not even register in the magnetic signal at all, probably due to the erosion of the upper part of the soil horizon, enriched by magnetic minerals — similar to that in the interglacial luvisols). The Rb/Sr ratio and CIA have been used to reflect paleoclimate changes in the loess of north-central China (Chen et al., 1999; Ding et al., 2001), the Danube region (Buggle et al., 2011; Bokhorst et al., 2009; Varga et al., 2011; Újvári et al., 2014) and Germany (Fischer et al., 2012) — in terms of their systematic variations in loess/paleosol sequences. Furthermore, in the Bohemian and Moravian loess/paleosol sequences these proxies reveal in an exemplary way the degree of chemical weathering and reflect the general course of climate development of the Upper Pleistocene — as is apparent through the correlation with deep sea oxygen isotopic records indicating the global climate changes (Lisiecki and Raymo, 2005; Fig. 8).

Despite the correlation between the Rb/Sr ratio and the global benthic $\delta^{18}O$ record being based on a visual comparison, we have several reasons to consider this correlation a reliable one: many lines of evidence indicate that the pedocomplexes PK III and PK II can be assigned to marine oxygen isotope stages MIS 5e–5a and PK I to MIS 3 (e.g. Kukla, 1975; Musson and Wintle, 1994; Zöller et al., 1994; Forster et al., 1996; Frechen et al., 1999; Fuchs et al., 2013). The well-determined pedostratigraphy of the last climatic cycle was mostly established based on detailed studies of the profile Dolní Věstonice (DV) brickyard and thus the successful correlation of the χ and litho-pedostratigraphical records of DV with the studied sections (Fig. 5) have allowed us to compare the obtained proxy records with the global climatic scale. This kind of correlation is supported by OSL dates adopted from DV which in turn can be correlated unambiguously to the sections under study. Yet, it is to be remembered that, in general, an accurate synchronization of land and ocean records and reliable stratigraphic correlation between them is still an unresolved task for several reasons. This also applied to LPSs, where the sedimentary record is often incomplete (as discussed above) and the absolute chronology, based on the OSL dating, is uncertain to often ~5–10 ky. Moreover, as suggested by studies comparing biological and geochemical proxy-records of well-dated varved lake sediments or speleothems with benthic and Greenland $\delta^{18}O$, synchronity often cannot be proven, and these records may not be exactly synchronous (e.g. Sánchez-Goñi et al., 1999; Shackleton et al., 2003; Drysdale et al., 2007; Boch et al., 2011).

In this study we used a simplistic explanation for the correlation between peaks and troughs of the Rb/Sr ratio on one hand and the global benthic $\delta^{18}O$ record on the other hand: benthic foraminiferal marine $\delta^{18}O$ records are directly linked to deep sea water temperature and to global ice volume. Such records may be used as a proxy for the water content of the atmosphere and consequently also for the mainly precipitation controlled climatic humidity on continents. The humidity, in turn, controls weathering and soil formation and therefore the geochemical and magnetic proxies seems to be generally in-phase with the $\delta^{18}O$ records. This assumption has been the basis for a number of studies which have demonstrated a close correspondence of magnetic and geochemical variations within LPSs to signatures of past global climatic change derived from oceanic benthic $\delta^{18}O$ records (e.g. Heller and Liu, 1984; Kukla, 1975; Kukla et al., 1988; Bloemendal et al., 1995; Chen et al., 1997; Heslop et al., 2000; Yang et al., 2004; Buggle et al., 2009; Basarin et al., 2014).

5.2. Paleoenvironmental implications and paleogeographic context

The rock-magnetic and geochemical records (Fig. 3) visually divide both studied sequences into two parts: (1) the lower parts (corresponding to MIS 5), with higher values and fluctuations; and (2) the upper part (interpreted as MIS 4-2), characterized by their lower values and a trend of further decreases towards the top of the sequences. The records reflect the main features of climate development and allow us to correlate these individual profiles.

Sea surface temperature reconstruction for the North Atlantic (Imbrie et al., 1992) or globally benthic $\delta^{18}O$ records (Lisiecki and Raymo, 2005; see also Fig. 8), and also proxy data from Greenland (North Greenland Ice Core Project (NGRIP) Members, 2004), indicates that the beginning of the Weichselian (MIS 5d–a) was on average not dramatically cooler than the Eemian interglacial (MIS 5e). However, this period was characterized by large-amplitude oscillations and with the abrupt appearance of rather drier conditions, which is also widely suggested by the regional biological evidence (Ložek, 1964; Woillard, 1978; Urban, 1984; Behre, 1989; Guiot, 1990; Kühl et al., 2007) and geochemical and sedimentological records (Caspers and Freund, 2001; Sirocko et al., 2005; Rousseau et al., 2006; Drysdale et al., 2007) from the land. In Europe, climate desiccation was most pronounced in continental areas, whereas the region influenced by the Atlantic was considerably wetter (Kühl et al., 2007). This is also reflected in the (paleo) pedological evidence: the east central European soils generally indicate somewhat drier and therefore less favorable conditions for leaching than more westerly areas (Haesaerts and Mestdagh, 2000). Along a transect from northwestern Europe towards the east and south-east, redoximorphic features and pseudogley characteristics in soils (known, for example, from Gleyic Chernozems and Gleyic or Stagnic Phaeozems) decrease and vanish in the Pannonian Basin. Typical steppe chernozem/kastanozem soils become predominant (Eckmeier et al., 2007; Marković et al., 2008; Gozhik et al., 2013).

Our studied LPSs are situated in eastern central Europe in a transitional area of high value for reconstructing past regional atmospheric conditions and their interaction with North Atlantic/continental climate systems (e.g. Kukla, 1977; Rousseau et al., 2013).

In this respect, the situation in the Central Bohemian section Zeměchy shows aspects of the Atlantic part of Europe more clearly than the South Moravian Dobšice section situated on the northwestern edge of the Pannonian Basin. The Pannonian Basin is marked in the Upper Pleistocene by continuous dry continental climate conditions, under the effects of a temperate sub-Mediterranean climatic influence (Sümegi and Krolopp, 2002).

The differences in the proxy records between the two sites can be clearly linked to geographical differences influencing chemical weathering processes. For example, whereas in Zeměchy all interstadial soils show (from the micromorphological point of view) quite pronounced pseudogley features and recalcification processes, in Dobšice these features are only very weakly developed (see Table 2). Regarding the rock-magnetic and geochemical results, the most pronounced differences were found in the lower Weichselian parts of the pedosedimentary records.

A lower Sr/Ca ratio, as well as almost featureless variations of Rb/Sr or CEC in the PK II of Dobšice, indicates weaker pedogenic carbonate dissolution and feldspar weathering, as well as weaker formation/

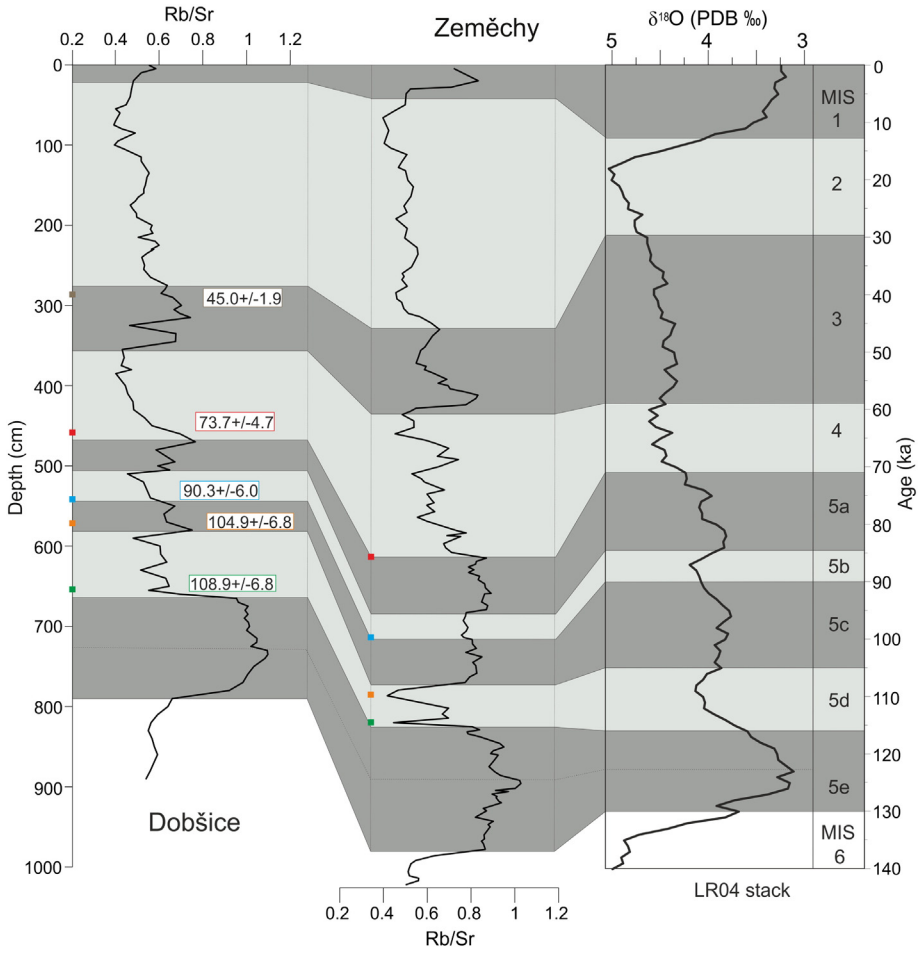

Fig. 8. Correlation of the Rb/Sr ratios from Dobšice and Zeměchy to the $\delta^{18}O$ record from the deep sea (LR04; Lisiecki and Raymo, 2005). OSL dates (color boxes) adopted from Fig. 4. (For interpretation of the references to color in this figure legend, the reader is referred to the web version of this article.)

transformation of clay minerals in the Moravian section compared to the Bohemian (Fig. 3). A stronger leaching process in Zeměchy is also supported by lower concentrations of Ca and Sr, indicating a considerable higher variability of these elements, a leaching of upper soil layers, and the formation of Ca-enriched horizons. In total, the relative concentrations of fine grained ferromagnets (χfd, ARM) are markedly higher in Zeměchy than in Dobšice, suggesting that pedogenic processes were more intense and/or bacterial production of magnetite (and/or maghemite) was higher. An increase in moisture has been found to be the key factor for stronger magnetic enhancement of many LPSs, as long as the soils are not affected by water-logging (e.g. Buggle et al., 2013a).

Regarding the geographical location of the studied sections, we suggest that the pronounced differences in chemical weathering and magnetic enhancement of the pedosedimentary sequences may be caused by differences in the amount of percolating water, which may be representative of the precipitation. Drier conditions during the Pleistocene, or at least a different seasonality with a pronounced dry season in the Pannonian Basin compared to other European regions, are widely supported by geochemical, pedological and biological approaches (Allen et al., 1999; Buggle et al., 2009, 2013b; Bokhorst et al., 2009; Zech et al., 2013; Újvári et al., 2014).

Our findings suggest that the transitional zone between the two climate regions, or the two different modes, of the Upper Pleistocene climate in central Europe could be quite narrow. Yet, to confirm this hypothesis, further data – in a transect from sites towards the Atlantic Ocean and further into the continental area – are required, either confirming or challenging the presented findings.

6. Conclusions

Loess/paleosols sequences from central Bohemia and south Moravia (eastern-central Europe) provide a suitable archive for a detailed study of the Upper Pleistocene paleoenvironmental changes in a transition zone between the oceanic and continental climate regimes. Using a multi-proxy approach combining sedimentological, rock-magnetic, geochemical and micromorphological methods — we demonstrate that:

(i) The stratigraphy of the studied sections conforms well to the general pattern of the Upper Pleistocene loess/paleosol successions in the relatively dry loess of central Europe. This is demonstrated by the correlation of the magnetic susceptibility record with the well-investigated section at Dolní Věstonice.

(ii) The magnetic signal of the studied sediments is dominated by the presence of fine grained (SP/SD) magnetite, and partially maghemite. The origin of these minerals in soils and loess is probably mainly pedogenetic. This is in accordance with the "China scenario" model of magnetic enhancement by pedogenesis.

(iii) Compared to chernozems, the distribution of magnetic minerals throughout the interglacial (MIS 5e) luvisol (para-brown soil) and interstadial (MIS 3) cambisol is nonlinear, probably due to

the erosion of the Ah horizons and later leaching of fine-grained magnetic grains. Rock-magnetic properties are thus not always a reliable proxy for deciphering paleoclimatic changes in the study area for the complete last climate cycle.

By contrast, proxies of chemical weathering – such as Rb/Sr ratio, CIA or CEC – reflect the main pattern of climate development through the whole Upper Pleistocene surprisingly well and they promise to provide a suitable correlation tool on the super-regional, or even hemispheric, scale.

(iv) The multi-proxy study reported in this paper revealed well-pronounced interegional differences in the leaching intensity of the loess/paleosols sequences. This suggests more humid conditions in central Bohemia than in south Moravia during the Upper Pleistocene, most probably due to the Moravian site's position close to the Pannonian Basin, where drier conditions during the Pleistocene predominated (in comparison to areas more to the north and west that are more exposed to the North Atlantic Ocean).

Acknowledgments

This research was supported by the Deutscher Akademischer Austausch Dienst (DAAD), Project no. 13-08169S of the Grant Agency of the Czech Republic (GAČR) and internal program of Institute of Geology ASCR in Prague RVO 67985831. We also thank AGICO Brno, s.r.o (especially Martin Chadima) for providing access to measuring equipment. Daniela Valentová is acknowledged for performing the grain-size analysis and Steve Ridgill for improving our English. Christian Zeeden and Gábor Újvári are thanked for their constructive comments, which helped to improve the manuscript enormously.

References

Allen, J.R.M., Brandt, U., Brauer, A., Hubberten, H.W., Huntley, B., Keller, J., Kraml, M., Mackensen, A., Mingram, J., Negendank, J.F.W., Nowaczyk, N.R., Oberhänsli, H., Watts, W.A., Wulf, S., Zolitschka, B., 1999. Rapid environmental changes in southern Europe during the last glacial period. Nature 400, 740–743.

Antoine, P., Rousseau, Moine, O., Rousseau, D.D., Kunesch, S., Hatté, C., Lang, A., Zöller, L., 2009. Evidence of rapid and cyclic eolian deposition during the Last Glacial in European loess series (Loess Events): the high-resolution records from Nussloch (Germany). Quat. Sci. Rev. 28, 2955e2973.

Antoine, A., Rousseau, D.-D., Moine, O., Kunesch, S., Hatté, C., Lang, A., 2010. Rapid and cyclic aeolian deposition during the Last Glacial in European loess: a high-resolution record from Nussloch. Quat. Sci. Rev. 28, 2955–2973.

Antoine, P., Rousseau, D.-D., Degeai, J.P., Moine, O., Lagroix, F., Kreutzer, S., Fuchs, M., Hatté, C., Gauthier, C., Svoboda, J., Lisá, L., 2013. High-resolution record of the environmental response to climatic variations during the Last Interglacial–Glacial cycle in Central Europe: the loess–paleosol sequence of Dolní Věstonice (Czech Republic). Quat. Sci. Rev. 67, 17–38.

Bábek, O., Chlachula, J., Grygar, J., 2011. Non-magnetic indicators of pedogenesis r elated to loess magnetic enhancement and depletion: examples from the Czech Republic and southern Siberia. Quat. Sci. Rev. 30, 967–979.

Basarin, B., Buggle, B., Hambach, U., Marković, S.B., Dhand, K.O.H., Kovačević, A., Lukić, T., 2014. Time-scale and astronomical forcing of Serbian loess–palaeosol sequences. Glob. Planet. Chang. 122, 82–96. http://dx.doi.org/10.1016/j.gloplacha.2014.08.007.

Baumgart, P., Hambach, U., Meszner, S., Faust, D., 2013. An environmental magnetic fingerprint of periglacial loess: records of Late Pleistocene loess paleosol sequences from Eastern Germany. Quat. Int. 296, 82–93.

Begét, J.E., Stone, D.B., Hawkins, D.B., 1990. Paleoclimatic forcing of magnetic susceptibility variations in Alaska loess during the late Quaternary. Geology 18, 40–43.

Behre, K.E., 1989. Biostratigraphy of the last glacial period in Europe. Quat. Sci. Rev. 8, 25–44.

Bloemendal, J., Liu, X.M., Rolph, T.C., 1995. Correlation of the magnetic susceptibility stratigraphy of Chinese loess and the marine oxygen isotope record, chronological and palaeoclimatic implications. Earth Planet. Sci. Lett. 131, 371–380.

Bloemendal, J., Liu, X.M., Sun, Y.B., Li, N.N., 2008. An assessment of magnetic and geochemical indicators of weathering and pedogenesis at two contrasting sites on the Chinese Loess plateau. Palaeogeogr. Palaeoclimatol. Palaeoecol. 257, 152–168.

Boch, R., Cheng, H., Spötl, C., Edwards, R.L., Wang, X., Häuselmann, P., 2011. NALPS: a precisely dated European climate record 120–60 ka. Clim. Past 7 (4), 1247–1259.

Bogucki, A., Maruszczak, H., Nawrocki, J., 1995. Stratigraphic and paleogeographic interpretation of analysis results of magnetic susceptibility of loesses at Bojanice NW Ukraine. Annales Universitatis Mariae Curie Sklodowskao B: Geographia, Geologia, Mineralogia et Petrographia 50, pp. 51–64.

Bokhorst, M.P., Beets, C.J., Marković, S.B., Gerasimenko, N.P., Matviishina, Z.N., 2009. Pedochemical climate proxies in Late Pleistocene Serbiane Ukranian loess sequences. Quat. Int. 198, 113–123.

Bronger, A., Heinkele, T., 1989. Paleosol sequences as witnesses of Pleistocene climatic history. Catena Suppl. 16, 163–186.

Buggle, B., Glaser, B., Zöller, L., Hambach, U., Marković, S., Glaser, I., Gerasimenko, N., 2008. Geochemical characterization and origin of Southeastern and Eastern European loesses (Serbia, Romania, Ukraine). Quat. Sci. Rev. 27, 1058–1075.

Buggle, B., Hambach, U., Glaser, B., Gerasimenko, N., Markovic, S., Glaser, I., Zöller, L., 2009. Stratigraphy, and spatial and temporal paleoclimatic trends in Southeastern/Eastern European loess–paleosol sequences. Quat. Int. 196, 186–206.

Buggle, B., Glaser, B., Hambach, U., Gerasimenko, N., Marković, S., 2011. An evaluation of geochemical weathering indices in loess–paleosol studies. Quat. Int. 240, 12–21.

Buggle, B., Hambach, U., Müller, K., Zöller, L., Markovic, S.B., Glaser, B., 2013a. Iron mineralogical proxies and Quaternary climate change in SE-Central European loess–paleosol sequences. Catena 117, 4–22.

Buggle, B., Hambach, U., Kehl, M., Zöller, L., Marković, S.B., Glaser, B., 2013b. The progressive evolution of a continental climate in SE-Central European lowlands during the Middle Pleistocene recorded in loess paleosol sequences. Geology 41, 771–774.

Bullock, P., Federoff, N., Jongerius, A., Stoops, G., Tursina, T., Babel, U., 1985. Handbook for Soil Thin Section Description. Waine Research Publications, Wolverhampton, UK (396 pp.).

Caspers, G., Freund, H., 2001. Vegetation and climate in the Early- and Pleni-Weichselian in northern central Europe. J. Quat. Sci. 16 (1), 31–48.

Chen, F.H., Bloemendal, J., Wang, J.M., Li, J.J., 1997. High-resolution multi-proxy climate records from Chinese loess: evidence for rapid climatic changes over the last 75 kyr. Palaeogeogr. Palaeoclimatol. Palaeoecol. 130, 323–335.

Chen, J., An, Z., Head, J., 1999. Variation of the Rb/Sr ratios in the loess / paleosol sequences of Central China during the last 130,000 years and their implications for monsoon paleoclimatology. Quat. Res. 51, 215–219.

Cílek, V., 1996. Sprašová rokle v Zeměchách u Kralup nad Vltavou. Zpr. geol. Výzk. v Roce 1995. pp. 31–33 (in Czech).

Demek, J., Kukla, J., 1969. Periglazialzone, Löss und Paläolithikum der Tschechoslowakei. Tschechoslowakische Akademie der Wissenschaften, Geographisches Institut, Brno (158 pp.).

Derbyshire, E., Billard, A., Van Vliet-Lanoë, B., Lautridou, J.-P., Cremaschi, M., 1988. Loess and palaeoenvironment: some results of a European joint programme of research. J. Quat. Sci. 3, 147–169.

Ding, Z.L., Sun, J.M., Yang, S.L., Liu, T.S., 2001. Geochemistry of the Pliocene red clay formation in the Chinese Loess Plateau and implications for its origin, source provenance and paleoclimatic change. Geochim. Cosmochim. Acta 65 (6), 901–913.

Drysdale, R.N., Zanchetta, G., Hellstrom, J.C., Fallick, A.E., McDonald, J., Cartwright, I., 2007. Stalagmite evidence for the precise timing of North Atlantic cold events during the early last glacial. Geology 35, 77–85.

Duan, L., Hao, J., Xie, S., Zhou, Z., Ye, X., 2002. Determining weathering rates of soils in China. Geoderma 110, 205–225.

Eckmeier, E., Gerlach, R., Gehrt, E., Schmidt, M.W.I., 2007. Pedogenesis of chernozems in Central Europe — a review. Geoderma 139, 288–299.

Evans, M.E., Heller, F., 2003. Environmental Magnetism: Principles and Applications of Enviromagnetics. Academic Press, New York (299 pp.).

Fink, J., Kukla, G., 1977. Pleistocene climates in central Europe: at least 17 interglacials after the Oiduvai Event. Quat. Res. 7, 363–371.

Fischer, P., Hilgers, A., Protze, J., Kels, H., Lehmkuhl, F., Gerlach, R., 2012. Formation and geochronology of Last Interglacial to Lower Weichselian loess/palaeosol sequences — case studies from the Lower Rhine Embayment, Germany. E & G Quat. Sci. J. 61, 48–63.

Fitzsimmons, K.E., Marković, S.B., Hambach, U., 2012. Pleistocene environmental dynamics recorded in the loess of the middle and lower Danube Basin. Quat. Sci. Rev. 41, 104–118.

Fontes, M.P.F., Weed, S.B., 1991. Iron Oxides in Selected Brazilian Oxisols: I. Mineralogy. Soil Sci. Soc. Am. J. 55, 1143–1149.

Forster, T., Evans, M.E., Havlíček, P., Heller, F., 1996. Loess in the Czech Republic: magnetic properties and paleoclimate. Stud. Geophys. Geod. 40, 243–261.

Frechen, M., 2011. Loess in Europe. E & G Quat. Sci. J. 60 (1), 3–5.

Frechen, M., Zander, A., Cilek, V., Ložek, V., 1999. Loess chronology of the Last Interglacial/Glacial cycle in Bohemia and Moravia, Czech Republic. Quat. Sci. Rev. 18, 1467–1493.

Fuchs, M., Kreutzer, S., Rousseau, D.-D., Antoine, P., Hatte, C., Lagroix, F., Moine, O., Gauthier, C., Svoboda, J., Lisa, L., 2013. The loess sequence of Dolni Vestonice, Czech Republic: a new OSL based chronology of the Last Climatic Cycle. Boreas 42, 664–677.

Gallet, S., Jahn, B.M., Torii, M., 1996. Geochemical characterization of the Luochuan loess–palaeosol sequence, China, and paaleoclimatic implications. Chem. Geol. 133, 67–88.

Gocke, M., Hambach, U., Eckmeier, E., Schwark, L., Zöller, L., Fuchs, M., Löscher, M., Wiesenberg, G.L.B., 2014. Introducing an improved multi-proxy approach for paleoenvironmental reconstruction of loess–paleosol archives applied on the Late Pleistocene Nussloch sequence (SW Germany). Palaeogeogr. Palaeoclimatol. Palaeoecol. 410, 300–315.

Gozhik, P., Komar, M., Łanczont, M., Fedorowicz, S., Bogucki, A., Mroczek, P., Prylypko, S., Kusiak, J., 2013. Paleoenvironmental history of the Middle Dnieper Area from the Dnieper to Weichselian Glaciation: a case study of the Maksymivka loess profile. Quat. Int. 334–335, 94–111.

Grygar, T., Kadlec, J., Žigová, A., Mihaljevič, M., Nekutová, T., Lojka, R., Světlík, I., 2009. Chemostratigraphic correlation of sediments containing expandable clay minerals based on ion exchange with Cu(II) complex with triethylenetetramine. Clay Clay Miner. 57, 168–182.

Guiot, J., 1990. Methodology of the last climatic cycle reconstruction in France from pollen data. Palaeogeogr. Palaeoclimatol. Palaeoecol. 80, 49–69.
Guo, B., Zhu, R.X., Roberts, A.P., Florindo, F., 2001. Lack of correlation between paleoprecipitation and magnetic susceptibility of Chinese loess/palaeosol sequences. Geophys. Res. Lett. 28, 4259–4262.
Haesaerts, P., Mestdagh, H., 2000. Pedosedimentary evolution of the last interglacial and early glacial sequence in the European loess belt from Belgium to central Russia. Neth. J. Geosci. 79, 313–324.
Hambach, U., 2010. Paleoclimatic and stratigraphic implications of high resolution magnetic susceptibility logging of Würmian Loess at the Upper Paleolithic KremseWachtberg Site. In: Neugebauer-Maresch, C., Owen, L.R. (Eds.), New Aspects of the Central and Eastern European Upper Palaeolithic — Methods, Chronology, Technology and Subsistence. Proceedings of the Prehistoric Commission of the Austrian Academy of Sciences. Vienna, pp. 295–304.
Han, J., Lu, H., Wu, N., Guo, Z., 1996. Magnetic susceptibility of modern soils in China and climate conditions. Stud. Geophys. Geod. 40, 262–275.
Hatté, C., Pessenda, L.C.R., Lang, A., Paterne, M., 2001. Development of an accurate and reliable ^{14}C chronology for loess sequences: application to the loess sequence of Nussloch (Rhine valley, Germany). Radiocarbon 43, 611–618.
Havlíček, P., Smolíková, L., 1995. Vývoj svrchnopleistocenních eolických sedimentů ve Znojmě-Dřevařských závodech. Vest. CGÚ 70/1 pp. 67–74 (in Czech).
Heller, F., Evans, M., 1995. Loess magnetism. Rev. Geophys. 33, 211–240.
Heller, F., Liu, T., 1984. Magnetism of Chinese loess deposits. Geophys. J. R. Astron. Soc. 77, 125–141.
Heller, F., Shen, C.D., Beer, J., Liu, X.M., Liu, T.S., Bronger, A., Suter, M., Bonani, B., 1993. Quantitative estimates of pedogenic ferromagnetic mineral formation in Chinese loess and paleoclimatic implications, Earth Planet. Sci. Lett. 114, 385–390.
Herbauts, J., 1982. Chemical and mineralogical properties of sandy and loamy–sandy ochreous brown earths in relation to incipient podzolization in a brown-podzol evolutive sequence. J. Soil Sci. 33, 743–762.
Heslop, D., Langereis, C.G., Dekkers, M.J., 2000. A new astronomical timescale for the loess deposits of northern China. Earth Planet. Sci. Lett. 184, 125–139.
Horáček, I., Ložek, V., 1988. Paleozoology and Mid-European Quaternary past: scope of the approach and selected results. Rozpr. ČSAV-MPV 94, 1–106.
Hošek, J., Lisá, L., Meszner, S., Knésl, I., 2012. Upper Pleistocene loess/paleosols sequence from Central Bohemia. In: Zöller, L., Peterek, A. (Eds.), From Paleozoic to Quaternary: a field trip from the Franconian Alb to Bohemia. 36. Hauptversammlung der Deutschen Quartärvereinigung DEUQUA, pp. 111–113.
Hošek, J., Pokorný, P., Kubovčík, V., Horáček, I., Žáčková, P., Kadlec, J., Rojik, F., Lisá, L., Bučkuliaková, S., 2014. Late Glacial climatic and environmental changes in Eastern-Central Europe: correlation of multiple biotic and abiotic proxies from the Lake Švarcenberk, Czech Republic. Palaeogeogr. Palaeoclimatol. Palaeoecol. 396, 155–172.
Huang, C., Zhao, W., Liu, F., Tan, W., Koopal, L.K., 2011. Environmental significance of mineral weathering and pedogenesis of loess on the southernmost Loess Plateau, China. Geoderma 163, 219–226.
Hunt, C.P., Banerjee, S.K., Han, J.M., 1995. Rock-magnetic proxies of climate change in the loess–palaeosol sequences of the western Loess Plateau of China. Geophys. J. Int. 123 (1), 232–244.
Imbrie, J., Boyle, E.A., Clemens, S.C., Duffy, A., Howard, W.R., Kukla, G., Kutzbach, J., Martinson, D.G., McIntyre, A., Mix, A.C., Molfino, B., Morley, J.J., Peterson, L.C., Pisias, N.G., Prell, W.L., Raymo, M.E., Shackleton, N.J., Toggweiler, J.R., 1992. On the structure and origin of major glaciation cycles. 1. Linear responses to Milankovitch forcing. Paleoceanography 7, 701–738.
Jary, Z., Ciszek, D., 2013. Late Pleistocene loess–palaeosol sequences in Poland and western Ukraine. Quat. Int. 296, 37–50.
Jordanova, D., Grygar, T., Jordanova, N., Petrov, P., 2011. Palaeoclimatic significance of hematite/goethite ratio in Bulgarian loess–palaeosol sediments deduced by DRS and rock magnetic measurements. In: Petrovsky, E., Ivers, D., Harinarayana, T., Herrero-Bervera, E. (Eds.), The Earth's Magnetic Interior. IAGA Special Sopron Book Series. Springer-Verlag, Berlin.
Jordanova, N., Jordanova, D., Liu, Q., Hu, P., Petrov, P., Petrovský, E., 2013. Soil formation and mineralogy of a Rhodic Luvisol — insights from magnetic and geochemical studies. Global Planet. Chang. 110, 397–413.
Kadereit, A., Kind, C.-J., Wagner, G.A., 2013. The chronological position of the Lohne Soil in the Nussloch loess section e re-evaluation for a European loess-marker horizon. Quat. Sci. Rev. 59, 67–86.
Kemp, R., 2001. Pedogenic modification of loess: significance for palaeoclimatic reconstructions. Earth Sci. Rev. 54, 145–156.
Klíma, B., Kukla, G., Ložek, V., Vries, H., 1962. Stratigraphie des Pleistozäns und Alter des paläolithischen Rastplatzes in der Ziegelei von Dolní Věstonice (Unter-Wisternitz). Anthropozoikum 11, 93–145.
Kravchinsky, V.A., Zykina, V.S., Zykin, V.S., 2008. Magnetic indicator of global paleoclimate cycles in Siberian loess–paleosol sequences. Earth Planet. Sci. Lett. 265, 498–514.
Kühl, N., Litt, T., Schölzel, C., Hense, A., 2007. Eemian and Early Weichselian temperature and precipitation variability in northern Germany. Quat. Sci. Rev. 26, 3311–3317.
Kukla, G.J., 1961. Lithologische Leithorizonte der tschechoslowakischen Lössprofile. Věstník 36, 369–372.
Kukla, G., 1975. Loess stratigraphy of Central Europe. In: Butzer, K.W., Isaac, G.L. (Eds.), After the Australopithecines. Mouton Publishers, The Hague, pp. 99–188.
Kukla, G., 1977. Pleistocene land-sea correlations I. Europe. Earth-Sci. Rev. 13, 307–374.
Kukla, G.J., Heller, F., Liu, X.M., Xu, T.C., Liu, T.S., An, Z.S., 1988. Pleistocene climates in China dated by magnetic susceptibility. Geology 16, 811–814.
Kukla, G., Cílek, V., 1996. Plio-Pleistocene megacycles: record of climate and tectonics. Palaeogeogr. Palaeoclimatol. Palaeoecol. 120, 171–194.
Lang, A., Hatté, C., Rousseau, D.-D., Antoine, P., Fontugne, M., Zöller, L., Hambach, U., 2003. High-resolution chronologies for loess: comparing AMS 14C and optical dating results. Quat. Sci. Rev. 22, 953–959.
Li, G., Chen, J., Chen, Y., Yang, J., Ji, J., Liu, L., 2007. Dolomite as a tracer for the source regions of Asian dust. J. Geophys. Res. 112, D17201. http://dx.doi.org/10.1029/2006JD007924.
Lisá, L., Hošek, J., Grygar, T., Bajer, A., Vandenberghe, D., 2014. Geoarchaeology of Upper Paleolithic loess sites located within transect through Moravian valleys, Czech Republic. Quat. Int. 351, 25–37. http://dx.doi.org/10.1016/j.quaint.2013.08.058.
Lisiecki, L.E., Raymo, M.E., 2005. A Pliocene–Pleistocene stack of 57 globally distributed benthic d ^{18}O records. Paleoceanography 20, 1–17.
Liu, X.M., Rolph, T., Bloemendal, J., Shaw, J., Liu, T.S., 1995. Quantitative estimates of paleoprecipitation at Xifeng, in the Loess Plateau of China. Palaeogeogr. Palaeoclimatol. Palaeoecol. 13, 243–248.
Liu, Q., Deng, C., Yu, Y., Torrent, J., Jackson, M.J., Banerjee, S.K., Zhu, R., 2005. Temperature dependence of magnetic susceptibility in an argon environment: implications for pedogenesis of Chinese loess/paleosols. Geophys. J. Int. 161, 102–112.
Liu, Q., Deng, C., Torrent, J., Zhu, R.X., 2007. Review of recent developments in mineral magnetism of the Chinese loess. Quat. Sci. Rev. 26, 368–385.
Liu, Q., Roberts, A.P., Larrasoaña, J.C., Banerjee, S.K., Guyodo, Y., Tauxe, L., Oldfield, F., 2012. Environmental magnetism: principles and applications. Rev. Geophys. 50, RG4002. http://dx.doi.org/10.1029/2012RG000393.
Ložek, V., 1964. Quartärmollusken der Tschechoslowakei. Rozp. Ú.ú. geol., Praha 31 (374 pp.).
Ložek, V., 1968. Mittel- und jungpleistozäne Löss Serien in der Tschechoslowakei und ihre Bedeutung für die Löss-Stratigraphie Mitteleuropas. INQUA-Report of the VIth International Congress on Quaternary-Warsaw, pp. 525–549.
Ložek, V., 1995. Sprašová rokle u Zeměch. 15/1. Nika Praha, pp. 30–31 (in Czech).
Maher, B.A., 1986. Characterisation of soils by mineral magnetic measurements. Phys. Earth Planet. Inter. 42, 76–92.
Maher, B.A., 1998. Magnetic properties of modern soils and Quaternary loessic paleosols: paleoclimatic implications. Palaeogeogr. Palaeoclimatol. Palaeoecol. 137, 25–54.
Maher, B.A., Alekseev, A., Alekseeva, T., 2003. Magnetic mineralogy of soils across the Russian Steppe: climatic dependence of pedogenic magnetite formation. Paleogeography Paleoclimatololy Paleoecology 201, 321–341.
Marković, S., Oches, E., Sumegi, P., Jovanovic, M., Gaudenyi, T., 2006. An introduction to the Upper and Middle Pleistocene loess–paleosol sequences of Ruma section (Vojvodina, Yugoslavia). Quat. Int. 149, 80–86.
Marković, S.B., Bokhorst, M.P., Vandenberghe, J., Mc Coy, W.D., Oches, E.A., Hambach, U., 2008. Late Pleistocene loess–paleosol sequences in the Vojvodina region, north Serbia. J. Quat. Sci. 23, 73–84.
Marković, S.B., Hambach, U., Catto, N., Jovanović, M., Buggle, B., Machalett, B., Zöller, L., Glaser, B., Frechen, M., 2009. Middle and Late Pleistocene loess sequences at Batajnica, Vojvodina, Serbia. Quat. Int. 198, 255–266.
Meier, L.P., Kahr, G., 1999. Determination of the cation exchange capacity (CEC) of clay minerals using the complexes of copper(II) ion with triethylenetetramine and tetraethylenepentamine. Clay Clay Miner. 47, 386–388.
Muhs, D.R., 2013. The geologic records of dust in the Quaternary. Aeolian Res. 9, 3–48.
Muhs, D.R., Bettis III, E.A., Been, J., McGeehin, J., 2001. Impact of climate and parent material on chemical weathering in loess-derived soils of the Mississippi River Valley. Soil Sci. Soc. Am. J. 65, 1761–1777.
Musson, F.M., Wintle, A.G., 1994. Luminescence dating of the loess profile at Dolní Věstonice, Czech Republic. Quat. Sci. Rev. 13, 411–416.
Nawrocki, J., Wojcik, A., Bogucki, A., 1996. The magnetic susceptibility record in the Polish and western Ukrainian loess-palaeosol sequences conditioned by palaeoclimate. Boreas 25, 161–169.
Nesbitt, H.W., Markovics, G., Price, R.C., 1980. Chemical processes affecting alkalis and alkaline earths during continental weathering. Geochim. Cosmochim. Acta 44, 1659–1666.
Nesbitt, H.W., Young, G.M., 1982. Early Proterozoic climates and plate motions inferred from major element chemistry of lutites. Nature 299, 715–717.
Nesbitt, H.W., Young, G.M., McLennan, S.M., Keays, R.R., 1996. Effects of chemical weathering and sorting on the petrogenesis of siliciclastic sediments, with implications for provenance studies. J. Geol. 104, 525–542.
North Greenland Ice Core Project (NGRIP) Members, 2004. High-resolution record of Northern Hemisphere climate extending into the last interglacial period. Nature 431, 147–151.
Oches, E.A., Banerjee, K., 1996. Rock-magnetic proxies of climate change from loess–paleosol sediments of the Czech Republic. Stud. Geophys. Geod. 40 (3), 287–300.
Oldfield, F., 2007. Sources of fine-grained magnetic minerals in sediments: a problem revisited. The Holocene 17, 1265–1271.
Panaiotu, C.G., Panaiotu, E.C., Grama, A., Necula, C., 2001. Paleoclimatic record from a loess–paleosol profile in southeastern Romania. Phys. Chem. Earth 26, 893–898.
Pécsi, M., 1990. Loess is not just the accumulation of dust. Quat. Int. 7, 1–21.
Perel'man, A., 1977. Geochemistry of Elements in the Supergene Zone. Keterpress Enterprises, Jerusalem (266 pp.).
Pye, K., 1987. Aeolian Dust and Dust Deposit. Academic Press, London (334 pp.).
Rivas, J., Ortega, B., Sedov, S., Solleiro, E., Sychera, S., 2006. Rock Magnetism & pedogenetic processes in Luvisol profiles: Examples from Central Russia & Central Mexico. Quanternary International. 156–157, 212–223.
Rolf, C., Hambach, U., Novothny, A., Horváth, E., Schnepp, E., 2014. Dating of a Last Glacial loess sequence by relative geomagnetic palaeointensity: a case study from the Middle Danube Basin (Sütto, Hungary). Quat. Int. 319, 99–108.
Rousseau, D.-D., Wu, N.Q., 1997. A new molluscan record of the monsoon variability over the past 130,000 yr in the Luochuan loess sequence, China. Geology 25, 275–278.

Rousseau, D.-D., Hatté, C., Guiot, J., Duzer, D., Schevin, P., Kukla, G., 2006. Reconstruction of the Grande Pile Eemian using inverse modeling of biomes and d13C. Quat. Sci. Rev. 25, 2806–2819.
Rousseau, D.-D., Ghil, M., Kukla, G., Sima, A., Antoine, P., Fuchs, M., Hatté, C., Debret, M., Moine, O., 2013. Major dust events in Europe during marine isotope stage 5 (130–74 ka): a climatic interpretation of the "markers". Clim. Past 9, 2213–2230.
Sánchez-Goñi, M.F., Eynaud, F., Turon, J.L., Shackleton, N.J., 1999. High resolution palynological record off the Iberian margin: direct land–sea correlation for the last interglacial complex. Earth Planet. Sci. Lett. 171, 123–137.
Schatz, A.-K., Scholten, T., Kühn, P., 2014. Paleoclimate and weathering of the Tokaj (NE Hungary) loess–paleosol sequence: a comparison of geochemical weathering indices and paleoclimate parameters. Clim. Past Discuss. 10, 469–507. http://dx.doi.org/10.5194/cpd-10-469-2014.
Shackleton, N.J., Sánchez-Goñi, M.F., Pailler, D., Lancelot, Y., 2003. Marine isotope substage 5e and the Eemian interglacial. Glob. Planet. Chang. 36 (3), 151–155.
Sirocko, F., Seelos, K., Schaber, K., Rein, B., Dreher, F., Diehl, M., Lèhne, R., Jäger, K., Krbetschek, M., Degering, D., 2005. A Late Eemian Aridity Pulse in central Europe during the last glacial inception. Nature 436, 833–836.
Smolíková, L., 1982. Fossil soils in loess series. Stud. Geophys. 80, 107–133.
Stoops, G., 2003. Guidelines for Analysis and Description of Soil and Regolith Thin Sections. Soil Science Society of America, Madison, Wisconsin (348 pp.).
Stoops, G., Marcelino, V., Mees, F., 2010. Interpretation of Micromorphological Features of Soils and Regoliths. Elseiver.
Sümegi, P., Krolopp, E., 2002. Quartermalacological analyses for modeling of the Upper Weichselian paleoenvironmental changes in the Carpathian basin. Quat. Int. 91, 53–63.
Sun, W.W., Banerjee, S.K., Hunt, C.P., 1995. The role of maghemite in the enhancement of magnetic signal in the Chinese loess–paleosol sequence: an extensive rock magnetic study combined with citrate-bicarbonatedithionite treatment. Earth Planet. Sci. Lett. 133, 493–505.
Svoboda, J., Škrdla, P., Ložek, V., Svobodová, H., Frechen, M., 1996. Predmosti II, excavations 1989–1992. In: Svoboda, J. (Ed.), Paleolithic in the Middle Danube Region. Spisy Archeologického Ústavu AVČR v Brně, Svazek 5, Brno, pp. 147–171.
Taylor, S.N., Lagroix, F., Rousseau, D.D., Antoine, P., 2014. Mineral magnetic characterization of the Upper Pleniglacial Nussloch loess sequence (Germany): an insight into local environmental processes. Geophys. J. Int. 199 (3), 1463–1480.
Thompson, R., Oldfield, F., 1986. Environmental Magnetism. Allen & Unwin Ltd., London (280 pp.).
Torrent, J., Barrón, V., Liu, Q., 2006. Magnetic enhancement is linked to and precedes hematite formation in aerobic soil. Geophys. Res. Lett. 33, L02401. http://dx.doi.org/10.1029/2005GL024818.
Tyráček, J., 1995. Zeměchy — loess gorge. In: Schirmer, W. (Ed.), Quaternary Field Trips in Central Europe, Eastern Alps Traverse. INQUA, Berlin, pp. 84–86.
Újvári, G., Varga, A., Balogh-Brunstad, Z., 2008. Origin, weathering, and geochemical composition of loess in southwestern Hungary. Quat. Res. 69, 421–437.
Újvári, G., Varga, A., Raucsik, B., Kovács, J., 2014. The Paks loess–paleosol sequence: a record of chemical weathering and provenance for the last 800 ka in the mid-Carpathian Basin. Quat. Int. 319, 22–37.
Urban, B., 1984. Palynology of central European loess–soil sequences. In: Pecsi, M. (Ed.), Lithology and Stratigraphy of Loess and Paleosols. Geographical Research Institute. Hungarian Academy of Sciences, Budapest, pp. 229–247.
van Velzen, A.J., Dekkers, M.J., 1999. Low-temperature oxidation of magnetite in loess–paleosol sequences: a correction of rock magnetic parameters. Stud. Geophys. Geod. 43, 357–375.
Vandenberghe, J., 2013. Grain size of fine-grained windblown sediment: a powerful proxy for process identification. Earth Sci. Rev. 121, 18–30.
Varga, A., Újvári, G., Raucsik, B., 2011. Tectonic versus climatic control on the evolution of a loess–paleosol sequence at Beremend, Hungary: an integrated approach based on paleoecological, clay mineralogical, and geochemical data. Quat. Int. 240, 71–86.
Vodyanitskii, Y.N., Vasil'ev, A.A., Gilev, V.Y., 2007. Iron minerals in soils on red earth deposits in the Cis-Ural region. Eurasian Soil Sci. 40, 432–444.
Wang, F., Sun, D., Guo, F., Wang, X., Li, Z., Zhang, Y., Li, B., Wu, S., 2012. Quantitative reconstruction of paleo-temperature and paleo-precipitation of Lingtai profile in Loess Plateau during the past 7 Ma. J. Earth Environ. 3, 781–791.
Woillard, G., 1978. Grand Pile Peat Bog: a continuous pollen record for the last 140 000 years. Quat. Res. 9, 1–21.
Yang, S.Y., Li, C.X., Yang, D.Y., Li, X.S., 2004. Chemical weathering of the loess deposits in the lower Changjiang Valley China, and paleoclimatic implications. Quat. Int. 117, 27–34.
Zander, A., Duller, G.A.T., Wintle, A.G., 2000. Multiple and single aliquot luminescence dating techniques applied to quartz extracted from Middle and Upper Weichselian loess, Zemechy, Czech Republic. J. Quat. Sci. 15, 51–60.
Zech, M., Zech, R., Zech, W., Glaser, B., Brodowski, S., Amelung, W., 2008. Characterisation and palaeoclimate of a loess-like permafrost palaeosol sequence in NE Siberia. Geoderma 143, 281–295.
Zech, R., Zech, M., Marković, S., Hambach, U., Huang, Y., 2013. Humid glacials, arid interglacials? Critical thoughts on pedogenesis and paleoclimate based on multi-proxy analyses of the loess–paleosol sequence Crvenka, Northern Serbia. Palaeogeogr. Palaeoclimatol. Palaeoecol. 387, 165–175.
Zeeden, C., Hambach, U., Steguweit, A., Anghelinu, M., 2010. Loess stratigraphy using palaeomagnetism: application to the Poiana Cireului archaeological site (Romania). Quat. Int. 240, 100–107.
Zeng, Q.Z., Brown, P.H., 2000. Soil potassium mobility and uptake by corn under differential soil moisture regimes. Plant Soil 221, 121–134.
Zhang, W., Yu, L., Lu, M., Zheng, X., Shi, Y., 2007. Magnetic properties and geochemistry of the Xiashu Loess in the present subtropical area of China, and their implications for pedogenic intensity. Earth Planet. Sci. Lett. 260, 86–97.
Zhu, R.X., Shi, C.D., Suchý, V., Zeman, A., Guo, B., Pan, Y.X., 2001. Magnetic properties and paleoclimatic implications of loess–paleosol sequences of Czech Republic. Sci. China Ser. D Earth Sci. 44, 385–394.
Zöller, L., Oches, E.A., McCoy, W.D., 1994. Towards a revised chronostratigraphy of loess in Austria with respect to key sections in the Czech Republic and in Hungary. Quat. Geochronol. (Quat. Sci. Rev.) 13, 465–472.

PŘÍLOHA II

Hošek, J. – Lisá, L. – Petr, L. – Vejrostová, L. – Bajer, A. – Grygar, T.M. – Moska, P. – Gottvald, Z. – Horsák, M.: Middle Pleniglacial pedogenesis on the north-western edge of the Carpathian Basin: a multidisciplinary investigation of the pedo-sedimentary section Bíňa, SW Slovakia. – submitted in Palaeogeography, Palaeoclimatology, Palaeoecology 418, 344-358.

Middle Pleniglacial pedogenesis on the north-western edge of the Carpathian Basin: a multidisciplinary investigation of the Bíňa pedo-sedimentary section, SW Slovakia

Jan Hošek[1,2*], Lenka Lisá[3], Ulrich Hambach[4,5] , Libor Petr[6], Lenka Vejrostová[7], Aleš Bajer[8], Tomáš M. Grygar[9], Piotr Moska[10], Zdeněk Gottvald[8], Michal Horsák[6]

[1]Czech Geological Survey, Klárov 3, Prague 1, Czech Republic
[2]Institute of Geology and Paleontology, Faculty of Science, Charles University in Prague, Albertov 6, Prague 2, Czech Republic
[3]BayCEER & Chair of Geomorphology, University of Bayreuth, 94450 Bayreuth, Germany
[4] Laboratory for Paleoenvironmental Reconstruction, Faculty of Sciences, University of Novi Sad, Trg Dositeja Obradovića 2, 21000 Novi Sad, Serbia
[5]Institute of Geology of Czech Academy of Science, Rozvojová 269, Prague 6, Czech Republic
[6]Department of Botany and Zoology, Faculty of Science, Masaryk University, Kotlářská 2, Brno, Czech Republic
[7]Department of Physical Geography, Faculty of Science, Charles University, Albertov 6, Prague 2, Czech Republic
[8]Faculty of Forestry and Wood Technology, Mendel University in Brno, Brno, Czech Republic
[9]Institute of Inorganic Chemistry of Czech Academy of Science, Řež 1001, Czech Republic
[10]Department of Radioisotopes, Institute of Physics, Silesian University of Technology, GADAM Centre of Excellence, Konarskiego 22B, Gliwice, Poland

**corresponding author*
email: johan.hosek@gmail.com

Abstract

The Middle Pleniglacial on the northern hemisphere is characterized by millennial scale, frequent, and high amplitude environmental climatic shifts. In loess-paleosol sequences (LPSs) the transition from the Lower (MIS 4) to the Middle Pleniglacial (MIS 3) was accompanied by significant erosion events, as recorded in various terrestrial archives across Central Europe. As a result, potentially existing paleosol horizons of the particular period have been widely erased from the (LPSs) and only little is known about pedogenesis in this vast area. This study tries to fill this gap in our knowledge through studying a pedo-sedimentary record from Bíňa, a site situated in a relatively poorly investigated area on the north-western edge of the Carpathian Basin. We investigated a 12 m high and more than 500 m wide outcrop along the Hron River, where a well-structured sequence of fluvio-lacustrine sediments, paleosols, and loess is preserved. The paleoenvironmental development within the studied area is presented and discussed on the basis of soil micromorphology, rock-magnetic and geochemical measurements, grain size analyses, and a malacological record accomplished by luminescence dating. Based on the OSL dating of the central profile, the sequence provides a high resolution record of the time period 60 – 20 ka BP (MIS 4 – MIS 2). The most developed paleosol horizons (Phaeozem and two Bw horizons of Gleyic Cambisols) were dated to the early stage of the MIS 3 (60 – 50 ka BP) and correlated with the Greenland interstadials GI-17/16, GI-14/13 and/or GI-12 (the north-western European interstadials Oerel, Glinde and Moershoofd). The development of the Bw horizon of a Cambisol recorded within the younger loess body was dated to c. 35 ka BP and it probably corresponds to the late MIS 3 intestadials GI-8–5 (Denekamp). The preservation as well as the development of the well-stratified record were closely related to the specific hydro- and geomorphological settings of the paleo-channel structure in which the sequence developed. Although soil development benefited from the specific local settings, we suggest that the recorded paleosols can also be related to the interregional climate differences of the Carpathian Basin: Within the northerly pericarpathian zones, a moister climate predominated during the last Pleniglacial, in contrast to the drier continental areas to the South. Thus, a sharp

climatic boundary existed separating a semi-arid steppe region from a climatic zone under the persistent influence of Atlantic air masses.

keywords: loess/paleosol sequence; Middle Pleniglacial (MIS 3); Pannonian/Carpathian Basin; soil micromorphology; paleomalacology; paleopedology

1. Introduction

As revealed in high-resolution deep sea and ice core oxygen isotope records, the Middle Pleniglacial (MPG; MIS 3; ~ 60-30 ka BP) is characterized by frequent and abrupt climatic changes of high amplitude, represented by repetitive fluctuations in climate systems (Johnsen et al., 1992; Dansgaard et al., 1993; Huber et al., 2006). In terrestrial settings these climatic shifts evoked distinct interactions within and between the different components of terrestrial environments, including vegetation as well as erosion and pedogenesis dynamics (Sirocko et al., 2016). Loess/paleosol sequences (LPSs) and colluvial sediments both provide an opportunity to study the intensity and rates of pedogenesis during the last glacial cycle. Different soil types preserved in these sequences can be used as indicators of past environmental conditions. Detailed micromorphological-sedimentological studies, supported by environmental magnetism and geochemical approaches, can contribute to an improved understanding of past climate fingerprints in loess and corresponding environments (e.g. Kemp et al., 1998; Kühn et al., 2006; Kühn et al., 2013, Lisá et al., 2014, Hošek et al., 2015; Hošek et al., 2016).

Paleosols of the Middle Pleniglacial are considered as marker horizons in European loess and are fundamental elements in understanding the terrestrial environment during the Last Glacial period (Kukla, 1977; Fitzsimmons et al., 2012). However, as during the Last Glacial, significant paleoenvironmental diversity controls the intensity and type of pedogenesis over the European loess belt, and the resulting MPG paleosols represent a wide variety of habitats, from humid soils and gleysols in western and north-western Europe (Meszner et al., 2012; Antoine et al. 2016; Haesaerts, 2016) and feeble boreal soils and Cambisols in central and eastern-central Europe (Demek and Kukla, 1969; Haesaerts, 1990; Lehmkuhl et al., 2016) to dry steppe soils in eastern Europe and around the Black Sea coast (Buggle et al., 2009; Marković et al., 2015). In addition, recovered climatic and stratigraphic information from the LPSs is complicated by the local geomorphological context, erosional unconformities, environmental settings, and the internal variability of each loess-paleosol site (Winkler and Matthews, 2010; Schrimer, 2010; Lehmkuhl et al., 2016), as well as by uncertainties in loess age models (Timar-Gabor et al., 2016). A promising approach in current loess research is the detailed reconstruction of the pedological evolution of particular regions within the European loess belt and the subsequent correlation of paleopedological records to individual north-western European interstadials of the middle, late MIS 3 (Denekamp, Hengelo), and early MIS 3 (Oerel, Glinde) (Frechen, 2011; Feurdean et al., 2014).

Such an approach, however, is often hampered by the occurrence of significant erosion events at the transition from MIS 4 to MIS 3, as recorded in various terrestrial archives across Central Europe (Huissteden et al., 2001). In LPSs, this erosion might have resulted from the extensive degradation of permafrost during a rapid warming phase that probably marked the beginning of the first interstadial of the MPG (Antoine et al., 2016). Also, repeated phases of torrential rain occurring especially at the transitions from stadials to interstadials might also have caused pervasive erosion events, depending on the vegetation coverage and regional morphology (Brunk et al., 2016) Because of this and also as a result of research history and the limitations of radiocarbon dating (e.g. Behre, 1989; Sauer et al., 2016), MPG paleosols have, in the past, usually been dated to the middle and late phase of

the MIS 3 and broadly correlated with Hengelo-Denekamp interstadials, which were thought to be the most prominent during the MPG (Kukla, 1975). Furthermore, poor chronometric data and widespread chronological misinterpretations of LPSs still complicate paleoenvironmental interpretations (e.g. Kadereit et al., 2013). Consequently, reliable data on paleosols in central Europe dated to the Early MPG (59 - 40 ka) is very scarce; their preservation is connected mostly to local geomorphological settings with high dynamics of colluvial and aeolian deposition (foot slopes and depressions), which have protected underlying units from erosion (Frechen, 2003; Schirmer, 2012). In contrast, the more continental areas of Eurasia seem to be less affected by erosional processes, as documented for instance in the Molodova (Ukraine) and Mitoc-Malu Galben (Romania) loess sections as well as the Kurtak locality in Siberia (Haesaerts et al. 2003; 2009).

In the central European context, the Carpathian/Pannonian Basin contains the largest and most significant loess region preserving a paleoenvironmental record that extends back over the last million years (Marković et al., 2011; 2015; Zeeden at al., 2016; Obreht et al., 2016). Various kinds of findings obtained from numerous LPSs in the last few years (see Marković et al., 2015 and references within) provide renewed information on Middle and Upper Pleistocene sequences. These studies confirm the findings of previous research, i.e. that the Carpathian Basin was warmer and drier than elsewhere in Europe during the Middle and Upper Pleistocene (Buggle et al., 2013). As a result, interglacial/interstadial soils preserved in LPSs show obvious differences from those from north-central and western Europe, especially regarding the weaker level of illuviation processes.

However, it should be noted that the majority of investigated LPSs are situated in the plateau position within the central and southern part of the Carpathian Basin (see LPSs sites distribution on Fig. 1) and comparatively little attention has been given to the paleopedological development of the northerly-situated upland pericarpathian zones, which differ from the inner part of the Carpathian Basin by having a considerably wetter climate (Spinoni et al., 2016). Similarly, while substantial work has been undertaken to characterize climatic fluctuations of the first order (interglacial paleosols), very little is known about soil development during second and third order climatic fluctuations, i.e. during interstadials.

To fill these gaps in our knowledge, we investigated the Bíňa LPS situated in the Pohronská Uplands (SW Slovakia), in the area of the northern limit of the Pannonian loess (Fig. 1). Our investigations in this relatively poorly documented region on the north-western edge of the Carpathian Basin provide valuable information and add important knowledge to already-detailed southeast and south-central European loess records.

In this study we present the results of multiproxy research (soil micromorphology, granulometry, environmental magnetism, malacology, and geochemistry) on the Pleniglacial (MIS 2-4) sequence of sediments and paleosols. The main goal was to interpret results concerning local pedogenic evolution and pedostratigraphy (with special attention to the early Middle Pleniglacial period) and to discuss these findings in the context of the facies variability of the Last Glacial European pedosedimentary record. This study also highlights the role of local geomorphological and hydrological settings on soil development and preservation.

2. Regional and local settings

The research area is situated on the northwestern edge of the Carpathian Basin along the Danube Uplands (Fig. 1). This part of the basin consists mainly of Neogene carbonate rocks of the Danube Basin covered by Quaternary colluvial and fluvial sediments, loess, and loess-like sediments. The border between loess and loess-like sediments is very sharp, situated approximately 15 km north of the study sites. The prevailing soil type is chernozem developed on loess; alluvial deposits are covered mostly by fluvisols. Within the Hron River valley, willow-poplar forests and relicts of alluvial forests with *Salix*, *Quercus* and *Ulmus* dominate, whereas the rest of the area is currently arable land. The climate is warm and rather dry, with a mild winter. The mean

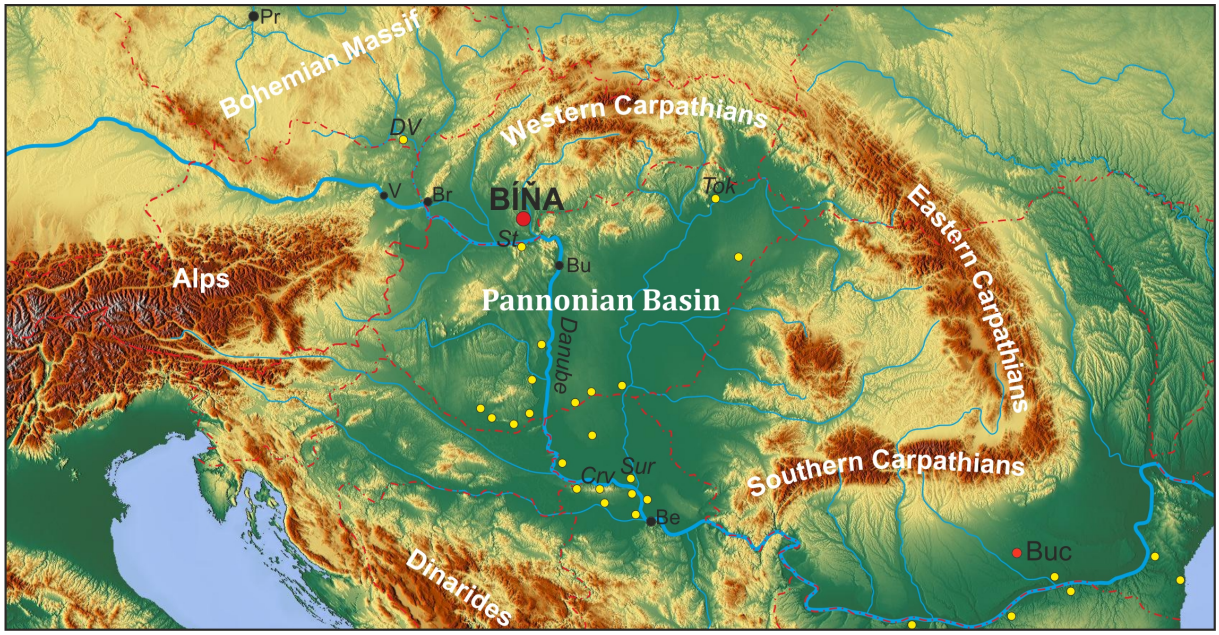

Fig. 1: Topographic map showing the location of the Bíňa site in south-eastern Europe. The sites mentioned in this paper are abbreviated as: DV (Dolní Věstonice), St (Sütto), Tok (Tokaj), Crv (Ćrvenka), and Sur (Surduk).

annual temperature is 8.5 °C (January -2.5 °C; July 20 °C) and the annual precipitation is 500-550 mm. The wind direction is predominantly northwesterly.

The studied outcrop is exposed on the right bank of the Hron River between the villages of Bíňa and Bíňa (47.942° N, 18.649 E°; 111 m a.s.l.; Fig. 2) and is up to 12 m high and 600 m wide. An overview scheme of the section and sampled profiles are shown in Figs 2 and 3. Fluvial gravel and sand of the Hron River are covered by a sequence of loess, loess derivatives, and colluvial sediments with intercalated paleosol horizons. The general lithostratigraphy of the section is provided by Halouzka and Smidt (1979), who assigned the sequences to the Weichselian Glacial. The first malacological investigations of the site were performed by Ložek (1952; 1965; 1976); this work was limited to the northern part of the loess section (without paleosols horizons), which were accessible at the time of his investigations.

3. Methods

3.1. Field work and sampling

The exposed outcrop was described and sampled during the spring of 2015. This study refers to three profiles: a 10.5 m long profile, P2, sampled in the central part of the outcrop, and a10 m long profile, P1, and a 3.5 long profile, P3, which were sampled in the northern part of the outcrop (see Fig. 2). Unoriented samples for laboratory analyses were collected continuously at 5 cm intervals from the cleaned profiles P2 and P1. The descriptions of the soils and sediments of the studied section are based on field observations and micromorphological studies.

3.2. Rock magnetic measurements

Mass-specific low frequency magnetic susceptibility (χlf, here referred to as χ) was measured at 0.976 kHz, and high frequency magnetic susceptibility (χhf) at 3.904 kHz, using a KLY-4 kappabridge (AGICO, Brno). The difference between the two measurements gives the frequency-dependent susceptibility, expressed here as a percentage of χfd using the following equation:

$$\chi fd\% = (\chi lf - \chi hf) / (\chi lf) \times 100.$$

3.3. Geochemical and grain size analyses

X-ray fluorescence (XRF) measurements were performed on bulk samples collected at 5 cm intervals from profiles P2 and P1 using a NITON XL3t 950 GOLDD + (Thermo Scientific) spectrometer with a 50 kV Ag tube and large-area SD detector. The XRF signals of some 20 elements were determined, but only

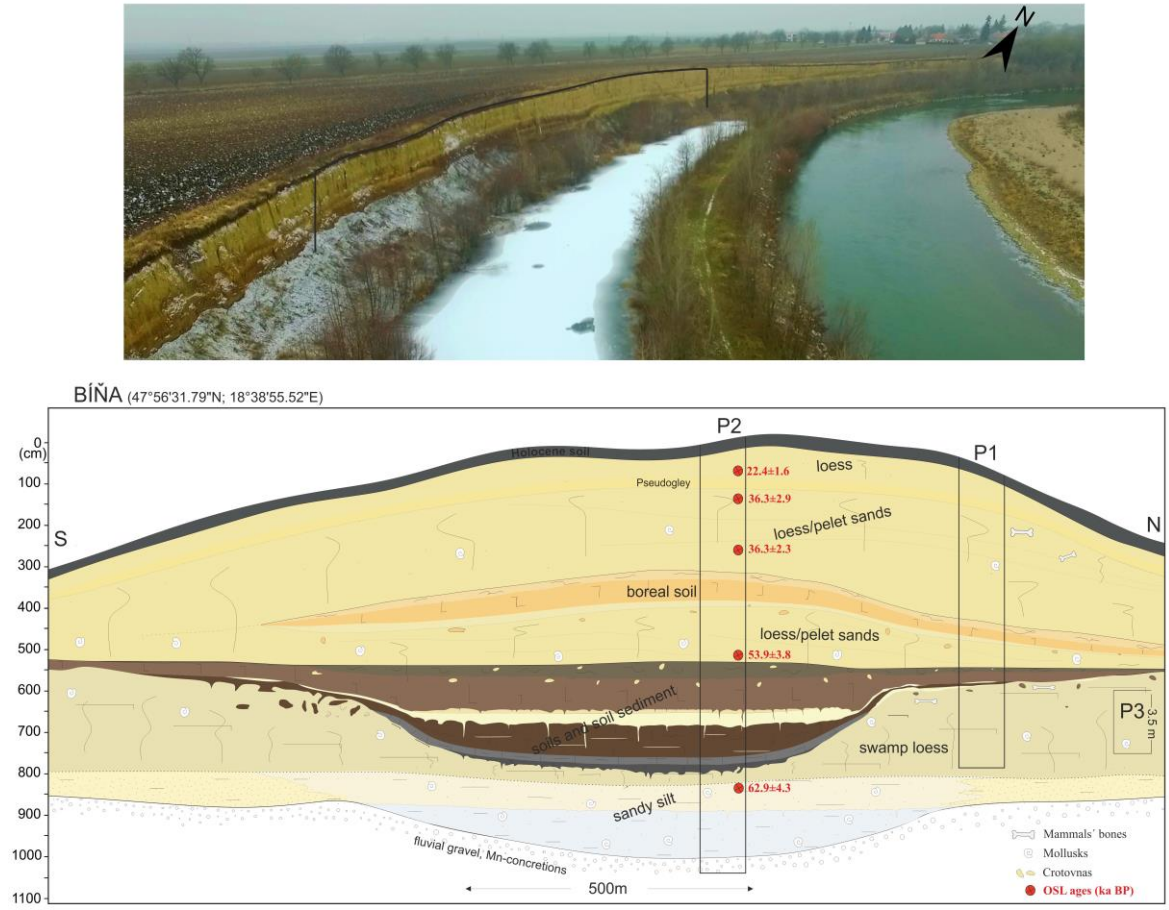

Fig. 2: A - Panoramic photograph of the exposed wall; B - Overview scheme of the studied outcrop and investigated profiles P1, P2 and P3.

the results for Ca, Sr, and Rb are discussed in this paper.

After removal of carbonate and organic matter by H_2O_2 and HCl, respectively, the particle size distribution of samples from profile P1 was obtained using a CILAS 1190 LD laser granulometer, which provides a measurement range from 0.04 to 2500 µm.

3.4. Micromorphology

Oriented soil samples from each lithological layer of profile P1 (10 samples) and profile P2 (8 samples) were placed into small Kubiena boxes (dimensions 3 × 5 cm). After slow drying and subsequent impregnation with a polymer resin, thin sections were produced from samples at the laboratory of the Institute of Geology CAS (equivalent to Bullock et al., 1985; Stoops, 2003). The thin sections were studied under a polarizing microscope at a magnification of 16–800× and interpreted according to Stoops et al. (2010).

3.5. Malacological analyses

Bulk samples for malacological analyses (15-20 dm^3) were collected continuously at 20 cm intervals from profile P3 and from selected horizons of profile P1. The samples were washed through a sieve of mesh size 0.5 mm and air dried. Shells and their fragments were hand sorted under a dissecting stereomicroscope and identified using the methodology devised by Ložek (1964) and Horsák et al. (2013). The latter was also used for mollusc nomenclature with some updates according to Horsák et al. (2015).

3.6 Luminiscence dating

For standard OSL measurements, fine grains of quartz (4–11 µm) were extracted from the samples. The laboratory protocol includes several chemical treatment steps such as treatment with 20% HCl, 20% H_2O_2, and H_2SiF_6. Subsequently, the sediment was rinsed in deionized water. After drying, the sediment was suspended in alcohol and grains in the desired diameter range were extracted by sedimentation. The cleaned quartz grains were suspended in 50 ml of acetone, and 2 ml of the

suspension was pipetted into flat bottomed tubes with stainless steel discs placed in them. The grains settled on the disc surface and after evaporation of the acetone, discs with a monolayer of fine polymineral grains were obtained.

All OSL measurements were made using an automated Daybreak 2200 TL/OSL reader. Laboratory irradiations were performed using a calibrated $^{90}Sr/^{90}Y$ beta source mounted onto the reader delivering a dose rate of 2.8 Gy/min, and a 6 mm Hoya U-340 filter was used for the OSL. Equivalent doses were determined using the single-aliquot regenerative-dose (SAR) protocol (Murray and Wintle, 2000). Ages were calculated using the Central Age Model (CAM) (Galbraith et al., 1999).

4. Results and interpretations

4.1 Litho- and pedostratigraphy

As visible on the overview scheme (Fig. 2), the study outcrop shows considerable lateral divergence. The pedo-sedimentary record is most stratified in the central part of the outcrop, whereas in the marginal parts of the study outcrop the sequence did not develop due to local geomorphology and eventually eroded in the later phases. On the basis of our field observations, we divided the sedimentary record of the central part into four main sequences (A-B-C-D), corresponding to major environmental changes that occurred during the formation (Fig. 3):

Sequence A – sandy silt and laminated loess;
Sequence B – dark brown soils and soil sediment;
Sequence C – pellet sands and light brown paleosol;
Sequence D – loess, pellet sands, and weakly developed grey-brown paleosol in the upper part.

Within the four divided zones, 13 lithological units (LUs) can be distinguished (profile P2). Units 1-4 and 6 were recorded also in the northern part of the outcrop (profile P1, Fig. 2). Correlation between profiles P1 and P 2 was based on macroscopic and microscopic evaluations as well as on the comparison of geochemical/rock-magnetic proxies. The general lithological description of these units, reported from the base of the section upwards, is as follows:

14 – fluvial sandy gravel with abundant Fe/Mn concretions (only in the profile P2)
13b – up to 1.5 m thick greenish grey (5GY 6/1) calcareous sandy silt, strongly marked by ox/redox. signs (Fe and Mn concretions and belts) (only in the profile P2)
13a –yellow (10YR 8/6) calcareous sandy silt, cryoturbation (ice wedges) (only in the profile P2)
12b – pale yellow (5YR 8/3) calcareous silt (loess) with well-discernible laminated structure
12a – laminated loess with crotovinas (unit 12 is not diferenced in the profile P2)
11 – up to 50 cm thick very dark brown (7.5YR 8/0) soil with prismatic structure; cryoturbation (ice wedges) (only in the profile P2)
10 – dark grey (5YR 3/1) silt and sand with the horizontal lamination (only in the profile P2)
9b – 80 cm thick dark brown (10YR 4/3) soil with significant prismatic structure and sand admixture (only in the profile P2)
9a– reddish brown (5YR 4/3) silt and sand with the horizontal lamination; soil sediment (only in the profile P2)
8 – up to 60 cm thick white carbonate horizon with flaky structure (only in the profile P2)
7b – dark reddish brown (5YR 2.5/2) soil with significant prismatic structure and crotovinas in the upper part, cryoturbation (ice wedges)
7a – reddish grey (5YR 5/1) silt and sand with the horizontal lamination; soil sediment
6 – yellow (10YR8/4) loess and pellet sands (*sensu* Kukla, 1961)
5 – up to 110 cm thick horizon of reddish yellow (7.5YR 7/6) soil with carbonate horizon and crotovinas below
4 – yellow (10YR8/6) loess and pellet sands (*sensu* Kukla, 1961) with aggregates up to 0.4 cm in diameter
3 – slightly grey 25-50 cm thick horizon of very weak develop soil
2 – pale yellow (2.5Y8/3) loess
1 – black (2.5Y3/3) Ah horizon of recent soil

4.2. Chronology

The results on 5 OSL data are presented in Table 1. The ages show good stratigraphic consistency, with no inversions outside error limits. According to absolute chronology, zone A (sandy silt and laminated loess) accumulated mostly up to approximately 63 ka BP, zone B (dark/brown soils and soil sediment) developed approximately from 60 to 50 ka BP, and zones C and D (loess, pellet sands and weakly developed paleosols) correspond to the period 50-20 ka BP.

Lab. Code	Sample ID	Sampling Depth (cm)	H_2O (%)	U (Bq/kg)	Th (Bq/kg)	K (Bq/kg)	Dose rate (Gy/ka)	OSL Age (ka)
2319	P2_125	125	15±5	30±1	39±1	427±11	2.49±0.16	22.4±1.6
2320	P2_200	200	15±5	29±1	44±1	408± 11	2.48±0.16	36.3±2.9
2321	P2_400	400	15±5	32±1	49±1	458±12	2.72±0.17	36.3±2.3
2322	P2_600	600	15±5	29±1	44±1	451±11	2.54±0.16	53.9±3.8
2323	P2_840	840	15±5	27±1	44±1	514±14	2.67±0.18	62.9±4.3

Table 1: Dose rate. equivalent dose data and OSL ages. H_2O % = measured water content (water mass over dry sediment mass); U = Uranium; Th = Thorium; K = Potassium.

Ten samples from P2 and five samples from P1 were taken from significant horizons of these profiles for micromorphological evaluation. The main features of these horizons are summarized in Table 2 and shown in Figure 4. The final interpretation of macroscopically distinguished horizons was based on micromorphological observations, mainly in cases of soil horizons where post-sedimentary processes tended to overprint the original features. Finally, features connected with a wet environment were confirmed at the base of the section, followed by loess sedimentation interrupted by soil development still in a quite wet environment (until a depth of 550 cm, sample P2/8). Glacial aridisation reflected by loess sedimentation with typical freezing structures and the sedimentation of pellet sands was recorded in the upper part of the studied section.

4.4. Grain size, rock magnetism, geochemical results, and their interpretation

4.4.1. Grain size results

A continuous record of grain size variations along the 10.5 m high profile, P2, showed good agreement with pedo-lithostratigraphy (Fig. 3). Within sequence A, coarse silt (20-50 μm) predominated (~76%) and clay content (<4 μm) ranged between 6 and 11%. Within the uppermost part of LU_12b, sand (>63 μm) was found to comprise up to 40% of the total content.

In general, sequence B (soil horizons and soil sediments) was enriched in clay in comparison with deposits located below and above. The clay content ranged between 9 and 18%. The highest amount of clay was found in upper dark soil (LU6). The increase in the sand fraction corresponded with the sediment horizons (LU_5 and LU_8).

Within sequence C, the highest content of clay (up to 24%) corresponded to the horizon of light brown paleosol (LU_5). The underlying horizon of pellet sands (LU_6) was marked by a distinct increase in sand (up to 35%). The above-situated loess (LU_4; sequence D) exhibited continually decreasing clay content at the expense of coarse silt and sand. Within this unit, the slight increase in clay content correlated with a weak soil horizon (LU_3). Holocene soil (LU_1) was also enriched in clay relative to the sedimentary record below.

4.4.2. Rock magnetism

Likewise, rock magnetic records (Fig. 3) correlated well with the lithology. In general, paleosols were characterized by magnetic enhancement, unlike loess, pellet sands and basal sandy silts. Maximum χ values as well as χfd occurred in Holocene topsoil (LU_1), whereas minimum values were measured in the basal sandy silts of profile P1.

The magnetic enhancement of paleosol horizons can be related to a higher concentration of fine-grained magnetite formed in situ. This is suggested by elevated values of χfd, which indicate the proportion of fine viscous magnetic grains just below the SP/SD boundary (~0.02 μm; Thompson and Oldfield, 1986). This grain-size fraction is preferably formed during pedogenesis (Heller and Evans, 1995). In our study, the increased magnetic values for pellet sands (LU_6) probably related to the amount of top-soil particles in the reworked sediment. These findings are in accordance with the basic principle of environmental magnetism in loess – i.e., that the enhancement of magnetic minerals derived from silicate minerals occurs through pedogenesis (Maher, 1991; Hambach et al., 2008).

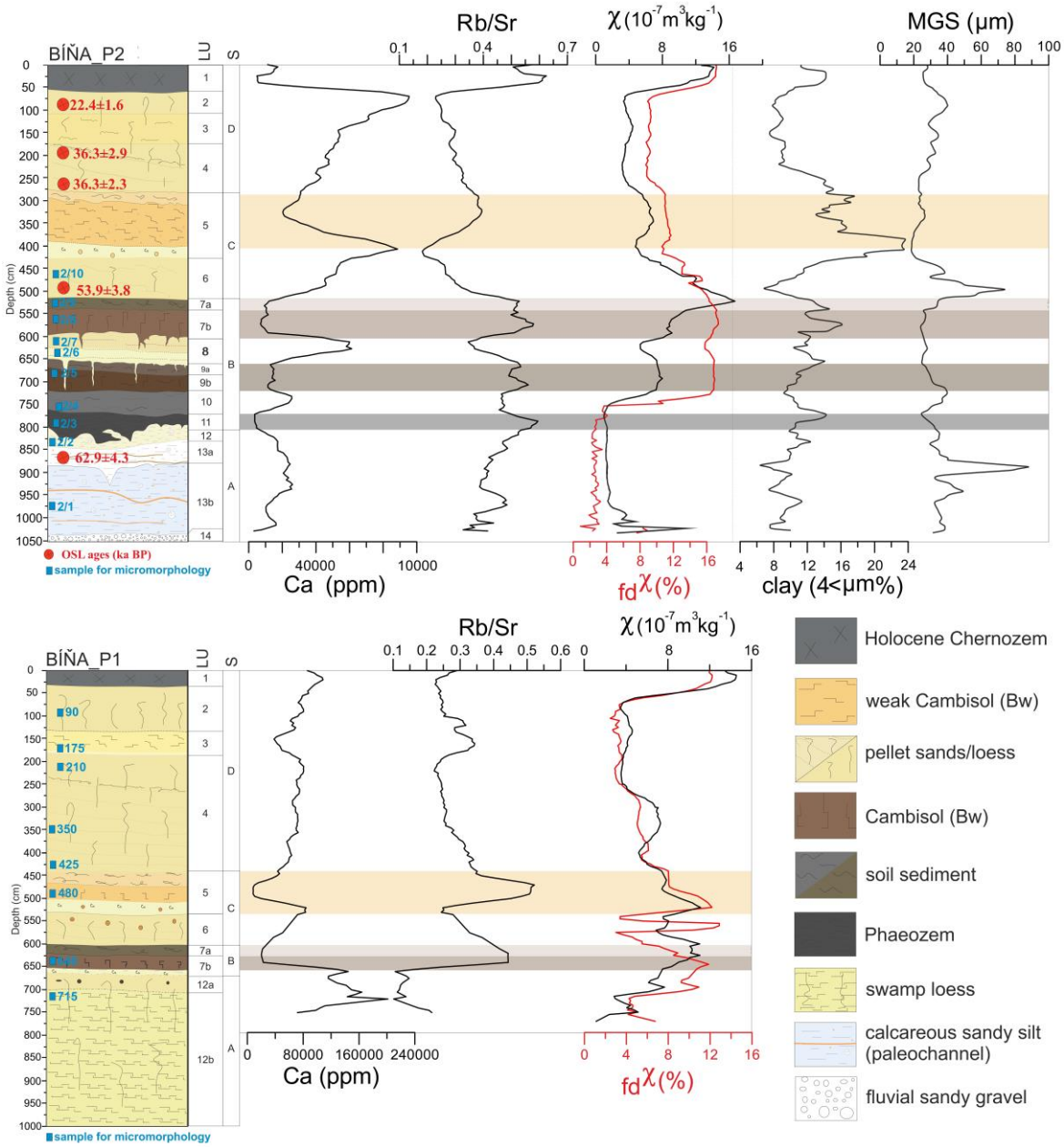

Fig. 3: Graphs of Rb/Sr, Ca, magnetic susceptibility, and grain size variation together with the lithostratigraphy of the sampled profiles.

In both profiles, magnetic enhancement (increasing χfd and χ values) was obvious in all strata, except for the initial pseudogley horizon (LU_3), where signs of depletion of primary MD and SD grains relative to SP particles were found, probably due to the effect of waterlogging.

4.4.3. Geochemical results

The values of Rb/Sr and Ca content from profiles P2 and P1 are summarized in Fig. 3. The Rb/Sr ratio was used to evaluate the intensity of chemical weathering in particular horizons. Rb is little affected by sediment diagenesis/pedogenesis, as it is strongly retained in the weathering zone by its sorption onto clay minerals (Nesbitt et al., 1980). In contrast, Sr is a mobile element bound in Ca-feldspars and primary carbonates and is easily soluble during leaching and chemical weathering processes. Such a simple ratio of more mobile (Sr) to relatively immobile (Rb) elements can be used as a reliable indicator of the degree of chemical weathering and the intensity of leaching in sediments (Gallet et al., 1996; Chen et al., 1999) or as a useful climatostratigraphic tool

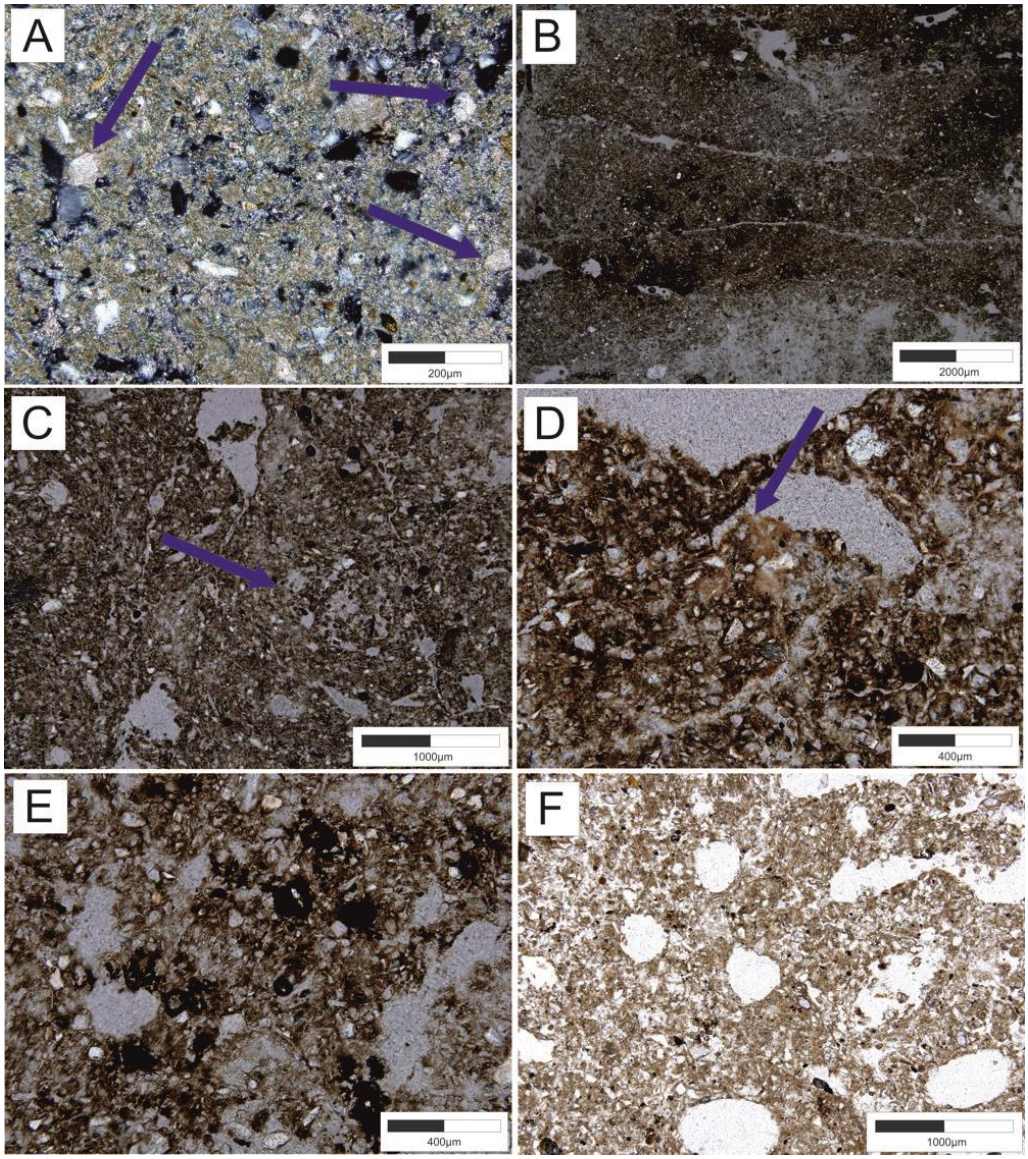

Fig. 4: Micromorphological features of the significant horizons of profiles P1 and P2; a - micritic impregnation of the matrix with the presence of sparitic pseudomorphoses after the root cells (blue arrows); b - platy microstructure as a result of freezing thawing processes. Fe/Mn concentrations developed mainly in the upper part of the picture have a different shape and size; c - well developed passage features and excremental features (blue arrows) representing intensive bioturbation; d - clay neoformation (blue arrow), e - gleying indicated by redoximorphic features composed mainly of neoformed dendritic Fe/Mn aggregated nodules; f - small redoximorphic nodules and the brownish matrix as a result of initial braunification.

(Hošek et al., 2015). The Rb/Sr ratio has previously been applied to LPSs in the European loess belt (Bokhorst et al., 2009; Bábek et al., 2011; Hošek et al., 2015; Profe et al., 2016) including several sites inside the Carpathian Basin (Buggle et al., 2011). In our study, the Rb/Sr ratio for both studied profiles reflected the lithology: maximum values correlated with the soil horizons (LUs_11, 9, 7 and 5), and with minimum values in loess, pellet sands and colluvial sediment. The values of Rb/Sr within units LU_2-4 exhibited a continually decreasing trend towards the Holocene soil, except for the weak soil horizon (LU_3), where these values were slightly increased.

The positive relationships between Rb/Sr ratio, clay content, and magnetic susceptibility (Fig. 3) suggests that all these proxies are driven by interrelated processes, most probably by the intensity of the pedogenesis and chemical weathering of the primary (silty) material. In our study, the highest Ca values in both sections corresponded with carbonate horizons of paleosols. Calcareous sandy silt, loess, as well as pellet sands were also enriched in carbonates. In contrast, the non-calcareous character of all recognized soils indicated decarbonisation as a result of pedogenesis processes.

sample	microstructure	porosity	texture class and sorting	C/F ratio distribution	nature of groundmass	b-fabric of groundmass (XPL)	mineral composition	residues of organic matter	amorphous organic matter	punctuations	pland residues	charred organic matter	coating	hypocoating	infilling	depleations	nodules	excrements	textural pedofeatures	notes	general interpretation
P2/1	channel	channels, voids, complex packing voilds	sorted silty clay	50µm=20:80 0µm=20:80	light brown	crystallic	calcite, mica, Q, Ptg	phytolites - r, mollusca shells - p	r	p				+		p			root bioturbation - p	micritic as well as sparitic form of carbonates, hypocoating is carbonatic	**overbank deposit, swamp loess**
P2/2	platy	horizontal plates, voids and cracks	sorted clayley silt	50µm=40:60 0µm=40:60	brown	crystallic	mica, Q, Ptg, calcite		p	p		microcharcoal-r		+	r	c	c		root bioturbation - r	nodules are dendritic (black) and oval (dark brown), composed of Fe and Mn , hypocoating is Fe rich, infiling is composed of Ca as well as Fe	**changing water level, freezing processes, depleation, aleolian imput (silt)**
P2/3	cracky	zig-zag cracks, voids	sorted clayley silt	50µm=40:60 0µm=40:60	varying from dark brown to light grey and orange	crystallic; locally porostriatic	clay minerals, Q, Ptg, mica	phytolites - r	c	vc	r			/-		vc			passage features - vc	hypocoating composed of Fe and clay minerals	**humic horizon of Phaeozem**
P2/4	cracky	zig-zag and horizontal cracks, vesicles, chambers	sorted silty clay	50µm=10:90 0µm=10:90	brown grey	crystallic	micritic and sparitic calcite	mollusca shells - c	r	c				vc	p	c	p	r	root bioturbation - p, passage features - r	rounded Fe nodules -r, dendirtic black Mn/Fe nodules r to c; hypocoating and infilling is composed of carbonates; excrements of microfauna	**wet alcaline environment, changing water level**
P2/5	vesicular	vesicles, channels, cracks	sorted silt	50µm=70:30 0µm=70:30	brown	crystallic	Q, mica Ptg	fragment of bone - r	r	p				c	r		vc	p	passage features - c	black Fe/Mn rounded nodules are vc, in diameter app. 100 - 200 µm; thick hypocoating and infilling composed of carbonates; excremental features are from microfauna	**weakly developed Bw horizon of Cambisol**
P2/6	cracky	cracks, vesicles and chambers	sorted silty clay	50µm=10:90 0µm=10:90	grey	crystallic	micritic carbonates, r Q, Ptg and			p		microcharcoal-r					p			black Fe/Mn dendritic nodules, matrix is micritic composed of carbonates	**Ca horizon composed of micritic carbonate and silt**
P2/7	channel	channels, cracks, vesicles	sorted silt	50µm=70:30 0µm=70:30	brown	crystallic	Q, mica Ptg		r	p					r		vc	p	passage features - c, root bioturbation - c	black Fe/Mn rounded nodules and small dendritic nodules are vc, in diameter app. 100 µm; excremental features are from microfauna, infilling composed of micritic carbonate	**hydromorphic type of soil**
P2/8	channel	channels, vesicles, cracks, compound packing voids	sorted silt	50µm=40:60 0µm=40:60	orange brown	porostriatic	Q, mica Ptg			p			clay coating-r				c	r	pasage features - p	microstructure is generally channel, but in the upper part is the huge passage feature or the microstructure change into granular; black rounded nodules in diameter of 500 µm - r, smaller rounded and detitic nodules in diamter of 100 - 200 µm	**Gleyic Cambisol (Bw)**
P2/9	vesicular	vesicles, channels, compound packing voids	moderately sorted silt	50µm=70:30 0µm=70:30	orange brown	crystalic	Q, mica Ptg		r	p		r			r	p	c	r	passage features - p	infillings are composed of carbonates coloured by Fe, small, dendritic black nodules of Fe/Mn are in diamter of 50 µ	**loess, pelet sands**
P2/10	vesicular	compound packing voids, vesicles, channels	unsorted silt	50µm=60:40 0µm=60:40	orange brown	crystalic	Q, mica Ptg, rock fragments			p							r		passage features and root bioturbation - r	rounded as well as dendritic black Fe/Mn nodules, unsorted	**loess, pelet sands or colluvium?**

Table 2. Micromorphological characterization of the significant lithological horizons of profiles P2 and P1; r = rare (up to 3 %), p = present (up to 10 %), c = common (up to 30 %), vc = very common (more than 30 %)

sample	microstructure	porosity	texture class and sorting	C/F ratio distribution	nature of groundmass	b-fabric of groundmass (XPL)	mineral compositiion	residues of organic matter	amorphous organic matter	punctuations	pland residues	charred organic matter	coating	hypocoating	infilling	depleations	nodules	excrements	textural pedofeatures	notes	general interpretation
P1 - 90	vesicular	vesicles, channles, cracks	moderatelly sorted silt	50µm=30:705 0µm=30:70	brown	crystalic	Q, mica, Ptg		r	p	r			r				p	passage features c, root bioturbation p	matrix is highly carbonatic, not well developed carbonate hypocoating, plant residues are reped by recent roots	**loess?**
P1 - 180	vesicular	vesicles, channles, cracks	moderatelly sorted silt	50µm=30:705 0µm=30:70	orange brown	crystalic	Q, mica, Ptg		r	p						c	p	c	passage features c root bioturbatiion p	small up to 100 µm sizes black Fe/Mn nodule	**initial pseudogley**
P1-210	vesicular	vesicles, channels	sorted silt	50µm=30:705 0µm=30:70	orange brown	crystalic	Q, mica, Ptg, sparitic calcite	mollusca shell fragments - r		p							r	r	passage features - c, root bioturbation r	matrix is highly carbonatic	**loess?**
P1 - 350	granular	compound packing voids, cracks, vesicles	moderatelly sorted silt, granulae are sandy	50µm=40:605 0µm=40:60	orange brown	crystalic	Q, mica, Ptg			p		r					r		passage features and root bioturbation are r	material is packed into the granulae of different size ranging from fine to coarse sand	**pelet sands**
P1 - 425	vesicular to granular	vesicles, compound packing voids, chambers	moderatelly sorted silt	50µm=40:605 0µm=40:60	light brown	crystallic	Q, mica, Ptg			p				r			p	p	passage features - c, root bioturbation - p	matrix is highly carbonatic, black Fe/Mn dendritic nodules of different size ranging from 100 - 500 µm, r hypocoating is composed of carbonates	**loess, pelet sands**
P1 - 480	vughy	channels, star shaped vughs,	silt	50µm=60:40	orange brown	crystalic	Q, mica Ptg		r	p							p	r	passage features - p, root bioturbation - c	nodules are black dendritic up to 50 µm, slight signs of illuviation?	**Cambisol (Bw)**
P1 - 641	vughy	vughs, channels, cracks	sorted silty clay	50µm=10:90	orange	crystallic	Q, mica, micritic carbonate accum.		r	p		r			r	p	p	r	passage features - p, root bioturbation p	infillings are composed of carbonates coloured by Fe, small, dendritic black nodules of Fe/Mn are in diamter of 50 µ	**Gleyic Cambisol (Bw)**
P1 - 716	vughy	zig-zag cracks and star shaped vughs, r channels and vesicles	sorted silty clay	50µm=20:80	grey	crystallic	Q, mica, Ptg, sparitic calcite	shell fragments - r	r	r							r		passage features and root bioturbation r	black nodules of different size, unsorted	**wet alcaline environment, changing water level**

Table 2 (continued...)

4.5. Interpretation of the malacofauna

Both sections provided rich mollusc records covering in total 12,742 shells identified as 45 The assemblages consisted mostly of open land species (e.g. *Vallonia* and *Pupilla* spp.) and species characteristic of glacial steppe conditions (e.g. *V. tenuilabris*, *P. loessica* and *Columella columella*) with a significant share

Lithological unit	Depth (cm)	Forest-shrubs					Open-country													
		Clausilia pumila (C. Pfeiffer, 1828)	*Ruthenica filograna* (Rossmässler, 1836)	*Vitrea crystallina* (O. F. Müller, 1774)	*Fruticicola fruticum* (O. F. Müller, 1774)	*Arianta arbustorum* (Linné, 1758)	*Vallonia pulchella* (O.F. Müller, 1774)	**Vallonia tenuilabris* (Al. Braun, 1842)	*Vallonia costata* (O. F. Müller, 1774)	*Vertigo pygmaea* (Draparnaud, 1801)	**Vertigo pseudosubstriata* (Ložek, 1954)	**Pupilla loessica* (Ložek, 1954)	*Pupilla sterri* (Forster, 1840)	*Pupilla triplicata* (Studer, 1820)	*Pupilla muscorum* (Linné, 1758)	**Columella columella* (Martens, 1830)	*Truncatellina cylindrica* (A. Férussac, 1807)	*Chondrula tridens* (O. F. Müller, 1774)	*Granaria frumentum* (Draparnaud, 1801)	*Helicopsis striata* (O. F. Müller, 1774)
1	10-30																			1
2	75-100							12		21			152	92						
3	125-150							153					297	245	491	119				52
4	180-210							1										2		1
4	210-250								1					6	1			3		7
5	340-360													1				8	1	4
6	450-470												1					1		1
7a	510-530								1									2	3	2
8	610-630																			
8	630-650																			1
9a	650-675							58	12			12	103	207		19				6
9b	690-710																			
10	710-720																			
10	720-730							1												
10	730-760																			
11	760-770					1														
11	770-780					1														
12	780-790	2				3														
12	790-800	2				2	1	18			1					16				
12	800-810	2				2	6	36			5	2		2		77				
12	810-820	6				4	2	43			14	2	1	2		118				1
12	820-830	10				7	3	40			16		2		2	74				
12	830-840	4				5		16			4	1				31				
13a	840-850	1				4		5								15				
13a	850-860	6				40		15								5				
13a	860-870	4				26		2								2				
13b	870-880	6				26		3		3	4									
13b	880-890					1														
13b	890-900																			
13b	900-970																			
P-3	0-20					1		39			17		3			19				1
P-3	20-40	14					6	44		32	4		3			4				1
P-3	40-60	24		45		2		129		7		10	2	15		21				
P-3	60-80	5		5		1	1	31	1			6	7			31				1
P-3	80-100	24		10	3	1	23	54		15		2				7				
P-3	100-120	6		6			1	39				2				26				
P-3	120-140	4		1				1								8				
P-3	140-190		1					21		1		4				9	1			

Lithological unit	Depth (cm)	Generalist				Wetland				
		Cochlicopa lubrica (O. F. Müller, 1774)	*Trochulus hispidus* (Linné, 1758)	*Clausilia dubia* (Draparnaud, 1805)	*Deroceras* sp.	*Pupilla alpicola* (Charpentier, 1837)	*Succinella oblonga* (Draparnaud, 1801)	*Oxyloma* cf. *sarsii* (Esmark, 1886)	*Euconulus* cf. *praticola* (Reinhardt, 1883)	*Pseudotrichia rubiginosa* (Rossmässler, 1838)
1	10-30		3				1			
2	75-100		16			132	68			
3	125-150		142			139	329			
4	180-210		8				6			
4	210-250		5		1	2				
5	340-360						3			
6	450-470						2			
7a	510-530		3				3			
8	610-630		3				2			
8	630-650		14				22			
9a	650-675		19			192	207			
9b	690-710		5				4			
10	710-720									
10	720-730									
10	730-760									
11	760-770				1					
11	770-780						1			
12	780-790	2	8				10			
12	790-800	10	12			58	94	2	2	5
12	800-810	64	9			148	128		25	28
12	810-820	19	29			187	148		4	12
12	820-830	10	22			146	112		2	
12	830-840	17	12			42	48		2	
13a	840-850	9	11			5	28		4	
13a	850-860	16	21			29	33			
13a	860-870	36	12			14	25			
13b	870-880	10	18			17	12			
13b	880-890				2					
13b	890-900									
13b	900-970									
P-3	0-20		2	1		104	52	1		
P-3	20-40	3	2			385	226			3
P-3	40-60	38	22			644	312			12
P-3	60-80	29	18			262	178			1
P-3	80-100	34	15			484	162			
P-3	100-120	9	22			231	275			
P-3	120-140	4	18			8	89			
P-3	140-190		3			17	108			

Lithological unit	Depth (cm)	Aquatic																
		Bithynia transsilvanica (Bielz, 1853)	*Marstoniopsis* cf. *insubrica* juv. (Küster, 1853)	*Valvata macrostoma* (Mörch, 1864)	*Galba truncatula* (O. F. Müller, 1774)	*Ladislavella terebra* (Westerlund, 1885)	*Radix labiata* (Rossmässler, 1835)	*Lymnaea stagnalis* (Linné, 1758)	*Physa fontinalis* (Linné, 1758)	*Planorbis planorbis* (Linné, 1758)	*Anisus leucostoma* (Millet, 1813)	*Anisus vortex* (Linné, 1758)	*Gyraulus laevis* (Alder, 1838)	*Pisidium obtusale* (Lamarck, 1818)	**Pisidium stewarti* (Preston, 1909)	*Pisidium casertanum* (Poli, 1791)	*Pisidium milium* (Held, 1836)	*Musculium lacustre* (O. F. Müller, 1774)
1	10-30																	
2	75-100																	
3	125-150																	
4	180-210																	
4	210-250																	
5	340-360				1	3					1							
6	450-470																	
7a	510-530																	
8	610-630																	
8	630-650																	
9a	650-675																	
9b	690-710																	
10	710-720			53			211	176	18	143			441					42
10	720-730			14		1	78	17	1	19			154	1		6		32
10	730-760			44		2	165	20		31			245	2		1		55
11	760-770																	
11	770-780																	
12	780-790																	
12	790-800			2	36		6	1				2	1	4	2			1
12	800-810				24		7	2		1		5	5		4			2
12	810-820				9		11						4	1		1		4
12	820-830				8		3	2			1	2	5	2	2			2
12	830-840	1			8						1			3	2			1
13a	840-850			2	4										3			
13a	850-860	2			1						2			3	4			
13a	860-870	4			2						1			4	6		1	
13b	870-880		4											2	2			
13b	880-890	2																
13b	890-900	1																
13b	900-970																	
P-3	0-20				1						1				1			
P-3	20-40			1	38						1			1				
P-3	40-60																	
P-3	60-80				6													
P-3	80-100				2													
P-3	100-120				1													
P-3	120-140																	
P-3	140-190				1													

Fig. 5: Taxonomic list of molluscs from P1 and P3 profiles.

of moisture-demanding species (e.g. *Pupilla alpicola* and *Vertigo pseudosubstriata*) and many aquatic molluscs (e.g. *Pisidium stewarti*) (Fig.6).
The bottom part of profile P2 (Sequence A) was very poor in shells, but starting at a depth of 880 cm, the mollusc record became robust. The assemblages were composed of a mixture of many typical glacial species with a rather low proportion of xerophilous steppe species (at depths of 830-800 cm), an abundant species of damp habitats, and many aquatic species.

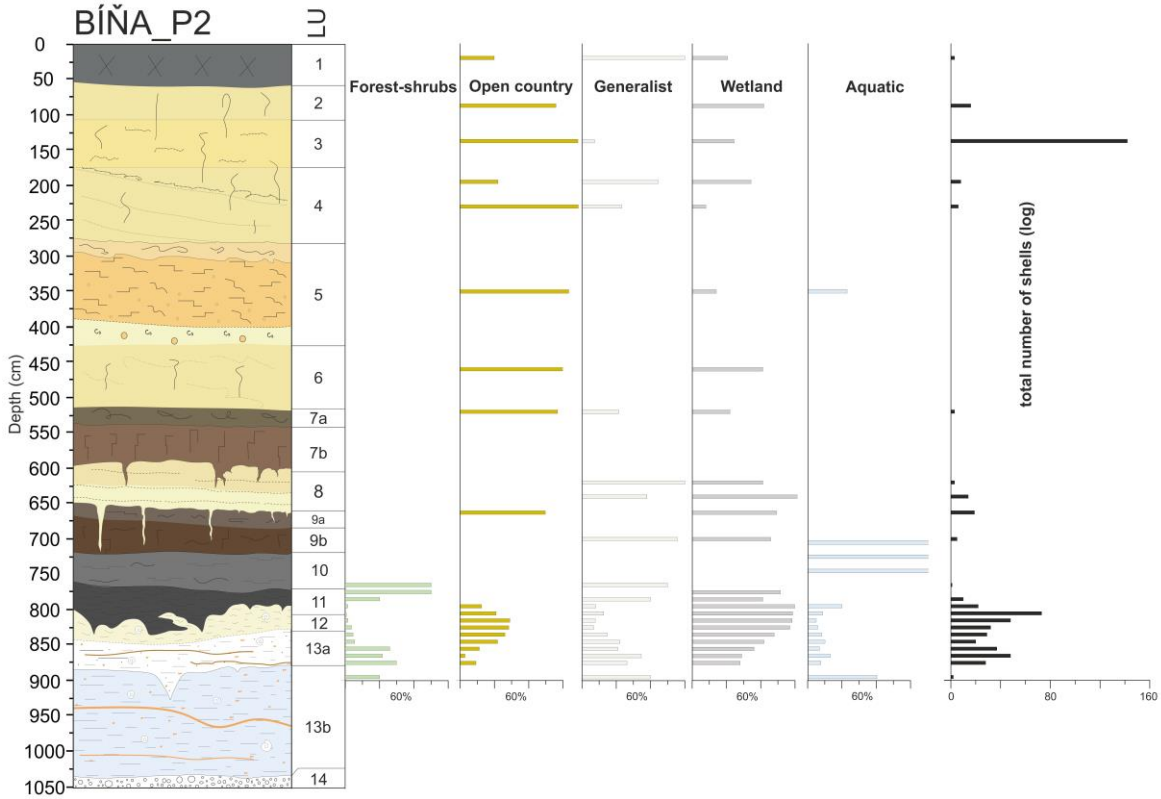

Fig. 6: Plots showing the percent abundance within major ecological groups and total

Within sequence B, the mollusc record was variable, as, at a depth of 780-760 cm (LU_11), virtually no shells were recorded, but rich assemblages of aquatic species were found between 760 and 710 cm (LU_10). The rest of this sequence (between 710-510 cm; LU_9-7) was in general similar to the lower part (especially at depths of 650-675 cm) before the presence of purely aquatic assemblages, though the assemblages were notably poorer both in individuals and species, these consisting mostly of generalist and xerophilous species. The same was found for sequence C, which was also poor in individuals and species, providing records for some generalist,xerophilous and/or steppe species (e.g. *Helicopsis striata* and *Chondrula tridens*).
The uppermost sequence, D, was again rich in shells, especially in the upper part (at a depth of 150-75 cm; LU_3-2), hosting mostly species of steppe habitats and two species of mesic-wet habitats. Generally, an important shift in the environment was detected from a depth of 710 cm, since no aquatic species were recorded, except for five shells of three species at depths of 360-340 cm (LU_5).

5. Discussion

5.1. Lithostratigraphy and environmental development of the site

On the basis of its stratigraphic position and OSL ages (Fig. 2, Table 1), the sedimentary record of the Bíňa site was accumulated during the last Pleniglacial. Using a multi-proxy approach that combined sedimentological, geochemical, and geophysical methods with the malacological record and soil micromorphology, we were able to reconstruct the environ-

mental evolution at the study site. The reconstructed development comprises four main phases of sedimentation and pedogenesis (Figs 7-10): MIS 4, Early MIS 3, Middle and late MIS 3, and MIS 2, which are discussed in detail below.

5.1.1. MIS 4 (sequence A; Fig. 7)

The snail assemblages (Figs. 5 and 6) obtained from calcareous silt with a significant laminated structure (LUs_13a -12; upper part of the profile P3; Fig. 2) are characterized by a specific combination of wetland and aquatic species (e.g. *Pupilla alpicola* and *Pisidium stewarti*), with an admixture of common loess steppe elements (e.g. *Vallonia tenuilabris* and *Columella columella*). The calcification of this stratum took place *in situ* as indicated by micritic impregnation of the matrix with the presence of sparitic pseudomorphoses of root cells (sample P1 - 715 cm, Fig. 4a.). Rare passage features and the limited presence of channels reflect the unclear biogenic influence of these strata. The mollusc record, along with textural and structural features of the sediment, indicate an environment of ephemeral swamp or water body in the overbank alluvial area, in which dust was deposited - so called 'swamp loess' or 'Sumpflöss' (*sensu* Ložek, 2001).

Within these overbank alluvials, a paleo-channel structure filled by loess and colluvial deposits (LU 13b, Figs. 2 and 3) was identified. Fe-Mn oxide precipitations of various types indicate pervasive gleying related to repeated oscillation of the ground water table (sample P2/2, Fig. 4b). On the macroscopic level, this is expressed by a predominantly reduced greenish grey background, accompanied by rusty mottles and concretions. This sedimentation resembles a limnic environment, but with shallow water conditions, in which water mostly stagnated and in which only a small amount of sediment was periodically deposited. This is clearly supported by the malacological record consisting of species characteristic of a loess environment enriched by several aquatic species of shallow waters (e.g. *Bithynia transsilvanica* and *Pisidium obtusale*). On the basis of the OSL 62.9±2.9 ka (Tab. 1, Fig. 3), the sedimentary record of sequence A probably correlates with the Early Pleniglacial, i.e. MIS 4 (60-71 ka). This interpretation is supported by the presence of cold-adapted species within this horizon (e.g. *Pupilla loessica*, *Columella columella* and *Vertigo pseudosubstriata*) and by cryoturbation features (ice wedges) founded in horizon LU_13a (Figs. 2 and 3). The general platy microstructure of this stratum provides further evidence of alternating freeze/thaw processes related to the presence of permafrost (sample P2/2; Fig. 4b). This finding is in accordance with observations from the central and eastern parts of Poland and western Ukraine, where permafrost developed in the latest part of the Early Pleniglacial (potentially equivalent to Heinrich Event 6) (Jary, 2009).

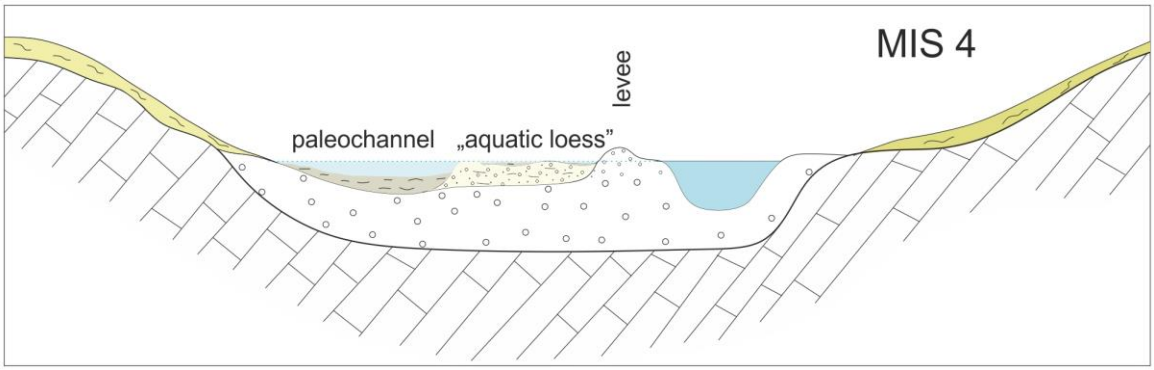

Fig. 7: Schematical cross-section of the site illustrating the pedo-sedimentary evolution during the MIS 4 (~70-60 ka BP).

5.1.2. Early MIS 3 (sequence B; Fig. 8)

The elevated Rb/Sr ratio and increased clay content in the dark layer developed on the paleo-channel deposits (LU_11, Fig. 3) indicate more intensive weathering processes related to this horizon. The *in situ* pedogenic origin of this layer is suggested by micromorphological features such as abundant bioturba-

tions, redoximorphosis, a hypocoating composed of Fe-bearing structures, and clay minerals (sample P2/3, Fig. 4c). Taking into account the position of this soil on the top of the paleo-channel, this soil would be classified as a humic horizon of Phaeozem – a hydromorphic type of chernozem (FAO, 2014) based on the presence of amorphous organic matter and a significant depletion of the matrix (see Tab. 2). On the basis of the OSL age of 62.9±2.9 ka obtained from the layer below (the uppermost part of sequence A), the occurrence of the humic horizon can be correlated with the beginning of the MPG (MIS 3; ~ 60-30 ka BP). Thus, our pedostratigrpahic and chronostratigraphic observations and interpretations are in obvious contradiction with the previous lithostratigraphical conclusions of Halouzka and Smidt (1979), who correlated the pedocomplex of sequence B with Eemian/Early Weichselian paleosols.

The intensive cryoturbation of the Phaeozem horizon observed at the transition of the substratum to a distinct colluvial sediment layer (LU_10, Fig. 3) on the surface of the Phaeozem reflects some short-term climatic deterioration which followed pedogenesis and was accompanied by erosion events and frost-thaw processes. The intensity of this cryoturbation might be connected with the presence of waterlogging.

After this cold event, climatic amelioration occurred. A warmer and more humid period was recorded in two genetically independent soil horizons of prismatic macrostructure (LU_9b and LU_7b) separated by colluvial sediment (LU_9a). The increased Rb/Sr ratio, enhanced magnetic susceptibility, and, in the case of the upper soil of the complex, significantly higher clay content (Fig. 3) are clear signs of enhanced *in situ* weathering and pedogenesis. The non-calcareous character of most of these soils and a porostriatic b-fabric points to decalcification that was followed by clay neoformation (dusty dark brown clay coatings in the upper soil (LU_7b, sample P2/8; Fig. 4d). Soils of this pedocomplex represent Bw horizons of Gleyic Cambisol, although the lower one (LU_9b) is rather weakly developed and probably also affected to some extent by relocation, as evident from the low clay content and relocated fragments of clay coatings and Fe-oxide nodules. Loess and/or silty colluvial sediment was probably the sub-

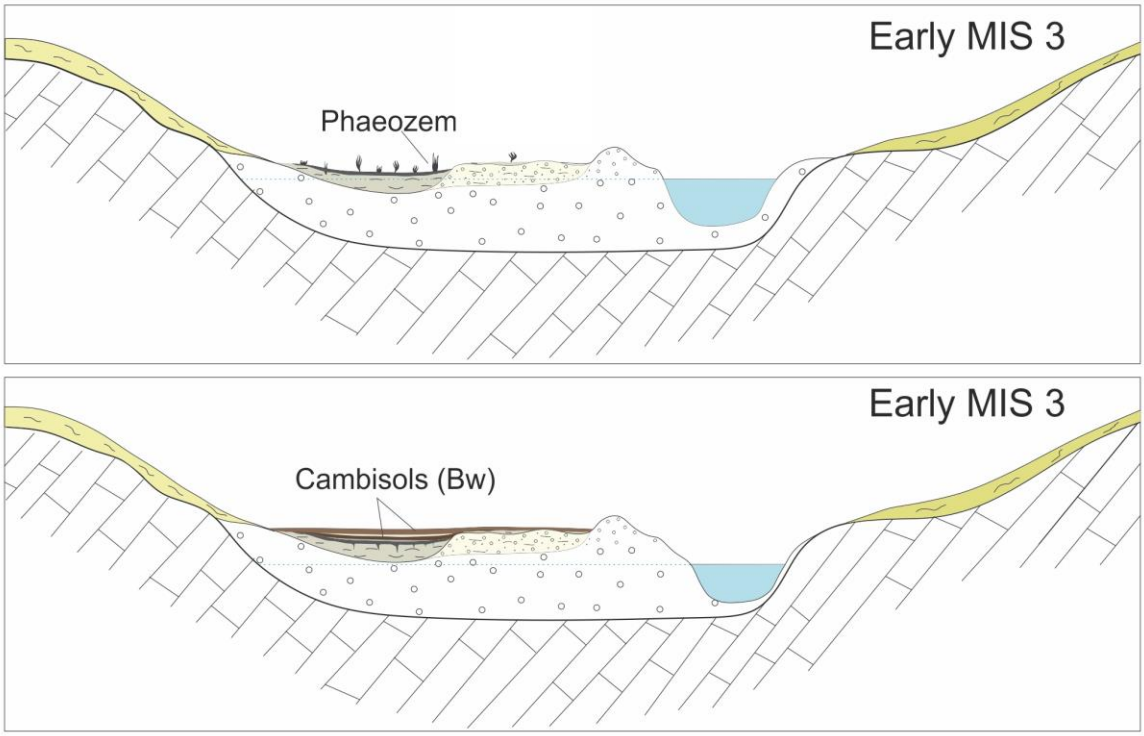

Fig. 8: Schematical cross-sections of the site illustrating the pedo-sedimentary evolution during the Early MIS 3 (~60-50 ka BP).

strate of the upper soil. Later soil forming processes transformed this material into a white layer of silt with a flaky structure (LU_8), which we interpret as a Ca horizon of the upper soil. This interpretation is supported by the micritic carbonate prevailing in the matrix and by the absence of molluscs and other biological residues of the aquatic environment (table 2).

The gleying process in both soils is indicated by abundant redoximorphosis composed mainly of neoformed dendritic Fe-Mn oxides (aggregate nodules) (P2/8, Fig. 4e).

However, it should be noted that these nodules cannot be interpreted only as a result of coeval pedogenesis, since they occur in all strata including soil horizons, loess layers, and loess derivatives (see Tab. 2). These nodules obviously resulted from *in situ*, but post-depositional redoximorphic processes (Lindbo et al., 2010). In some parts, visible bacterial Fe oxide staining is a clear sign of water table oscillations and frost-thaw processes (Van Vliet-Lanoë, 1998).

In contrast, the position of sequence B above the paleo-channel (Fig. 2), where more moisture was available, could be attributed to pedogenesis of remarkable intensity. A similar situation was previously described at the Datthausen site along the upper Danube River in SW Germany (Sauer et al., 2016). Together, convex morphology and the cohesive surface of the channel structure, where a high dynamic of colluvial sediment aggradation would be expected, promoted distinct soil differentiation (soil divergence) and allowed the formation of the pedocomplex. In contrast, soil development outside the paleo-channel, in flat relief, would have been limited; that is, polygenetic soil forming processes (soil divergence) resulted in less differentiation of the particular soil sequence. The thickness of the soil horizons outside the paleo-channel depression could also have been significantly reduced by later erosion processes.

In the context of the Carpathian Basin, there is no evidence for this kind of paleosol development during the early MPG. The described pedo-sedimentary sequence is much more similar to records from north-west Europe. Among these, the sequence at the Schwalbenberg section in the Middle Rhine valley bears, in particular, a striking resemblance to the record from Bíňa. At Schwalbenberg, the basal soils of the lithostratigraphic Ahrgau Member unit – two individual Bw horizons of calcic Cambisol separated by soil sediments (Remagen R1 and R2) – have been evaluated as the most mature MPG soils (Frechen and Schrimer, 2011; Schirmer, 2012; Schirmer, 2016). The development of these soils has been dated, similarly to those from Bíňa, to between 62.4±6.5 ka and 50.6±6.0 ka (Klasen et al., 2015), and they have been directly correlated with the Greenland interstadials GI-17+16 and GI-14 (Shirmer, 2016). Further evidence of a stratigraphically corresponding pedogenesis during the early MPG has been found at the Nussloch site in the Upper Rhine area (Gräselberger soils), within the area of Northern France (the lower horizon of the Villiers-Adam soil complex; Antoine et al., 2003), and in Belgium (the Les Vaux Soil; Haesaerts, 1985). All these Cambisols have been dated to ±55 ka. However, in comparison with these soils, the diminution of the particular paleosols of sequence B at Bíňa seems to be less pronounced and thus these Cambisols at Bíňa are preserved in a more complete state.

Further pedostratigraphic and paleogeographic implications of the paleosols from sequence B are discussed in section 5.2.

5.1.3. Middle and late MIS 3 (sequence C, Fig. 9.)

The accumulation of the 0.3-0.5 m thick layer of loess and pellet sands at the base of sequence C correlates with the climatic deterioration after the preceding warm (and humid) period of the early MPG. The age of 53.9 ± 2.5 ka obtained from that strata is remarkably similar to the ages of MPG loess units from many Carpathian sites ('VL1L2' loess of Marković et al., 2008); for instance, 56±4 ka from the Serbian Crvenka site (Stevens et al., 2011) and 53±4 ka and 47±4 ka from the Hungarian sites Tokaj, (Schatz et al., 2012) and Süttő, (Novothny et al., 2011), respectively. This increase in aeolian activity during the middle

MIS 3 has, however, been observed throughout the European Loess Belt.

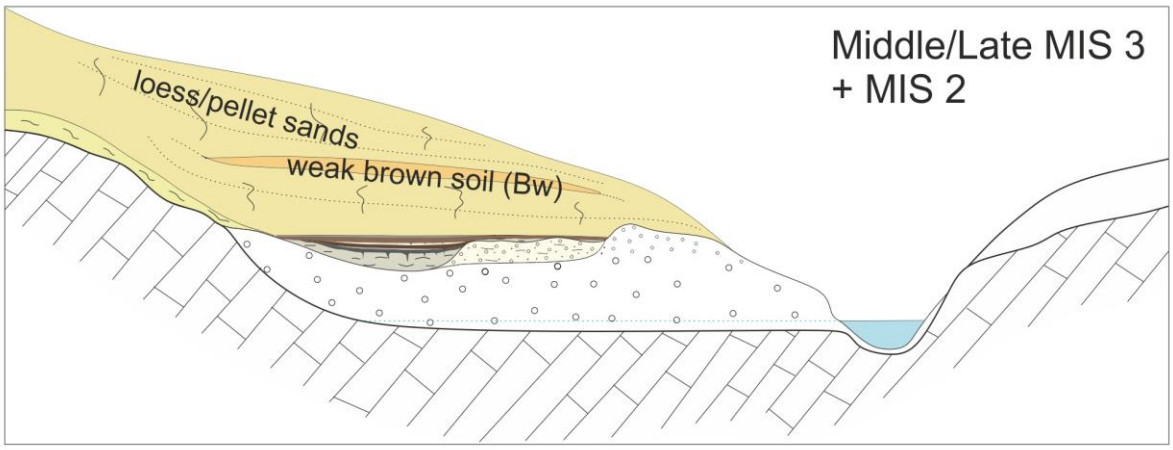

Fig. 9: Schematical cross-section of the site illustrating the pedo-sedimentary evolution during the Middle and Late MIS 3 and MIS 2 (~50-20 ka BP).

The steep increase in Rb/Sr ratio and clay content as well as in magnetic enhancement observed in the above lying soil horizon (LU_5) indicate moister and warmer climate conditions than those prevailing during the accumulation of loess- and pellet-sand before. Several micromorphological features, such as the presence of Fe-Mn-oxides (brunification), indicate the beginning of cambic processes connected with the pseudogleying in this horizon (Fig. 4g sample P1 - 480), which are probably the result of climatic warming in combination with increased precipitation. The presence of micromorphological common passage features reflects high bioturbation activity. In comparison with the lower paleosols (sequence B), this horizon exhibits remarkably weaker signs of hydromorphic processes, which is probably because of changes in the local topography. This observation can be connected with the Hron River incision (Fig. 9) and a subsequent decrease in the water table, which hampered the availability of additional moisture and hence influenced the pedogenesis and diagenesis of the upper sequences (C and D).

According to its stratigraphic position and the OSL date of 36±1.4 ka obtained from the layer above the uppermost Cambisol horizon (LU_5), this paleosol probably corresponds to the boreal brown soil of the lower half of the MPG soil complex PKI (Stillfried B), known from many central European loess sites (see Kukla, 1975). This soil formation is broadly correlated with the NW European interstadial Denekamp (ca 35.5–32.5 ka, GI-8–5), although the lower boundary of this complex may belong to the interval denoted Hengelo (ca 43.5–41.5 ka, GI-11+10) (Richter et al., 2009; Antoine et al., 2013). In NW Europe, these soils correspond, for instance, to Cambisol horizons of the Saint-Acheul/Villiers-Adamm in France (Bahain et al., 1996), Lohner Boden in Germany (Bibus et al., 1989), and the les Vaux soil complexes Haesaerts and Van Vliet-Lanoë, 1974). Across the middle and lower Danube Basin, paleosol horizons of corresponding ages have been documented from numerous LPSs (e.g. Fuchs et al., 2008, 2013; Novothny et al., 2011; Stevens et al., 2011; Timar-Gabor et al., 2016; Constantin et al., 2014). They vary here along the NW-SE transect from boreal brown soils and soils related to the parklands and grasslands of the Middle Danube, to the dry steppe soils of the Lower Danube lowlands (Marković et al., 2015).

From this point of view, the relatively strong cambic processes related to the uppermost Cambisol horizon at the study site suggest that this paleosol is more similar to the bioclimatopedo-zones of the more westerly situated areas of the European Loess Belt rather than to those from the inner parts of the Carpathian Basins.

5.1.3. MIS 3/2 – MIS 2 (sequence D; Figs. 9 and 10)

Some recent studies from the Middle and

Lower Danube Basin (Obreht et al., 2011; Zeeden et al., 2016) as well as palynological records from Western Europe (Sirocko et al., 2016) report a significant trend of continentalization during the late MIS 3 culminating in an increase in aeolian sedimentation and a shift from boreal forest to steppe conditions at ~37 ka BP. At the study site, this climatic shift might be represented by the thick layer of pellet sands (LU_4; Figs. 2 and 3) dated to 36.3±1.4 ka and 36.3±1.9 ka BP. The presence of these slope deposits within the sedimentary sequence has a direct climate-indicative significance, since they probably represent torrential rains that followed prolonged warm and dry seasons (Kukla et al., 1961; Butzer and Isaac, 1975). Such interpretations correspond to the stratigraphic position of the pellet sands in our profiles, as they cover the clayey soil horizons (LU_7 and 5). The presence of soil particles in this sediment is also supported by elevated χ values within the pellet sands (Fig. 3). Malacological records from these strata (Figs. 5 and 6) indicate the environmental conditions of a glacial steppe with the presence of some damper tundra habitats (wetland snail *Pupilla alpicola*). However, as no single aquatic species was found, climatic conditions would probably have been rather dry compared to the older sequences.

The loess body separated from the pellet sands by a distinct erosion event (Fig. 3) probably represents the MIS 2 peak in loess accumulation observed elsewhere in the Carpathian Basin (e.g. Fuchs et al., 2008, Novothny et al. 2011; Stevens et al., 2011) as well as from other sites of the European loess belt (see Frechen, 2011). A weakly developed soil horizon intercalating basal loess accumulation slightly affected by cryogenic processes (cryo-desiccation micro-cracks) is interpreted as an initial pseudogley (LU_3) (Fig. 4f, sample P1_180). These pseudogley characteristics are reflected by the presence of small redoximorphic nodules and initial brunification resulting from short-term increased precipitation in combination with a non-permeable substratum (the presence of permafrost). Weathering/pedogenetic processes during phases of low sedimentation rates are also reflected in the higher Rb/Sr ratio, slight magnetic enhancement, an increase in clay content, and decalcifcation of the particular horizon (Fig. 3). Compared especially to the loess horizons below and generally to the neighboring sediment layers, a notable increase in the number of preserved mollusc shells is observed (see Figs. 5 and 5b), probably linked to the stable environment of a developed grassland vegetation. Thus, during short-term interstadial warming, pedogenesis was promoted revealing the main characteristics of the interstadial phases of the Upper Weichselian. Tundra gleys, which are rather rare in the continental interior and more frequent in the Atlantic part of Europe, were formed at many European sites during the first half of the Late Pleniglacial (~26-20 ka); molluscan assemblages found in the uppermost part of sequence D (LU_2) indicate, similarly to LU_6, a relative increase in cold steppe

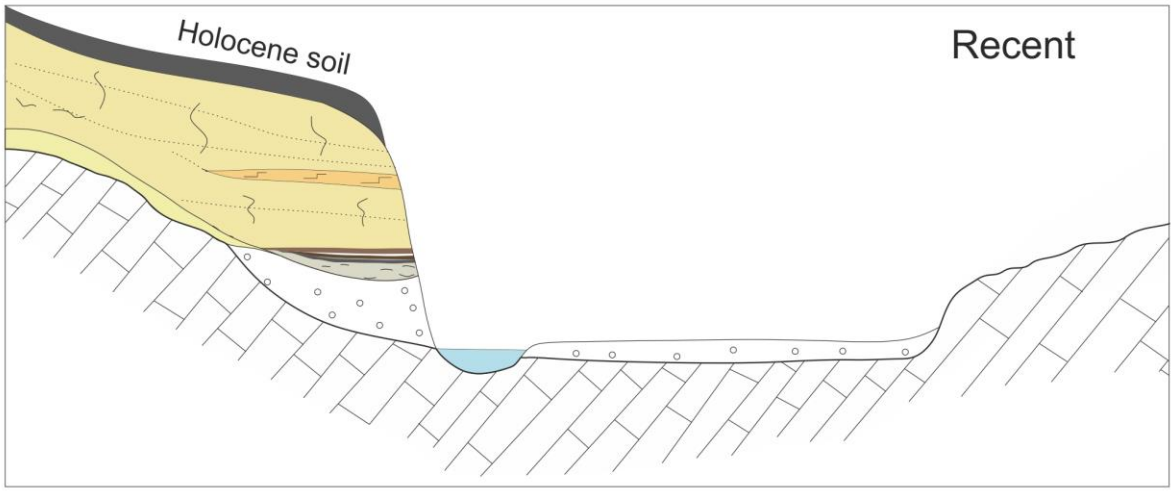

Fig. 10: Schematical cross-section of the site at the present time.

conditions relating these strata to the LGM, during which open-country species such as *Columella columella* and *Vallonia tenuilabris* predominated (Fig. 5). The younger loess layers have probably been eroded, as shown by the sharp boundary that occurs between the loess and the Holocene topsoil. This finding is in accordance with observations at the Tokaj site (NE Hungary; Schatz et al., 2012), and also from many other LPSs throughout the Carpathian Basin (Marković et al., 2015).

5.2. Local pedostratigraphy of the Early MIS 3 in the supraregional context

As recognized in ice-cores and marine records from the North Atlantic, the warmest period of the MIS 3 occurred in the lower part of this isotope stage, during the time interval from approx. 58–48 ka (NGRIP Members, 2004). Recently, the most detailed insight into the environmental responses of terrestrial ecosystems to NA climatic shifts is provided by sedimentological and palaeobiological proxy data from lacustrine archives of the Eifel region (ELSA stacks, western Central Europe; Sirocko et al., 2016). Paleobotanic records clearly demonstrate a distinct increase in thermophylous vegetation between 60–49 ka BP with maxima corresponding to the Greenland Interstadials GI-17 and GI-16, and GI-13 and GI-14, (Landscape Evolution Zones – LEZs 9 and 8). These peaks in tree pollen are in accordance with other records from peat and lacustrine sediments of sub-Atlantic regions (Woillard and Mook, 1982; de Beaulieu and Reille, 1984; Guiot et al., 1989), where these warm and wet periods are usually associated with the NW-European interstadials Oerel and Glinde dated to 58-54 ka BP and 51-48 ka BP, respectively (Behre and van der Plicht, 1992). The increased moisture and vegetation cover and consequently suppressed aeolian sedimentation should have made pedogenesis more dynamic. However, rapid warming of the MPG is, at many sites, represented by a strong erosion event and is rather linked to thermo-karst processes than to soil formation (Antoine et al., 2016). Consequently, a potentially existing early MPG paleosol horizon could have been eroded by subsequent climatic extremes (Huissteden et al., 2001). Furthermore, the dating uncertainty of many LPS is large, which makes it difficult to assign individual paleosols to particular MIS 3 interstadials, and thus some soils or soil complexes tend to date from more than one interstadial (e.g., Frechen et al., 2001). For these reasons the unambiguous correlation of the formation and preservation of paleopedological and loessic horizons during the MIS 3 to individual NW European pollen-based interstadials or the Greenland Interstadials remains difficult (Marković et al, 2015). Well-stratified records of contemporaneous or alternating sedimentation and pedogenesis can thus only be preserved in specific hydroclimatic and geomorphological settings, where pedogenesis was promoted and paleosols were protected from erosion.

Up to now, such kinds of records have only been known from the extra-Pannonian part of Europe. Among these, the most complete and detailed record of MPG paleosols was found at Schwalbenberg in the Middle Rhine valley, which revealed for the first time that paleosols developed during all MIS 3 interstadials, especially during the early MIS 3 (Schirmer, 2016). At this site, two individual Bw horizons of calcic Cambisol can be correlated to LPZs 9 (60-55 ka BP) and 8 (55-49 ka BP) (*sensu* Sirocko et al., 2016), clearly demonstrating the close relationship between climate, vegetation and soil development.

The pedo-sedimentary record of the Bíňa site suggests that the effect of early MPG humid phases, primarily known from the sub-Atlantic region, were not necessarily restricted to the western part of Europe. On the basis of the OSL ages (62.9±2.9 ka and 53.9±2.5 ka) obtained from the sediments under and above sequence B (Figs. 2 and 3), we can correlate the Phaeozem horizon (LU_11) and the lower Bw horizons of the Cambisol (LU_9b) to the Greenland interstadials GI-17/16 (NW-European Oerel interstadial). These soils may be equivalent to the Remagen R1 Cambisol from Schwalbenberg and could reflect the climatic amelioration detected in the Eifel maar record

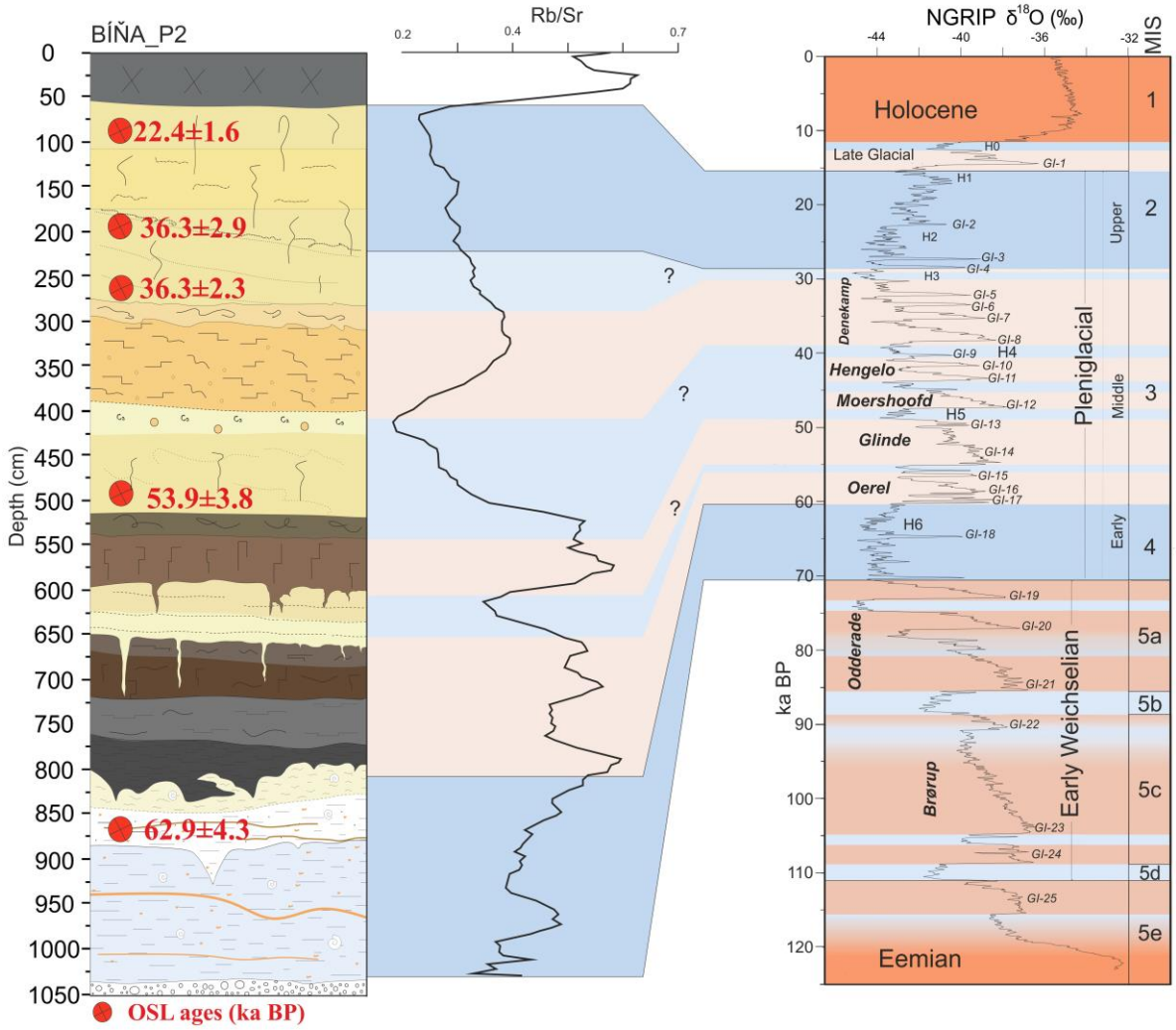

Fig. 11: Lithostratigraphy of the profile P2 and Rb/Sr record (proxy for chemical weathering intensity) correlated with the NGRIP oxygen isotope record (NGRIP members, 2004) and NW-European Weichselian interstadials.

(LPZ 8, Sirocko et al., 2016). The development of the upper and more strongly developed Cambisol (LU_7b) probably corresponds to GI-14 (the Glinde interstadial). This interstadial are recognized in the ELSA stack record as the longest warm period of the MIS 3, characterized by spruce and hornbeam forest with thermophilous trees (LPZ 8; Sirocko et al., 2016). This Cambisol (LU_7b) eventually belonged to the most prominent Greenland interstadial GI-12, associated with the NW-European interstadial Moershoofd (see Fig. 11). The layer of soil sediment and silt (LU_8), which was transformed into the Ca horizon of the upper soil, was then probably deposited during the cold oscillation between the Oerel and Glinde interstadials (Ebersdorf stadial; Heinrich Event 5.2) and the overlaying loess and pellet sands probably during the prominent cold oscillation HE 5.

Although the pedogenesis in sequence B surely benefited from the specific local hydro- and geomorphological settings, this pedosedimentary record is not necessarily limited to this particular site. A very similar record within the Carpathian Basin can be found at the Süttő site (approx. 30 km away; northern Hungary), where two thin horizons of weak brown soils are bordered with loess layers dated to 48.0±4 ka, 59.1±4.6 ka, and 64.8±5.2 ka (Novothny et al., 2009), but attributed to the Early Weichselian period. Furthermore, along the lower Hron River there are several outcrops with preserved humic paleosols. They have not been dated so far; however, their stratigraphic position is very similar to those from Bíňa (e.g. Kamenica nad Hronom, Malá n. Hronom, Velké Ľudanice – Halouzka

and Schmidt, 1979; Schmidt, 1979). In contrast, unambiguous correlation of the pedo-sedimentary records of sequence B from Bíňa to records of the plateau-loess-facies from the Middle and Lower Danube regions is presently not possible. The dry to semi-arid conditions, prevailing during the entire MIS 3 around the threshold between loess formation and initial pedogenesis (Marković et al., 2016), have resulted in hardly distinguishable differences between loess and initial pedogenic layers.

Our observations support the idea that during the MPG the northern rim of the Carpathian Basin was climatically different from the central and southern areas, where more continental conditions prevailed.
Nowadays, cloud cover is further north and east than south and west of the Carpathians, which seem to block the clouds and the air masses coming from the regions north of the Carpathians (Philipp et al., 2010; Spinoni et al., 2016). As a result, there is higher precipitation in the northern pericarpathian zones relative to the inner part of the Carpathian Basin. In the study area, the precipitation reaches up to 700 mm per annum, more than twice that in the inner part of the Carpathian Basin. Furthermore, the precipitation is significantly influenced by the regional topography, creating a sharp boundary between loess and decalcified loess-like sediments: loess-like sediments have been found at the same altitude only 15 km to the North.
Whereas during cold phases of the last Glacial, the maximum extent of the northern European ice sheet may have partially blocked the penetration of Atlantic air masses to the east (Dodonov and Baiguzina, 1995, Wohlfarth, 2008), a sudden resumption of Atlantic Thermohaline Circulation during the MIS3 caused the reorganisation of atmospheric circulation. The low-pressure was shifted to the east and slightly to the south, resulting in dominant westerly air circulation which provided the moisture for easterly located regions of the North and West Carpathians (Barron and Pollard, 2002). General climatic conditions could thus have been similar to those prevailing nowadays, with the highest precipitation in the mountains and up-slopes.
In the Western Carpathians, the climatic amelioration connected with the beginning of the MPG can be correlated with the humid phase revealed from the pollen record of the Šafářka site (Jankovská et al., 2002), situated in the Carpathian foothills (450 m a.s.l.) approx. 170 km NE of the study site. In the pollen spectrum this phase was characterized by forest succession from *Larix decidua* to dense *Picea abies* taiga. Another western Carpathian MIS 3 pollen and plant macrofossil record from peat deposits provides evidence for dense taiga forest cover until the onset of the Last Glacial Maximum (Jankovská and Pokorný, 2008; Kuneš et al., 2008). Similarly, at two sites in the southern foothills of the Western Carpathians (approx. 80 km NE of the study site) a number of thermophile molluscs species characteristic of woodlands were found, indicating the presence of relatively dense forest during the last Pleniglacial (Ložek, 2006).

6. Conclusion

Here, we present the results of an interdisciplinary study of a new LPS site situated on the north-eastern edge of the Carpathian Basin along the Danube Uplands. Using a multi-proxy approach based on sedimentological, geochemical, and rock-magnetic methods combined with a malacological record, soil micromorphology, and OSL dating, we reconstructed the genetic sequence of erosion/sedimentation processes and pedogenesis during the Last Pleniglacial (~ 60 to 20 ka BP). The study sequence represents the most complete pedo-sedimentary record of the middle Pleniglacial (MIS 3) within the northern Carpathian Basin, where the high dynamics of erosion during the last Pleniglacial significantly limited sediment accumulation and soil preservation.
The preservation as well as development of the well-stratified study record is closely related to the specific hydro- and geomorphological settings of a paleo-channel structure, which promoted the distinct differentiation of soils and allowed the formation of the well-developed pedocomplex. Particular paleosols (Bw horizons of Cambisols) were correlated

with the early MIS 3 Glinde and Oerel interstadials in north-western Europe and with the middle/late MIS 3 Denekamp-Hengelo interstadials. Although the soil development benefited from the specific local settings, we propose that the recorded paleosols can also be related to the interregional climate differences of the Carpathian Basin: Within the northerly pericarpathian zones, moister climates predominated during the last Pleniglacial, in contrast to the drier more continental areas to the South. Our observations and interpretations suggest that the transitional zone between the two climate modes of the Upper Pleistocene within the Carpathian Basin was probably quite narrow. Yet, to confirm or reject this hypothesis, further data from this northerly region are required.

Acknowledgement.

This research was possible thanks to Project no. 13-08169S of the Grant Agency of the Czech Republic (GAČR). Matthew Nicholls is acknowledged for improving our English.

References:

Antoine, P., Catt, J., Lautridou, J.-P., Sommé, J., 2003. The loess and coversands of northern France and southern England. Journal of Quaternary Science 18, 309–318.

Antoine, P., Rousseau, D. D.D.-D., Degeai, J. P., Moine, O., Lagroix, F., Kreutzer, S., Fuchs, M., Hatté, C., Gauthier, C., Svoboda, J., Lisá, L., 2013. High-resolution record of the environmental response to climatic variations during the Last Interglacial-Glacial cycle in Central Europe: the loess-paleosol sequence of Dolní Věstonice (Czech Republic). Quaternary Science Reviews 67, 17-38.

Antoine, P., Coutard, S., Guerin, G., Deschodt, L., Goval, E., Locht, J.-L., Paris, C., 2016. Upper Pleistocene loess-palaeosol records from Northern France in the European context: Environmental background and dating of the Middle Palaeolithic. Quaternary International 411, 4–24.

Bábek, O., Chlachula, J., Grygar, J., 2011. Non-magnetic indicators of pedogenesis r elated to loess magnetic enhancement and depletion: Examples from the Czech Republic and southern Siberia. Quaternary Science Reviews 30, 967–979.

Bahain, J.J., Locht, J.L., Drwila, G., Raymond, P., Antoine, P., Caspar, J. P., Debenham, N., Gauthier, A., Krier, V. & Limondin, N., 1996. Le gisement paléolithique moyen du "Petit-Saule" et la séquence pléistocènes du "Chamesson" de Villiers-Adam (Val d'Oise). Document Final de Synthése, AFAN/SRA Ile de France/SDA Val d'Oise, 78 pp.

Barron, E., Pollard, D., 2002. High-Resolution Climate Simulations of Oxygen Isotope Stage 3 in Europe. Quaternary Research 58, 296–309.

Beaulieu, J.L. de, Reille, M., 1984. A long Upper Pleistocene pollen record from Les Echets, near Lyon, France. Boreas 13, 111-132.

Behre, K.E., 1989. Biostratigraphy of the last glacial period in Europe. Quaternary Science Reviews 8 (1), 25-44.

Behre, K.E., van der Plicht, J., 1992. Towards an absolute chronology for the last glacial period in Europe: radiocarbon dates from Oerel, northern Germany. Vegetation History and Archaeobotany, 1 (2), 111–117.

Berger, A., 1978. Long-Term Variations of Daily Insolation and Quaternary Climatic Changes. Journal of the Atmospheric Sciences 35, 2362–2367.

Bibus, E., von Rähle, B., Zöller, L., 1989. Programm und Exkursionsführer zur 8. Tagung des Arbeitskreises "Paläoboden" des Deutschen Bodenkundlichen Gesellschaft, Heilbronn, 31.

Bokhorst, M.P., Beets, C.J., Marković, S.B., Gerasimenko, N.P., Matviishina, Z.N., Frechen M., 2009. Pedo-chemical climate proxies in Late Pleistocene Serbian–Ukrainian loess sequences. Quaternary International 198 (1–2), 113–123.

Brunck, H., Sirocko, F., Albert, J., 2016. The ELSA-Flood-Stack: A reconstruction from the laminated sediments of Eifel maar structures during the last 60000 years. Global and Planetary Change 142, 136-146.

Buggle, B., Glaser, B., Zöller, L., Hambach, U., Marković, S.B., Glaser, I., Gerasimenko, N., 2008. Geochemical characterization and origin of Southeastern and Eastern European loesses (Serbia, Romania, Ukraine). Quaternary Science Reviews 27, 1058-1075.

Buggle, B., Glaser, B., Hambach, U., Gerasimenko, N., Marković, S., 2011. An evaluation of geochemical weathering indices in loess–paleosol studies. Quat. Int. 240, 12–21.

Buggle, B., Hambach, U., Kehl, M., Markovic, S.B., Zoller, L., Glaser, B., 2013. The progressive evolution of a continental climate in southeast-central European lowlands during the Middle Pleistocene recorded in loess paleosol sequences. Geology 41, 771–774.

Bullock, P., Federoff, N., Jongerius, A., Stoops, G., Tursina, T., Babel U., 1985. Handbook for soil thin section description. Waine Research Publications, Wolverhampton, UK, 396 pp.

Butzer, K.W., Isaac, G.L., 1975. After the Australopithecines: stratigraphy, ecology, and culture change in the Middle Pleistocene. Mouton, The Hague.

Chen, J., An, Z., Head, J., 1999. Variation of the Rb/Sr ratios in the loess / paleosol sequences of Central China

during the last 130,000 years and their implications for monsoon paleoclimatology. Quaternary Research 51, 215-219.

Cílek V., 2001. The loess of the Bohemian Massif: silt provenance, palaeometeorology and loessification processes. Quaternary International 76-77, 123-128.

Dansgaard, W., Gundestrup, N., 1993. Greenland: a temptation and a challenge. Endeavour 17, 12–16.

Demek, J., Kukla, J. (Eds.), 1969: Periglazialzone, Löss und Paläolithikum der Tschechoslowakei. Czechoslovak Academy of Sciences – Institute of Gegraphy, Brno, 156 pp.

Dodonov, A.E., Baiguzina, L.L., 1995. Loess stratigraphy of Central Asia: Palaeoclimatic and palaeoenvironmental aspects. Quaternary Science Reviews 14 (7–8), 707–720.

Elias, S.A., 2013. Encyclopedia of quaternary science. Elsevier, Ansterdam.

Engels, S., Bohncke, S.J.P., Heiri, O., Schaber, K., Sirocko, F., 2008. The lacustrine sediment record of Oberwinkler Maar (Eifel, Germany): Chironomid and macro-remain-based inferences of environmental changes during Oxygen Isotope Stage 3. Boreas 37, 414–425.

Feurdean, A., Persoiu, A., Tantau, I., Stevens, T., Magyari, E.K., Onac, B.B., Markovic. S., Andric, M., Connor, S., Galka, M., Hoek, W.S., Lamentowicz, M., Sümegi, P., Persoiu, I., Kolaczek, P., Kuneš, P., Marinova, E., Slowinski, M., Michczyńska, D., Stancikaite, M., Svensson, A., Veski, S., Fărcaş, S., Tămaş, T., Zernitskaya, V., Timar, A., Tonkov, S., Toth, M., Willis, K.J., Płóciennik, M., Gaudeny, T., 2014. Climate variability and associated vegetation response throughout Central and Eastern Europe (CEE) between 60 and 8 ka. Quaternary Science Reviews 106, 206-224.

Fitzsimmons, K.E., Marković, S.B., Hambach, U., 2012. Pleistocene environmental dynamics recorded in the loess of the middle and lower Danube basin. Quaternary Science Reviews 41, 104–118.

Frechen, M., Oches, E.A., Kohfeld, K. E., 2003. Loess in Europe—mass accumulation rates during the Last Glacial Period. Quaternary Science Reviews 22 (18), 1835-1857.

Frechen, M., 2011. Loess in Eurasia. Quaternary International 234, 1–3.

Frechen, M., Schirmer, W., 2011. Luminescence chronology of the Schwalbenberg II loess in the middle Rhine valley. Quat. Sci. J. 60, 78-89. http://dx.doi.org/10.3285/eg.60.1.05.

Fuchs, M., Rousseau, D.D., Antoine, P., Hatté, C., Gauthier, C., Marković, S., Zöller, L., 2008. Chronology of the last climatic cycle (Upper Pleistocene) of the Surduk loess sequence, Vojvodina, Serbia. Boreas 37, 66–73.

Fuchs, M., Kreutzer, S., Rousseau, D.D., Antoine, P., Hatté, C., Lagroix, F.,Moine, O., Gauthier, C., Svoboda, J., Lisá, L., 2013. The loess sequence of Dolní Věstonice, Czech Republic: a new OSL-based chronology of the Last Climatic Cycle. Boreas 42, 664–677.

Galbraith, R.F., Roberts, R.G., Laslett, G.M., Yoshida, H., Olley, J.M., 1999. Optical dating of single and multiple grains of quartz from Jinminum Rock Shelter, Northern 12 Australia. Part I, experimental design and statistical models. Archaeometry 41, 1835- 1857 Guerin, G., Mercier, N., Adamiec, G., 2011. Dose-rate conversion factors: update. Ancient TL 29, 5-8.

Gallet, S., Jahn, B.M., Torii, M., 1996. Geochemical characterization of the Luochuan loess-palaeosol sequence, China, and paaleoclimatic implications. Chemical Geology 133, 67-88.

Genty, D., Blamart, D., Ouahdi, R., Gilmour, M., Baker, A., Jouzel, J., Van-Exter, S., 2003. Precise dating of Dansgaard–Oeschger climate oscillations in western Europe from stalagmite data. Nature 421, 833–837.

Guiot, J., Pons, A., Beaulieu, J. L. de, Reille, M., 1989. A 140,000 year climatic reconstruction from two European pollen records. Nature 338, 309-313.

Haesaerts P., 1985. Les loess du Pléistocène supérieur en Belgique. Comparaisons avec les séquences d'Europe centrale. Bulletin de l'Association Française pour l'Etude du Quaternaire (Paris) 22–23(2–3), 105–15.

Haesaerts, P., Van Vliet-Lanoë, B., 1974. Compte-rendu de l'excursion du 25 mai 1974 consacrée à la stratigraphie des limons aux environs de Mons. Annales de la Société Géologique de Belgique 97 (2), 547–560.

Haesaerts, P., Borziak, I., Chirica, V., Damblon, F., Koulakovska, L., Plicht, J.V.D., 2003. The east Carpathian loess record : a reference for the middle and late pleniglacial stratigraphy in central Europe [La séquence loessique du domaine est-carpatique : une référence pour le Pléniglaciaire moyen et supérieur d'Europe centrale.]. Quaternaire 14, 163–188.

Haesaerts, P., Borziac, I., Chekha, V.P., Chirica, V., Damblon, F., Drozdov, N.I., Orlova, L.A., Pirson, S., Plicht, J.V.D., 2009. Climatic Signature and Radiocarbon Chronology of Middle and Late Pleniglacial Loess from Eurasia: Comparison with the Marine and Greenland Records. Radiocarbon 51, 301–318.

Haesaerts, P., Damblon, F., Gerasimenko, N., Spagna, P., Pirson, S., 2016. The Late Pleistocene loess-palaeosol sequence of Middle Belgium. Quaternary International 411, 25–43.

Halouzka, R., Schmidt, Z., 1979. Brief report on the new climatic-stratigraphic interpretation of late Pleistocene loess series in the Danube Lowland, Slovakia. In: Sibrava, V. and Shotton, F. (eds). Quaternary glaciations in the Northern Hemisphere, International Geological Correlation Programme (IGCP), Project 24, Report 5, 138-145.

Hambach, U., 2010. Paleoclimatic and stratigraphic implications of high resolution magnetic susceptibility logging of Würmian Loess at the Upper Paleolithic KremseWachtberg Site, in: Neugebauer-Maresch, C., Owen, L.R. (Eds.), New Aspects of the Central and Eastern European Upper Palaeolithic - Methods, Chronology, Technology and Subsistence. Proceedings of the Prehistoric Commission of the Austrian Academy of Sciences. Vienna, pp. 295-304.

Horsák, M., Chytrý, M., Pokryszko, B.M., Danihelka, J., Ermakov, N., Hájek, M., Hájková, P., Kintrová, K., Kočí, M., Kubešová, S., Lustyk, P., Otýpková, Z., Pelánková, B., Valachovič, M. 2010. Habitats of relict terrestrial snails in southern Siberia: lessons for the reconstruction of palaeoenvironments of full-glacial Europe. Journal of Biogeography 37 (8), 1450-1462.

Horsák M., Juřičková L., Picka J. 2013. Měkkýši České a Slovenské republiky. Molluscs of the Czech and Slovak Republics. Kabourek, Zlín.

Horsák, M., Chytrý, M., Hájková, P., Hájek, M., Danihelka, J., Horsáková, V., Ermakov, N., German, D. A., Kočí, M., Lustyk, P., Nekola, J. C., Preislerová, Z., Valachovič, M. 2015. European glacial relict snails and plants: environmental context of their modern refugial occurrence in southern Siberia. Boreas 44 (4), 638-657.

Hošek, J., Hambach, U., Lisá, L., Grygar, T.M., Horáček, I., Meszner, S., Knésl, I., 2015. An integrated rock-magnetic and geochemical approach to loess/paleosol sequences from Bohemia and Moravia (Czech Republic): Implications for the Upper Pleistocene paleoenvironment in central Europe. Palaeogeography, Palaeoclimatology, Palaeoecology 418, 344–358.

Hošek, J., Pokorný, P., Prach, J., Lisá, L., Grygar, T.M., Knésl, I., Trubač, J., 2017. Late Glacial erosion and pedogenesis dynamics: Evidence from high-resolution lacustrine archives and paleosols in south Bohemia (Czech Republic). Catena 150, 261–278.

Huber, C., Leuenberger, M., Spahni, R., Flückiger, J., Schwander, J., Stocker, T.F., Johnsen, S., Landais, A., Jouzel, J., 2006. Isotope calibrated Greenland temperature record over Marine Isotope Stage 3 and its relation to CH4. Earth and Planetary Science Letters 243, 504–519.

Huissteden, J.K.V., Gibbard, P., Briant, R., 2001. Periglacial fluvial systems in northwest Europe during marine isotope stages 4 and 3. Quaternary International 79, 75–88.

IUSS Working Group WRB, 2014. World Reference Base for Soil Resources 2014. International soil classification system for naming soils and creating legends for soil maps. Rome.

Jankovská, V., Pokorný, P., 2008. Forest vegetation of the last full-glacial period in the Western Carpathians (Slovakia and Czech Republic). Preslia 80, 307–324.

Jankovská, V., Chromý, P., Nižnanská, M., 2002. „Šafárka“ - first palaeobotanical data of the char-acter of Last Glacial vegetation and landscape n the West Carpathians (Slovakia). Acta Palaeobo-tanica, Kraków, 42, 1, 29 - 52.

Jary, Z., 2009. Periglacial markers within the Late Pleistocene loess–paleosol sequences in Poland and Western Ukraine. Quaternary International 198, 124–135.

Johnsen, S.J., Dansgaard, W., 1992. On Flow Model Dating of Stable Isotope Records from Greenland Ice Cores. The Last Deglaciation: Absolute and Radiocarbon Chronologies 13–24.

Kadereit, A., Kind, C.-J., and Wagner, G. A., 2013. The chronological position of the Lohne Soil in the Nussloch loess section – reevaluation for a European loess-marker horizon. Quaternary Sci. Rev. 59, 67–86, doi:10.1016/j.quascirev.2012.10.026.

Kemp, R.A., 1998. Role of micromorphology in paleopedological research. Quaternary International 51-52, 133–141.

Klasen, N., Fischer, P., Lehmkuhl, F., Hilgers, A., 2015. Luminescence Dating of Loess Deposits from the Remagen-Schwalbenberg site, Western Germany. Geochronometria 42, 67-77.

Kühn, P., Billwitz, K., Bauriegel, A., Kühn, D., Eckelmann, W., 2006. Distribution and genesis of Fahlerden (Albeluvisols) in Germany. Journal of Plant Nutrition and Soil Science 169, 420–433.

Kühn, P., Techmer, A., Weidenfeller, M., 2013. Lower to middle Weichselian pedogenesis and palaeoclimate in Central Europe using combined micromorphology and geochemistry: the loess-paleosol sequence of Alsheim (Mainz Basin, Germany). Quaternary Science Reviews 75, 43–58.

Kukla, J., Ložek, V., Záruba, Q., 1961. Zur stratigraphie der Lösse in der Tschekoslowakei. Quartär, 13, 1-29.

Kukla, J., 1975. Loess stratigraphy of Central Europe. After the Australopithecines (eds. Butzer, K. W., Isaac, G. L.). The Hague: Mouton, 99-188.

Kuneš, P., Pelánková, B., Chytrý, M., Jankovská, V., Pokorný, P., Petr, L., 2008. Interpretation of the last-glacial vegetation of eastern-central Europe using modern analogues from southern Siberia. Journal of Biogeography 35, 2223-2236.

Lehmkuhl, F., Zens, J., Krauß, L., Schulte, P., Kels, H., 2016. Loess-paleosol sequences at the northern European loess belt in Germany: Distribution, geomorphology and stratigraphy. Quaternary Science Reviews 153, 11–30.

Lindbo, D.L., Stolt, M.H., Vepraskas, M.J., 2010. Redoximorphic features, in: Stoops, G., Marcelino, V., Mees, F. (Eds.), Interpretation of Micromorphological features in soils and regoliths, Elsevier, pp. 129-147.

Lisá, L., Hošek, J., Bajer, A., Grygar, T.M., Vandenberghe, D., 2014. Geoarchaeology of Upper Palaeo-

lithic loess sites located within a transect through Moravian valleys, Czech Republic. Quaternary International 351, 25–37.

Ložek, V., 1952. Zpráva o paleontologickém výzkumu kvarteru v okolí Štúrova. Věstník Ústředního ústavu geologického 27(3–4), 174–179.

Ložek, V., 1964. Quartärmollusken der Tschechoslowakei: Mit 32 fotographischen Tafeln. Nakladatelství Československé akademie věd.

Ložek, V., 1965. Das Problem der Lößbildung und die Lössmollusken. Eiszeitalter und Gegenwart 16, 61–75.

Ložek, V., 1976. Klimaabhängige Zyklen der Sedimentation und Bodenbildung während des Quartärs im Lichte malakozoologischer Untersuchungen. Monography of Rozpravy Československé akademie věd, Řada matematických a přírodních věd 86(8), 1–97.

Ložek, V., 2001. Molluscan fauna from the loess series of Bohemia and Moravia. Quaternary International 76-77, 141-156.

Ložek, V., 2006. Last Glacial paleoenvironments of theWest Carpathians in the light of fossil malacofauna. Anthropozoikum 26, 73–84.

Maher, B.A., 1998. Magnetic properties of modern soils and Quaternary loessic paleosols: paleoclimatic implications. Paleogeography Paleoclimatology Paleoecology 137, 25–54.

Margari, V., Gibbard, P., Bryant, C., Tzedakis, P., 2009. Character of vegetational and environmental changes in southern Europe during the last glacial period; evidence from Lesvos Island, Greece. Quaternary Science Reviews 28, 1317–1339.

Markovic, S., Bokhorst, M. P., Vandenberghe, J., Mc Coy, W. D., Oches, E. A., Hambach, U., 2008. Late Pleistocene loess-palaeosol sequences in the Vojvodina region, north Serbia. J. Quat. Sci., 23, 73-84.

Marković, S.B., Hambach, U., Stevens, T., Kukla, G.J., Heller, F., McCoy, W.D., Oches, E.A., Buggle, B., Zöller, L., 2011. The last million years recorded at the Stari Slankamen loess–palaeosol sequence: revised chronostratigraphy and long-term environmental trends. Quaternary Science Reviews 30, 1142–1154.

Marković, S.B., Stevens, T., Kukla, G.J., Hambach, U., Fitzsimmons, K.E., Gibbard, P., Buggle, B., Zech, M., Guo, Z., Hao, Q., Wu, H., O'Hara Dhand, K., Smalley, I.J., Újvari, G., Sümegi, P., Timar-Gabor, A., Veres, D., Sirocko, F., Vasiljević, D.A., Jary, Z., Svensson, A., Jovic, V., Lehmkuhl, F., Kovacs, J., Svircev, Z., 2015. Danube loess stratigraphy - towards a pan-European loess stratigraphic model. Earth-Sciences Reviews 148, 228-258.

Meszner, S., 2012. Loess-paleosol-sequences in Saxony – A terrestrial archive for paleoenvironmental evolution. Quaternary International 279-280, 324.

Murray, A.S., Wintle, A.G., 2000. Luminescence dating of quartz using an improved single-aliquot regenerative-dose protocol. Radiation measurements 32(1), 57-73.

Nesbitt, H.W., Young, G.M., McLennan, S.M., Keays, R.R., 1996. Effects of chemical weathering and sorting on the petrogenesis of siliciclastic sediments, with implications for provenance studies. Journal of Geology 104, 525-542.

Nesbitt, H.W., Markovics, G., Price, R.C., 1980. Chemical processes affecting alkalis and alkaline earths during continental weathering. Geochim. Cosmochim. Acta 44, 1659–1666.

North Greenland Ice Core Project NGRIP Members, 2004. High-resolution record of Northern Hemisphere climate extending into the last interglacial period. Nature 431, 147–151.

Novothny, A., Frechen, M., Horváth, E., Bradák, B., Oches, E. A., McCoy, W. D., Stevens, T., 2009. Luminescence and amino acid racemisation chronology of the loess-paleosol sequence at Süttő, Hungary. Quaternary International 198, 62-76.

Novothny, Á., Frechen, M., Horváth, E., Wacha, L., Rolf, C., 2011. Investigating the penultimate and last glacial cycles of the Süttő loess section (Hungary) using luminescence dating, high-resolution grain size, and magnetic susceptibility data. Quaternary International 234 (1), 75-85.

Obreht, I., Zeeden, C., Schulte, P., Hambach, U., Eckmeier, E., Timar-Gabor, A., Lehmkuhl, F., 2015. Aeolian dynamics at the Orlovat loess–paleosol sequence, northern Serbia, based on detailed textural and geochemical evidence. Aeolian Research 18, 69–81.

Obreht, I., Zeeden, C., Hambach, U., Veres, D., Marković, S.B., Bösken, J., Svirčev, Z., Bačević, N., Gavrilov, M.B., Lehmkuhl, F., 2016. Tracing the influence of Mediterranean climate on Southeastern Europe during the past 350,000 years. Scientific Reports 6.

Philipp, A., Bartholy, J., Beck, C., Erpicum, M., Esteban, P., Fettweis, X., Huth, R., James, P., Jourdain, S., Kreienkamp, F., Krennert, T., Lykoudis, S., Michalides, S.C., Pianko-Kluczynska, K., Post, P., Álvarez, D.R., Schiemann, R., Spekat, A., Tymvios, F.S., 2010. Cost733cat – A database of weather and circulation type classifications. Physics and Chemistry of the Earth, Parts A/B/C 35, 360–373.

Profe, J., Zolitschka, B., Schirmer, W., Frechen, M., Ohlendorf, C., 2016. Geochemistry unravels MIS 3/2 paleoenvironmental dynamics at the loess–paleosol sequence Schwalbenberg II, Germany. Palaeogeography, Palaeoclimatology, Palaeoecology 459, 537-551.

Richter, D., Tostevin, G., Skrdla, P., Davies, W., 2009. New radiometric ages for the Early Upper Palaeolithic type locality of Brno-Bohunice (Czech Republic): comparison of OSL, IRSL, TL and 14C dating results. Journal of Archaeological Science 36, 708-720.

Sauer, D., Kadereit, A., Kühn, P., Kösel, M., Miller,

C.E., Shinonaga, T., Kreutzer, S., Herrmann, L., Fleck, W., Starkovich, B.M., Stahr, K., 2016. The loess-palaeosol sequence of Datthausen, SW Germany: Characteristics, chronology, and implications for the use of the Lohne Soil as a marker soil. Catena 146, 10–29.

Schatz, A.-K., Buylaert, J.-P., Murray, A., Stevens, T., Scholten, T., 2012. Establishing a luminescence chronology for a paleosol-loess profile at Tokaj (Hungary): A comparison of quartz OSL and polymineral IRSL signals. Quaternary Geochronology 10, 68–74.

Schirmer, W., 2012. Rhine loess at Schwalbenberg IIeMIS 4 and 3. Eiszeitalter und Gegenwart Quat. Sci. J. 61.

Schirmer, W., 2016. Late Pleistocene loess of the Lower Rhine. Quaternary International 411, 44-61.

Smidt, Z., Horniš, J. Halouzka, R., 1979. Výskum kvartéru južných častí dolného Pohronia, Ipeľskej pahorkatiny a dolného Piplia. MS, GUDŠ, Bratislava.

Schmidt, E., Machalett, B., Marković, S., Tsukamoto, S., Frechen, M., 2010. Luminescence chronology of the upper part of the Stari Slankamen loess sequence (Vojvodina, Serbia). Quaternary Geochronology 5, climatologies and trends of 10 variables. International Journal of Climatology 35, 1322–1341.

Stevens, T., Marković, S.B., Zech, M., Hambach, U., Sümegi, P., 2011. Dust deposition and climate in the Carpathian Basin over an independently dated last glacial–interglacial cycle. Quaternary Science Reviews 30, 662–681.

Stoops, G., 2003. Guidelines for Analysis and Description of Soil and Regolith Thin Sections. Soil Science Society of America, Madison, Wisconsin, 348 pp.

Stoops, G., Marcelino, V., Mees, F., 2010. Interpretation of Micromorphological Features of Soils and Regoliths. Elseiver.

Thompson R., Oldfield F., 1986. Environmental Magnetism. London, Allen & Unwin Ltd., 280 pp.

Timar-Gabor, A., Panaiotu, C., Vereş, D., Necula, C., Constantin, D., 2016. The Lower Danube Loess, New Age Constraints from Luminescence Dating, Magnetic Proxies and Isochronous Tephra Markers, in Radoane, M., Vespremeanu-Stroe, A. (Eds.), Landform Dynamics and Evolution in Romania, Springer Geography, pp. 679–697.

Van Vliet-Lanoe, B., 1998. Frost and soils: implications for paleosols, paleo-climates and stratigraphy. Catena 34, 157-183.

Winkler, S., Matthews, J.A., 2010. Holocene glacier chronologies: Are 'high-resolution' global and interhemispheric comparisons possible? The Holocene 20, 1137–1147.

Woillard, G.M., Mook, W.G., 1982. Carbon-14 dates at Grande Pile: Correlation of land and sea chronologies. Science 2l5, 159- 161.

137–142.

Sirocko, F., 2016. The ELSA - Stacks (Eifel-Laminated-Sediment-Archive): An introduction. Global and Planetary Change 142, 96–99.

Sirocko, F., Knapp, H., Dreher, F., Förster, M., Albert, J., Brunck, H., Veres, D., Dietrich, S., Zech, M., Hambach, U., Röhner, M., Rudert, S., Schwibus, K., Adams, C., Sigl, P., 2016. The ELSA-Vegetation-Stack: Reconstruction of Landscape Evolution Zones (LEZ) from laminated Eifel maar sediments of the last 60,000 years. Global and Planetary Change 142, 108–135.

Spinoni, J., Szalai, S., Szentimrey, T., Lakatos, M., Bihari, Z., Nagy, A., Németh, Á., Kovács, T., Mihic, D., Dacic, M., Petrovic, P., Kržič, A., Hiebl, J., Auer, I., Milkovic, J., Štepánek, P., Zahradnícek, P., Kilar, P., Limanowka, D., Pyrc, R., Cheval, S., Birsan, M.-V., Dumitrescu, A., Deak, G., Matei, M., Antolovic, I., Nejedlík, P., Štastný, P., Kajaba, P., Bochnícek, O., Galo, D., Mikulová, K., Nabyvanets, Y., Skrynyk, O., Krakovska, S., Gnatiuk, N., Tolasz, R., Antofie, T., Vogt, J., 2014. Climate of the Carpathian Region in the period 1961-2010:

Wohlfarth, B., Veres, D., Ampel, L., Lacourse, T., Blaauw, M., Preusser, F., Andrieu-Ponel, V., Kéravis, D., Lallier-Vergès, E., Björck, S., Davies, S.M., Beaulieu, J.-L.D., Risberg, J., Hormes, A., Kasper, H.U., Possnert, G., Reille, M., Thouveny, N., Zander, A., 2008. Rapid ecosystem response to abrupt climate changes during the last glacial period in western Europe, 40–16 ka. Geology 36, 407.

Zeeden, C., Hambach, U., Veres, D., Fitzsimmons, K., Obreht, I., Bösken, J., Lehmkuhl, F., 2016. Millennial scale climate oscillations recorded in the Lower Danube loess over the last glacial period. Palaeogeography, Palaeoclimatology, Palaeoecology, in press.

PŘÍLOHA III

Lisá, L. – Hošek, J. – Matys Grygar, T. – Bajer, A. – Vandenberghe, D. (2014): Geoarchaeology of Upper Palaeolithic loess sites located within a transect through Moravian valleys, Czech Republic. – Quaternary International 351, 25-37.

Quaternary International 351 (2014) 25–37

Contents lists available at ScienceDirect

Quaternary International

journal homepage: www.elsevier.com/locate/quaint

Geoarchaeology of Upper Palaeolithic loess sites located within a transect through Moravian valleys, Czech Republic

L. Lisá [a, *], J. Hošek [b, c], A. Bajer [d], T. Matys Grygar [e], D. Vandenberghe [f]

[a] Institute of Geology, Academy of Sciences of the Czech Republic, Rozvojova 269, Prague 165 00, Czech Republic
[b] Czech Geological Survey, Klárov 3, Prague 118 21, Czech Republic
[c] Institute of Geology and Palaeontology, Faculty of Science, Charles University in Prague, Albertov 6, Prague 2, Czech Republic
[d] Faculty of Forestry and Wood Technology, Mendel University, Zemědělská 3, Brno 613 00, Czech Republic
[e] Institute of Inorganic Chemistry, Academy of Sciences of the Czech Republic, 250 68 Řež, Czech Republic
[f] The Research Foundation – Flanders (FWO – Vlaanderen), Laboratory of Mineralogy and Petrology (Luminescence Research Group), Department of Geology and Soil Science, Ghent University, Krijgslaan 281 (S8), B-9000 Gent, Belgium

ARTICLE INFO

Article history:
Available online 3 October 2013

ABSTRACT

The Middle and Upper Palaeolithic sites situated within the system of Moravian and South Silesian valleys are key localities for understanding the patterns of seasonal mobility that enabled humans to exploit the North European Plain, and a possibility to distinguish the importance of the weather and climate for their subsistence practises. Loess accumulations that have covered the best preserved open air Palaeolithic sites in Central Europe display the climatic record covering at least 30,000 years. The sedimentological, microstratigraphical and geochemical record of three studied Upper Palaeolithic loess sites show significant changes, documenting increased precipitation towards the north. A progressive coarsening of the loess deposits during the Upper Pleniglacial, contrasting with the progressive fining toward the North European glaciation was detected. This methodological approach explains more precisely the context of formation processes connected also with human activity within the corridor between the North European Plain and the Danube Basin, through which a wide range of organisms, including humans and their prey species, were channelled.

1. Introduction

Upper Palaeolithic sites located along a transect between the Danube region, Moravian valleys, and the North European Plain offer unique insights into an early episode of modern human adaptations to the landscape (Otte, 1981; Svoboda et al., 2002; Oliva, 2005, 2007; Lisá et al., 2013). The system of Moravian valleys, oriented mainly N–S or NE–SW (Czudek, 1997), provides a valuable archaeological trap for two reasons. First, it constitutes wide river valleys between transcontinental mountain ranges through which a wide range of organisms, including humans and their prey species, were channelled: this has always been the principal access route to the North European Plain from the Danube Basin (Skutil, 1955; Valoch, 1979; Svoboda et al., 2002; Trinkaus and Svoboda, 2006). Second, it is also a trap for wind-blown sediments flowing preferentially from the W or NW, SW to the E or NE, SE (Lisá, 2004; Lisá and Uher, 2006; Lisá et al., 2009) that have accumulated to considerable depths around many a hilly protuberance in that landscape. It is these deep accumulations of loess that have covered the best preserved open air Palaeolithic sites in Europe (Svoboda et al., 2002). The lithological record of those localities was described mainly in the case of the famous Dolní Věstonice old brickyard section (Klíma et al., 1962; Bábek et al., 2011; Antoine et al., 2013), but the geochemical and micromorphological record of other localities situated more northerly in Moravia was less studied. Instrumental sedimentological analyses can bring valuable information about environmental conditions which Palaeolithic hunters had to accept in hunting large mammals. The main question addressed in this paper is, therefore: is it possible to distinguish any significant lithological or geochemical differences between three of the most important Upper Palaeolithic regions within Moravia and use the interpretations of those differences to discuss climatic changes of Middle and Upper Pleniglacial and the reasons which enabled humans to exploit the North European Plain, and subsequently even colder regions?

* Corresponding author.
E-mail address: lisa@gli.cas.cz (L. Lisá).

1040-6182/$ – see front matter © 2013 Elsevier Ltd and INQUA. All rights reserved.
http://dx.doi.org/10.1016/j.quaint.2013.08.058

2. Geographical and sedimentological background

Three key localities for Moravian Upper Palaeolithic history are used in this study. The localities are typical for long term temporary Gravettian occupation (Nývltová Fišáková, 2013) and are situated along a transect between South Moravia (Dolní Věstonice), Central Moravia within Moravian Gate (Předmostí), and North–East Moravia (Hošťálkovice locality near Petřkovice). The imaginary section connecting those three localities provides information about the different sedimentological records preserved, and the differences of environmental conditions which Palaeolithic hunters had to accept in hunting large mammals.

The Last Glacial loess formation within the area of Central Europe was strongly influenced by its geographical position between two glaciers. In that time Moravia and Silesia were situated in the narrowest part of the non-glaciated area and became very important for loess formation as well as for the fauna (Ložek, 1968; Horáček and Ložek, 1988), flora (Frenzel, 1968) and human migrations (Svoboda et al., 2002).

2.1. Dolní Věstonice II (DV II)

This section was excavated in the context of the archaeological research of the Gravettian site during the 2005 season. The studied section is located in anthropogenic terraces on the slope above the famous Dolní Věstonice – old brickyard section. The 4.2 m thick profile DV II covers the Gravettian cultural layer and the Upper Pleniglacial sedimentary record correlated with the upper part of the old brickyard section. The section in the old brickyard represents the most prominent loess section accessible today in Central Europe and, therefore, enormous numbers of different research efforts were made there (Klima et al., 1962; Demek and Kukla, 1969; Haesaerts and Mestdagh, 2000; Fuchs et al., 2012; Antoine et al., 2013). Approximately 18 m of loess, loess like deposits, and paleosols cover a relatively complete Last climatic cycle and display warming, cooling, and wetting trends. The loess was in this case derived mainly from frost shattered and weathered magmatic and metamorphic rocks situated to the west, deposited as eluvial deposits or as river alluvium (Lisá, 2004; Lisá and Uher, 2006; Lisá et al., 2009), and calcareous Miocene deposits (Adamová, Havlíček, 1998). The provenance during the last glacial period did not change (Lisá et al., 2009) and the grain size differences depend mostly on the wind speed or post-depositional weathering.

2.2. Předmostí

Close to the town of Přerov, and to the southern entrance to the Moravian Gate, a series of loess deposits has been extensively excavated. A rescue excavation in the last century produced a considerable body of data relating to various Palaeolithic episodes, mainly of Gravettian Age (Svoboda et al., 1994). Předmostí is located at the southern entrance of the Moravian Gate, one of the most important passing points of prehistoric routes in Central Europe (Svoboda et al., 1994). Originally two limestone formations, at Skalka in the south and Hradisko in the north, emerged from the Neogene and Quaternary deposits. Both of them have nearly disappeared due to limestone exploitation. Several mineral spring sources are known close to the site, which formed travertine deposits (Kovanda, 1971). One, with a constant temperature of 12 °C was located directly at the foot of the former Skalka hill (Svoboda et al., 1994). The cultural content of this locality has been classified as Gravettian or Pavlovian with a hypothetical Aurignacian horizon below. The Gravettian was dated approximately to 26–27 ka (Svoboda et al., 1994).

2.3. Hošťálkovice

Hošťálkovice is situated in Northern Moravia in the Ostrava region. This locality is 1.5 km from Petřkovice, famous for the Venus finding (Svoboda, 2004). Unfortunately, Petřkovice could not be included in this research because of technical problems. Hošťálkovice, nevertheless, offers the similar stratigraphy (Folprecht, 1934; Neruda and Nerudová, 2000) and its location was suitable for our research. The site was excavated in 1992 by P. Neruda (Neruda and Nerudová, 2000). This site lies beyond the Moravian Gate at the opening of the North European Plain. It has also a significant history of archaeological investigation, allowing us to target location of an approximately 1.6 deep test pit to capture the layer with Gravettian artefacts.

3. Methodology

3.1. Micromorphology

Microstratigraphical study, micromorphology in archaeological context, was applied in all three localities. In total, 53 samples for thin sections were taken. A micromorphological approach covers descriptive microstratigraphical analyses (Bullock et al., 1985) including microfabric types, structural and porosity features, natural inclusions, anthropogenic inclusions, and pedofeatures (Macphail and Cruise, 2001). Such application of soil micromorphology to archaeology was introduced mainly by Goldberg (1983) and latelyis well established in the literature (French, 2003; Goldberg and Macphail, 2006). Samples were taken in Kubiena boxes (9 × 5 cm), slowly dried, impregnated by a polymer resin, processed into thin sections and then studied according to Bullock et al. (1985) and Stoops (2003). A record was made of the microfabric types, structural and porosity features, natural inclusions, anthropogenic inclusions and pedofeatures (Macphail and Cruise, 2001).

3.2. Geochemistry – quantitative analysis of expandable clay minerals (CEC)

The cation exchange capacity (CEC) was determined using a procedure proposed by Meier and Kahr (1999) for pure clay mineral specimens and then optimised for sediments and soils (Grygar et al., 2009). $[Cu(trien)]^{2+}$ solution was obtained from $CuSO_4 \cdot 5H_2O$ (Penta, Czech Republic) and trien, triethylenetetramine (1,4,7,10-tetraazadekane, Sigma–Aldrich), to the final concentration 0.01 M with a potentiometric control of the constant ligand-to-metal ratio (Grygar et al., 2009). A fine dry powder (100–500 mg) was placed in a 50 mL beaker, wetted and then suspended by stirring in 5 mL of distilled water; then 5 mL 0.01 M Cu-trien solution was added, and the suspension stirred for a further 5 min using a magnetic stirrer. The suspension was then filtered into a 50 mL flask and the solid washed with several aliquots of distilled water, and the final volume of the filtrate made to 50 mL. The solutions were analyzed by AAS (Cu and Mg) and AES (Ca and Na). The sample weight for analysis was adjusted depending on its actual CEC to consume about 50% of $[Cu(trien)]^{2+}$ using the routine described by Grygar et al. (2009).

3.3. Bulk magnetic susceptibility (MS)

Unoriented samples were collected at 5 cm intervals from cleaned profiles. Low frequency magnetic susceptibility (χlf) was measured at 0.976 kHz and high frequency magnetic susceptibility (χhf), at 3.904 kHz, using a MFK1 kappabridge (AGICO, Brno). The difference between the two measurements gives the frequency dependent susceptibility, expressed here as a percentage of χfd

($\chi fd\% = (\chi lf - \chi hf)/\chi lf \times 100$). This parameter is widely used to determine the concentration of magnetic particles close to superparamagnetic (SP)/stable single domain (SSD) boundary (Liu et al., 2005). This grain size fraction is proposed to have formed during pedogenesis (Evans and Heller, 2003; Dearing et al., 1996).

3.4. Particle size distribution function (PSDF)

Samples for particle size distribution were collected at 5 cm intervals from cleaned profiles from all three studied section (Figs. 2 and 3). Particle-size analysis (PSA) is a measurement of the size distribution of individual particles in a soil sample (Gee and Bauder, 1986). Particle size distribution was established using a Malvern Mastersizer 2000. Samples of air dried and roughly crushed sediments were gently disaggregated and dispersed in deionized water. Organic matter was removed by addition of hydrogen peroxide accompanied by gentle warming at 40 °C until effervescence stopped. The supernatant was removed after centrifugation and the sample rinsed with two changes of deionised water. The samples were then re-homogenised in a minimum of water using a whirly mixer and then sub-sampled for particle size analysis. Two sub-samples were taken from each sample and analysed sequentially, and the graphs presented are the mean of the two measurements.

3.5. OSL dating

DV II section was sampled in two positions. DV2/1 comes from the depth of 435 cm and corresponds to the base of cultural layer mixed with soil material. DV2/2 comes from the depth of 265 cm and corresponds to the position directly above gley II. layer (Fig. 2). Three locations were sampled at Hošťálkovice. HB 13 came from 160 cm depth at the very base of the section on the contact between redeposited terrace sediments and redeposited loess-like sediments. THV2 came from a depth of 65 cm where some of the artefacts occurred. THV1 came from 35 cm depth, on the contact between E soil horizon and the loess-like sediment below (Fig. 2). Předmostí was not sampled due to the technical problems during the fieldwork organisation.

Samples were dated by OSL in the Laboratory of Mineralogy and Petrology (Luminescence Research Group), Department of Geology and Soil Science, Ghent University in Belgium. by applying the SAR-OSL protocol to sand-sized (63–90 μm) quartz. This fraction was extracted from the inner material of the sampling tubes using conventional sample preparation procedures (HCl, H_2O_2, sieving, heavy liquids, and HF). OSL measurements were performed using an automated Risø TL/OSL-DA-12 reader. The equivalent dose (De) was determined using the single-aliquot regenerative-dose (SAR) protocol as described by Murray and Wintle (2000, 2003). Low-level high-resolution gamma-ray spectrometry was used for the determination of the natural dose rate. The annual dose was calculated from the present-day radionuclide activities using the conversion factors of Adamiec and Aitken (1998). An internal dose rate of 0.013 ± 0.003 Gy ka^{-1} was assumed (Vandenberghe et al., 2008). Both the beta and gamma contributions were corrected for the effect of moisture by generally accepted procedures.

4. Results

4.1. Stratigraphy

4.1.1. Southern Dolní Věstonice section

The lithostratigraphy was examined in a 4.2 m high freshly cleaned vertical section (Fig. 2) containing several horizons with different contexts, coded as DV II. Generally, the profile is mainly composed of fine grained loess and loess-like sediments which

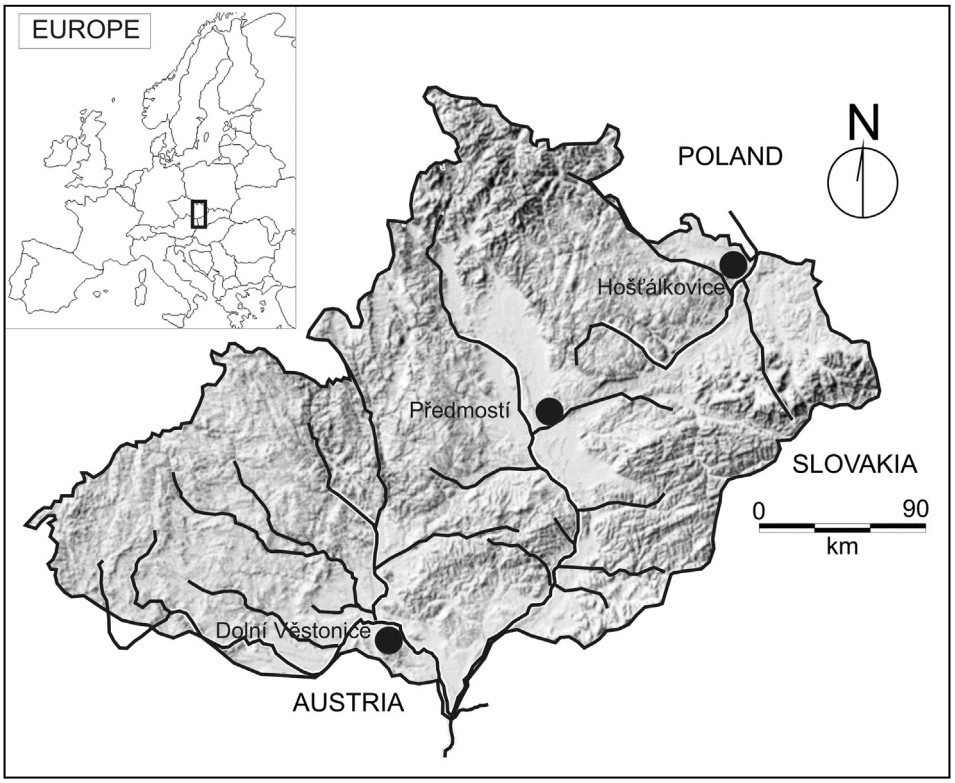

Fig. 1. Location of studied sites.

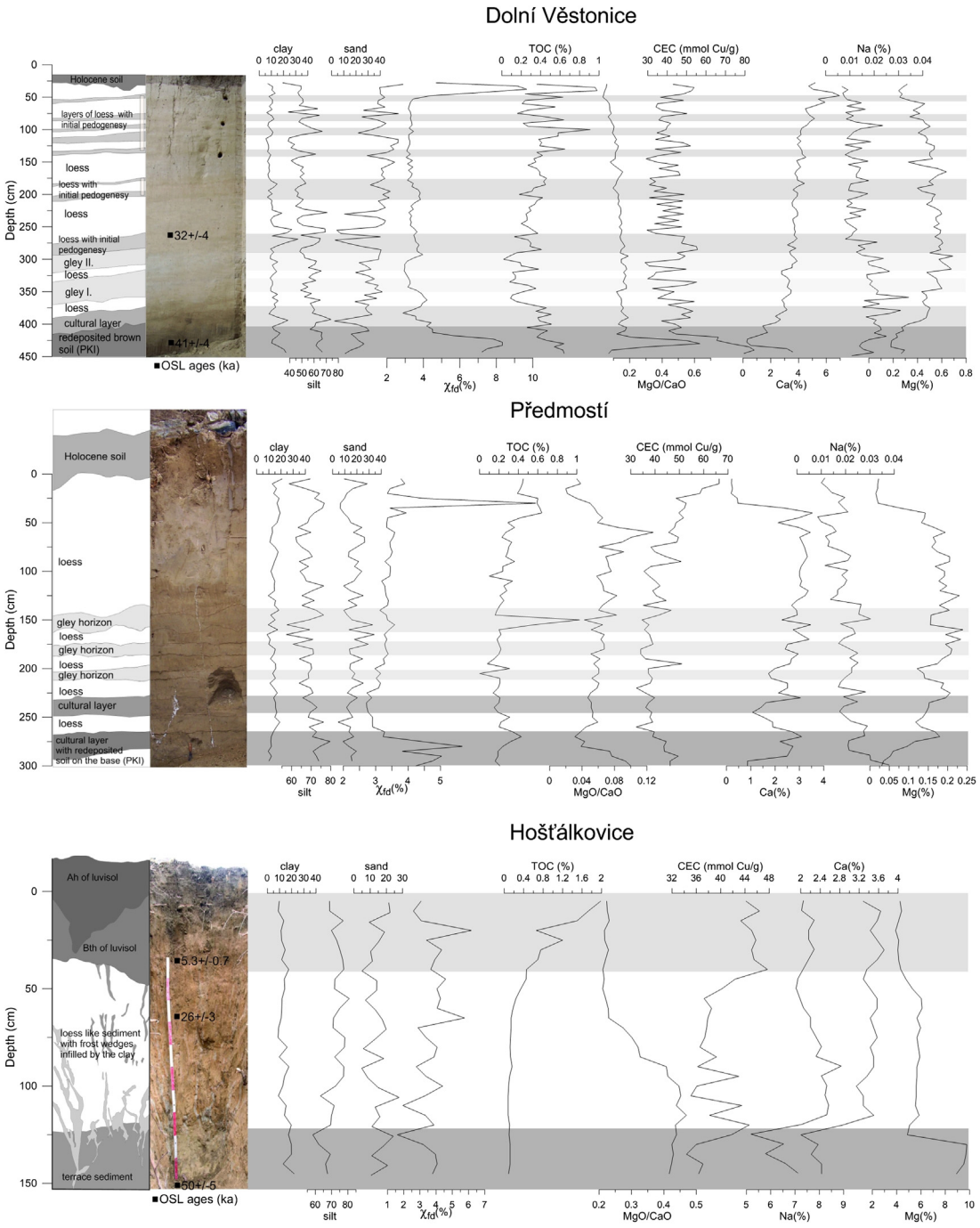

Fig. 2. The sedimentological description of loess sections Dolní Věstonice, Předmostí and Hošťálkovice together with the main geochemical, magnetic and grain size proxies.

were post-depositionally influenced by changing climatic conditions. There is a dark brown horizon of re-deposited laminated soil, probably of Cambisol type (40 cm) found in the very bottom, followed by the complex of thin loess layers (approximately 15 cm each), and one darker layer (10 cm), described as Gravettian occupational layer (10 cm) with the macroscopic presence of charcoal and fine freezing and thawing laminae (less than 1 cm) in the loess layers below and above. The loess deposition grades into two lighter horizons (17 and 10 cm) divided by a loess horizon (10 cm). Those horizons were interpreted as gley horizons. The part of the section above is composed by loessic material with a group of slightly browner horizons (1–5 cm). The section is ended by a dark brown aggraded Chernozem-type Holocene soil horizon.

4.1.2. *Intermediate Předmostí u Přerova section*

In contrast to the cultural layer excavated in the DV II sections, in which burnt charcoal is a conspicuous hearth component, burnt mammoth bones predominate here, suggestive of a difference in resource availability between the sites (Beresford-Jones et al., 2010). However, another, microcharcoal containing layer was micromorphologically confirmed the cultural layer. The lithological section of Předmostí (Fig. 2) contained a dark brown horizon of re-

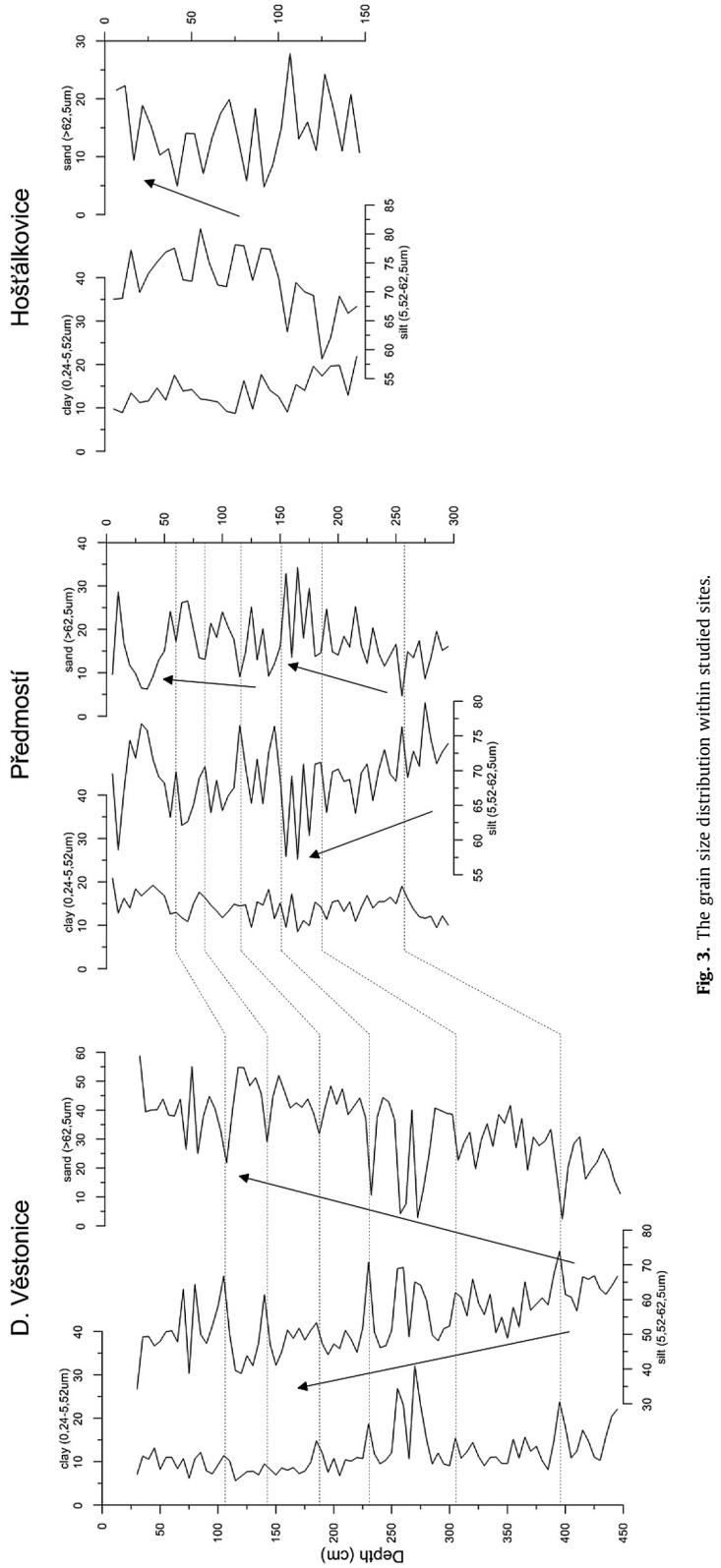

Fig. 3. The grain size distribution within studied sites.

deposited arctic soil in the very bottom followed by a thick cultural layer containing mammoth bones and burned bones together with charcoal and loess-like sediment intercalations (Fig. 2). There is evidently slight re-deposition by gelifluction. This layer is overlain by loess deposits with a number of features typical of frost action, including frost wedges and other micromorphologically detected features. Three thin gley horizons were present. The upper part of the section continues with monotonous loess deposition containing thin darker layers containing decomposed organic matter. The section is capped by a Holocene Cambisol.

4.1.3. Northern Hošťálkovice near Petřkovice loess like sedimentary section

Approximately 1.5 m thick sedimentary cover (Fig. 2) lies on the ridge between Petřkovice and Hošťálkovice. The geological background of Hošťálkovice section is composed of re-deposited terrace deposits. Colluviated loess-like deposits include approximately 30 cm of the section. Gravettian artefacts are distributed mainly on the contact of terrace deposits and loess-like sediments (Fig. 2) (Neruda and Nerudová, 2000), but occasionally were detected within loess-like sediments above. Loess-like deposits contain small frost edges filled by clays as a record of boreal illuviation. The section is capped by a Holocene Luvisol, lately degraded into Pseudogley.

4.2. Microstratigraphy and micromorphology

4.2.1. Dolní Věstonice

The base of the section is composed of re-deposited interstadial soil of the boreal to arctic brown soil type with ferric oxide nodules (Fig. 4C), interpreted as the consequence of relatively humid conditions causing erosion and reduction processes. This soil can be

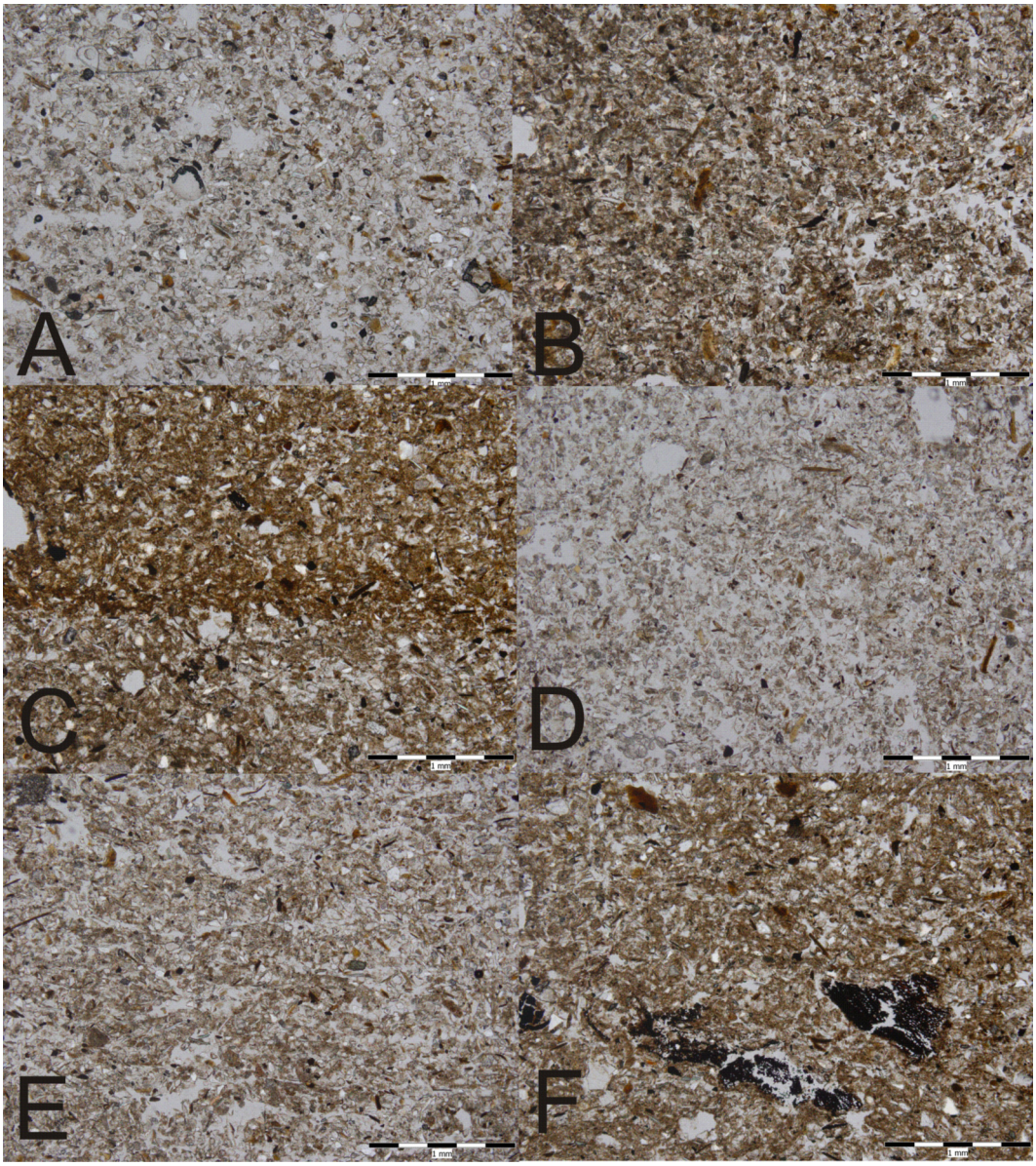

Fig. 4. Typical micromorphogical features from Dolní Věstonice site: A – loess s.s.; B – initial soil horizon with visible brunification, location above Gley II.; C – redeposited arctic brown soil on the base of section with, visible FeOH nodules due to the gleying; D – Gley II with leaching, but without FeOH features typical of gleying; E – horizontal pores documenting phases of freezing and thawing, location above the cultural layer; F – charcoal distributed widely within the cultural layer. This layer also contains redeposited arctic brown soil material.

interpreted as an early stage cambisol. Gelifluction features are connected mainly with the cultural layer (Fig. 4F), which show a continuing relatively cold and humid environment. Freezing – thawing features (Fig. 4E) above the cultural layer indicate frost heaving, related to the development of ice lenses as the consequence of cold and relatively humid conditions. Those features are not very common, in contrast to Předmostí and Hošťálkovice. Two horizons of the frost gley surprisingly do not contain ferric oxide (Fig. 4D) nodules. The absence of freezing – thawing features toward the Holocene layer is probably the result of a cold and dry LGM environment. The slightly darker horizons differ from pure loess (Fig. 4A) by initial brunification (Fig. 4B). The presence of darker horizons (Fig. 4) within this part of the section is therefore the result of transitory periods of increased humidity and initial stages of pedogenic weathering.

4.2.2. Předmostí

Re-deposited interstadial soil of the boreal to arctic brown soil type at the base (Fig. 5A) has ferric oxide nodules formed under relatively humid conditions causing erosion and reduction processes. A thick cultural layer with bioturbation (Fig. 5B) indicates stable humid conditions. The cultural layer contains frequently fragments of burned bones (Fig. 5B), but little or no charcoal. A layer which contains microcharcoal was micromorphologically identified above the first cultural layer. The presence of freezing and thawing structures (Fig. 5C) above the cultural layer is the result of persistent cold and relatively humid conditions. The presence of frost wedges (without flat bottoms) and gleying above (Fig. 5D) is the result of cold, humid conditions and probably also an initial stage of permafrost. Continuing freezing and thawing features toward the Holocene horizon with thin horizons containing

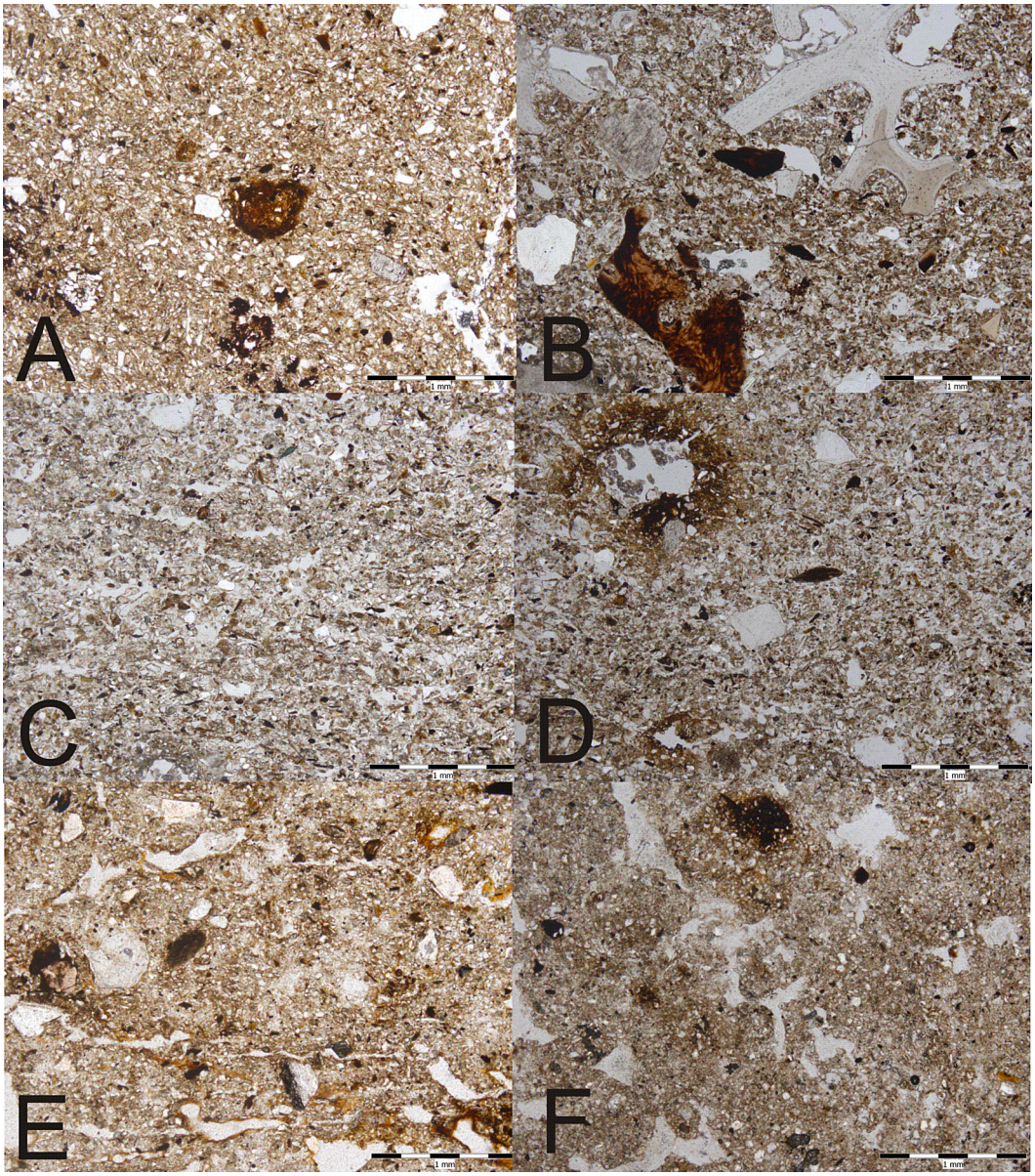

Fig. 5. Typical micromorphological features from Předmostí and Hošťálkovice sections: A – redeposited arctic brown soil at the base of Předmostí section containing nodules of FeOH; B – cultural layer with burned and unburned bones from Předmostí; C – horizontal pores documenting phases of freezing and thawing, location above the cultural layer in Předmostí and appearance of such features within all rest of section; D – Gley horizon with FeOH nodules from Předmostí; E – horizontal pores documenting phases of freezing and thawing (Hošťálkovice). Those pores were secondary during Holocene pedogenesis, iluviated by clays; F – Luvic horizon from locality Hošťálkovice.

decomposed organic matter and initial stages of brunification is the consequence of a cold and relatively wet LGM environment with short stages of increased humidity.

4.2.3. Hošťálkovice

Terrace sediments on the base of the section are partly distributed within the loess-like deposits, overlain by unsorted sediment. This record is the result of gelifluction. The presence of ferric hydroxide nodules and gleying is the consequence of a wet environment responsible for erosion and reduction processes, probably under permafrost conditions. The Gravettian artefacts are more or less incorporated into the re-deposited terrace and loess-like sediments above, probably the result of post-sedimentary cryoturbation. Freezing and thawing features (Fig. 5E) up to the Holocene soil and within the cultural layer can be attributed to persistent cold and relatively humid LGM conditions. Those features are infilled by clay illuviation as a consequence of Holocene pedogenic processes. Desiccation cracks 50 cm below the surface (Fig. 2) are the result of extremely cold and dry conditions. Boreal clay illuviation is the result of the Bölling climate. The sediment was lately influenced by Holocene illimerisation (Fig. 5F).

4.3. Frequency dependent magnetic susceptibility

The values of χfd are basically a concentration-dependent parameter. It depends on the grain-size and amount of magnetic materials present in the sediment, indicating the proportion of fine viscous grains close to the SP/SD boundary ($\sim$0.02 μm) in the total (Thompson and Oldfield, 1986). This grain size fraction formed during pedogenesis (Evans and Heller, 2003). χfd vary considerably within the studied localities (Fig. 2), but the trends in Dolní Věstonice and Předmostí are more or less similar. The highest values were detected within the horizon with re-deposited interstadial arctic brown soil (Cambisol) and within Holocene soil cover, whereas the loess typically has lower values (Fig. 2). Předmostí shows a relatively increasing trend of values, in comparison with the consistency at Dolní Věstonice. In the case of Dolní Věstonice, higher values were obtained also within horizons with initial soil horizons. In the case of Hošťálkovice, the highest values were detected within the Holocene Luvisol. The record of the Hošťálkovice section shows high variability with slightly increasing trend toward the Holocene soil (Fig. 2).

4.4. Geochemistry

The geochemical record of the profiles shows numerous similarities and is influenced by lithology (Fig. 2). Cation Exchange Capacity (CEC) of Dolní Věstonice shows a relatively stable trend with microfluctuation, except for enhancement within the lower part of the section, where re-deposited interstadial soil and cultural layer were identified. Increased values were found in the loess with initial pedogenesis, and a slightly increased trend is visible in the upper part of the profile (Fig. 2).

The profile in Předmostí shows a similar trend of CEC to Dolní Věstonice. The elevated values are visible mainly within the lower part of the section where the relicts of interstadial soil were detected. In the middle part of the profile with gley and loess horizons, a stable trend is apparent with slighter higher values in gley horizons. In the upper loess above the gley III increasing trend of values up to the Holocene soil is apparent.

In Hošťálkovice, the highest CEC values were detected within the base of the section where the weathered sandy loam with carbonate pebbles was detected. A sharp decrease of those values follows the appearance of pure loess-like deposits with the artefacts. The percentage content of Na shows a slightly declining trend in the lower part of the profile in Dolní Věstonice, whereas in Předmostí a slightly increasing trend in the whole profile is visible. Mg and Ca contents of the DV profile show the same increasing trend up to the layer of loess with initial pedogenesis. Above this layer, Ca increases whereas Mg begins to decrease to the top of the profile. Ca and Mg content of the Předmostí show slightly increasing trends with relative stagnation in the upper part, above the gley III. In general, contents of Ca and Mg show the highest variations within the gley horizons and initial soil formations above those horizons in both sections. MgO/CaO ratio shows a gradual decrease in both profiles, but in the case of Předmostí this trend is less apparent. For the Hošťálkovice profile, the great difference in elements concentration between the lower and upper part is typical. Ca and Na contents are lowest in the horizon with weathered sandy loam and high in loess-like sediment, whereas the Mg content shows the opposite trend.

Another sharp decrease of measured components is visible within E and A horizons of the Holocene Luvisol. The contents of organic matter within the sections have more or less the same trend: the most obvious is the enhancement of organic matter within the interstadial brown soil of Dolní Věstonice and Předmostí as well as within the Holocene soil formation in all three localities. For Hošťálkovic, a stable trend is typical, with a slight increase below the Holocene soil.

4.5. Grain size

Grain size measurements show the same significant trend in all three studied localities. Toward the Holocene layer significant coarsening of sand fraction is obvious (Figs. 2 and 3), while toward the north there is a fining trend. Dolní Věstonice section has probably the best preserved long-time depositional record, and consequently the deposits have much more fine composition than in other studied localities (Figs. 2 and 3). It is also possible to see a connection between the appearance of darker, more humid layers and the contemporary increase of clay fraction (depth about 1.2, 1.8–2.2 and between 3 and 4 m). In the case of Předmostí and Hošťálkovice this connection was not found. Předmostí and Hošťálkovice sections display much coarser deposits and the trend of coarsening is visible not only toward the Holocene but also toward the north, toward the edge of the North European glaciation. Předmostí section has a visible enhancement of sand fraction within 1.0–1.5 m where the cultural layer was detected. In the case of Hošťálkovice, there is a visible enhancement of clay at the expense of silt in the upper part of the section due to the Holocene pedogenic processes (Figs. 2 and 3).

4.6. Dating

A sufficient amount of pure quartz grains could be extracted from all samples. The quartz extracts showed satisfactory luminescence characteristics in terms of brightness (clearly distinguishable from background), OSL decay (dominated by the fast component), recycling ratio (consistent with unity), recuperation (generally less than 1% of the sensitivity corrected natural OSL signal) and dose recovery (a known dose given to a bleached sample prior to any heating can be accurately measured). These characteristics suggest that the samples are well-suited for optical dating. Sample GLL-091927 behaved differently from the other samples, however, in that a poor dose recovery was achieved using a preheat for 10 s at 240 °C; a lower preheat (200 °C) was required to achieve a good dose recovery. The ages are consistent with the stratigraphic position of the samples. Based on the observed spread in D_e (large aliquots), the date for sample GLL-081901 is not thought

to be an accurate sedimentation age. This sample may be affected by postdepositional mixing and/or incomplete resetting.

4.6.1. Luminescence characteristics and D_e-determination

Fig. 1 shows a representative luminescence decay and growth curve for sample GLL-081902. The luminescence signal decays rapidly with stimulation time (Fig. 1, inset); this is characteristic for quartz dominated by the fast component. The dose–response curve can be approximated satisfactorily by the sum of a single saturating exponential and a linear component. Fig. 1 also illustrates the generally good behaviour of the samples in the SAR protocol; the recycling ratios are close to unity (indicating that sensitivity changes occurring throughout the measurement procedure are accurately corrected for) and the growth curves pass close to the origin (demonstrating that recuperation is negligible).

Fig. 2 summarises the dose recovery data. Within analytical uncertainty, the measured dose does not differ from the given dose by more than 5% (Fig. 2A); the average recovered to given dose ratio for the five samples is 1.01 ± 0.02. Fig. 2B shows the corresponding values for the recycling ratio and recuperation; the average values are 0.98 ± 0.01 and 0.05 ± 0.01%, respectively. For each sample, at least 18 replicate measurements of D_e were made. Values were accepted if recuperation did not exceed 5% of the corrected natural OSL signal and if the recycling or depletion ratio did not deviate by more than 10% from unity. The average D_e's (±1 standard error) are summarised in Table 1.

Table 1
Radionuclide concentrations used for dose rate evaluation, estimates of past water content (F^*W), calculated dose rates, equivalent doses (D_e), optical ages, and random (σ_r), systematic (σ_{sys}) and total (σ_{tot}) uncertainties. The uncertainties mentioned with the D_e and dosimetry data are random; all uncertainties represent 1σ.

Sample (field code)	Sample (GLL code)	Depth (cm)	^{234}Th (Bq kg^{-1})	^{226}Ra (Bq kg^{-1})	^{210}Pb (Bq kg^{-1})	^{232}Th (Bq kg^{-1})	^{40}K (Bq kg^{-1})	F^*W (%)	Total dose rate (Gy ka^{-1})	D_e (Gy)	Age (ka)	σ_r (%)	σ_{sys} (%)	σ_{tot} (%)	σ_{tot} (ka)
THV1	081901	35	42 ± 3	45 ± 1	39 ± 1	49.5 ± 0.3	573 ± 4	24 ± 6	2.95 ± 0.02	15 ± 2 $_{(17)}$	5.3	9.9	9.8	14.0	0.7
THV2	081902	65	36 ± 2	48 ± 1	42 ± 2	52.7 ± 0.5	600 ± 5	25 ± 6	3.03 ± 0.03	77 ± 2 $_{(18)}$	26	2.3	10.2	10.5	3
HB13	091927	160	36 ± 3	43 ± 1	40 ± 2	47.7 ± 0.4	521 ± 5	21 ± 5	2.81 ± 0.03	141 ± 4 $_{(24)}$	50	3.3	9.1	9.7	5
DV2/2	091902	265	36 ± 2	43 ± 1	39 ± 1	52 ± 1	559 ± 5	23 ± 6	2.86 ± 0.02	92 ± 6 $_{(17)}$	32	6.1	9.8	11.5	4
DV2/1	091901	435	45 ± 3	49 ± 1	41 ± 2	57 ± 1	482 ± 5	23 ± 6	2.78 ± 0.02	115 ± 5 $_{(18)}$	41	4.2	9.9	10.7	4

Radionuclide concentrations used for dose rate evaluation, estimates of past water content (F^*W), calculated dose rates, equivalent doses (D_e), optical ages, and random (σ_r), systematic (σ_{sys}) and total (σ_{tot}) uncertainties. The uncertainties mentioned with the D_e and dosimetry data are random; all uncertainties represent 1σ.

4.6.2. Dose rate determination

The radionuclide activity concentrations and calculated total dose rates are given in Table 1.

4.6.3. Optical ages

Table 1 summarises all analytical results, and shows the calculated optical ages. The present-day dose rate was assumed to have prevailed throughout the entire period of burial. Uncertainties on the luminescence ages were calculated following the error assessment system proposed by Aitken and Alldred (1972) and Aitken (1976). All sources of systematic uncertainty were as quantified by Vandenberghe et al. (2004; see also Vandenberghe, 2004).

For most samples, the systematic uncertainty is dominant in the overall uncertainty on the ages and varies between ~9 and 10% (1 sigma). For sample GLL-081901, both the random and systematic uncertainty are ~10%.

5. Discussion

5.1. Sedimentary and micromorphological record of Middle Pleniglacial (MIS3) and Upper Pleniglacial (MIS 2) in Moravia

The environmental record of the Middle and Upper Pleniglacial in Moravia was studied in detail mainly in context of loess deposits (Ložek, 1953, 1964; Kukla, 1975; Frechen et al., 1999; Antoine et al., 2013). The Middle Pleniglacial in Europe is marked by the appearance of brown soil complexes as Stillfried-B from Lower Austria (Haesaerts et al., 2003), Vytachiv soil complex of Ukraine (Gerasimenko, 2006), the Gräselberger and Lohne Boden in Germany (Frechen, 1999; Antoine et al., 2009) the Saint-Acheul-Villiers-Adam soil complex in Northern France (Antoine et al., 2003), and Les Vaux soil in Belgium (Haesaerts, 1985). The soil development in this case corresponds to warmer and more humid conditions and it is widely associated with the Hengelo and Denekamp insterstadials. Those periods were interrupted mainly by the phases of erosion, and thus the sedimentary record is usually very fragmented. In Moravia the three interstadials of the Middle Pleniglacial are supposed to be preserved as the PKI pedo-complex described by Klima (1969) and dated at ~30–35 ka, and by the Bohunice soil (Valoch, 1976) dated at ~45–50 ka (Richter et al., 2009). Antoine et al. (2013) mentioned erosion processes resulting from warming phases of one of those interstadials that enhanced the seasonal degradation of the permafrost active layer leading to solifluxion-related deformation and alteration of the gley horizon preserved above the re-deposited interstadial soil.

Two sections included in our research, Dolní Věstonice and Předmostí, contain re-deposited arctic brown soil (Cambisol), which corresponds to one or more of those interstadials. In both cases, the soil sediment was re-deposited and contains ferric oxide nodules indicating the presence of water and buried organic matter (Fig. 4). Berendorf-Jones et al. (2011) described this horizon as an Interstadial A Cambisol horizon with the weak B-horizon above and covered by redeposited reworked palaeosol loam. However, micromorphological study did not confirm preservation of the *in situ* A horizon. A similar situation appeared in case of Předmostí locality. The weak interstadial soil horizon was eroded and redeposited. The interstadial soil was not preserved at Hošťálkovice. This finding corresponds to the results of the excavations of Neruda and Nerudová (2000). This type of paleosol is not known from this area, probably because of strong erosion and fragmentation of the sediment record and also because the environment of Northern Moravia and Lower Silesia was probably generally much colder than Central and Southern Moravia. Due to the fragmentation of sedimentary record of the Hošťálkovice section, it is quite difficult to use it for geochemical comparison with the sedimentary record preserved in central and southern Moravia. The first OSL data from Ostrava region concerning this context estimated the base of the section at 50 ka, which indicates that the arctic soil did not develop here or was removed by erosion.

Typical cultural layers containing charcoal or burned bones were described only in Dolní Věstonice and Předmostí, while in Hošťálkovice only the accumulations of artefacts were detected. ^{14}C data recently published by Berensdorf-Jones et al. (2011) from the DV II show a wide range between 25.570 and 28.850 ka uncal. After

calibration, this fits the date from the cultural layer by OSL dating, 32 ka. The artefact accumulation from Hošťálkovice was dated as 26 ka, which make the finding a little bit older than the findings from nearby Petřkovice (Svoboda, 2008).

The tundra gley horizons preserved above the soil sediments of the Middle Pleniglacial were described in Dolní Věstonice (Klima et al., 1962; Antoine et al., 2013) and interpreted as cold humid episodes of the Middle and Upper Pleinglacial. In the old Věstonice brickyard, Antoine et al. (2013) have recently described one gley horizon connected with the Middle Pleniglacial which underwent strong solifluction process due to one of the humid interstadial phases of the Middle Pleniglacial (frost creep). The solifluction resulted in thin, discontinuous undulated iron oxide bands throughout the unit, and two gley horizons connected with the Upper Pleniglacial. The section situated above the old brickyard displays only two gley horizons which are *in situ* and have no ferric oxide nodules or accumulations. The third gley horizon was probably redeposited together with the paleosol, which would explain redoximorphic features founded within this redeposited horizon. Such an interpretation would also fit to the findings of Antoine et al. (2013) from the old brickyard. It is quite possible that those ferric oxide accumulations described by Antoine et al. (2013) were formed mainly due to the specific geomorphologic position in the landscape. Berensdorf-Jones et al. (2011) described from this section only lenses of gley above the cultural layer and gleyic features from the cultural layer, but not from redeposited soil below. Our OSL date sampled in the uppermost part of the upper gley horizon was estimated as 32 ka. That position in the old brickyard was in contrast to the date by Fuchs et al. (2012) at 21.7 ka.

One or more gley horizons together with frost features including frost wedges were also mentioned by Žebera et al. (1955) and lately by Svoboda et al. (1994) in Předmostí with no further details of interpretation. Demek and Svoboda (2008) described strong leaching and the presence of frost wedges in Petřkovice. In the same publication, Svoboda (2008) partly rejected Demek and Svoboda's interpretation, and interpreted those wedges as the result of Holocene pedogenesis. According to our OSL data, the infilling of the frost wedges is estimated at 5.3 ka, but the infilling could be much younger than the development of the wedges.

According to Antoine et al. (2013) the transition from Middle Pleniglacial gley horizons to the Upper Pleniglacial loess in Dolní Věstonice is abrupt and marked by a drastic increase in sedimentation rate due to a return of cold and arid conditions. In the studied sections, this phase of the sedimentary record is quite homogenous and the cold and arid conditions are recorded by the increased number of frost features, which are much more evident in Předmostí and Hošťálkovice. In the case of Věstonice and Předmostí, the sedimentary record of wind deposition is interrupted by thin layers of organic-matter rich layers corresponding to short phases of increased humidity. Toward the north there is an evident decrease of the mass of sediment, which could correspond to the increased wind intensity due to the geomorphology and position much closer to the North European glaciation that did not allow aeolian material deposition.

5.2. The interpretation of geochemical, magnetic and grain size proxies of studied sections in context of Middle and Upper Pleniglacial

The profiles from Dolní Věstonice and Předmostí are much more suitable for detailed correlation and paleoenvironmental interpretation from proxy analyses than is Hošťálkovice. The reason is a fragmentation of the sedimentary record and weaker pedogenesis in the case of Hošťálkovice, where the paleoenvironmental record was mainly inferred from micromorphological and sedimentological approaches.

Grain size records of Dolní Věstonice and Předmostí show similar features. Above the interstadial soils, the silt fraction continuously decreases, whereas the sand fraction of the sediment shows an increasing trend. Based on the interval of a higher sand input it is possible to correlate these profiles (Fig. 3). Several cycles can be seen, each being characterised by an abrupt increase of the sand component, followed by a short-term decrease. In these sites strong colluvial or water transport has not been noted. Therefore, these variations can be entirely attributed to the input of aeolian sand associated with climatic deterioration, increase of wind intensity and higher accumulation rate during MIS 2. Grain-size analyses from both sites are generally in accordance with previous measurements from the Upper Weichselian part of the old brickyard profile in Dolní Věstonice (Shi et al., 2003; Antoine et al., 2013). Inputs of coarse aeolian material during the Upper Pleniglacial were also reported and correlated within several sites from sub-Atlantic region to the western Ukraine (Antoine et al., 2009; Bokhorst et al., 2010; Rousseau et al., 2011) as well as in China Loess Plateau (Nugteren et al., 2004). These events were correlated with a dust median in NGRIP record and associated to Heinrich events H3–H1 (Antoine et al., 2009). While a gradual coarsening trend is a significant feature in Dolní Věstonice, in the upper part of Předmostí this trend is not so apparent. That can be a signal of lower wind intensity in the final phase of the Upper Pleniglacial in the Central Moravia in comparison with South Moravia. A distinctly higher percentage of sand in the sediment of Dolní Věstonice as compared with Předmostí indicates lower energy of wind transport during Upper Pleniglacial in Central Moravia. Evident fining of the grain composition toward to the north is also visible (Fig. 3), together with the progressive reduction of the thickness of the deposited material. The fining trend probably reflects the changing provenance (Lisá, 2004; Lisá and Uher, 2006; Lisá et al., 2009) especially the possible appearance of glacial deposits (Lisá, 2004) toward the north. The geomorphology and the lack of westerly situated wide valleys with thick alluvial plain also play a role.

Higher values of frequency dependent magnetic susceptibility suggest the presence of ultra-fine grained (pedogenetic) magnetite or maghemite (Worn, 1998; Liu et al., 2005). In Dolní Věstonice and Předmostí, slightly higher values were found in the horizons with initial pedogenesis (and gley horizons) and significant high values in redeposited brown soil horizons. The magnetic enhancement is probably caused by increased activity of soil bacteria during the Middle Pleniglacial and climatically favourable periods (micro-interstadials) of the Upper Pleniglacial. Good correlation of the frequency-dependent magnetic susceptibility with the organic content was found in both sections. That denotes a connection between vegetation development (humid climate?) and the intensity of pedogenesis. In contrast, weak magnetic signal of pure loess accumulation indicates colder (and drier) condition and minimal pedogenetic processes. With regard to relatively narrow provenance source of the Moravian loess during Upper Pleistocene (Lisá, 2004), changes in the chemical composition in the profiles could relate to postdepositional processes.

Continuously decreasing Mg–Ca ratio (expressed here as MgO/CaO) in the pedo-sedimentary record could be caused by gradual decline of precipitation in the study area during MIS 2. Mg and Ca are present in primary carbonates, abundant in the loess deposits. Free Mg content can be enhanced by weathering of pyroxene, amphibole, and biotite, and Ca mainly from Ca-feldspar. Mg is retained much more strongly on clay than Ca, due to the large difference in atomic diameter (Perel'mman, 1977). A higher amount of percolating rainwater therefore leads to stronger leaching of Ca relative to Mg and increasing of Mg/Ca ratio (MgO/CaO) (Bokhorst

et al., 2009). Both elements are also taken up by plants, although Ca is much more important with a biogenic coefficient of 0.17, versus 0.02 for Mg (Perel'man, 1977). The ratio could be, therefore, also influenced by the density of the vegetation cover. In comparison with the decreasing trend in Dolní Věstonice, Předmostí shows a slightly increasing MgO/CaO trend, suggesting wetter conditions in Central Moravia during MIS 2.

During chemical weathering of loess, ion exchange and layers transformation of clay minerals occurs, that leads to modified of their structure and clay neoformation. The $[Cu(trien)]^{2+}$ ion is rather selective to expandable clay minerals, and thus increased CEC values are most likely attributable to a higher concentration of the most common expandable clay minerals, i.e. smectite structures, whereas lower concentrations indicate increased presence of the weak expandable clay mineral, i.e. illite (Bábek et al., 2011). The structure of expanded clay minerals is typical for more humid environments, and its low amount in the sediment suggests that conditions were likely arid (and acidic) and they has been largely depleted or least altered. The smectite/illite ratio in the loess series can be used as a proxy for humidity. Even if CEC has rarely been used for loess/paleosols sequences, several studies suggest CEC can be correlated with other indicators of weathering intensity related to precipitation such as magnetic susceptibility, diffuse reflectance spectroscopy and element ratios of Rb, Ca and Sr (Maher, 1998; Bokhorst et al., 2008; Bábek et al., 2011). In DV and Předmostí, that is suggested by an apparent relationship of CEC with MgO/CaO ratio and magnetic susceptibility that denotes a connection of weathering intensity with pedogenesis and amount of precipitation.

In general, the sedimentological, magnetic and geochemical results from all sections show significant climatic deterioration in Upper Pleniglacial by comparison with Upper Middle Pleniglacial conditions. That is recorded as gradual increasing wind intensity and a relative decline of precipitation. Nevertheless, in comparison with Dolní Věstonice, the proxy record from Předmostí suggests relatively more favorable climatic conditions.

5.3. Gravettian migrations during the Middle and Upper Pleniglacial within Moravian valleys

One of the goals set at the beginning of this paper was to discuss reasons which enabled humans during the Upper Pleniglacial to exploit the North European Plain, and subsequently even colder regions. One of the possible explanations is the presence of the water in the cold, and subsequently very dry glacial landscape (Lisá et al., 2013). Humidity seems to be the most important factor for the presence of vegetation, and subsequently animals and humans. The most important factors limiting the presence of human camps in the landscape is the presence of tectonically predisposed wide open valleys with the river network and with the close proximity of narrowing in the landscape. Oliva (2007) and Svoboda et al. (2003) discuss the importance of the presence of a river network. During the Glacial period, braided rivers (French et al., 2007) resulting from appreciable sediment load, rapid and large variations in discharge, and erosion formed the fluvial landscape of the Paleolithic in Central Europe. The alluvial zone differed from the recent one quite significantly. The presence of water in the landscape raised the temperature below rivers and along the margins, which resulted in further melting of permafrost along the banks and distinct bank morphology. Tectonic activity often brings water to the surface as course and springs. Deep water circulations were probably alsi active during the LGM.

Another important factor is the precipitation, which was probably distributed differently within the Moravian landscape. As visible from the sedimentological micromorphological and the geochemical record, Central and Northern Moravia was during the Middle and Upper Pleniglacial more humid than Southern Moravia. This fact can be connected with the more hilly geomorphology (Czudek, 1997), but also with the shorter distance from the North European glaciation. The proposed movement to the more cold, but subsequently also more humid regions in the transect from the Danube to the North European Plains can be compared with the movement to the Carpathians valleys as described by Svoboda (2001). Those valleys were described as warmer refugia (Musil, 2003), but the key factor was possibly the presence of humidity. Together with the possible presence of permafrost, such areas were much more suitable for the vegetation growth than the drier south. Rich vegetation growing over permafrost, because the permafrost layer catches the humidity, are known from recent arctic areas (Beilman, 2001; Payette et al., 2004). The presence of water connected with growing vegetation is one of the limiting factors of mammoth migrations (Gröning and Saller, 1998), and therefore also the limiting factor for Gravettian hunters' migrations.

6. Conclusions

Studied loess sites from Northern, Southern and Central Moravia provide a suitable archive for detailed study of the palaeoenvironmental changes during Upper Paleolithic period. Using a multi-proxy approach combining micromorphological, sedimentological, rock-magnetic, and geochemical methods, we have demonstrated that:

1. The sedimentary record within the studied transect differs, the amount of deposited or preserved sedimentary record decreases toward the north.
2. The most evident difference in micromorphological record is the increasing presence of freezing and thawing features toward the north. The strong postsedimentary influence at Hošťálkovice precluded detailed study.
3. The particle grain distribution record of three studied Upper Palaeolithic loess sites show a progressive coarsening of the loess deposits during the Upper Pleniglacial. A progressive fining is visible toward the North European glaciation.
4. The geochemical record of the studied sections shows numerous similarities and is influenced by lithology. Cation Exchange Capacity (CEC) of Dolní Věstonice shows a relatively stable trend with microfluctuations except for enhancement within the lower part of the section, where the re-deposited interstadial soil and cultural layer were identified. Increased values were found in the loess with initial pedogenesis, and a slightly increased trend is visible in the upper part of the profile. The profile in Předmostí shows a similar trend. Hošťálkovice section displayed the highest CEC values within the base, due to the weathered sandy loam with carbonate pebbles. A sharp decrease of those values follows the appearance of pure loess-like deposits with the artefacts.
5. New OSL Ages were determined for Dolní Věstonice, and the first OSL dating for Hošťálkovice. In Dolní Věstonice the age of the cultural layer was estimated to 41 ka and the age of the gley layer to 32 ka. Hošťálkovice, the age of the base of the section was estimated to 50 ka, the position of artefact findings 26 ka, and the infilling of frost edges 5.3 ka. OSL dating for Dolní Věstonice and Hošťálkovice brought slightly older dates than expected.
6. The reason that humans could exploit the North European Plain and even colder regions could have been the presence of water in the cold and arid glacial landscape. According to sedimentological and geochemical records, the more northerly regions were more humid than the regions to the south.

Acknowledgements

The authors would like to thank the Archaeological Department of the University of Cambridge and the European Commission Marie Curie Intra-European Fellowship program for support. This research was also financed by the institutional research plan of the Institute of Geology AS CR, v. v. i, No. AV0 Z 30130516 and by the Institutional research plan of FWT Mendel University in Brno, No. MSM 6215648902. We would like to thank Dr. M. Chadima from Agico a.s. company for allowing measurement of magnetic properties of studied sediments, to Prof. Jiří Svoboda and Martin K. Jones to provide us with access to the excavation in Dolni Vestonice, to Mgr. P. Drechsler for providing access to the section in Předmost, and especially to dr. Peter Neruda for the possibility to sample material from the Hoštálkovice locality. Authors would also like to thank Alena Šamonilová for the very helpful comments and editing of the English text.

References

Adamiec, G., Aitken, M., 1998. Dose-rate conversion factors: update. Ancient TL 16, 37–50.
Adamová, M., Havlíček, P., 1998. Fossil soils geochemistry of the most important Moravianlocalities. Zpr. geol. Výzk. v Roce 1997, 54–62.
Aitken, M.J., 1976. Thermoluminescence age evaluation and assessment of error limits: revised system. Archaeometry 18, 233–238.
Aitken, M.J., Alldred, J.C., 1972. The assessment of error limits in thermoluminescence dating. Archaeometry 14, 257–267.
Antoine, P., Catt, J., Lautridou, J.P., Sommé, J., 2003. The loess and coversands of Northern France and Southern England. Journal of Quaternary Sciences 18, 309–318.
Antoine, P., Rousseau, Moine, O., Rousseau, D.D., Kunesch, S., Hatté, C., Lang, A., Zöller, L., 2009. Evidence of rapid and cyclic eolian deposition during the Last Glacial in European loess series (Loess Events): the high-resolution records from Nussloch (Germany). Quaternary Science Reviews 28, 2955–2973.
Antoine, P., Rosseau, D.D., Degeai, J.P., Moine, O., Lagroix, F., Kreutzer, S., Fuchs, M., Hatté, Ch., Gauthier, C., Svoboda, J., Lisa, L., 2013. High-resolution record of the environmental response to climatic variations during the last interglacial-glacial cycle in central Europe: the loess-palaeosol sequence of Dolní Věstonice (Czech Republic). Quaternary Science Reviews 67, 17–38.
Bábek, O., Chlachula, J., Grygar, T.M., 2011. Non-magnetic indicators of pedogenesis related to loess magnetic enhancement and depletion: examples from the Czech Republic and southern Siberia. Quaternary Science Reviews 30, 967–979.
Beilman, D.W., 2001. Plant community and diversity change due to localized permafrost dynamics in bogs of western Canada. Canadian Journal of Botany 79, 983–993.
Beresford-Jones, D., Johnson, K., Pullen, A.G., Pryor, A.J.E., Svoboda, J., Jones, M., 2010. Burning wood or burning bone? A reconsideration of flotation evidence from Upper Palaeolithic (Gravettian) sites in Moravian Corridor. Journal of Archaeological Science 37, 2799–2811.
Beresford-Jones, D., Taylor, S., Paine, C., Pryor, A., Svoboda, J., Jones, M., 2011. Rapid climate change in the Upper Palaeolithic: the record of charcoal conifer rings from the Gravettian site of Dolní Věstonice, Czech Republic. Quaternary Science Reviews 30, 1948–1964.
Bokhorst, S., Bjerke, J.W., Bowles, F.P., Melillo, J.M., Callaghan, T.V., Phoenix, G.K., 2008. Impacts of extreme winter warming in the sub-Arctic: growing season responses of dwarf-shrub heathland. Global Change Biology 14, 2603–2612.
Bokhorst, S., Bjerke, J.W., Davey, M., Taulavuori, K., Taulavuori, E., Laine, K., Callaghan, T.V., Phoenix, G.K., 2010. Impacts of extreme winter warming events on plant physiology in a sub-Arctic heath community. Physiol Plant 140, 128–140.
Bullock, P., Federoff, N., Jongerius, A., Stoops, G., Tursina, T., Babel, U., 1985. Handbook for Soil Thin Section Description. Waine Research Publications, Wolverhampton, UK.
Czudek, T., 1997. Reliéf Moravy a Slezska v kvartéru. SURSUM, Tišnov (in Czech).
Dearing, J.A., Dann, R.J.L., Hay, K., Lees, J.A., Loveland, P.J., Maher, B.A., O'Grady, K., 1996. Frequency-dependent susceptibility measurements of environmental materials. Geophysical Journal International 124, 228–240.
Demek, J., Kukla, J., 1969. Periglazialzone, Löss und Paläolithicum der Tschechoslowakei. Tsechoslowakische Akademie der Wissenschaften, Geographisches Institut, Brno, p. 158 (in German).
Demek, J., Svoboda, J., 2008. Quaternary stratigraphy. In: Svoboda, J. (Ed.), Petřkovice on Shouldered Points and Female Figurines. Institute of Archaeology at Brno, Academy of Sciences of the Czech Republic, Brno, pp. 28–30.
Evans, M.E., Heller, F., 2003. Environmental Magnetism, Principles and Applications of Enviromagnetics. Academic Press, An imprint of Elsevier Science, Oxford.
Folprecht, J., 1934. Výzkumné práce na praehistorickém sídlišti v Petřkovicích. Příroda 27 (3), 77 (in Czech).
Frechen, M., 1999. Upper Pleistocene loess stratigraphy in Southern Germany. Quaternary Geochronology 18, 243–269.
Frechen, M., Zander, A., Cílek, V., Ložek, V., 1999. Loess chronology of the Last Interglacial/Glacial cycle in Bohemia and Moravia, Czech Republic. Quaternary Science Rewiews 18, 1467–1493.
French, Ch.A., 2003. Geoarchaeology in Action: Studies in Soil Micromorphology and Landscape Evolution. Routhledge.
French, C., Lewis, H., Green, M., Allen, M.J., Scaife, R., Gardiner, J., Samarsundera, E., 2007. Studying land use from monuments: archaeology and environment on Bottlebush, Wyke and Gussage Cow Downs'. In: Prehistoric landscape development and human impact in the upper Allen valley, Cranborne Chase, Dorset. McDonald Institute for Archaeological Research, Cambridge.
Frenzel, B., 1968. Grundzűge der pleistozänen Vegetationsgeschichte Nord-Eurasiens. Erdwissenschaftliche Forschungen (I), Wiesbaden (in German).
Fuchs, M., Kreutzer, S., Rousseau, D.D., Antoine, P., Hatté, C., Lagroix, F., Moine, O., Gauthier, C., Svoboda, J., Lisá, L., 2012. The loess sequence of Dolní Věstonice, Czech Republic: a new OSL-based chronology of the Last Climatic Cycle. Boreas. http://dx.doi.org/10.1111/j.1502–3885.2012.00299.x.
Gee, W., Bauder, J.W., 1986. Particle-size analyses. In: Klute, Arnold (Ed.), Methods of Soil Analysis: Part 1—Physical and Mineralogical Methods. SSSA book series 5.1.
Gerasimenko, N., 2006. Upper Pleistocene loess-palaeosol and vegetational successions in the Middle Dnieper Area, Ukraine. Quaternary Int. 149, 55–66.
Goldberg, P., 1983. Applications of micromorphology in archaeology. In: Bullock, P., Murphy, C.P. (Eds.), Soil Micromorphology, Techniques and Applications, vol. 1. AB Academic Publishers, Berkhamsted, United Kingdom, pp. 139–150.
Goldberg, P., Macphail, R.I., 2006. Practical and Theroetical Geoarchaeology. Blackwell Publishing, Oxford, 455pp.
Gröning, K., Saller, M., 1998. Der Elefant in Natur und Kulturgeschichte. Könemann, Köln.
Grygar, T., Světlík, I., Lisá, L., Koptíková, L., Bajer, A., Wray, D.S., Ettler, V., Mihaljevič, M., Nováková, T., Koubková, M., Novák, J., Máčka, Z., Smetana, M., 2009. Geochemical tools for the stratigraphic correlation of floodplain deposits of the Morava River in Strážnické Pomoraví, Czech Republic from last millennium. Catena 80, 106–121.
Haesaerts, P., 1985. Les læss du Pléistocène supérieur en Belgique ; comparaisons avec les séquences d'Europe centrale. Bulletin de l'Association Française pour l'Etude du Quaternaire 2/3, 105–115.
Haesaerts, P., Mestdagh, H., 2000. Pedosedimentary evolution of the last interglacial and the early glacial sequence in the European loess belt from Belgium to central Russia. Geologie en Mijnbouw/Netherlands Journal of Geosciences 79 (2/3), 313–324.
Haesaerts, P., Borziak, I., Chirica, V., Damblon, F., Koulakovska, L., Van der Plicht, J., 2003. The East-Carpathian loess record: a reference for the Middle and Late Pleniglacial stratigraphy in central Europe. Quaternaire 14 (3), 163–188.
Horáček, I., Ložek, I., 1988. Paleozoology and mid-European quaternary past: scope of the approach and selected results. Rozpravy ČSAV-MPV 94, 1–106.
Klíma, B., 1969. Petřkovice II. Nová Paleolitická stanice v Ostravě. Archeologické Rozhledy 21, 583–595 (in Czech).
Klima, B., Kukla, J., Lozek, V., De Vries, H., 1962. Stratigraphie des Pleistozäns und Alter des Paläolithischen Rastplatzes in der Ziegelei von Dolni Vestonice (Unter-Wisternitz). Antropozoikum 11, 93–145 (in German).
Kovanda, J., 1971. Kvartérní vápence Československa. Anthropozoikum 7, 7–236 (in Czech).
Kukla, G., 1975. Loess stratigraphy of central Europe. In: Butzer, K.W., Isaac, G.L. (Eds.), After the Australopithecines. Mouton Publishers, The Hague, pp. 99–188.
Lisá, L., 2004. Exoscopy of Moravian eolian sediments. Bulletin Geosciences 79 (3), 177–182.
Lisá, L., Uher, P., 2006. Provenance of Wurmian loess and loess-like sediments of Moravia and Silesia (Czech Republic): a study of zircon typology and cathodoluminiscence. Geologica carpatica 57 (5), 397–403.
Lisá, L., Buriánek, D., Uher, P., 2009. New approach to garnet redistribution during aeolian transport. Geological Quarterly 53 (3), 333–340.
Lisá, L., Škrdla, P., Havlín Nováková, D., Bajer, A., Čejchan, P., Nývltová Fišáková, M., Lisý, P., 2013. The role of abiotic factors in ecological strategies of Gravettian hunter-gatherers within Moravia, Czech Republic. Quaternary International 294, 71–81.
Liu, Q.S., Torrent, J., Maher, B.A., Yu, Y.J., Deng, C.L., Zhu, R.X., Zhao, X.X., 2005. Quantifying grain size distribution of pedogenic magnetic particles in Chinese loess and its significance for pedogenesis. Journal of Geophysical Research 110, B11102. http://dx.doi.org/10.1029/2005JB003726.
Ložek, V., 1953. Pleistocénní mekkýši z gravettského sídliště u Dolních Věstonic. Monumenta Archeologica 2, 45–51.
Ložek, V., 1964. Mittel- und jungpleistozäne Löß-Serien in der Tschechoslowakei und ihre Bedeutung für die Löß-Stratigraphie Mitteleuropas. Report of the IV International Congress on Quaternary, pp. 525–549. Warschau.
Ložek, V., 1968. Über die malakozoologische Charakteristik der pleistozänen Warmzeiten mit besonderer Berücksichtigung des letzten Interglazials. Berichte der Deutschen Ges. f. Geol. Wiss., R.A 14 (4), 439–469. Berlin.
Macphail, R.I., Cruise, G.M., 2001. The soil micromorphologist as team player: a multianalytical approach to the study of European microstratigraphy. In: Goldberg, P., Holliday, V., Ferring, R. (Eds.), Earth Science and Archaeology. Kluwer Academic/Plenum Publishers, New York, pp. 241–267.

Maher, B.A., 1998. Magnetic properties of modern soils and loessic paleosols: implications for paleoclimate. Palaeogeography, Palaeoclimatology, Palaeoecology 137, 25–54.
Meier, L.P., Kahr, G., 1999. Determination of the cation exchange capacity (CEC) of clay minerals using the complexes of copper (II) ion with triethylenetetramine and tetraethylenepentamine. Clays Clay Miner. 47, 386–388.
Murray, A.S., Wintle, A.G., 2000. Luminescence dating of quartz using an improved single-aliquot regenerative-dose protocol. Radiation Measurements 32, 57–73.
Murray, A.S., Wintle, A.G., 2003. The single aliquot regenerative dose protocol: potential for improvements in reliability. Radiation Measurements 37, 377–381.
Musil, R., 2003. The Middle and Upper Palaeolithic game suite in central and Southeastern Europe. In: van Andel, T.H., Davies, W. (Eds.), Neanderthals and Modern Humans in the European Landscape during the Last Glaciations: Archaeological Results of the Stage 3 Project. McDonald Institute Monographs, Cambridge, pp. 167–190.
Neruda, P., Nerudová, Z., 2000. Archeologická sondáž na lokalitě Hošťálkovice II – Hladová vrch o. Ostrava. Acta Historica et museologica Universitatis Silesianae Opaviensis. 5, 116–122 (in Czech).
Nývltová Fišáková, M., 2013. Seasonality of Gravettian sites in the Middle Danube Region and adjoining areas of Central Europe. Quaternary International 294, 120–134. http://dx.doi.org/10.1016/j.quaint.2011.08.017.
Nugteren, G., Vandenberghe, J., Ko van Huissteden, J., Zhisheng, A., 2004. A Quaternary climate record based on grain size analysis from the Luochuan loess section on the Central Loess Plateau, China. Global and Planetary Change 41 (3-4), 167–183.
Oliva, M., 2005. Palaeolithic and Mesolithic Moravia. MZM, Brno.
Oliva, M., 2007. Gravettien na Moravě. Dissertatiiones archaeologicae Brunheses/Pragensesque Brno, Praha.
Otte, M., 1981. Le gravettien en Europe centrale. Disertationes archeologicae Gandenses 20. Brugge.
Payette, S., Delwaide, A., Caccianiga, M., Beauchemin, M., 2004. Accelerated thawing of subarctic peatland permafrost over the last 50 years. Geophysical Research Letters 31, L18208. http://dx.doi.org/10.1029/2004GL020358.
Perel'man, A.I., 1977. Geochemistry of Elements in the Supergene Zone. Keterpress Enterprises, Jerusalem.
Richter, D., Tostevin, G., Skrdla, P., Davies, W., 2009. New radiometric ages for the Early Upper Palaeolithic type locality of Brno-Bohunice (Czech Republic): comparison of OSL, IRSL, TL and 14C dating results. Journal of Archaeological Science 36, 708–720.
Rousseau, D.D., Antoine, P., Gerasimenko, N., Sima, A., Fuchs, M., Hatté, C., Moine, O., Zöller, L., 2011. North Atlantic abrupt climatic events of the Last Glacial period recorded in Ukrainian loess deposits? Clim. Past 7, 221–234.
Shi, C., Zhu, R., Glass, B.P., Liu, Q., Zeman, A., Suchy, V., 2003. Climate variations since the last interglacial recorded in Czech loess. Geophysical Research Letters 30 (11), 1562.
Skutil, J., 1955. Příspěvek k poznání paleolitika Moravské brány. Anthropozoikum 4, 447–468 (in Czech).
Stoops, G., 2003. Guidelines for Analysis and Description of Soil and Regolith Thin Sections. Soil Science Society of America, Inc., Madison, Wisconsin, USA.
Svoboda, J., 2001. On the Middle to Upper Paleolithic transition in north Eurasia. Archaeol. Ethnol. Anthropol. Eurasia 4 (8), 30–37. Rusko: Institute of Archaeology and Ethnography.
Svoboda, J. (Ed.), 2008. Petřkovice on Shouldered Points and Female Figurines. Institute of Archaeology at Brno, Academy of Sciences of the Czech Republic, Brno.
Svoboda, J., Ložek, V., Svobodová, H., Škrdla, P., 1994. Předmostí after 110 years. Journal of Field Archaeology 21, 457–472.
Svoboda, J., Havlíček, P., Ložek, V., Macoun, J., Musil, R., Přichystal, A., Svobodová, H., Vlček, E., 2002. Paleolithic of Moravia and Silesia. In: The Dolní Věstonice Studies, vol. 8. Brno.
Svoboda, J., Havlíček, P., Ložek, V., Macoun, J., Musil, R., Přichystal, A., Svobodová, H., Vlček, E., 2003. Paleolit Moravy a Slezska, 2., aktualizované vydání – Paleolithic of Moravia and Silesia, 2nd revised edition. Dolní Věstonice Studies vol. 8. Brno 2002.
Svoboda, J., 2004. Continuities, discontinuities, and interactions in Early Upper Paleolithic technologies. In: The Early Upper Paleolithic beyond Western Europe. University of California Press, USA, pp. 30–49.
Thompson, R., Oldfield, F., 1986. Environmental Magnetism. Allen and Unwin, London.
Trinkaus, E., Svoboda, J., 2006. Early Modern Human Evolution in Central Europe: the People of Dolní Věstonice and Pavlov. Oxford University Press, Oxford.
Valoch, K., 1976. Die altsteinzeitliche Fundstelle in Brno-Bohunice, vol. 4. Studi Archeologickeho ustavu Ceskoslovenske Akademie ved v Brne, Brno.
Valoch, K., 1979. Paleolit středního pomoraví. Studie Muzea Kroměřížska 1, 22–35 (in Czech).
Vandenberghe, D., 2004. Investigation of the Optically Stimulated Luminescence Dating Method for Application to Young Geological Samples. Ph.D. thesis. Ghent University.
Vandenberghe, D., Kasse, C., Hossain, S.M., De Corte, F., Van den haute, P., Fuchs, M., Murray, A.S., 2004. Exploring the method of optical dating and comparison of optical and 14C ages of Late Weichselian coversands in the southern Netherlands. Journal of Quaternary Science 19, 73–86.
Vandenberghe, D., De Corte, F., Buylaert, J.-P., Kučera, J., Van den haute, P., 2008. On the internal radioactivity in quartz. Radiation Measurements 43, 771–775.
Worn, H.U., 1998. On the superparamagnetic—stable single domain transition for magnetite, and frequency dependence of susceptibility. Geophys. J. Int 133, 201–206.
Žebera, K., Ložek, V., Kneblová, V., Fejfar, O., Mazánek, M., 1955. Zpráva o druhé etapě geologického výzkumu kvartéru v Předmostí u Přerova na Moravě. Anthropozoikum 4, 291–362.

PŘÍLOHA IV

Hošek, J. – Pokorny, P. – Prach, J. – Lisa, L. – Matys Grygar, T. – Knesl, I. – Trubac, J. (2017): Late Glacial erosion and pedogenesis dynamics: Evidence from high-resolution lacustrine archives and paleosols in south Bohemia (Czech Republic). – Catena 150, 261-278.

Catena 150 (2017) 261–278

Contents lists available at ScienceDirect

Catena

journal homepage: www.elsevier.com/locate/catena

Late Glacial erosion and pedogenesis dynamics: Evidence from high-resolution lacustrine archives and paleosols in south Bohemia (Czech Republic)

Jan Hošek [a,b,*], Petr Pokorný [c], Jindřich Prach [c,e], Lenka Lisá [d], Tomáš Matys Grygar [f], Ilja Knésl [a], Jakub Trubač [g]

[a] Czech Geological Survey, Klárov 3, Prague 1, Czech Republic
[b] Institute of Geology and Paleontology, Faculty of Science, Charles University in Prague, Albertov 6, Prague 2, Czech Republic
[c] Center for Theoretical Study, Charles University in Prague; Jilská 1, Praha 1, Czech Republic
[d] Institute of Geology of Czech Academy of Science, Rozvojová 269, Prague 6, Czech Republic
[e] Department of Botany, Faculty of Science, Charles University in Prague, Benátská 2, Prague 2, Czech Republic
[f] Institute of Inorganic Chemistry of Czech Academy of Science, Řež 1001, Czech Republic
[g] Institute of Geochemistry, Mineralogy and Mineral Resources, Faculty of Science, Charles University in Prague, Albertov 6, Prague 2, Czech Republic

ARTICLE INFO

Article history:
Received 10 August 2016
Received in revised form 1 November 2016
Accepted 21 November 2016
Available online xxxx

Keywords:
Late Pleistocene
Landscape evolution
Climate
Lake geochemistry
Soil micromorphology
Podzolization

ABSTRACT

Sediments from three paleolakes and two paleosol horizons in south Bohemia, Czech Republic, provide evidence of climate change and landscape evolution in central-eastern Europe on millennial to centennial timescales over the Late Glacial (~16–11.5 ky). Based on a combination of geochemical, sedimentological and geophysical proxy indicators, along with the pollen record and soil micromorphology, we propose a relationship between vegetation cover, soil development, and erosional processes. Four major and two minor environmental stages, identified in all investigated paleo-lakes, were broadly correlated with the Late Glacial climatostratigraphy. Short-term (decadal to centennial) climatic deteriorations between the Bølling and Allerød, and within the Allerød, have been correlated with the Older Dryas and the Intra-Allerød Cold Period (IACP) respectively. B horizons of two (gleyic) podzols discovered under aeolian sand dunes in the lake catchments were dated to the Allerød interstadial and were parallelized with Usselo soils – pedostratigraphical marker horizons of west- and northern-central Europe. The upper parts of these soils have signs of colluvial processes. According to the radiocarbon dating, the erosion occurred at 13,155 ± 150 cal. yr BP and can be associated with the IACP event, which is marked by a significant input of allogenic material into the lake basins. We attribute the significant increase in the iron and consequent phosphorus content in the lake sediments during the Allerød to the podzolization that occurred with the humid interstadial conditions.

1. Introduction

As demonstrated by numerous paleoenvironmental studies worldwide, changes in climate regimes associated with the Late Glacial (LG) period (~16–11.5 ky ago) caused deep ecosystem conversions and evoked distinct interactions within and between the different components of terrestrial environments (Roberts, 2014).

Although most research has demonstrated the effects of the LG climatic oscillations on the biological components of the environment (Firbas, 1949; Watts, 1979; Ammann and Lotter, 1989; Ammann et al., 1993; Goslar et al., 1993; Hoek, 1997), significant insight into the LG climatic and, consequently landscape, dynamics can also be gained by the study of the associated erosion and pedogenesis dynamics. These processes are directly connected with climatic changes: the more favourable climatic conditions would usually favour pedogenesis, greater soil-binding by the denser vegetation, and the limiting of surface erosion, while cooling conditions tend immediately to cause surface instability, limited chemical weathering, increased erosion, and reinforced aeolian activity (Engstrom and Wright, 1984).

Some studies have shown that lacustrine sediments are able to record physical erosion, weathering, and soil development (Bakke et al., 2010; Mckay and Kaufman, 2009; Rosqvist and Schuber, 2003; Simonneau et al., 2014).

In a Pan-European context, the most straightforward evidence on the LG climatic oscillations (including the minor cooling episodes such as the Older Dryas or Intra-Allerød Cold Period) has come from the

* Corresponding author at: Czech Geological Survey, Klárov 3, Prague 1, 118 00, Czech Republic.
E-mail addresses: johan.hosek@gmail.com (J. Hošek), pokorny@cts.cuni.cz (P. Pokorný), jindraprach@gmail.com (J. Prach), lisa@gli.cas.cz (L. Lisá), grygar@iic.cas.cz (T.M. Grygar), ilja.knesl@geology.cz (I. Knésl), jakub.trubac@gmail.com (J. Trubač).

http://dx.doi.org/10.1016/j.catena.2016.11.022
0341-8162/

North-Atlantic (NA) region; further into the European sub-continent, namely into central-eastern Europe (hereafter CEE), the impact of these short-term climatic episodes has as yet been poorly documented. This could be due to: (1) geographical position, since the N and NW Europe is supposedly more heavily influenced by the hydroclimatic changes in the NA; and/or (2) the relative scarcity of suitable CEE sedimentary archives, such that would cover the complete period of the LG in sufficient resolution, compared to N and NW Europe. Consequently, many questions related to particular episodes in paleoenvironmental history remain virtually unclear throughout the territory of the Czech Republic, situated as it is in an important transition zone between the macro-climatic settings of the Atlantic and European continent. Such unanswered questions include those relating to the spatiotemporal variation of the timing of LG climatic changes and their impact on terrestrial ecosystems.

The investigation of Lake Švarcenberk in South Bohemia (Czech Republic) has already proved to be one of the most valuable archives for this period of interest in the entire CEE (Hošek et al., 2014). With a sediment thickness of over 10 m, from which 4–5 m cover just the LG period, this site provides the most complete and detailed record of the last 16 ky in the European interior. Though a wide range of paleoecological information has already been obtained from this site (Pokorný and Jankovská, 2000; Pokorný, 2002; Hošek et al., 2014), some crucial questions remain unclear. These include the interplay between terrestrial and lake ecosystems, and the wide-scale landscape evolution during the Last Termination.

To fill in some of those gaps, we hereafter report on some high-resolution lacustrine records discovered recently in in two other individually-closed paleolakes and the LG interstadial paleosol horizons that represent the former catchment surfaces.

Our aim has been to obtain evidence for the environmental changes surrounding the LG in high temporal resolution, with particular focus on how the rapid climatic shifts had affected pedogenesis, erosion, and weathering. To address these questions, we have applied geochemical, sedimentological, rock-magnetic and micromorphological methods to both the lacustrine sequences and paleosol horizons. Because of the crucial role of vegetation cover in erosion-weathering processes, we compared the geochemical data with the pollen record, currently available from Lake Švarcenberk (Pokorný, 2002, Hošek et al., 2014).

Last, but not least, this study has highlighted some challenges for paleoenvironmental reconstruction from the geochemistry and rock-magnetism of non-laminated lacustrine sequences.

2. Regional setting

The study area is situated in South Bohemia, the Czech Republic, in the north-eastern margin of the Třeboň Mega-basin (Fig. 1). This Mega basin is filled mostly by Cretaceous clastic sediments consisting of sandstones, conglomerates and mudstones. Cretaceous sediments are partially covered by Middle and Late Miocene fluvio-lacustrine clayey sands filling the NNE-SSW graben.

During the Last Glacial Maximum (c. 24–22 ky BP) the study area was located ~110 km north of the Alpine piedmont glaciers and ~ 420 km from the southern edge of the North European continental Ice Sheet. Quaternary periglacial sediments include Pleistocene colluvial loamy sands, fluvial sandy gravels and the Holocene floodplain of the Lužnice River. Along this axial river, numerous aeolian sand dunes formed during the Younger Dryas (Pokorný and Růžičková, 2000). The sand dunes were formed, according to their morphology, by north-westerly winds. The source material originated both from fluvial sand and unconsolidated Cretaceous sandy bedrock. Because of its altitudinal position (420 m asl) and flat landscape, the loess cover has not been preserved in the Třeboň Mega-basin. Nevertheless, remnants of loess-like sediments can be found in the NW neighbourhood of this vast area.

Due to the nature of the geological substratum of this Mega basin, local soils are deficient in calcium carbonate. Currently, most soils are leached and show a tendency towards podzolization. The soils are thus mostly acidic (pH down to 3.3).

The study area is located in the temperate transitional climatic zone between west oceanic and east continental climatic settings. The present climate is controlled by prevailing westerly air masses, already significantly reduced in moisture by their passage across central Europe. Present mean annual precipitation is 627 mm and mean annual temperature is 7.8 °C (at the town of Třeboň; 30-year observation sequence).

Nineteen depressions filled by lacustrine sediments were recently discovered in the study area (Fig. 1, for details see Hošek et al., 2013; Hošek et al., 2016), most of them covered by artificial fishponds of Medieval and Modern foundation. These basins vary in size (several tens up to several hundreds of metres in diameter), and in the depth of their post-glacial infilling (2–12 m); nevertheless, they share several common features such as their location on Miocene sedimentary bedrock, elongated shape, and the presence of tectonic faults that often run along their major axis. Although research on the origin of the lake basins is still in progress, we assume that these basins are the result of the complex of thermokarst processes (formation and collapse of alases/pingos and surface degradation of the permafrost) that occurred during the periglacial conditions of the late LGM. Another explanation which should be taken into account is that their origin is connected with short-distance neotectonic horizontal movements (pull-apart basins). The local geological settings of these study lakes and the bathymetry of the lake basins are shown in Figs. 1 and 2.

The stratigraphy of the infilling of all the basins under investigation is very similar, and the time-successive changes in sediment character are highly contrasting, reflecting well the changes in environmental conditions during the millennia of sedimentation.

3. Material and methods

This paper is based on data obtained from the three most-intensively investigated lakes: Velký Tisý – 'VT' (49°02′58.01″N; 14°43′39.60″E), Švarcenberk – 'SV' (49°08′42.01″N; 14°42′45.22″E) and Lake Veselí – 'VS' (49° 10′14.67″N; 14°40′36.06″E). All of them were closed in terms of their hydrology and with relatively small catchments (4–6 km^2).

Reference cores VTC and VSC were taken in the summer seasons of 2014 and 2015 with a pneumatic hammer-operated piston corer (tube 50 mm in diameter). The SVC core from the central part of the SV lake was taken already in 2000 (Pokorný, 2002). After a visual description of the cores, these were subsampled continuously with intervals of 2.5 cm (core VTC) and 1 cm (VSC). In the case of Lake Švarcenberk, we used archived samples from the central core (SV), sampled with 4 cm intervals.

Although the study area has been severely influenced by agricultural management over the last centuries, we were able to discover Late Glacial paleosols within two (from the total of three) investigated catchments (Fig. 1), and the erosional surfaces associated with them, preserved under thick aeolian sand dune deposits. These sections were dug manually and the soils subsampled continuously for micromorphological, geochemical and rock-magnetic investigations.

3.1. Chronology and depth-age modelling

The chronology of the VTC core is based on seven radiocarbon ages determined on terrestrial plant macroremains (2 samples) and 5 bulk sediment samples (due to the general scarcity of macroremains). From the VSC core, two samples of terrestrial plants and one bulk sediment sample were used for dating. In the case of the SVC core, we used the already published radiocarbon measurements (Pokorný, 2002; Hošek et al., 2014).

From the soil buried under the Vlkovský přesyp sand dune (VLK), two charcoal samples were taken for radiocarbon dating, and one radiocarbon date (also obtained from a charcoal sample) used from a previous investigation of the site (Pokorný, 2002) (Table 1). Samples were

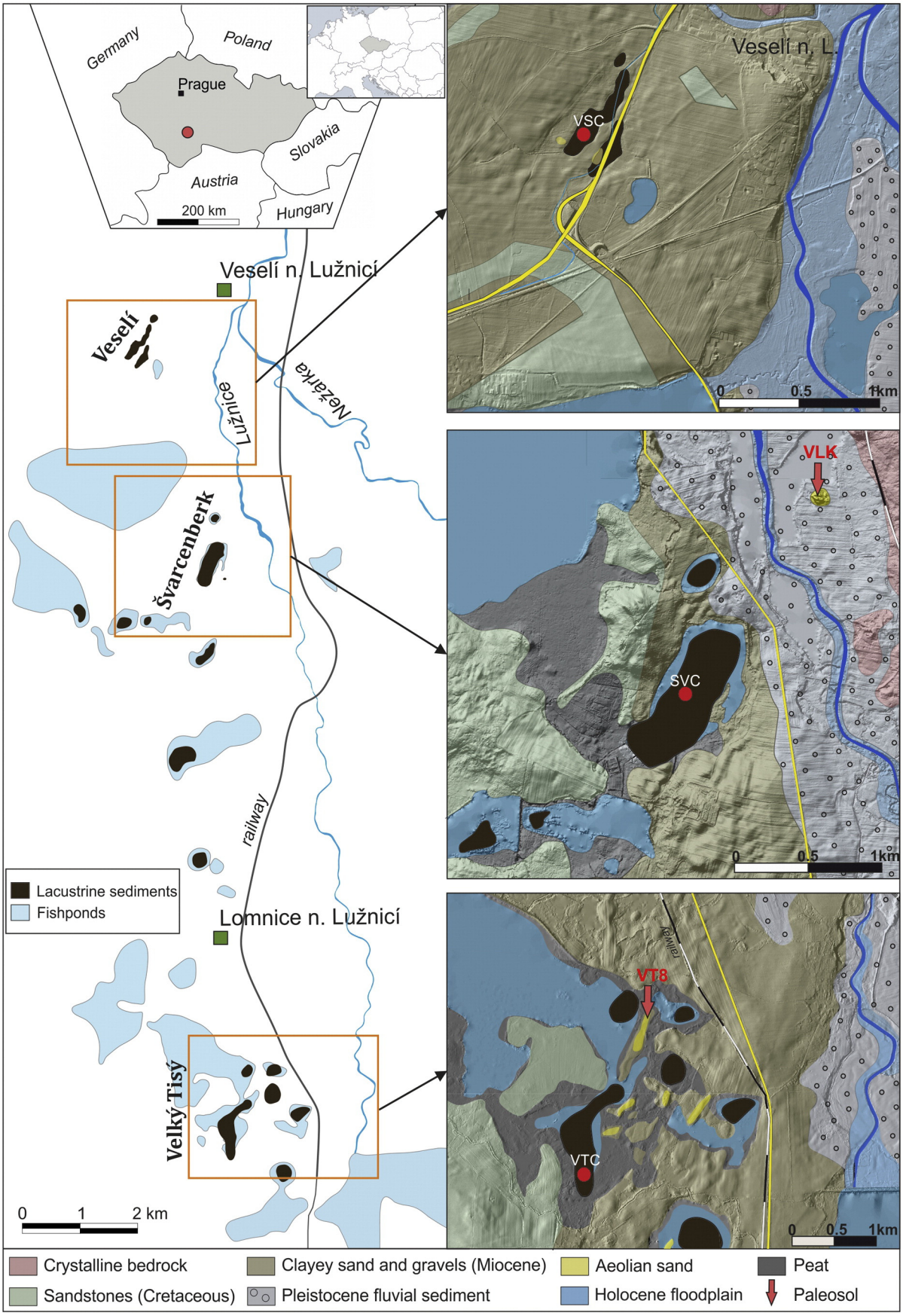

Fig. 1. Location of the study area and simplified geological map with positions of coring sites. Red arrows mark the sites with paleosol horizons buried by sand dunes. (For interpretation of the references to colour in this figure legend, the reader is referred to the web version of this article.)

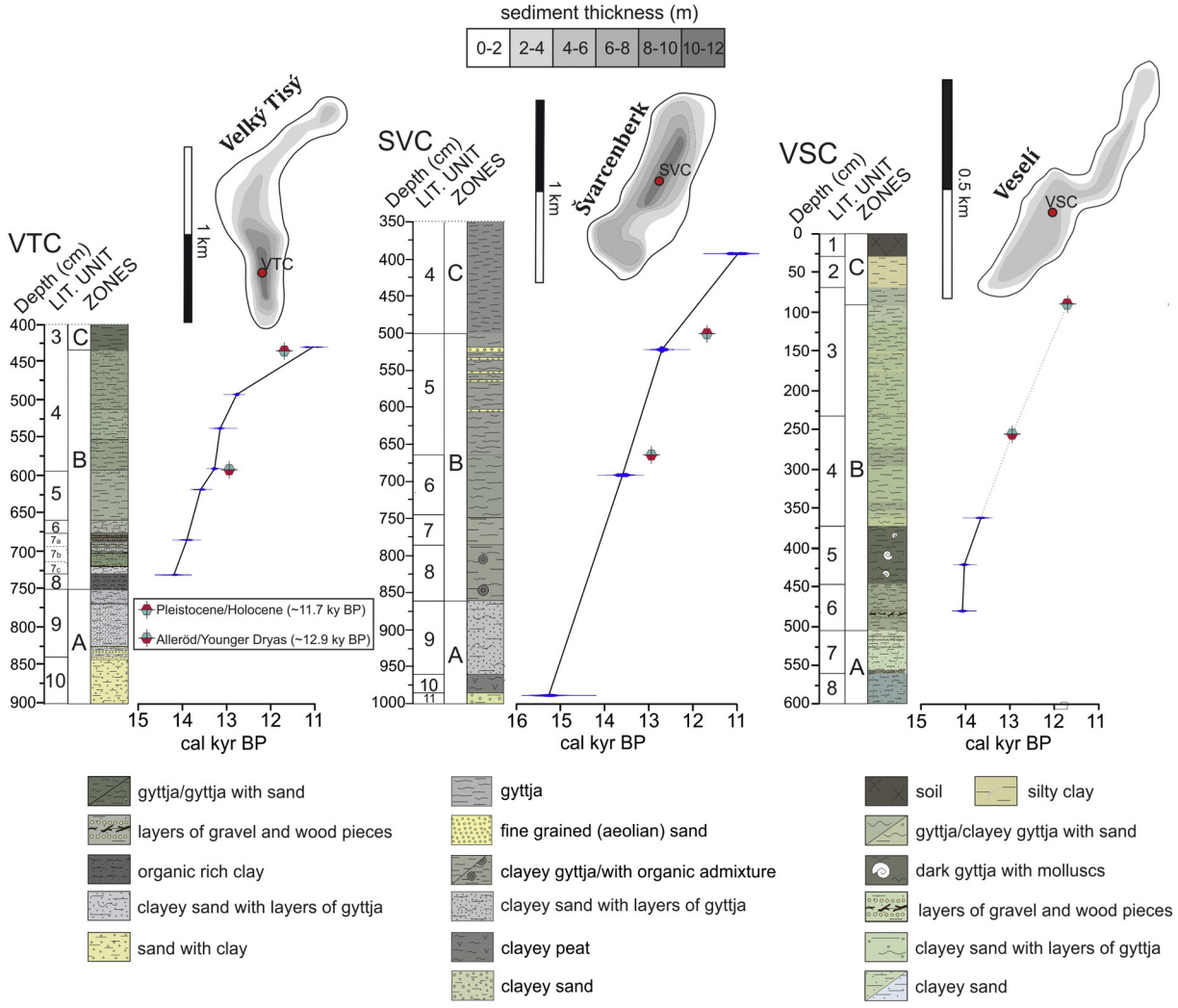

Fig. 2. Lithology and age-depth relation for VTC, SVC and VSC cores together with the bathymetry of studied lakes. Boundaries between Alleröd-Younger Dryas (~12.9 ky BP) and Pleistocene-Holocene (~11.7 ky BP; both defined following Lowe et al., 2008) were added based on chemostratigraphy and, in the case of the SVC core, also based on palynostratigraphy (adopted from Hošek et al., 2014).

prepared for ^{14}C accelerated mass spectrometry (AMS) and dated at the Poznan radiocarbon laboratory in Poland (abrr. Poz-), at the Center for Applied Isotope Studies, University of Georgia in USA (abrr. UGAMS-), and at the Radiocarbon Dating Laboratory, Department of Quaternary Geology, Lund/Sweden (abrr. LuA-; see Table 1). Samples were treated with 5% HCl at the temperature 80 °C for 1 hour, then they were washed with deionized water on the fiberglass filter and rinsed with diluted NaOH to remove possible contamination by humic acids. After that samples were treated with diluted HCL again, washed with deionized water and dried at 60 °C. The cleaned samples were combusted at 900 °C in evacuated/sealed quartz ampoule in the present CuO.

The depth-age relationship of the cores was performed using a depth-age model constructed in the software CLAM 2.2 (Blaauw, 2010). The model is based on the linear interpolation of dates calibrated according to the northern hemisphere terrestrial curve IntCal13.14C (Reimer et al., 2013).

3.2. Geochemical, LOI, $\delta^{15}N$, and grain-size analyses

We included data on the elemental concentration of titanium (Ti), rubidium (Rb), strontium (Sr), iron (Fe), calcium (Ca) and phosphorus (P) in our study in order to detect changes in the lithogenic influx and chemical weathering intensity in the catchments. X-ray fluorescence (XRF) measurements were performed on split cores at a resolution of 1–2.5 cm using a NITON XL3t 950 GOLDD + (Thermo Scientific) spectrometer with 50 kV Ag tube and large-area SD detector (used for the cores VTC and SVC) and Delta Professional spectrometer with 50 kV Rh tube (used for the core VSC).

For better assessment of the erosion-weathering processes in the study area, samples from the VTC core were used to carry out additional analyses.

The stable isotopic composition of nitrogen was measured from samples at a depth of 770–400 cm in 2.5–8 cm intervals at the Laboratory of Geochemistry of the Faculty of Science of Charles University in Prague. Samples were decarbonized with 0.5 mol/L HCl, wrapped in tin capsules and combusted or high-temperature pyrolysed. $\delta^{15}N$ was determined using a Thermo Flash 2000 elemental analyzer connected to a Thermo Delta V Advantage isotope-ratio mass spectrometer in a Continuous Flow IV system and oxygen. $\delta^{15}N$ is expressed relative to atmospheric nitrogen and normalized to a calibration curve based on international standards.

LOI (%) was calculated as the difference in weight between the sediment dried at 110 °C and ash produced at 550 °C within a high temperature muffle furnace (Heiri et al., 2001).

Ash residual material from the VTC core was used for granulometric analyses using a laser size analyzer CILAS 1190 LD that provides a measurement range from 0.04 to 2500 μm. Following Syvitski (1991) and Sperazza et al. (2004), the samples were treated with 0.5 mol/L HCl,

Table 1
Results on radiocarbon dating from the cores VTC, SVC, VSC and paleosol VLK.

Lab. code	Profile, depth (cm)	Type of material	^{14}C age BP	Calibrated age range cal. yr BP	Reference
LuA-4590	SVC, 390–393	Woody stem fragment	9640 ± 115	10,801–11,147 (68%)	Pokorný, 2002
LuA-4591	SVC, 520–523	Bulk gyttja sample	10,780 ± 115	12,654–12,877 (68%)	Pokorný, 2002
LuA-4738	SVC, 680–683	Bulk gyttja sample	11,750 ± 120	13,464–13,813 (68%)	Pokorný, 2002
LuA-4737	SVC, 985–995	Salix twigs	12,800 ± 120	14,943–15,617(68%)	Hošek et al., 2014
Poz-72027	VTC, 422–423	Bulk gyttja sample	9670 ± 60	11,061–11,214 (50.7%) 10,786–10,981 (39.2%) 10,986–11,033 (5.1%)	This study
Poz-72212	VTC, 487–488	Bulk gyttja sample	10.840 ± 60	12,672–12,823 (95%)	This study
Poz-72071	VTC, 536–537	Bulk gyttja sample	11.250 ± 60	13,019–13,249 (95%)	This study
UGAMS-25537	VTC, 590	Bulk gyttja sample	11.400 ± 30	13,152–13,306 (95%)	This study
Poz-72028	VTC, 617–618	Bulk gyttja sample	11.730 ± 70	13,448–13,717 (95%)	This study
Poz-71860	VTC, 678–679	Betula (fruit, seeds)	12.000 ± 60	13,729–14,037 (95%)	This study
Poz-71861	VTC, 730–735	Woody fragment	12.240 ± 60	13,960–14,449 (95%)	This study
UGAMS-25536	VSC, 282.5	Bulk gyttja sample	11.890 ± 35	13,580–13,776 (95%)	This study
UGAMS-23611	VSC, 355–360	??? Carex	11.830 ± 70	13,534–13,772 (89.8%) 13,483–13,527 (5.2%)	This study
UGAMS-23612	VSC, 420–422	Salix/Populus (wood fragment)	12.140 ± 30	13,905–14,152 (94.7%) 13,880–13,884 (0.3%)	This study
Poz-80136	VLK_surface, 185	Charcoal fragments	10.560 ± 70	12,380–12,705 (92.5%)12,239–12,274 (1.8%) 12,308–2325 (0.6%)	This study
LuA-4645	VLK_subsurface, 190	Charcoal fragments	11,260 ± 120	12,829–13,343 (95%)	Pokorný and Růžičková, 2000
Poz-80137	VLK_bottom, 198	Charcoal fragments	11,530 ± 60	13,263–13,475 (95%)	This study

dispersed with 5.5 g KOH 24 h prior to analysis, and 60 s of ultrasonication was used during analysis.

3.3. Rock-magnetic measurements

Rock-magnetic investigations were applied on the VTC core. The core was subsampled continuously at 2.5 cm intervals using plastic cubes with an inner volume of 6.7 cm^3. Values of saturated isothermal remanent magnetization (SIRM) were imparted with a MMPM 10 pulse magnetizer using a field of 2 T. The sample was then imparted in a back field at 200 mT (IRM_200 mT). Remanence measurements were made using a JR6-A spinner magnetometer with a noise level of 0.1×10^{-8} A/m^2. The S-ratio was calculated conventionally as IRM_200 mT/SIRM.

For the correlation of magnetic and geochemical parameters, as well as the chemical element concentration and pollen record, the Pearson's correlation coefficient r was used.

3.4. Micromorphology

Four oriented soil samples were taken in small Kubiena boxes (dimensions 3 × 5 cm) from the buried soil in the "Vlkoský přesyp" sand dune (VLK) and one from the paleosol in the proximity of Lake Velký Tisý (VT8) (Fig. 1). Upon slow drying followed by impregnation with resin, thin sections were produced from samples in the laboratory of the Czech Geological Survey (equivalent to Bullock et al., 1985; Stoops, 2003). The thin sections were studied under polarizing microscopes at a magnification of 16–800× and interpreted according to Stoops et al. (2010).

4. Results

4.1. Lithostratigraphy and chronology of lake sediments

General lithological descriptions of the studied cores are shown in Figs. 2–4. We were able to divide the studied sedimentary records into three main zones (A-B-C), corresponding to major environmental changes in the study area. Within these zones, particular lithological units (LUs) for each studied core were differentiated. The basal parts of the studied sections (zone A) consist of minerogenic sediments (clayed sand/gravel) with a very low content of organic matter. In the overlying 3 to 4-m-thick zone B, a slightly grey/greenish grey, fine-detritus gyttja prevails. In the lower part of this zone, an increased input of allochthonous mineral (fine-grained sand and silt) is found, whereas in the upper part the zone is characterized by quiet lacustrine sedimentation. The uppermost part of the studied cores (zone C) consists of organic-rich, fine- and coarse-detritus gyttja, sometimes rich in microscopic charcoal. In the case of the VSC core, only a thin layer from this upper zone is preserved, due to the destruction caused by agriculture management.

Based on 7 radiocarbon dates from the VTC, 3 dates from the VSC, and 3 dates from the SVC core (Table 1), zone B represents the Late Glacial period and the sediment from the studied cores provide a complete high-resolution record of this period. The underlying zone A was accumulated probably during the Pleniglacial (LGM), and zone C corresponds with the Holocene. In this paper, mainly the zone B (LG) are investigated.

4.2. Elemental variations in the sediment cores VTC, SVC, and VSC

The stratigraphic variations of selected elements in the individual cores from the three studied lakes are shown in Figs. 3 and 4. The gross trends in these proxies show considerable regularity between the three cores. Common features of the geochemical record of the Late Glacial part of all the studied cores (zone B) allowed us to subdivide this zone into particular subzones B1, B2, and B3.

In lacustrine environments, titanium has been found to be a good measure of the intensity of detrital input, similarly as in, for example, Whitlock et al. (2008). The highest concentrations of Ti were found in zones A (VTC, VSC) and B3 (SVC) (Figs. 3 and 4), denoting the significant input of mineral-clastic material to the lakes. In general, distinct phases of increased influx of detrital material are visible on the LG part of the records (zone B). The highest Ti concentrations have been found within subzones B3, whereas subzones B2 and the lower part of subzone B1 show rather lower concentrations. In zone C, Ti concentration significantly decreases.

The iron record of the lacustrine sediments (Figs. 3 and 4) is characterized by high values within subzone B2, relatively low (SVC) or descending (VTC and SVC) values within subzone B3, and rather low to

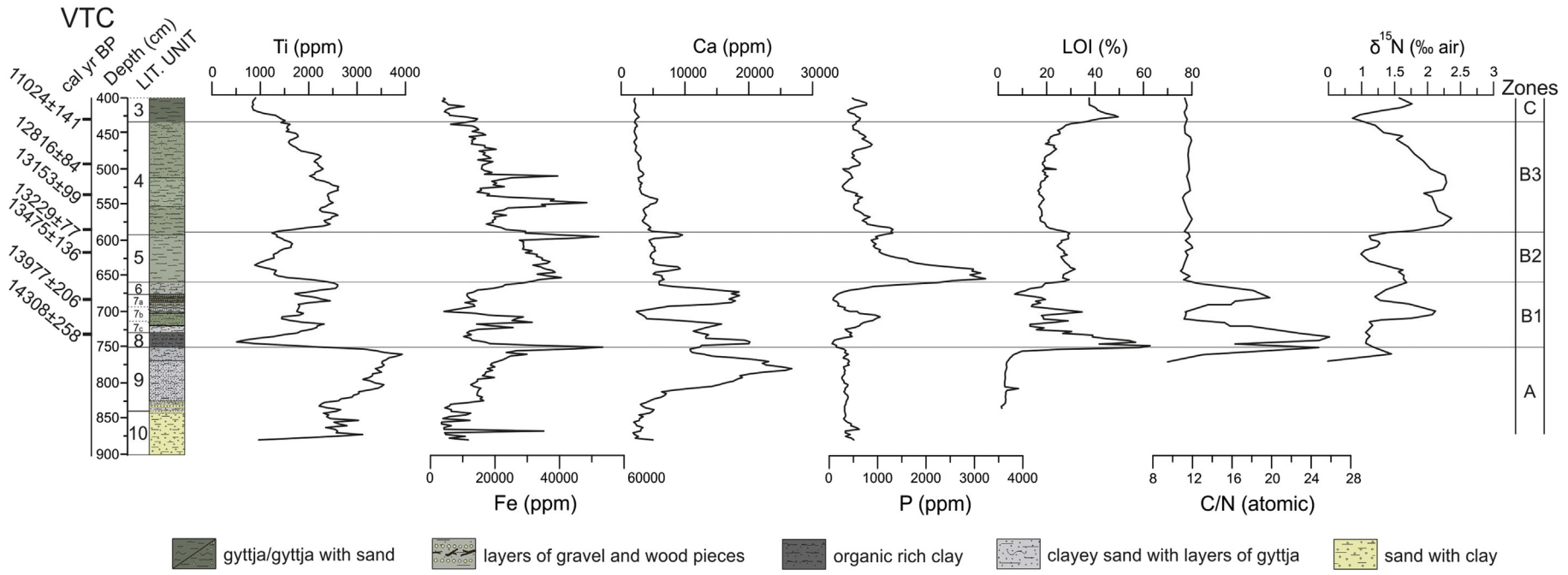

Fig. 3. Graphs of selected elements concentration, Loss on Ignition (LOI), C/N and $\delta^{15}N$ in the core VTC plotted by depth.

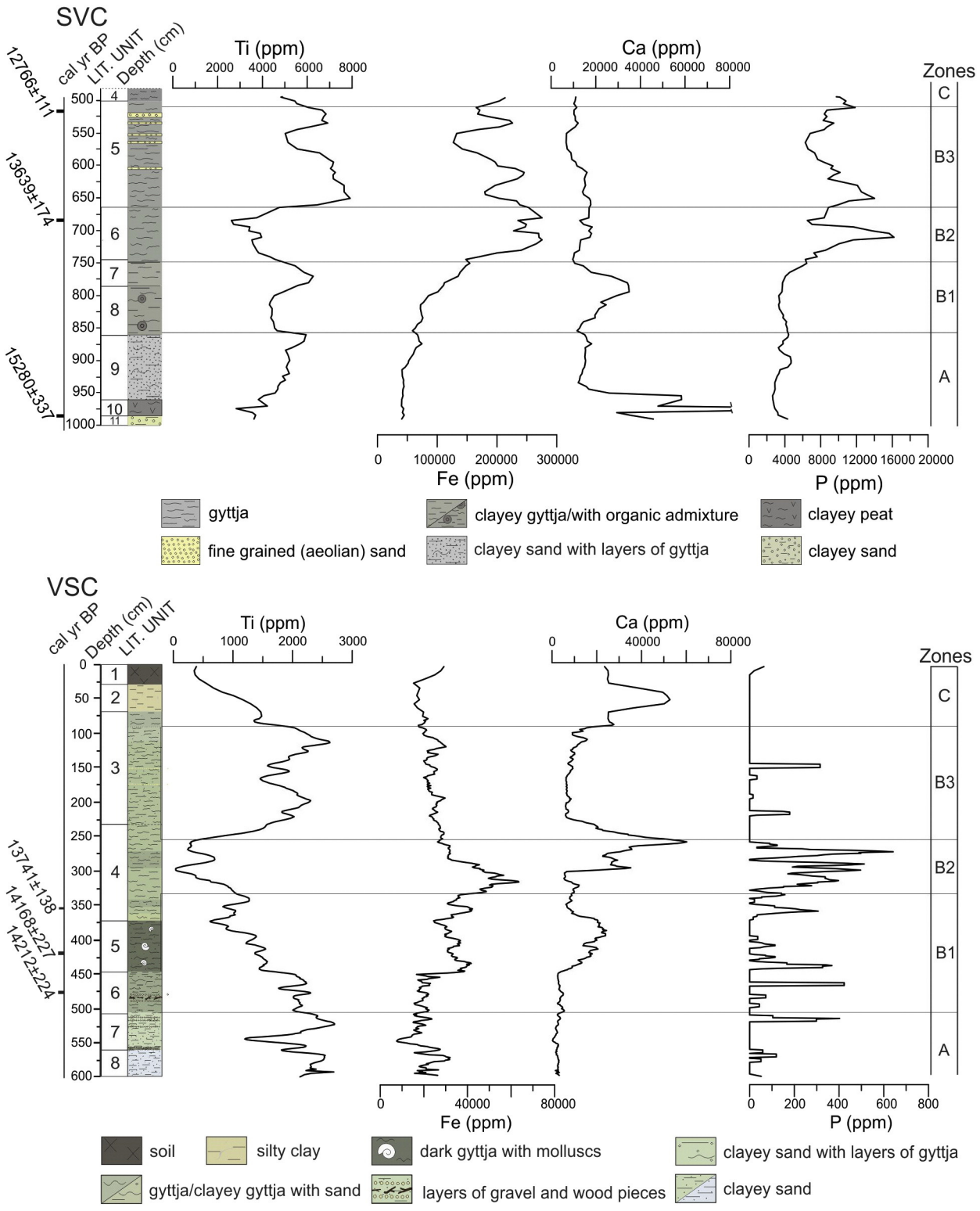

Fig. 4. Graphs of selected elements concentration in the cores SVC and VSC plotted by depth.

moderate values with subzone B1 and zone A, except for the lithological units VTC_7 and 8 and VSC_5, where increased concentrations of Fe were found. A weak correlation between Fe and Ti in VTC and SVC ($r = \sim 0.10, 0.22$) and even a weak negative correlation in VSC ($r = -0.14$) suggest that the enrichment of the lake sediments in Fe cannot be attributed to enhanced detrital input.

Although lacustrine sediments in the research area are found to be acidic and carbonate-poor, some horizons showed an enrichment in calcium. Depth variations of the Ca records have generally shown opposite trends to that of Fe (Figs. 3 and 4). In the VTC core (Fig. 3), the high concentrations of Ca correspond with the upper part of zone A (LU VTC_9) and subzone B1, whereas subzones B2 and B3 show a significantly lower concentration as well as a descending trend in Ca concentration. A similar record has also been found in the SVC core (Fig. 4); in this profile the highest Ca concentration relates to the LU SVC_10 (zone A) and SVC_7 (subzone B1). In the core VSC (Fig. 4) a higher content of

Ca has been found within LU VSC_5 (subzone B1) and subzone B2. In contrast, Zone A and subzone B3 seem to be almost calcium- (carbonate-) free.

Phosphorus reaches maximum concentrations within subzone B2, whereas zone A shows low values, both similarly in all cores. In the VTC and SVC cores (Figs. 3 and 4) there is some increase in the lower part of subzone B3 and, in the case of VTC, also in the middle part of subzone B1 (LU VTC_7). Phosphorus concentrations show a good positive linear relationship with Fe in the LG part (Zone B), in core VTC ($r = 0.61$) and SVC ($r = 0.71$). In the VSC core this relationship has only a weak correlation ($r = 0.44$).

4.3. Results from the VTC core

4.3.1. C/N and LOI

The organic matter (OM) in sediments is able to record the relative contributions of the particulate detritus of plants coming from a catchment (allochthonous) or from the aquatic environment (autochthonous). The origin of aquatic organic matter is conventionally distinguished from allochthonous (terrigenous) material by the C/N ratios. Lacustrine algae have low C/N ratios, commonly between 4 and 10, whereas upland vascular plants have C/N ratios of 20 or more (Meyers and Lallier-Vergès, 1999). In subzone B1, the C/N ratio ranges from 28 to 11 (Fig. 3), indicating the significant contribution of terrestrial OM in the lacustrine sediment. The maximum values correspond with LU VTC_8 (clayey peat) and the upper part of LU VTC_7 (silty gyttja with an admixture of plant macro-remains). Within subzones B2 and B3, the C/N ratios are rather stable, being around 11, denoting that the organic component of gyttja is mainly composed of the remains from autochthonic aquatic production. This interpretation is supported by microscopic examinations that revealed remnants of microscopic organisms, mainly algae.

Based on this finding, the values of LOI (Fig. 3) in the B2 and B3 subzones can be taken mostly as a proxy for primary lake productivity, which was definitely driven mainly by climate conditions (Heiri et al., 2001). The LOI values show an opposite trend to the Ti concentrations discussed above. The content of OM within zone A is very low, ranging from 0 to 3%. The highest content of OM (up to 60%) coincides with the layer of clayey peat in the bottom of subzone B1 (LU VTC_8). Subzone B2 also shows a higher content of OM (~25%), whereas within subzone B3 the content of OM again progressively decreases (~16%). The uppermost part of subzone B3 is characterized by a sudden increase of OM content, which reaches its maximum at the LG/Holocene boundary.

4.3.2. $\delta^{15}N$ and paleoclimatic interpretations

Although nitrogen isotope composition ($\delta^{15}N$) in lake sediments can be influenced by several mechanisms (see Xu et al., 2014 and references therein), a considerable factor influencing $\delta^{15}N$ can be, similar to C/N, the amount of terrigenous organic matter entering the lake. Lowering $\delta^{15}N$ values can thus be associated with a higher amount of terrigenous organic matter and vice versa. Consequently the denser vegetation cover and soil development during a warm-humid period leads to low $\delta^{15}N$ values in lake sediments, while elevated $\delta^{15}N$ values can indicate sparser vegetation, weak pedogenesis, and thus a cool (and dry) climate (Watanabe et al., 2004; Zhang et al., 2014).

The values of $\delta^{15}N$ (Fig. 3) vary between 0.47 and 2.73% with an average value of 1.54. The depth profile shows rather low values in subzone B1, except for its middle part (LU VTC_7), where a significant increase of $\delta^{15}N$ was found (Fig. 3). Another peak in $\delta^{15}N$ occurs at the B1/B2 boundary. Subzone B2 is characterized by a range of lower values ~1.1‰; slight increases of $\delta^{15}N$ have been detected in the upper part of this subzone (617.5–600 cm). In subzone B3 there is a sudden increase of $\delta^{15}N$; peak values are high (~2.3‰) within the lower part of the subzone (500 cm) and then continuously decrease up to the LG/Holocene threshold, when they rise again.

During the whole of LG the $\delta^{15}N$ values show very similar depth variations as the Ti record ($r = 0.54$) (Fig. 3). In subzone B1, the increases of $\delta^{15}N$ lag behind the peaks of Ti, resulting in a low/moderate correlation coefficient ($r = 0.20$), whereas in subzones B2 and B3 a strong correlation ($r = 0.85$) between these proxies has been found.

4.3.3. Grain-size variations

Depth-variations of clay-, silt-, and sand-grain sizes of the mineral clasts, together with the mean grain size (MGS), are shown in Fig. 5. Basal sediments in LU VTC_10 (880–750 cm) consist mainly of coarse silt to fine/medium coarse sand. In the over-lying grey sandy silt (LU VTC_9) the fraction 16–42 μm prevails. Average grain size in subzone B1 is 34 μm. This subzone is characterized by the higher dynamics of the coarse-grained input. The most prominent input of the coarse-grained clasts is coincident with LU VTC_6 (650–700 cm, MGS up to 72 μm, maximum grain size up to 500 μm). Within subzone B2 (LU VTC_3) a medium-coarse silt (23 μm) prevails. In the upper part of the unit gyttja is enriched by clay (up to 8%). Average grain-size of subzone B3 (LU VTC_4) is 27 μm; the striking feature of the upper part of this subzone is the high content of the clay fraction (up to 12%). By contrast, the middle part (depths 475–550 cm) is characterized by a distinct input of a coarse-grained fraction (MGS up to 45 μm, maximum grain size up to 200 μm).

4.3.4. SIRM and S-ratio

Rock-magnetic parameters, in concert with the geochemical and sedimentological characteristics, provide a valuable contribution to environmental reconstructions, since the magnetic properties can mirror both the environmental conditions on land and the intra-lake processes (Just et al., 2015).

Depth-variations of the SIRM and S-ratio are shown in Fig. 5. SIRM is a parameter providing information mostly on the concentration of fine-grained magnetite preferably formed by pedogenesis (Heller and Evans, 1995). The values of SIRM (in 10^{-3} A/m) vary between 0.5 and 610. In zone A and subzone B1, the rock magnetic record correlates with the lithology. On the bottom of zone A (LU VTC_10) are very low values of SIRM, apparently due to the presence of diamagnetic quartz sand. Maximum values correspond with LU VTC_9, where clayey silt dominates. A sharp decrease of magnetic values in zone B1 (LU VTC_8) is caused by a significantly high content of diamagnetic organic matter (up to 80%), which reduces the magnetic signal. Peaks of SIRM within subzone B1 correlate with layers of increased influxes of silt and fine-grained sand mixed with plant macro-remains (LU VCTC_7). Within subzones B2 and B3 (homogenous fine-detritus gyttja) rather low SIRM ($2-12$) was found. Increased values of SIRM (lower and upper part of B2, upper part of B3) have no lithological correlates.

The S-ratio is a concentration-independent proxy for the relative abundance of ferrimagnetic to antiferromagnetic minerals (Maher, 1986; Wang et al., 2012). Elevated values reflect the dominance of magnetite (or maghemite), while lower values represent increasing contributions from antiferromagnetic minerals, i.e. hematite or goethite. The S-Ratio is in general high and varies less in zone A (0.9 to 1), whereas in zone B the S-ratio is scattered between 0.75 and 1 (Fig. 5). The positive correlation of SIRM with the S-ratio ($r = 0.61$) suggests magnetically-soft ferrimagnetic minerals (magnetite or maghemite) as the main carriers of magnetic remanence. Consequently, the lower S-ratio values observed in some horizons (lower part of LU VTC_7, VTC_6, middle part of VTC5, VTC_4) signalize an increased presence of magnetically-harder antiferromagnetic minerals (hematite or goethite), which have overall weak magnetic signals (Robinson, 1986).

Elevated SIRM, and consequently a high S-ratio, within zone A indicates a magnetite/maghemite population that is probably of detrital origin because it occurs in mineral-clastic-rich sediments deposited with a minimum of organic matter (LOI 0.1–3%).

SIRM shows a weak/moderate positive correlation with Ti content within zone A ($r = 0.44$), a very weak correlation within subzone B1

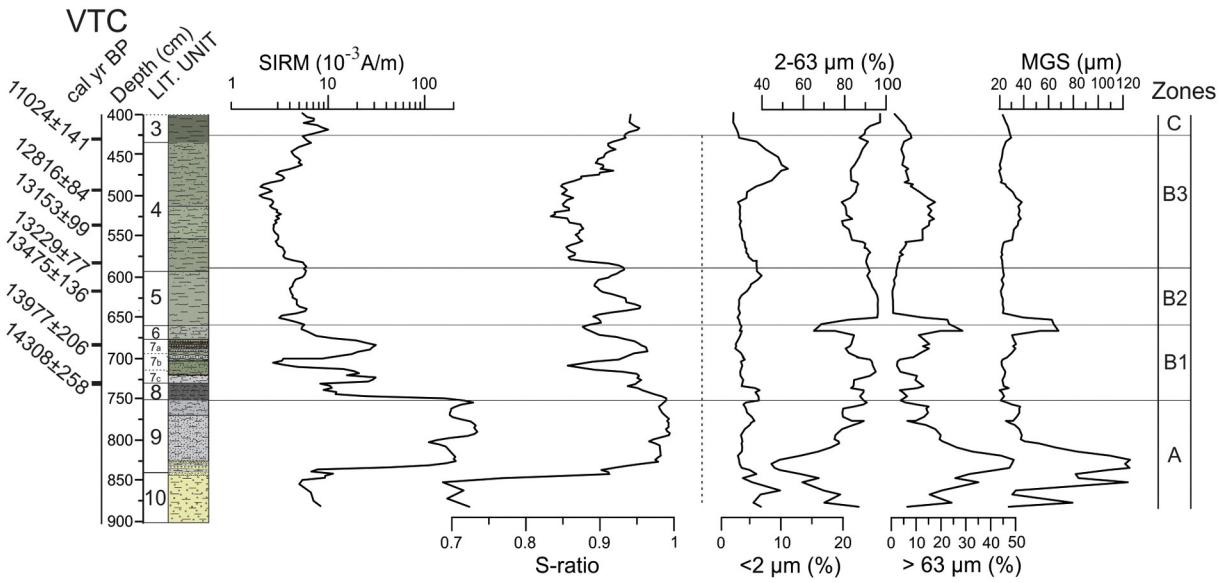

Fig. 5. SIRM, S-ratio and grain-size variations in the core VTC.

($r = 0.11$), and a strong negative correlation within subzones B2 and B3 ($r = -0.66$, Fig. 6). The correlation between the S-ratio and Ti shows a similar behaviour as the SIRM. It is slightly positive in zone A ($r = 0.32$), very weak in B1 and strongly negative in B2 and B3 ($r = -0.88$). Both magnetic parameters show positive correlation with Ca ($r = 0.43$ for SIRM and 0.57 for S-ratio) for zones A and B1, whereas in subzones B2 and B3 this relationship does not occur. Within subzones B2 and B3, where the fine-detritus gyttja dominates, the S-ratio as well as SIRM are obviously positively correlated with LOI ($r = 0.81$ and 0.72, Fig. 6), denoting that the magnetic enhancement of the lacustrine sediment occurred during periods with increased lake productivity, which we can assign to a warmer climate. Within subzone B1, SIRM and the S-ratio show linear correlation with C/N ($r = 0.58$ and 0.61, respectively) suggesting that the magnetic signal is positively influenced by an influx of terrestrial organic material.

The S-ratio and $\delta^{15}N$ have a significant strong correlation ($r = -0.75$) during the whole LG (Fig. 6). The SIRM and $\delta^{15}N$ anti-correlate moderately within subzone B1 ($r = -0.42$) and strongly ($r = -0.64$) within subzones B2 and B3.

4.4. The paleosols - field observations, micromorphological description, dating

We have discovered two paleosols under aeolian sand: VT8 paleosol, situated in the proximity of the former shore of Lake Velký Tisý, and VLK paleosol, located in the NE proximity of Lake Švarcenberk (Fig. 1). The profiles of these paleosols and superimposed sand dunes are sketched in Fig. 7. The basal part of the VLK profile consists of non-stratified, medium and coarse sand with fine gravel. A charcoal sample from the top of this basal layer provided a radiocarbon age of 13,427 ± 116 cal yr BP. The over-lying, 21-cm-thick, brownish-yellow (10YR6/8) soil horizon is characterized by its massive texture and low organic content (0.6–1.2%). The over-lying, 170-cm-thick, aeolian accumulation consists of well-sorted, fine to medium sand with a layer of coarse sand and gravel.

At the base of the profile from the VT8 site, clayey sand (Miocene sediment) has been found. This basal sediment is overlain by a 15-cm-thick layer of brownish-yellow (10YR6/6) clay mixed with fine- to medium-grained sand. Macroscopic charcoals and features of oxidation-reduction features (Fe and Mn nodules) are present. This layer is buried under a 90-cm-thick horizon of aeolian sand. A 15-cm-thick, podzol, horizon sequence (O-E-Bhs) developed on the top of this sequence and some placic horizons were recognized within the aeolian sand.

Four samples from the VLK paleosol and one sample from the VT8 paleosol were obtained from the above-discussed sequences; their significant micromorphological features are summarized in Table 2 and shown in Fig. 8.

According to the field and micromorphological observations on the VLK paleosol (see Table 2), the lower part (21–9 cm, sample VLK_2, Fig. 8a) consists of an intact, gley-spodic horizon of podzol, whereas the upper part (8–0 cm; VLK_1, 3, 4) is probably a redeposited B horizon mixed with sand and poorly-decomposed organic matter. Apart from the fragments of B horizon, possible fragments of humic A horizon (Fig. 8b) and albic E horizon (Fig. 8d) were found. This pedo-colluvial horizon was post-sedimentarily illuviated and gleyed. It contains abundant charcoal fragments that was dated to 13,155 ± 150 cal. yr BP. The pedo-colluvial horizon is overlain by a 2 to 4-cm-thick layer reddish yellow clay (7.5YR6/6) with sand and abundant size-sorted, charcoal and mineralized, wood fragments (average size 0.3 cm in diameter). The sample obtained from these organic fragments yielded a radiocarbon age of 12,492 ± 169 cal. yr BP.

Micromorphological analyses of the VT8 site (Fig. 8e–f, Table 2) have proved the nature of the material: soil sediment. This layer is similar to that found in the upper part of the VLK site; nevertheless, fragments of former soil horizons are rather rare. Post-sedimentary illuviation also took place, but its intensity was significantly lower compared to that from the VLK site.

5. Discussion

5.1. Titanium and magnetic proxies as indicators of erosion and pedogenesis processes

In order to remove the effects of the detrital chemistry, titanium (Ti) was taken to represent an element that is relatively immobile during weathering and stays predominantly in the allogenic phase (Young and Nesbitt, 1998). The minerals containing Ti are not dissolved in an exogenic environment (Demory et al., 2005) and are biologically not very active (Eusterhues et al., 2005), so their concentration in lacustrine sediment is mostly related to the erosion rate in the lake catchment. Since Ti is most enhanced in fine-grained, clastic-rich sediments (it is especially strongly bounded on the clay fraction) its higher values could also have originated from wind-blown/eroded loess or the

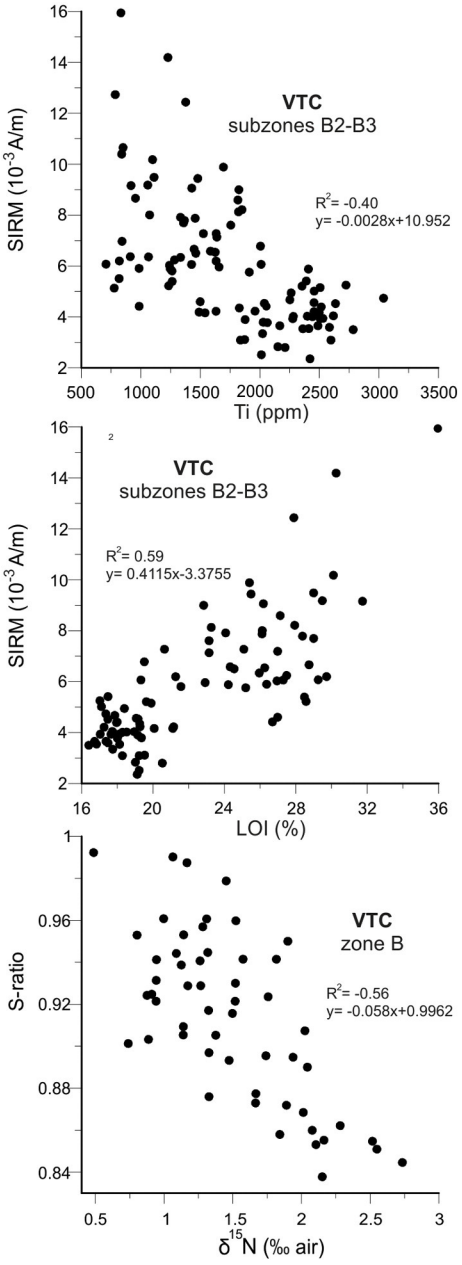

Fig. 6. Scatterplots of (a) SIRM versus Ti, (b) SIRM versus LOI and (c) and S-ratio versus $\delta^{15}N$ in the core VTC.

intensive erosion of catchment mineral soils (Yancheva et al., 2007; Dietrich and Sirocko, 2011).

In the study area, the Miocene clayey sand can be considered an appreciable contributor to Ti in the lake sediment. This is demonstrated in the relationship between Ti and concentration of reworked Tertiary palynomorphs in the SVC core, which shows an obvious similarity throughout zone A and subzones B2 and B3 (Fig. 9). A negative correlation (a decrease in the concentration of Tertiary palynomorphs with increasing content of Ti in LU SVC_7, subzone B1) could have been caused by the erosion of a former loess cover from the lake catchment. This interpretation is supported by a substantially-elevated concentration of Ca in these sedimentary strata (Fig. 4). Eroded (water-, or wind-transported) loess could also be the source of Ti in zone A and partially also in subzone B1. In these horizons the calcium content is ten times higher than in the present bedrock. The higher content of Ca further correlates with an increased presence of medium/coarse silt, i.e. grain-size fraction 16–42 μm typical for loess (Smalley, 1995).

Since humic soil horizons are usually enriched by fine-grained (single-domain and superparamagnetic) magnetite and maghemite (Jordanova et al., 2013), the elevated magnetic values in the monotonous, organo-mineral, lacustrine sediment can be connected with a more intensive pedogenesis in the lake catchment (Maher and Taylor, 1988). The good correlation between S-ratio and SIRM with LOI and $\delta^{15}N$ (Fig. 6) in the sediment strata where the fine-detritus gyttja dominates (subzones B2 and B3) suggests that the magnetite/maghemite enhancement of the lacustrine sediments can be attributed to warmer (more humid) periods and thus a humic soil-horizon development in the lake catchment.

On the other hand, a higher content of ferrimagnets in zone A and also in LU VTC_7a and 7c (subzone B1) can be attributed to the presence of eroded (wind-blown) loess, which is, in general, enriched in coarse-grained (lithogenic) magnetite (Maher and Thompson, 1991). This assumption is supported by the very similar depth variation of SIRM and Ca in these horizons (Figs. 3 and 5).

5.2. Paleoenvironmental implications and local climatostratigraphy

The close similarity of the Ti depth-variations in all studied lacustrine sedimentary sequences suggests that the dynamics of the allogenic input into the three studied lake basins was driven by the same mechanisms, most probably triggered by the climatic changes. We assume that the relationship between cold climate and higher amounts of Ti in the lake sediment was caused by the following process: when the climate deteriorated, vegetation was destabilized by ecological stress. Events, such as blowdowns and fires, became more frequent under such circumstances. The resulting disturbed surface was more prone to erosion, including aeolian transport and such processes would result in higher Ti contents in the lake basins as compared with more stable warm periods. In the study area this assumption is supported by: 1) the positive relationship between Ti and pollen percentages of *Artemisia* (Fig. 10), which is commonly used as an indicator of cold and dry climate and thus sparse vegetation cover (Hongyan et al., 2013); and 2) the strong positive correlation between Ti and $\delta^{15}N$ (Fig. 6). The former finding also confirms the observations from some other sites: that measurements of $\delta^{15}N$ in lacustrine sediments can be considered as a powerful proxy for climate reconstructions.

The idea that Ti is a suitable tracer of the climatic record in our study area is further supported by the close similarity between the $\delta^{18}O$ Greenland record (NGRIP Members, 2004) and the depth-variations of Ti content in all the studied lakes (Fig. 11). These findings allow us to subdivide the records into particular units, corresponding to already-known LG biostratigraphy (sensu Mangerud et al., 1974) and comparable with the event stratigraphy proposed by Lowe et al. (2008). Based on this syllogism, subzone B1 very probably corresponds with Bølling, subzone B2 with Allerød, subzone B3 matches to Younger Dryas and B/C threshold correlates with the Younger Dryas/Holocene transition.

Apart from this kind of wiggle-matching, our correlation is supported by radiocarbon dating, and in the case of the SVC core by the regional pollen stratigraphy as well (Pokorný, 2002; Hošek et al., 2014).

In addition to the prominent stages, some minor climatic events were identified in the study area.

5.2.1. Bølling-Allerød warm period and two minor cooling events within

In comparison with the preceding Pleniglacial, sudden climatic amelioration occurred during the onset of the Bølling interstadial (see e.g. steep increase of the LOI in the VTC core, Fig. 3). Nevertheless, Ti records in the VTC and VSC cores show that the soil surface in the research area was still rather unconsolidated, inclinable to erosion. The higher level of catchment erosion during the pre-Allerød period has also been referred to, for example, in the case of Łukie Lake in eastern Poland (Zawiska et al., 2015). In all study lakes, the most prominent erosion event has been found in the uppermost part of the B1 subzone, in the time interval that separates the Bølling and Allerød interstadials. This cooling episode could be associated with the Older Dryas (GI-1d reported by Björck

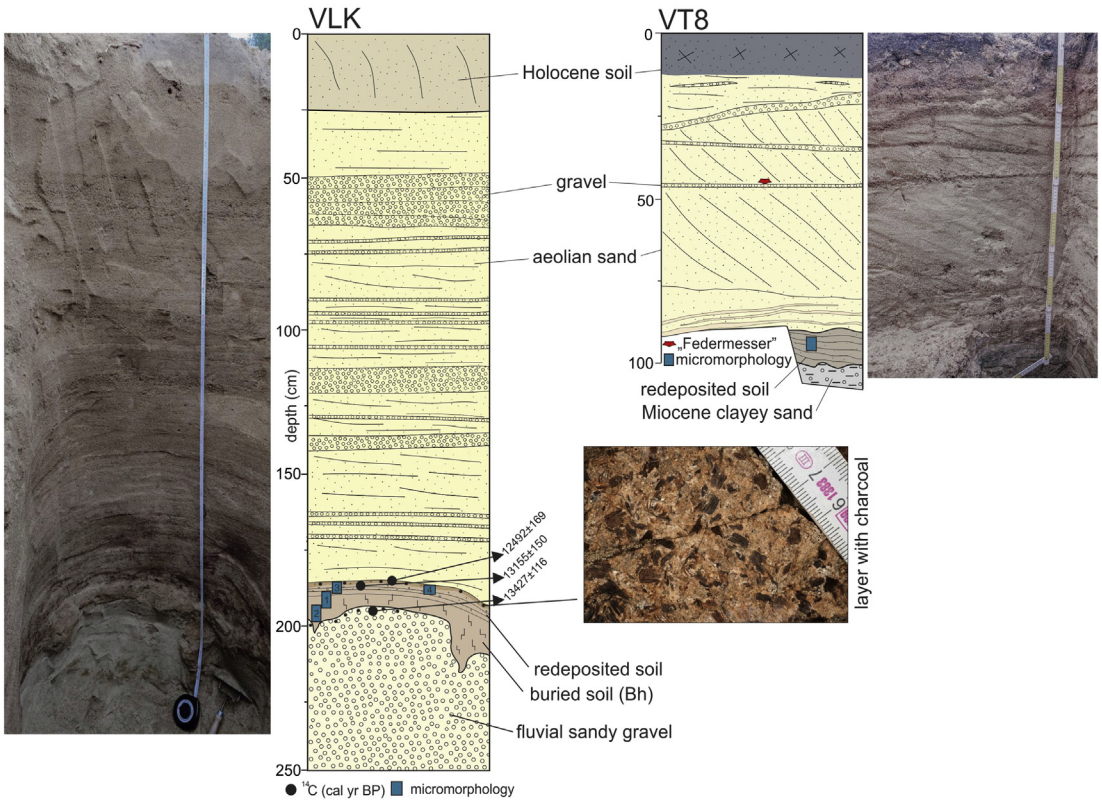

Fig. 7. Profile sketches of paleosol sections Vlkovský přesyp (VLK) and Velký Tisý (VT8). Photo shows a detail of the layer with abundant charcoal and wood fragments.

et al., 1998). This short-lived climatic deterioration is generally recognized in the pollen record in northern and western Europe (e.g. Walker, 1995; Brauer et al., 2000) and has also been found in the oxygen isotopic record of several lakes in southern central Europe, where it is dated to 14,044–13,908 yr BP (von Grafenstein et al., 1999; van Raden et al., 2013). Radiocarbon data 13,977 ± 206 cal. yr BP and 13,741 ± 138 cal. yr BP obtained from the discussed horizons of the VTC and VSC cores support this correlation. Identifying the Older Dryas outside of the NA region has been regarded as problematic, particularly due to the low temporal resolution of most sites already studied and/or the weak response of local vegetation to this climatic event (Lotter et al., 1992). Within the territory of the Czech Republic it has not been clearly detected in pollen records up to now.

The prominent peak of the sand fraction associated with the Older Dryas period in the VTC core (depth 648–677 cm, Fig. 5) could have been caused by a high intensity of erosion and/or by a higher level of aeolian activity. A significant aeolian influx in organic deposits during the Older Dryas has been reported from many sites in the Netherlands (e.g. Bohncke et al., 1993). The increasingly severe conditions during this period are indicated by the expansion of pine, suggesting a fall in mean winter temperatures, and an increase in the continentality of the climate (Pokorný, 2002).

Another signal of the erosion event (climatic deterioration) has been found within the Allerød interstadial (the upper part of subzone B2). This event can be associated with cooling and surface erosion of mineral soils, as suggested by the higher values of Ti and $\delta^{15}N$, and the lower S-ratio (Figs. 3–5). The stratigraphic position, together with the radiocarbon data in the VTC and SVC cores (Fig. 2 and Table 1), suggests that this climatic shift was coeval with the *Intra-Allerød Cold Period* (Amphi-Atlantic Oscillation of Levesque et al., 1993; GI-1b sensu Björck et al., 1998). This centennial-scale cooling event has been reported, for example, from Switzerland (the Gerzensee oscillation; Lotter et al., 1992), Canada (the Killarney Oscillation; Lesveque et al., 1993), Wales (Walker and Harkness 1991), and England (Gransmoor; Walker et al., 1993). At Lake Gerzensee, this event is dated to 13,274–12,989 varve yr BP (van Raden et al., 2013). From lakes in Denmark, the onset of the oscillation is dated between 11,400 and 11,300 ^{14}C BP (Andersen et al., 2000). In the Greenland oxygen isotopic record this event spans the period approximately 13,311–13,099 calendar yr BP (Rasmussen et al., 2006).

Evidence of IACP in all the studied lakes denotes the strong response of the regional environment to this event, which has been recorded only exceptionally and as a weak disruption outside the North Atlantic region (Björck et al., 1996; Velichko et al., 2002; Battarbee et al., 2004).

5.2.2. Younger Dryas

In subzone B3, a sudden increase of allogenic input (higher Ti content, Figs. 3 and 4), and a simultaneous decrease of aquatic and terrestrial organic production (lower LOI and higher $\delta^{15}N$ values in the VTC core; Fig. 3) occurred. These findings point to a rapid cooling, an acceleration of erosion intensity and thus a sparser vegetation cover than that during the preceding Allerød. We attribute this subzone to the Younger Dryas, although the radiocarbon data obtained from the same horizons seem to be obviously older (Table 1, Fig. 11). The discrepancy between radiocarbon measurement results and the rich contextual information provided by chemo- and palyno-stratigraphy (Pokorný, 2002; Hošek et al., 2014, see also Fig. 2) can best be explained by the significant radiocarbon plateaus that are repeatedly reported for the YD period (Ammann and Lotter, 1989; Björck et al., 1996; Wick, 2000).

The maxima of the aeolian dynamics are supposed to occur during the middle period of the YD, as visible on the grain-size record of the VTC core (zone B3, Fig. 5). This period is connected with a significant input of a coarse mineral fraction. In the SVC core, several layers of well-sorted sand are preserved in a position corresponding with the middle and upper part of the YD (see Fig. 4). These aeolian sand layers had already been correlated with the formation of the VLK sand dune, and with the opening up of forest cover (Pokorný and Růžičková, 2000). Higher aeolian activity during this period within the YD is in

Table 2
Micromorphological description of the paleosols from the VLK and VT8 sites.

Sample	Micromorphological features	Interpretation
VLK_2 (Fig. 8a)	Complex microstructure, horizontal pores, cracks, channels, vughs, complex packing voids C/F(500 μm) = 15:85; C/F(500 μm) = 30:70; sandy loam Coarse fraction: subrounded and rounded quartz and plagioclase, mica Matrix brown to dark brown stipple speckled to porostriated Organic components: fragment of partly decomposed organic matter – rare but present; brown decomposed elongated fragments of organic matter (50–100 μm – cca 5%); dark decomposed angular pieces of organic matter (50–100 μm – cca 20%) Pedofeatures: Fe oxide depleted groundmass, Fe/Mn oxidequasicoatings and impregnative nodules, clay infilling and coating	Gley-spodic horizon of podzol
VLK_1 (Fig. 8b)	Cracky microstructure; cracks pores, channels, vughs, complex packing voids C/F(500 μm) = 10:90; C/F(500 μm) = 30:70; sandy loam Coarse fraction: subrounded and rounded quartz and plagioclasse, mica Matrix: orange brown, dark brown to black, stipple speckled, grano and porostriated Organic components: black partly decomposed and decomposed organic matter – preserved as fragments, but composing horizon, brown decomposed elongated fragments of organic matter (50–100 μm – cca 20%); dark decomposed angular pieces of organic matter (50–100 μm – cca 30%) Pedofeatures: Fe oxide depleted groundmass, Fe/Mn oxidequasicoatings and impregnative nodules, Fe/Mn capping, clay infilling and intensive multilayered coating	Redeposited B horizon with fragments of A horizon; features of postsedimentary illuviation
VLK_3 upper part	Vughy microstructure; cracks pores, vughs, chambers C/F(500 μm) = 5:95; C/F(500 μm) = 30:70; sandy loam Coarse fraction: subrounded and rounded quartz and plagioclasse, mica Matrix: brown to light brown, stipple speckled, striated Organic components: dark decomposed angular pieces of organic matter (50–100 μm – cca 5%) Pedofeatures: clay and Fe/Mn oxide depleted matrix, occasional mottles of Fe impregnative nodules	Redeposited soil with features of postsedimentary illuviation and gleying
VLK_3 middle part	Vughy microstructure; cracks pores, vughs C/F(500 μm) = 5:95; C/F(500 μm) = 30:70; sandy loam Coarse fraction: subrounded and rounded quartz and plagioclasse, mica Matrix: orange brown, dark brown to black, stipple speckled, grano and porostriated Organic components: brown decomposed elongated fragments of organic matter (50–100 μm – cca 20%); dark decomposed angular pieces of organic matter (50–100 μm – cca 30%), charcoal – rare Pedofeatures: Fe/Mn oxidequasicoatings and impregnative nodules, Fe/Mn capping, clay infilling and intensive multilayered coating	Redeposited soil with features of postsedimentary? gleying
VLK_3 lower part (Fig. 8d)	Single packing void microstructure; single packing voids C/F(500 μm) = 15:85; C/F(500 μm) = 30:70; sandy loam Coarse fraction: subrounded and rounded quartz and plagioclasse, mica Matrix: orange, clayely, granostriated Organic components: charcoal, microcharcoal, black particle in clay coating Pedofeatures: clay coating	Relict of E horizon?
VLK_4 (Fig. 8d)	Complex microstructure; horizontal pores, cracks, channels, vughs, chambers, complex packing voids C/F(500 μm) = 20:80–50:50; C/F(500 μm) = 30:70; sandy loam to sands Coarse fraction: subrounded and rounded quartz and plagioclase, mica Matrix: stipple speckled to porostriated, brown to dark brown Organic components: fragment of partly decomposed organic matter – rare but present; brown decomposed elongated fragments of organic matter (50–100 μm – cca 10–50%); dark decomposed angular pieces of organic matter (50–100 μm – cca 20–50%) Pedofeatures: Fe oxide depleted groundmass, Fe/Mn oxidequasicoatings and impregnative nodules, clay infilling and coating	Redeposited soil influenced by illuviation of clay minerals and Gleying process
VT8 (Fig. 8e–f)	Massive microstructure; missing pores, only few channels filled with recent partly decomposed roots or rarely compose packing voids C/F(500 μm) = 20:88; C/F(50 μm) = 70:30; unsorted sandy loam Coarse fraction: subangular to subrounded quartz and plagioclase, mica Matrix: brown to light brown, crystalic Organic components: partly decomposed organic matter as roots in recent channels, brown decomposed elongated fragments of organic matter (50–100 μm – cca 1%); dark decomposed angular pieces of organic matter (50–100 μm – cca 20%), microcharcoal (50–100 μm – cca 20%) Pedofeatures: Fe oxide depleted groundmass, Fe/Mn oxide impregnated matrix, rare redeposited Fe/Mn nodules and clay coating, dirty dusty coating on grain surfaces	Redeposited soil with fragments of organic matter and charcoal; slightly postedoposition illuviation

accordance with observations from numerous other sites of northern-central Europe (Hoek, 1997).

From this point of view, the later part of the YD seems to be climatically more favourable. In all cores, Ti content declines. In the VTC core, the same period is associated with a distinct dominance of clay in the sediment (Fig. 5), which can be attributed to an increase of the lake level and/or enhanced pedogenesis in the catchment. The idea of accelerated soil formation in the catchment under more humid conditions (and its connection with the formation of fine-grained pedogenic magnetite/maghemite) is also supported by the magnetic and $\delta^{15}N$ records, which gradually increase (decrease) within the upper part of the YD towards the Holocene. The climatic amelioration associated with increased humidity has been previously observed throughout northern-central Europe (e.g., Kulesza et al., 2014; Karpińska-Kołaczek et al., 2016), eastern-central Europe (Hájková et al., 2016), and eastern Europe (Druzhinina et al., 2015; Stančikaitė et al., 2015; Zawiska et al., 2015). On the other hand, grain-size analyses of the littoral core from the Švarcenberk Lake (Hošek et al., 2014) suggest a lake-level rise in

the later phase of the YD and thus rather drier conditions along the Pleistocene/Holocene transition.

5.3. Evidence from paleosols

An exceptional opportunity to study the above-discussed processes is provided by the fossil soils discovered in the proximity of the Švarcenberk and Velký Tisý paleolakes (Fig. 1). On the surface of the Pleistocene sandy-gravel terrace of the Lužnice River, a spodic horizon of podzol was identified (VLK, Fig. 7). This soil is buried by up to 4 m of sand, which has been previously interpreted as aeolian by origin (Pokorný and Růžičková, 2000). Based on the radiocarbon data obtained from the base and top of this soil (Fig. 7, Table 1), the soil had developed during the second part of the Allerød. It can be parallelized with the stratigraphically-identical Usselo and Finow soils reported from west- and northern-central Europe, where they are usually considered to be stratigraphical-marker horizons for Late Glacial, aeolian landscapes (Hijszeler, 1957; Schlaak, 1997; Kowalkowski et al., 1999; Kasse, 2002; Kaiser et al., 2006; Kaiser et al., 2009; Jankowski, 2012). These paleosols consist of various soil types; nevertheless, the Finow soils are mostly characterized by silicate weathering, clay translocation and redoximorphism, whereas for the Usselo soils organic matter accumulation and podzolization are rather more characteristic (Kaiser et al., 2009). On the basis of the micromorphological investigations (Table 2), the latter type is pedologically more similar to that found within the VLK sand dune. Because of the influence of water table oscillations within the fluvial terrace, podzolization took place - consequently with the oxidation of iron and manganese after water saturation and desaturation. The buried soil horizon thus corresponds rather with the Gleyic Podzol. This type of Usselo soil has been previously described, for instance, in a closely-resembling, geomorphological and hydrological context from Poland, as the result of soil-forming processes and diagenesis along a buried slope (Jankowski, 2012). The Usselo horizon is usually 5–20 cm thick and is characterized by slight humus accumulation, the presence of charcoal and well-developed humic (Ahb), albic (Eb), and spodic (Bhs) horizons (Kaiser et al., 2009 and references therein). Nevertheless, in our studied profile the humic and albic horizons have not been detected. This we attribute to the erosion of the former Ah and Eb horizons shortly before the soil was buried under the aeolian sand. The same observations have also been made in some loess/paleosols sequences in central Europe where the Ah horizons of the Eemian Luvisol were eroded immediately after the climate deterioration at the end of the Last Interglacial (Hošek et al., 2015). Micromorphological investigations (Table 2) have shown that the upper part of the soil profile has signs of colluvial processes and surface runoff, such as horizontal lamination and the changing of 1 to 2-mm-thick layers of coarse- and fine-grained particles over a dense, structural seal. The higher content of the poorly-decomposed organic matter visible in the micromorphological sample VLK_1 (Fig. 8b) can be interpreted as the preserved fragment of a disturbed Ah horizon, which was mixed with the sand and underlying gley-spodic horizon during colluviation. Owing to the fact that the matrix in the lowermost part of sample VLK_3 is obviously depleted (Fig. 8c), only a relic of the albic horizon (E) could be preserved in this layer. All these findings indicate that some climatically-driven erosion event occurred within the Allerød. Based on the radiocarbon date 13,005–13,305 cal. yr BP obtained from the pedo-colluvial horizon, this event fits the above-described IACP cool event (GI-1b) dated from western Europe to 13,274–12,989 varve yr BP (van Raden et al., 2013). This clearly demonstrates a direct relationship between landscape processes, such as surface runoff/soil erosion, and the allogenic input to the lake basins, as indicated by the geochemical/magnetic records in all the lakes studied by us.

Another pedo-colluvial horizon buried by aeolian sand found in the proximity of Lake Velký Tisý (VT8, Figs. 1 and 7) seems to be the result of the same erosion event. Unfortunately, no radiocarbon date was obtained from this horizon. Nevertheless, a Late Paleolithic artifact (Federmesser culture; personal communication by P. Šída) discovered in the over-lying aeolian sand denotes that the sand accumulated during the YD (from the age of the Federmesser culture in central Europe; see Jochim, 2008). Thus we suggest that the soil was formed (and eroded) in the preceding warmer period. This horizon is, similarly to the VLK site, very rich in charcoal, pointing to the observation from northern-central Europe that towards the end of Allerød the occurrence of forest fires had increased (Van der Hammen, 1951).

The pedo-colluvial horizon and the uppermost part of the intact B horizon from the VLK paleosol are marked by a relatively strong clay illuviation connected with the gley process demonstrated by micromorphological analysis (sample VLK_4, Fig. 8d). The same, but less intensive, post-sedimentary illuviation was also recognized in the pedo-colluvial horizon from VT8 (Fig. 8e). It denotes that another pedological process took place on these sites after the erosion event. This soil weathering process could be related to a relatively short humid phase of the late Allerød (GI-1a in the NGRIP record) which occurred after the IACP cold event. Favourable climatic conditions during this period are indicated by all the abiotic proxies from the three studied lakes (Figs. 3–4) and it is also reflected in the biotic indicators from Lake Švarcenberk (Pokorný, 2002; Hošek et al., 2014). Nevertheless, due to the relatively short distance between the buried soils and recent surface, it should also be taken into account that the illuviation of the particular soil horizons could have taken place during the Holocene.

The formation of soils during the Allerød period required stable climatic conditions with little aeolian activity and a relatively-dense vegetation cover. The catchments of the lakes were covered by pine-dominated forest, which then became more closed, as reflected by a decrease in open-community indicators in the pollen spectra (Pokorný, 2002; Hošek et al., 2014). Woodland cover helped to prevent surface washes and slope processes. Considering this, it is not surprising that generally little erosion occurred in the lake catchments during the Allerød.

A combination of the acidic nature of the bedrock, the relatively dense cover by coniferous trees, and increased precipitation would have ensured that podzolization occurred in the study region (see Fig. 8a). The increase in precipitation, in particular, would have been the crucial factor for this process (Section 5.4). A supposed increase of precipitation in the study area at the beginning of the Allerød is in accordance with the higher lake level of the VT lake (see the fall in the mean grain size of the lacustrine sediment in this particular horizon, Fig. 5) and with the pollen record from Švarcenberk Lake (Hošek et al., 2014).

By contrast, the formation of aeolian sand dunes indicates severe climatic conditions. In the upland record from the VLK buried soil, the sudden climatic change at the Allerød/YD threshold is represented by the thin layer of sandy clay and abundant charcoal dated to 12,322–12,661 cal. yr BP (Fig. 7), i.e. the beginning of the YD. This layer with abundant charcoal has been referred to from numerous Usselo soils as well (Kaiser et al., 2009 and references within). Charcoal presence on the top of the soil probably resulted from the climatic deterioration which led to a wide-scale dieback of coniferous forests and subsequent extensive fire events. This climatic event is also probably reflected in the regional pollen record (Pokorný, 2002; Hošek et al., 2014), where a peak in microscopic charcoal particles precedes a phase of significant opening up of the vegetation during the Allerød/YD transition. A good size-sorting of the charcoal and rotten-wood particles (0.5 cm in diameter, see Fig. 7) denotes that the fragments of dead coniferous vegetation were wind transported together with the sand.

5.4. Evidence of early soil leaching and acidification

A striking feature of the geochemical records of all the studied lacustrine records of that particular period is the significant increase in iron, as well as phosphorus concentrations, which correspond with the beginning of the Allerød interstadial (subzone B2, Figs. 3–4). Because of the low correlation between these elements and Ti ($r = 0.1$–0.3) and

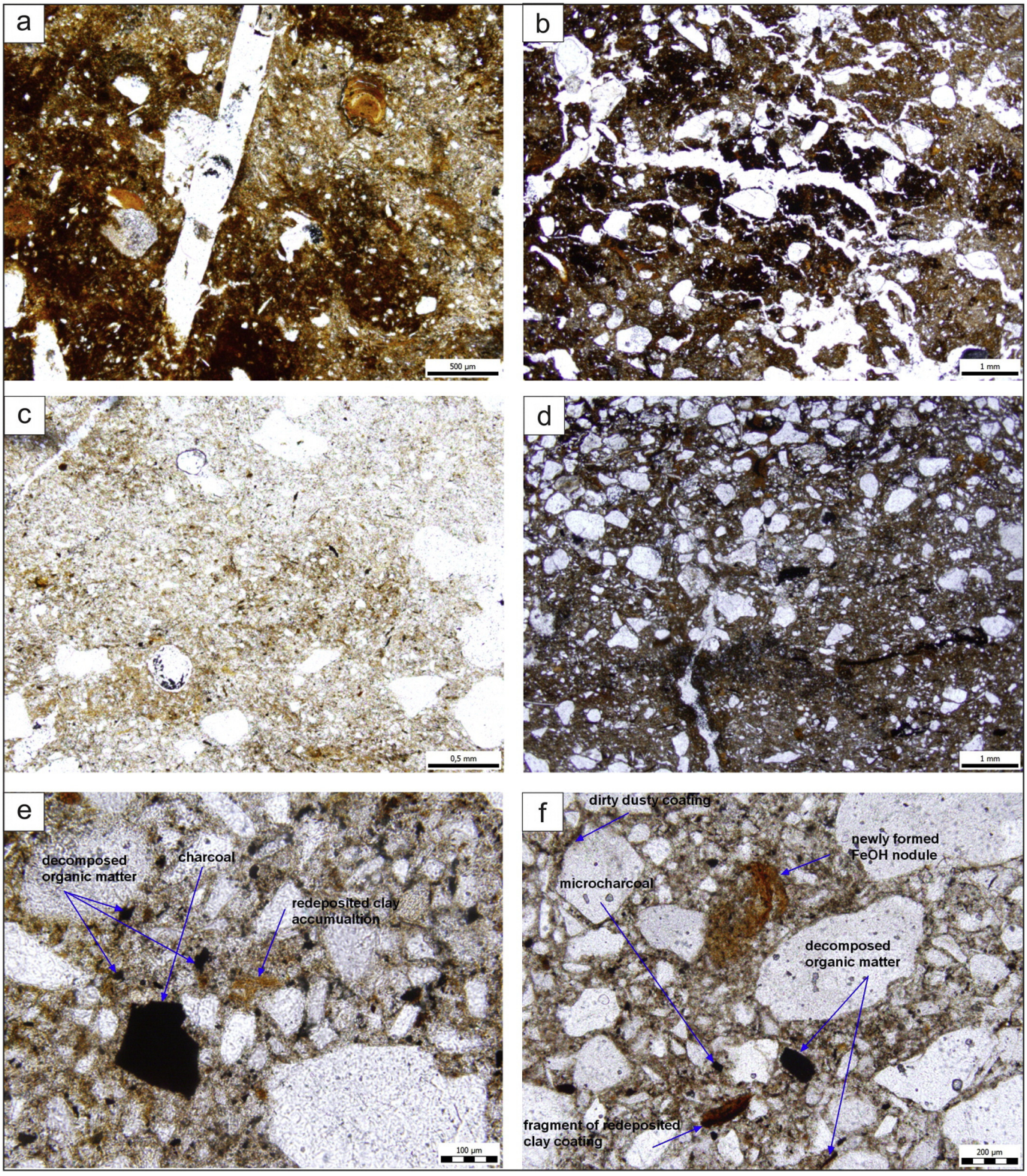

Fig. 8. Micromorphological features of the paleosols from the VLK (a–d) and VT8 (e, f); a – sample VLK_2, Fe oxide depleted groundmass (right part), Fe/Mn oxide quasi-coatings and impregnative nodules (central lower part and left corner) (PPL); b – sample VLK_1, horizon of black particles composed of partly and fully decomposed organic matter and coated by clay minerals. Visible crack pores (PPL); c – sample VLK_3, depleted silty matrix with vughs; d – sample VLK_4, the transition between silty loam and sands. Pieces of buried organic matter and microcharcoal are preserved there; e – sample VT8, microcharcoal, as well as relict of clay accumulation and dark pieces of buried organic matter (PPL); f – sample VT8, fragment of redeposited clay coating, black, decomposed organic matter, dirty dusty coating, microcharcoal and newly forming FeOH nodule (PPL).

the Fe/Ti ratio exceeding the mean upper-crustal value (approximately 10) by an order of magnitude, the enrichment of the lake sediments by iron and phosphorus probably did not occur via physical (colluvial or aeolian) processes. We attribute this phenomenon to the climate amelioration, particularly the increase in precipitation. It resulted in the onset of reducing conditions in soils (during podzolization), leaching of iron, and subsequent P loss related to the leaching of Fe as its main inorganic sorbent. The beginning of the Allerød was

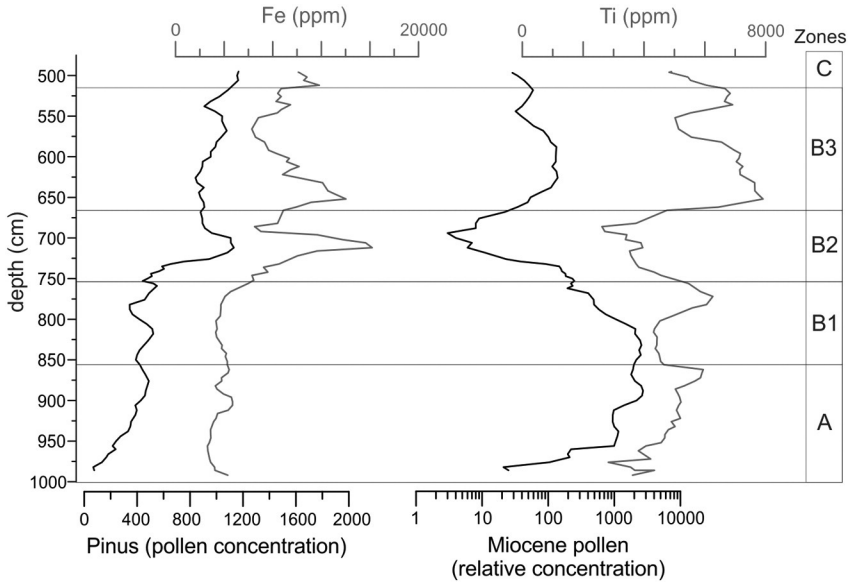

Fig. 9. SVC core: Depth variation of the Fe, *Pinus* pollen concentration, Ti and concentration of the Miocene reworked palynomorphs.

characterized by the establishment of relatively-dense coniferous forests (Pokorný, 2002; Hošek et al., 2014). Both the more humid climate and coniferous forests are factors that highly promote podzolization (Lundström et al., 2000). The relationship between Fe-mobilization (podzolization) and coniferous forest development is clearly illustrated through the correlation of Fe content and *Pinus* pollen concentration in the SVC core (Fig. 9).

The relatively high *Helianthemum* percentages (up to 3%) in the basal sediments of Lake Švarcenberk (Pokorný, 2002) indicate initially-carbonate-rich substrates in the area, most probably loess (see discussion above). All this is in obvious contrast with the acidic substratum that prevails there today. At the present time, most soils are leached, highly-acidic, and almost completely lacking calcium carbonate.

This finding indicates that in our research area, with its sandy and relatively acidic bedrock, mineral-rich soils were replaced by increasingly well-leached ones during the Allerød.

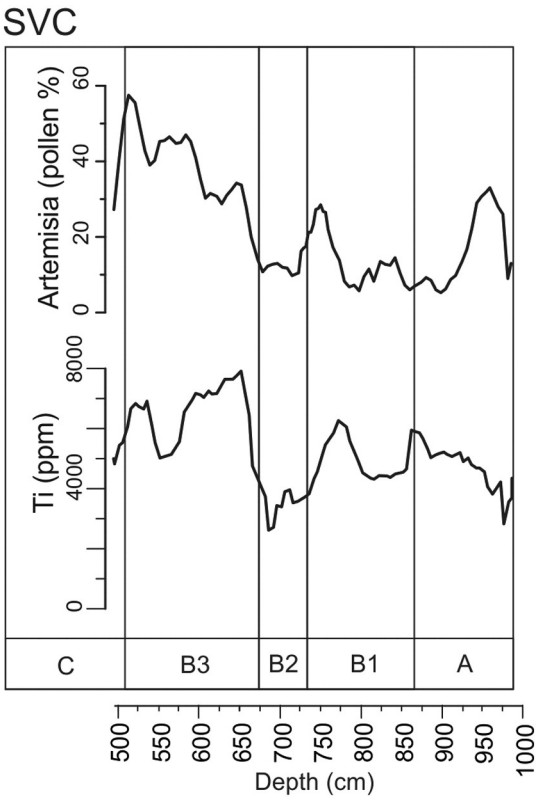

Fig. 10. SVC core: Comparison of the Ti-record with *Artemisia* pollen record (% of terrestrial pollen total sum).

6. Conclusions

Although the eastern part of central Europe is rather poor in Pleistocene lacustrine sequences, in recent years a large number of lake basins with relatively fast sediment deposition have been discovered in south Bohemia (Czech Republic). In this study we present the first results on newly-studied Late Glacial paleolakes and paleosols. Using a multi-proxy approach that combined sedimentological, geochemical, and geophysical methods with the pollen record and soil micromorphology, we have reconstructed the evolution of the erosion and pedogenic processes during the Last Termination (~16 to 11 ky BP). The conclusions of this study can be summarized as follows:

(i) Ti content in lacustrine sediment is a good tracer for erosion in the lake catchments. The highest erosion intensity occurred during cold periods with sparse vegetation cover, as suggested by the direct correlation between Ti and the pollen percentages of the *Artemisia* pollen record.

(ii) Four major and two minor environmental stages, identified geochemically in all the investigated paleo-lakes, were broadly correlated with Late Glacial climatostratigraphy. Based on wiggle-matching of the Ti record with the $\delta^{18}O$ Greenland record, local palynostratigraphy and ^{14}C-AMS dating, the main stages correspond with the Late Pleniglacial (geochemical zone A), Bølling (subzone B1), Allerød (subzone B2) and Younger Dryas (subzone B3). Short-term (centennial) climatic deteriorations situated between the Bølling and Allerød, and within the Allerød, have been correlated with the Older Dryas and the Intra-Allerød Cold Period, respectively. It suggests that the landscape of the study area responded sensitively to the climatic changes in the North Atlantic region and measurement of Ti in lacustrine sediments can be used as a reasonable climatostratigraphical tool for the subdivision of the Late Glacial part of studied records.

(iii) Magnetic properties (SIRM, S-ratio) are shown to be useful indicators of pedogenesis in the catchment, since the magnetic enhancement of the gyttja is probably connected with the

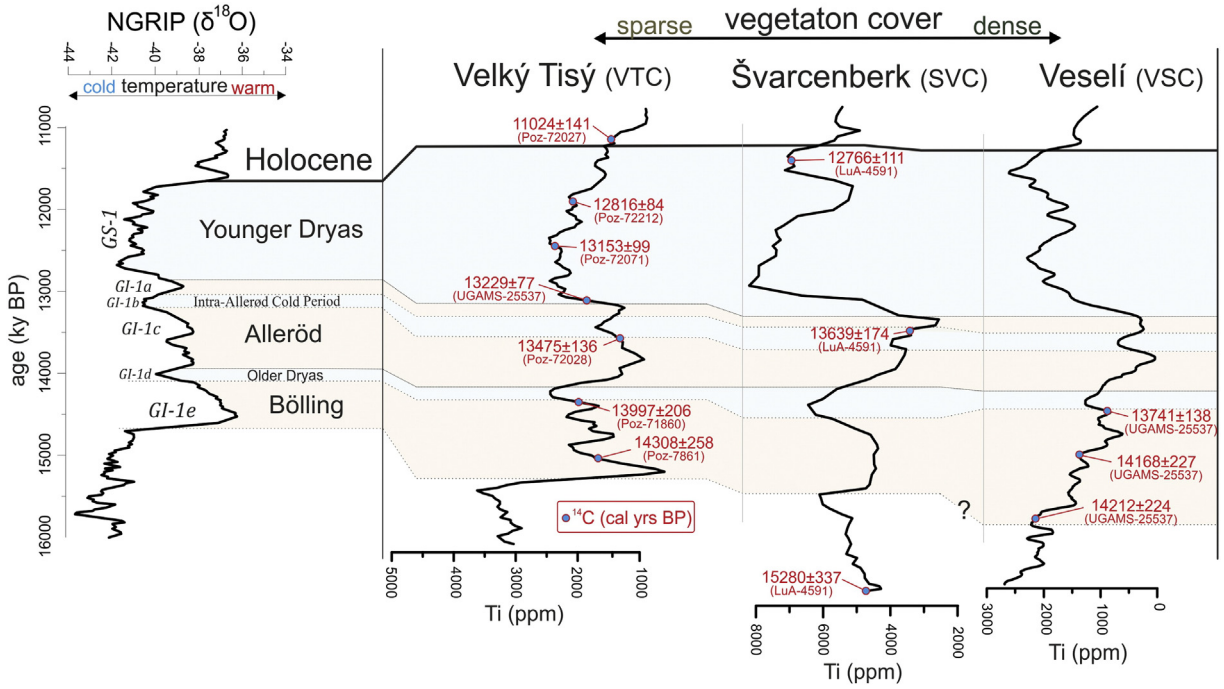

Fig. 11. Correlation of Ti-records from Velký Tisý, Švarcenberk and Veselí with $\delta^{18}O$ record from NGRIP (NGRIP Members, 2004).

development of humic soil horizons in the lake catchment. During the Late Pleniglacial, and partially also during the Bølling, the magnetic signal was influenced by the presence of eroded/wind-blown loess in the lake sediment.

(iv) Measurement of $\delta^{15}N$ in lacustrine sediments seems to be a promising method for the reconstruction of the humidity in the study area. Low $\delta^{15}N$ values relate with a warm-humid period, while elevated $\delta^{15}N$ values indicate a cool (and dry) climate.

(v) The B horizons of two (gleyic) Podzols discovered under aeolian sand dunes in the lake catchments were dated to the Allerød interstadial absolutely, by the ^{14}C-AMS dating (VLK section), and relatively, based on the stratigraphic position (VT8 section). These paleosols were parallelized with Usselo soils, up to now only known from northern-central Europe. According to the micromorphology investigations, the uppermost soil horizons had been eroded. In the case of the VLK paleosol, this erosion event was dated to 13,155 ± 150 cal. yr and associated with the IACP cold event. This clearly demonstrates a direct relationship between landscape processes, such as surface runoff/soil erosion, and allogenic input into the lake basins - as indicated by the geochemical/magnetic records in all studied lakes.

(vi) The geochemical, sedimentological, rock-magnetic, as well as pollen, records suggest that during the Late Pleniglacial and Bølling the study area was covered by a carbonate-rich substrate (loess), which is in sharp contrast with the acidic substratum that prevails in the study area at the present time. The significant increase in the iron and phosphorus content found in the lake sediments during the Allerød indicates that mineral-rich soils in the study area were replaced by increasingly-leached ones during the podzolization that took place under the humid, interstadial conditions.

Acknowledgements

This research was supported by Charles University in Prague, project GA UK no. 1472214 and by project no. 13-08169S of the Grant Agency of the Czech Republic. Stable isotopic analyses were made possible by the programme OPPK CZ.2.16/3.1.00/21516. Kristýna Kuncová and Barbora Koutská are acknowledged for performing the LOI and isotopic analysis and Pavla Žáčková for the separation and determination of plant macroremains. We are thankful to Petr Šída for providing samples from the archaeological site and for enriching discussions. Steve Ridgill is thanked for improving our English. This manuscript benefited from the thoughtful reviews of Knut Kaiser and an anonymous reviewer.

References

Ammann, B., Birks, H.J.B., Drescher–Schneider, R., Juggins, S., Lang, G., Lotter, A.F., 1993. Patterns of variation in late-glacial pollen stratigraphy along a northwest-southeast transect through Switzerland – a numerical analysis. Quat. Sci. Rev. 12, 277–286.

Ammann, B., Lotter, A.F., 1989. Late-glacial radiocarbon and palynostratigraphy of the Swiss plateau. Boreas 18, 109–126.

Andersen, C.S., Björck, S., Bennike, O., Heinemeier, J., Kromer, B., 2000. What do D 14C changes across the Gerzensee oscillation/GI–1b event imply for deglacial oscillation? J. Quat. Sci. 15, 203–214.

Bakke, J., Dahl, S.O., Paasche, Ø., Simonsen, J.R., Kvisvik, B., Bakke, K., Nesje, A., 2010. A complete record of Holocene glacier variability at Austre Okstindbreen, northern Norway: an integrated approach. Quat. Sci. Rev. 299, 1246–1262.

Battarbee, R.W., Gasse, F., Stickley, C.E., 2004. Past climate variability through Europe and Africa. In: Smol, J.P. (Ed.), Developments in Paleoenvironmental Research. Springer, New York, pp. 339–371.

Björck, S., Kromer, B., Johnson, S., Bennike, O., Hammerlund, D., Lemdahl, G., Possnert, G., Lander Rasmussen, T., Wolfahrt, B., Hammer, C.U., Spurk, M., 1996. Synchronized terrestrial-atmospheric deglacial records around the North Atlantic. Science 274, 1155–1160.

Björck, S., Walker, M.J.C., Cwynar, L.C., Johnsen, S., Knudsen, K.L., Lowe, J.J., Wohlfarth, B., INTIMATE Members, 1998. An event stratigraphy for the last termination in the North Atlantic region based on the Greenland ice-core record: a proposal by the INTIMATE group. J. Quat. Sci. 13, 283–292.

Blaauw, M., 2010. Methods and code for 'classical' age-modelling of radiocarbon sequences. Quat. Geochronol. 5, 512–518.

Bohncke, S., Vandenberghe, J., Huijzer, A., 1993. Periglacial environments during the Weichselian late glacial in the Maas valley, The Netherland. Geol. Mijnb. 72, 193–210.

Brauer, A., Günter, C., Johnsen, S.J., Negendank, J.F.W., 2000. Land–ice teleconnections of cold climatic periods during the last glacial/interglacial transition. Clim. Dyn. 16, 229–239.

Bullock, P., Federoff, N., Jongerius, A., Stoops, G., Tursina, T., Babel, U., 1985. Handbook for Soil Thin Section Description. Waine Research Publications, Wolverhampton.

Demory, F., Oberhänsli, H., Nowaczyk, N.R., Gottschalk, M., Wirth, R., Naumann, R., 2005. Detrital input and early diagenesis in sediments from Lake Baikal revealed by rock magnetism. Glob. Planet. Chang. 461, 145–166.

Dietrich, S., Sirocko, F., 2011. The potential of dust detection by means of μXRF scanning in Eifel maar lake sediments. E&G – Quat. Sci. J. 60 (1), 90–104.
Druzhinina, O., Subetto, D., Stančikaitė, M., Vaikutienė, G., Kublitsky, J., Arslanov, K., 2015. Sediment record from the Kamyshovoe Lake: history of vegetation during late Pleistocene and early Holocene Kaliningrad District, Russia. Baltica 28, 121–132.
Engstrom, D.R., Wright Jr., H.E., 1984. Chemical stratigraphy of lake sediments as a record of environmental change. In: Haworth, E.Y., Lund, J.W.G. (Eds.), Lake Sediments and Environmental History. Leicester University Press.
Eusterhues, K., Heinrichs, H., Schneider, J., 2005. Geochemical response on redox fluctuations in Holocene lake sediments, Lake Steisslingen, southern Germany. Chem. Geol. 2221, 1–22.
Firbas, F., 1949. Spät und nacheiszeitliche Waldgeschichte Mitteleuropas nördlich der Alpen. In: Fisher, J. (Ed.), Algemeine Waldgeschichte. Erster Band.
Goslar, T., Kuc, T., Ralska-Jasiewiczowa, M., Rózánski, K., Arnold, M., Bard, E., Pazdur, M.F., Szeroczyñska, K., Wicik, B., Wieckowski, K., Walanus, A., 1993. High–resolution lacustrine record of the late glacial/Holocene transition in central Europe. Quat. Sci. Rev. 12, 287–294.
Hájková, P., Pařil, P., Petr, L., Chattová, B., Grygar, T.M., Heiri, O., 2016. A first chironomid–based summer temperature reconstruction 13–5 ka BP around 49° N in inland Europe compared with local lake development. Quat. Sci. Rev. 141, 94–111.
Heiri, O., Lotter, A.F., Lemcke, G., 2001. Loss on ignition as a method for estimating organic and carbonate content in sediments: reproducibility and comparability of results. J. Paleolimnol. 25, 101–110.
Heller, F., Evans, M., 1995. Loess magnetism. Rev. Geophys. 33, 211–240.
Hijszeler, G.C.W.J., 1957. Late-glacial human cultures in the Netherlands. Geol. Mijnb. 19, 288–302.
Hoek, W., 1997. Palaeogeography of late glacial vegetations. Aspects of late glacial and early Holocene vegetation, abiotic landscape, and climate in The Netherlands. Neth. Geogr. Stud. 230, 1–147.
Hongyan, L., Kan, L., Fangling, W., Yuan, W., Min, L., 2013. Artemisia pollen–indicated steppe distribution in southern China during the last glacial maximum. J. Palaeogeogr. 23, 297–305.
Hošek, J., Pokorný, P., Šída, P., Prach, J., 2013. Newly discovered late glacial lakes in Třeboň region. Geosci. Res. 126–132 Reports for 2012.
Hošek, J., Pokorný, P., Kubovčík, V., Horáček, I., Žáčková, P., Kadlec, J., Rojik, F., Lisá, L., Bučkuliaková, S., 2014. Late glacial climatic and environmental changes in eastern–central Europe: correlation of multiple biotic and abiotic proxies from the Lake Švarcenberk, Czech Republic. Palaeogeogr. Palaeoclimatol. Palaeoecol. 396, 155–172.
Hošek, J., Hambach, U., Lisá, L., Grygar, T.M., Horáček, I., Meszner, S., Knésl, I., 2015. An integrated rock-magnetic and geochemical approach to loess/paleosol sequences from bohemia and Moravia Czech Republic: implications for the upper Pleistocene paleoenvironment in central Europe. Palaeogeogr. Palaeoclimatol. Palaeoecol. 418, 344–358.
Hošek, J., Prach, J., Šída, P., Houfková, P., Vondrák, D., Lisá, L., Pokorný, P., Chvojka, O., Dohnal, J., 2016. Sedimentary development of the late glacial lakes near Veselí nad Lužnicí south bohemia. Geosci. Res. 157–164 Reports for 2015.
Jankowski, M., 2012. Lateglacial soil paleocatena in inland-dune area of the Toruń Basin, northern Poland. Quat. Int. 265, 116–125.
Jochim, M.A., 2008. The Mesolithic of the Upper Danube and Upper Rhine. In: Bailey, G., Spikins, P. (Eds.), Mesolithic Europe. Cambridge University Press, New York, pp. 203–220.
Jordanova, N., Jordanova, D., Liu, Q., Hu, P., Petrov, P., Petrovský, E., 2013. Soil formation and mineralogy of a Rhodic Luvisol – insights from magnetic and geochemical studies. Global Planet. Change 110, 397–413.
Just, J., Nowaczyk, N., Francke, A., Sagnotti, L., Wagner, B., 2015. Climatic control on the occurrence of high-coercivity magnetic minerals and preservation of greigite in a 640 ka sediment sequence from Lake Ohrid Balkans. Biogeosci. Discuss. 12, 14215–14243.
Kaiser, K., Barthelmes, A., Czakó Pap, S., Hilgers, A., Janke, W., Kühn, P., Theuerkauf, M., 2006. A Lateglacial palaeosol cover in the Altdarss area, southern Baltic Sea coast northeast Germany: investigations on pedology, geochronology and botany. Netherlands Journal of Geosciences]–>Neth. J. Geosci. 85, 197–220.
Kaiser, K., Hilgers, A., Schlaak, N., Jankowski, M., Kühn, P., Bussemer, S., Przegietka, K., 2009. Palaeopedological marker horizons in northern central Europe: characteristics of Lateglacial Usselo and Finow soils. Boreas 38, 591–609.
Karpińska-Kołaczek, M., Stachowicz-Rybka, R., Obidowicz, A., Woszczyk, M., Kołaczek, P., 2016. A lake-bog succession vs. climate changes from 13,300 to 5900 cal. BP in NE Poland in the light of palaeobotanical and geochemical proxies. Rev. Palaeobot. Palynol. 233, 199–215.
Kasse, C., 2002. Sandy aeolian deposits and environments and their relation to climate during the last glacial maximum and Lateglacial in northwest and central Europe. Prog. Phys. Geogr. 26, 507–532.
Kowalkowski, A., Nowaczyk, B., Okuniewska–Nowaczyk, I., 1999. Chronosequence of biogenic deposits and fossil soils in the dune near Jasień, western Poland. In: Schirmer, W. (Ed.), Dunes and Fossil Soils. GeoArchaeoRhein. 3, pp. 107–127.
Levesque, A.J., Mayle, F.E., Walker, I.R., Cwynar, L.C., 1993. A previously unrecognized late-glacial cold event in eastern North-America. Nature 361, 623–626.
Lotter, A.F., Eicher, U., Birks, H.J.B., Siegenthaler, U., 1992. Late–glacial climatic oscillations as recorded in Swiss lake sediments. J. Quat. Sci. 7, 187–204.
Lowe, J.J., Rasmussen, S.O., Björck, S., Hoek, W.Z., Steffensen, J.P., Walker, M.J.C., Yu, Z., INTIMATE Group, 2008. Precise dating and correlation of events in the North Atlantic region during the last termination: a revised protocol recommended by the INTIMATE group. Quat. Sci. Rev. 27, 6–17.
Lundström, U.S., van Breemen, N., Bain, D., 2000. The podzolization process. A review. Geoderma 94 (2), 91–107.
Maher, B.A., 1986. Characterisation of soils by mineral magnetic measurements. Phys. Earth Planet. In. 42, 76–92.
Maher, B.A., Taylor, R.M., 1988. Formation of ultrafine–grained magnetite in soils. Nature 336, 368–370.
Maher, B.A., Thompson, R., 1991. Mineral magnetic record of the Chinese loess and paleosols. Geology 191, 3–6.
Mangerud, J., Andersen, S.T., Berglund, B.E., Donner, J.J., 1974. Quaternary stratigraphy of Norden, a propsal for terminology and classification. Boreas 3, 109–128.
Mckay, N.P., Kaufman, D.S., 2009. Holocene climate and glacier variability at Hallet and Greyling Lakes, Chugach Mountains, south-central Alaska. J. Paleolimnol. 41, 143–159.
Meyers, P.A., Lallier, V.E., 1999. Lacustrine sedimentary organic matter records of late quaternary paleoclimates. J. Paleolimnol. 21, 345–372.
North Greenland Ice Core Project NGRIP Members, 2004. High-resolution record of northern hemisphere climate extending into the last interglacial period. Nature 431, 147–151.
Pokorný, P., 2002. A high-resolution record of late-glacial and early-Holocene climatic and environmental change in Czech Republic. Quat. Int. 91, 101–122.
Pokorný, P., Jankovská, V., 2000. Long-term vegetation dynamics and the infilling process of a former lake Švarcenberk, Czech Republic. Folia Geogr. 35, 433–457.
Pokorný, P., Růžičková, E., 2000. Changing environments during the younger dryas climatic deterioration: correlation of aeolian deposits in southern Czech Republic. Geolines 11, 89–92.
Rasmussen, S.O., Andersen, K.K., Svensson, A.M., Steffensen, J.P., Vinther, B.M., Clausen, H.B., Bigler, M., 2006. A new Greenland ice core chronology for the last glacial termination. J. Geophys. Res. Atmos. 111, D06102.
Reimer, P.J., Bard, E., Bayliss, A., Beck, J.W., Blackwell, P.G., Bronk Ramsey, C., Buck, C.E., Cheng, H., Edwards, R.L., Friedrich, M., Grootes, P.M., Guilderson, T.P., Haflidason, H., Hajdas, I., Hatté, C., Heaton, T.J., Hoffmann, D.L., Hogg, A.G., Hughen, K.A., Kaiser, K.F., Kromer, B., Manning, S.W., Niu, M., Reimer, R.W., Richards, D.A., Scott, E.M., Southon, J.R., Staff, R.A., Turney, C.S.M., van der Plicht, J., 2013. IntCal13 and Marine13 radiocarbon age calibration curves 0–50,000 years cal BP. Radiocarbon 55, 1869–1887.
Roberts, N., 2014. The Holocene. An Environmental History, third ed. John Willey & Sons, Chichester, UK.
Robinson, S.G., 1986. The late Pleistocene paleoclimatic record of North Atlantic deep-sea sediments revealed by mineral-magnetic measurements. Phys. Earth Planet. In. 42, 22–47.
Rosqvist, G.C., Schuber, P., 2003. Millennial-scale climate changes on South Georgia, Southern Ocean. Quat. Res. 59, 470–475.
Schlaak, N., 1997. Äolische Dynamik im brandenburgischen Tiefland seit dem Weichselspätglazial. Humboldt Universität zu Berlin, Arbeitsberichte Geographisches Institut.
Simonneau, A., Chapron, E., Garçon, M., Winiarski, T., Graz, Y., Chauvel, C., Di Giovanni, C., 2014. Tracking Holocene glacial and high-altitude alpine environments fluctuations from minerogenic and organic markers in proglacial lake sediments Lake Blanc Huez, Western French Alps. Quat. Sci. Rev. 89, 27–43.
Smalley, I., 1995. Making the material: the formation of silt sized primary mineral particles for loess deposits. Quat. Sci. Rev. 147, 645–651.
Sperazza, M., Moore, J.N., Hendrix, M.S., 2004. High-resolution particle size analysis of naturally occurring very fine-grained sediment through laser diffractometry. J. Sediment. Res. 74 (5), 736–743.
Stančikaitė, M., Šeirienė, V., Kisielienė, D., Martma, T., Gryguc, G., Zinkutė, R., Mažeika, J., Šinkūnas, P., 2015. Lateglacial and early Holocene environmental dynamics in northern Lithuania: a multi-proxy record from Ginkūnai Lake. Quat. Int. http://dx.doi.org/10.1016/j.quaint.2014.08.036.
Stoops, G., 2003. Guidelines for Analysis and Description of Soil and Regolith Thin Sections. Soil Science Society of America, Madison, Wisconsin.
Stoops, G., Marcelino, V., Mees, F., 2010. Interpretation of Micromorphological Features of Soils and Regoliths. Elseiver.
Syvitski, J.P.M. (Ed.), 1991. Principles, Methods, and Application of Particle Size Analysis. Cambridge University Press, Cambridge.
Van der Hammen, T., 1951. Late-glacial flora and periglacial phenomena in the Netherlands. Leidse. Geol. Meded. 17, 71–183.
van Raden, U.J., Colombaroli, D., Gilli, A., Schwander, J., Bernasconi, S.M., van Leeuwen, J., Eicher, U., 2013. High-resolution late-glacial chronology for the Gerzensee lake record Switzerland: δ 18 O correlation between a Gerzensee-stack and NGRIP. Palaeogeogr. Palaeoclimatol. Palaeoecol. 391, 13–24.
Velichko, A.A., Catto, N., Drenova, A.N., Klimanov, V.A., Kremenetski, K.V., Nechaev, V.P., 2002. Climate changes in East Europe and Siberia at the late glacial–Holocene transition. Quat. Int. 91, 75–99.
von Grafenstein, U., Erlenkeuser, H., Brauer, A., Jouzel, J., Johnsen, S.J., 1999. A mid European decadal isotope-climate record from 15,500 to 5000 years BP. Science 284, 1654–1657.
Walker, M.J.C., 1995. Climatic changes in Europe during the last glacial/interglacial transition. Quat. Int. 28, 63–76.
Walker, M.J.C., Harkness, D.D., 1991. Radiocarbon dating the Devensian Lateglacial in Britain: new evidence from Llanilid, South Wales. J. Quat. Sci. 5, 135–144.
Walker, M.J.C., Coope, G.R., Lowe, J.J., 1993. The Devensian (Weichselian) Lateglacial Palaeoenvironmental Record from Gransmoor, East Yorkshire, England. Quat. Sci. Rev. 12, 659–680.
Wang, F., Sun, D., Guo, F., Wang, X., Li, Z., Zhang, Y., Li, B., Wu, S., 2012. Quantitative reconstruction of paleo-temperature and paleo-precipitation of Lingtai profile in Loess plateau during the past 7 Ma. J. Earth Environ. 3, 781–791.
Watanabe, T., Naraoka, H., Nishimura, M., Kawai, T., 2004. Biological and environmental changes in Lake Baikal during the late quaternary inferred from carbon, nitrogen and sulfur isotopes. Earth Planet. Sci. Lett. 222, 285–299.

Watts, W.A., 1979. Regional variations in the response of vegetation to late glacial climatic events in Europe. In: Lowe, J.J., Gray, J.M., Robinson, J.E. (Eds.), Studies in the Lateglacial of north-west Europe. Pergamon Press, Oxford. pp., pp. 1–21.
Whitlock, C., Marlon, J., Briles, C., Brunelle, A., Long, C., Bartlein, P., 2008. Long-term relations among fire, fuel, and climate in the north–western US based on lake-sediment studies. Int. J. Wildland Fire 171, 72–83.
Wick, L., 2000. Vegetational response to climatic changes recorded in Swiss late glacial lake sediments. Palaeogeogr. Palaeoclimatol. Palaeoecol. 159, 231–250.
Xu, H., Sheng, E., Lan, J., Liu, B., Yu, K., Che, S., 2014. Decadal/multi-decadal temperature discrepancies along the eastern margin of the Tibetan plateau. Quat. Sci. Rev. 89, 85–93.
Yancheva, G., Nowaczyk, N.R., Mingram, J., Dulski, P., Schettler, G., Negendank, J.F., Haug, G.H., 2007. Influence of the intertropical convergence zone on the east Asian monsoon. Nature 44, 74–77.
Young, G.M., Nesbitt, H.W., 1998. Processes controlling the distribution of Ti and Al in weathering profiles. Siliciclastic sediments and sedimentary rocks. J. Sediment. Res. 683, 448–455.
Zawiska, I., Słowiński, M., Correa-Metrio, A., Obremska, M., Luoto, T., Nevalainen, L., Woszczyk, M., Milecka, K., 2015. The response of a shallow lake and its catchment to Late Glacial climate changes. A case study from eastern Poland. Catena 126:1–10. http://dx.doi.org/10.1016/j.catena.2014.10.0070341-8162.
Zhang, W., Ming, Q., Shi, Z., Chen, G., Niu, J., Lei, G., Chang, F., Zhang, H., 2014. Lake sediment records on climate change and human activities in the Xingyun Lake catchment, SW China. PLoS One 97, 1–10.

PŘÍLOHA V

Hošek, J. – Pokorný, P. – Kubovčík, V. – Horáček, I. – Žáčková, P. – Kadlec, J. – Rojik, F. – Lisá, L. – Bučkuliaková, S. (2014): Late glacial climatic and environmental changes in eastern-central Europe: Correlation of multiple biotic and abiotic proxies from the Lake Švarcenberk, Czech Republic. – Palaeogeography, Palaeoclimatology, Palaeoecology 396, 155-172.

Palaeogeography, Palaeoclimatology, Palaeoecology 396 (2014) 155–172

Contents lists available at ScienceDirect

Palaeogeography, Palaeoclimatology, Palaeoecology

journal homepage: www.elsevier.com/locate/palaeo

Late glacial climatic and environmental changes in eastern-central Europe: Correlation of multiple biotic and abiotic proxies from the Lake Švarcenberk, Czech Republic

Jan Hošek [a,g,*], Petr Pokorný [b], Vladimír Kubovčík [c], Ivan Horáček [d], Pavla Žáčková [b,e], Jaroslav Kadlec [f], Filip Rojik [c], Lenka Lisá [f], Simona Bučkuliaková [c]

[a] Institute of Geology and Paleontology, Faculty of Science, Charles University in Prague, Albertov 6, Prague 2, Czech Republic
[b] Center for Theoretical Study, Charles University in Prague, Jilská 1, Praha 1, Czech Republic
[c] Faculty of Ecology and Environmental Sciences, Technical University in Zvolen, T. G. Masaryka, 2117/24, Slovak Republic
[d] Department of Zoology, Faculty of Science, Charles University, Viničná 7, Prague 2, Czech Republic
[e] Department of Botany, Faculty of Science, Charles University in Prague, Benátská 2, Prague 2, Czech Republic
[f] Academy of Sciences of the Czech Republic, Institute of Geology, Rozvojová 135, Prague 6, Czech Republic
[g] Czech Geological Survey, Klárov 3, Prague 1, Czech Republic

ARTICLE INFO

Article history:
Received 8 July 2013
Received in revised form 9 December 2013
Accepted 16 December 2013
Available online 03 January 2014

Keywords:
Last Glacial Termination
Lacustrine sediments
Climate changes
Biotic/abiotic responses
Eastern-Central Europe

ABSTRACT

Thick lake sediments discovered in the southern part of the Czech Republic provide a high-resolution archive for detailed study of paleoenvironmental changes during the Late Pleistocene to Holocene in eastern-central Europe. Until recently, no similar records were available for this important region in the transition from oceanic to continental macro-climatic settings. Using a multi-proxy approach that combines sedimentological, pollen-analytical, paleozoological (Chironomids), geochemical and mineral-magnetic methods we demonstrate that major climatic events of the Late Glacial can be correlated with Atlantic rather than continental regimes as reported in paleoclimatic literature for the area of the interest. The sensitivity of applied biological and abiological techniques to climatically-driven processes allows trans-regional comparisons and enables us to discuss the pattern of geographic variation in these processes. We are able to establish a clear relationship between vegetation cover, soil development and erosional processes. A short-term intra-Alleröd cool event has been correlated with the Gerzensee oscillation. Proxy evidence suggests that the early half of the Younger Dryas was rather humid, whereas the latter half was dry and had significant impact on vegetation, sedimentary dynamics and lake level status during the YD/Preboreal transition.

1. Introduction

The Last Glacial–Interglacial Transition (including the Late Weichselian period and onset of the Holocene) is marked by rapid and pronounced climatic oscillations associated with successive climatic steps during global deglaciation (Ruddiman and McIntyre, 1981; Lowe et al., 1994; Björck et al., 1996; Clark et al., 2001; Lowe et al., 2008). While these changes are well documented in the high-resolution record of the Greenland ice cores (Johnsen et al., 1992; Stuiver et al., 1995), as well as in marine sediments (Bergsten, 1994), our knowledge on environmental transformations of the continents is still relatively fragmental due to the heterogenic deployment of suitable sedimentary archives. In continent interiors, abrupt Late Glacial and Early Holocene climatic oscillations caused deep changes in local vegetation and soil development, resulting in changes in sedimentary processes. Yet, as indicated by a large scale geographic comparison of the pollen records throughout Europe (Davis et al., 2003), considerable interregional differences both in timing and intensity of the respective climatic and environmental rearrangements might have occurred. Consequently, geographic variation in the regional response to general climatic trends along the Weichselian–Holocene transition becomes a topic of urgent importance. A dense network of high resolution records from different geographic locations once available will present a basic prerequisite for its analysis.

The records of the lacustrine series providing data on the course of vegetation development and its relations to local erosion and lithogenetic dynamics are in these connections of particular significance (Walker, 1995; Brauer et al., 1999; von Grafenstein et al., 1999; Ammann et al., 2000; Birks and Wright, 2000; von Grafenstein et al., 2000). Yet, the geographic distribution of such series is far from being homogeneous. While a large number of lake deposits are available from northern and NW Europe, most of central Europe (except for the

* Corresponding author at: Albertov 6, Prague 2, 128 00, Czech Republic. Tel.: +420 731 905 752.
E-mail addresses: johan.hosek@gmail.com (J. Hošek), pokorny@cts.cuni.cz (P. Pokorný), kubovcik@tuzvo.sk (V. Kubovčík), ivan.horacek@natur.cuni.cz (I. Horáček), pa.zackova@seznam.cz (P. Žáčková), kadlec@gli.cas.cz (J. Kadlec).

0031-0182/$ – see front matter © 2014 Elsevier B.V. All rights reserved.
http://dx.doi.org/10.1016/j.palaeo.2013.12.024

Alpine piedmont and Panonnian basin) is rather poor in this respect. This very much holds for the area of the eastern part of Central Europe where the absence of lacustrine deposits is explained both by the high relief dynamics of the region and by its unfavorable hydrologic context, far from the sources related to either continental or Alpine glaciations. Until recently, only three sites with Late Weichselian lacustrine deposits were reported from the interior of the Czech Republic: Plešné Lake in Šumava Mts., Labský důl mire in Krkonoše Mts. (both with a total thickness of 200–250 cm: Engel et al., 2004; Jankovská, 2006), and the Švarcenberk Lake in Třeboň basin (Pokorný, 2002; Pokorný et al., 2010). In contrast to the former two that are high mountain deposits with rather specific conditions, the latter is situated at a medium altitude and represents a continuous lacustrine and peat series of a total thickness of over 10 m of which about 4 m cover just the Late Weichselian–Early Holocene transition.

The Švarcenberk Lake is, in this sense, a unique archive for environmental reconstructions and the best sedimentary record known for the Late Glacial and Early Holocene periods in the eastern-central Europe. The sensitivity of the site's setting to climatic oscillations of this particular period is due to its altitudinal position (412 m a.s.l.) that is transitional in terms of altitudinal zonation of vegetation. In addition, the character of the lake itself (small catchment, a single outlet) makes its water level sensitive to climatic oscillations. Detailed high-resolution data on the Late Glacial and Holocene vegetation development are already available from this site (Pokorný and Jankovská, 2000; Pokorný, 2002) together with data on the dynamics of the Mesolithic occupation of the lake catchment area (Šída et al., 2007; Pokorný et al., 2010).

The present paper supplements this information with the results from a multi-proxy approach, which combines several techniques of instrumental sedimentological analyses with the pollen record, plant macrofossils and analyses of insect (Chironomid) remains. We provide some new data on the former series (a core in the center of the lake), yet the paper is particularly based on a new core in the littoral area, where a relatively quiet, continuous sedimentation prevailed and allochtonous material from the catchment together with autochtonous biotic sediment accumulated. We correlate a record from both series and discuss a degree of correspondence between the results of particular techniques and, furthermore, the timing and intensity of paleoenvironmental changes in the lake catchment during the Alleröd and Younger Dryas periods.

2. The study area and site

The study site (49°08′45″ N, 14°42′45″ E) is situated in South Bohemia (Czech Republic) at 412 m a.s.l. (Fig. 1). The former lake Švarcenberk lies in the northern section of the flat landscape of the Třeboň Basin. The geological substratum of the lake catchment is represented by sandy Cretaceous sandstones and Tertiary sandy/clayey fluvio-lacustrine sediments. Depressions are filled with Quaternary fluvial silt and sandy gravel, aeolian sands, and particularly organic lake and peat sediments (Fig. 3). Various types of podsols and sandy or peaty gleysols prevail in the area. The present climate is suboceanic and is determined by prevailing westerly air masses, already significantly reduced in moisture by their passage across central Europe.

Lacustrine clastic sediments of the Lake Švarcenberk basin are overlain by peat, which have formed after the natural infilling of the lake occurred at approx. 5500 years BP according to ^{14}C dating (Pokorný and Jankovská, 2000). Nowadays, the site is heavily influenced by intensive management: between 1698 and 1701 a fishpond was constructed directly on the site, and its waters have almost completely flooded over the peat and the underlying lake sediments.

3. Basin morphology and stratigraphy of deposits

The extent of lake deposits and morphology of the basin was mapped using approximately 150 hand borings (Pokorný, 2002) and

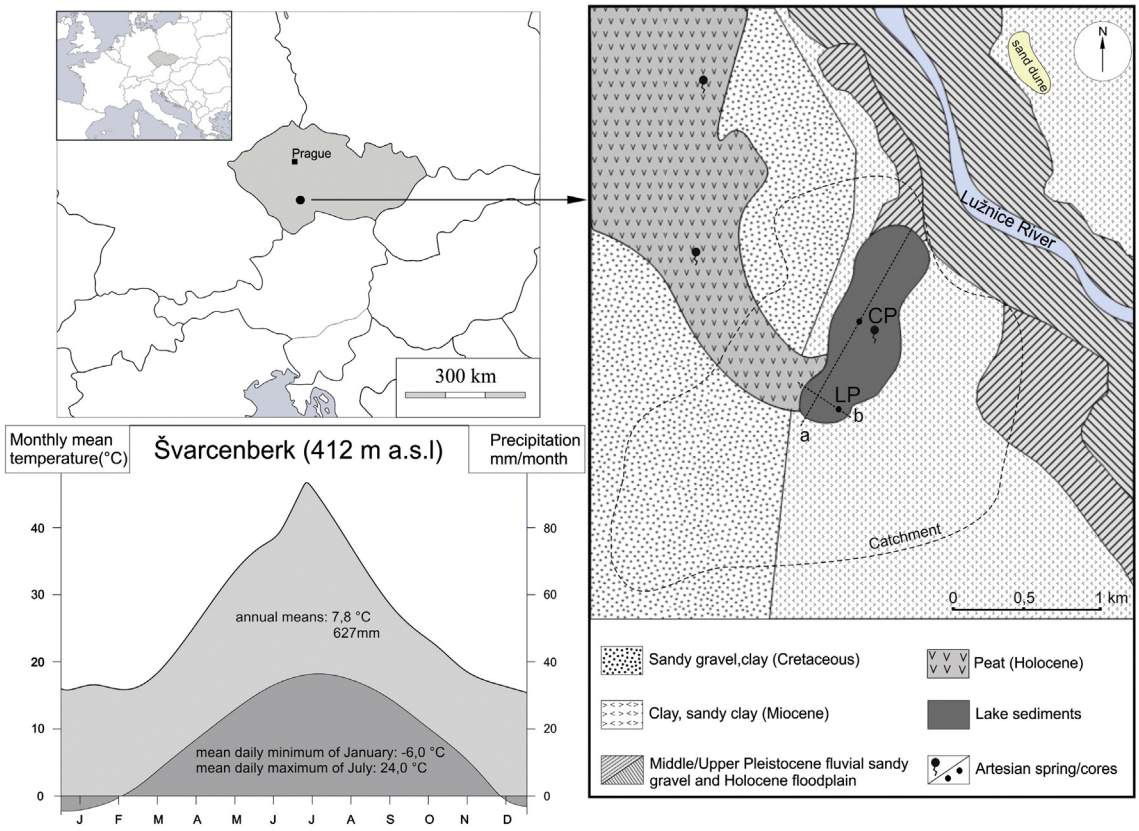

Fig. 1. Location of Švarcenberk lake; simplified geological situation of the site; climatic diagram for Třeboň (16 km south from the site); a,b — two cross sections used for stratigraphic investigation.

another 30 detailed hand borings in the southern littoral segment. The altitude of individual stratigraphic sections was obtained by relative leveling using the altitude of the present water level as a reference. The former lake was found to have a maximum surface of 0.51 km^2 and the ratio of the surface to drainage basin to be about 1:8 (Fig. 1). A longitudinal section of the southern littoral (Fig. 3a) shows the morphometry and infilling of the depression. Notable features of the basin morphometry are its kidney-shaped form, surprising depth and declivity (Fig. 2).

The maximum thickness (11 m) of Quaternary deposits was found in the center of the basin. The layer of basal mineral sediment, 2–3 m thick, consists of clay with organic admixture in some horizons. Overlaying this is a 1–2 m thick layer consisting of clayey gyttja, or clay with very fine organic detritus, the mineral components prevailing. Above this layer the mineral content decreases and the sediment (*gyttja*) is more organic. The last lithological member of the paleo-lake infilling is coarse-detritus *gyttja*. After the final infilling of the lake, oligotrophic lingo-herbaceous peat accumulated. Visual stratigraphy reflects well the environmental conditions during the time of sedimentation and was used for a basic correlation of individual hand borings.

The SE littoral is relatively separated from the rest of the basin. A cross-section through the littoral is shown in Fig. 3b. In the western part of the littoral sandy gravel basal sediments accumulated because of the erosion from the Cretaceous bedrock, whereas in the more distant eastern part clayey sand is present. The lithology of the southwestern part could also have been influenced by fluvial sedimentation from a small tributary; evidence for this are layers of sandy gravels in the upper part of the lake sediment with a rapidly declining thickness towards the center of the basin. Nevertheless, the SE part of the basin was not influenced by the dynamics of this weak tributary: relatively calm sedimentation took place here. In this SE littoral, the sediments are composed mainly of colluvial materials, autochthonous organic sediment, suspension silt and in some places aeolian sand. Therefore the littoral core taken here (littoral profile; LP) is most suitable for a reconstruction of paleoenvironmental changes in the lake catchment and water level oscillations.

The other core presented in this paper comes from the center of the basin (central profile; CP). This is a reference core for the site, and has already been analyzed for palynostratigraphy, geochemical composition and macrofossils by Pokorný (2002). However, new analyses (content of Rb and Chironomids) were made for this core. Information from this core was mainly used for correlation with the LP core.

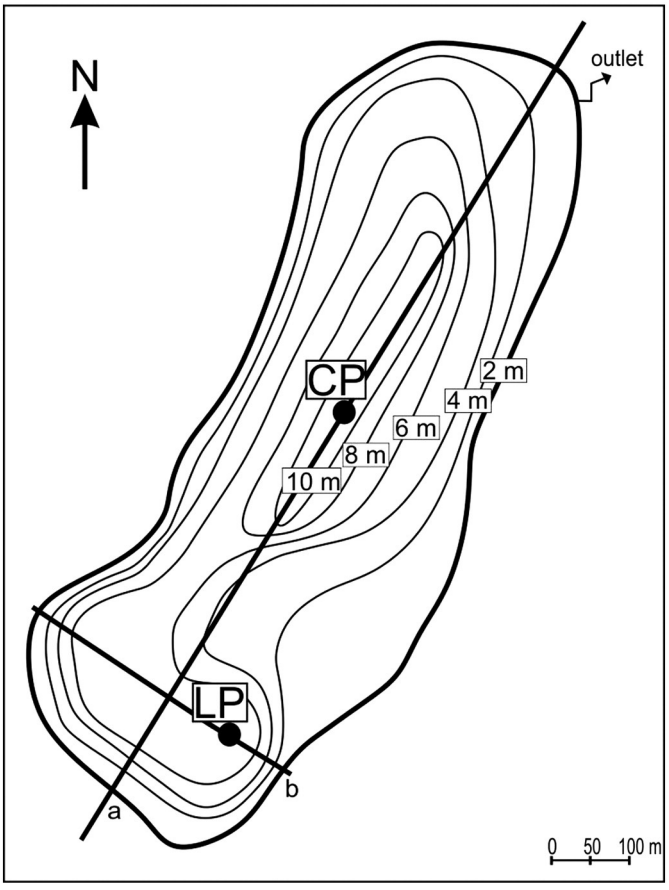

Fig. 2. Bathymetry of the lake basin.

4. Material and methods

The results discussed in this paper refer to data from the littoral core LP (total depth of 464 cm) and the central core CP (total depth of 990 cm). These cores were taken with a pneumatic hammer-operated piston corer (tube 50 mm in diameter).

Subsamples of 1 to 20 cm^3 of the sediment of the core LP (depending on the type of analysis) were analyzed with the following techniques: magnetic measurements, pollen and plant macrofossils analyses, loss-on-ignition (LOI), Rb concentration measurement, and grain size analyses.

Results of pollen analyses and total organic carbon (TOC) in the core CP summarized by Pokorný (2002) are here supplemented with results of Chironomid analyses and instrumental data on Rb concentrations. Due to insufficient material from the lower part of the core CP, Rb concentration measurements from depths between 780 and 1000 cm are incomplete and relatively fragmental.

Petrographic description of mineral grains was performed on a binocular microscope Olympus ZX-65.

4.1. Stratigraphic analyses

The complete series of the fine-scaled primary record obtained by their respective analytic techniques were separately subdivided into particular units based on the degree of similarity among compared horizons. The stratigraphical units are independently established based on magnetostratigraphic data, sedimentological characteristics and the Rb record. The pollen record, plant macrofossils, and Chironomids are treated separately. Their mutual correspondence and meaning for reconstructions of the environmental dynamics, as well as presumed correlations of the studied series with the units of standard stratigraphic scales, are hence a matter for discussion.

4.2. Chronostratigraphy

AMS radiocarbon measurements were performed on selected horizons using plant macrofossils: items extracted from the sediment of core LP at 437, 308, 268–270 and 190 cm depths were dated (Table 1). Five AMS dates for the CP core are adopted from Pokorný (2002) and one basal age (LuA-4737) is newly presented here. Measurements were performed at the Lund University Radiocarbon Dating Laboratory, Lund, Sweden (sample lab. codes LuA-xxxx) and at Poznań Radiocarbon Laboratory, Adam Mickiewicz University, Poznań, Poland (sample lab. codes Poz-xxxxx). All the samples were pre-treated by an acid–alkali–acid method.

Radiocarbon ages were calibrated using the CalPal Online program (http://www.calpal-online.de/) that uses the calibration curve hyperlink http://www.calpal.de/wp/?page_id=5%22CalPal2007_HULU.

4.3. Pollen stratigraphy

The samples used for pollen and other microfossil analyses were treated using a modified acetolysis method with hydrofluoric acid (HF) treatment (Faegri and Iversen, 1989; Moore et al., 1991). The

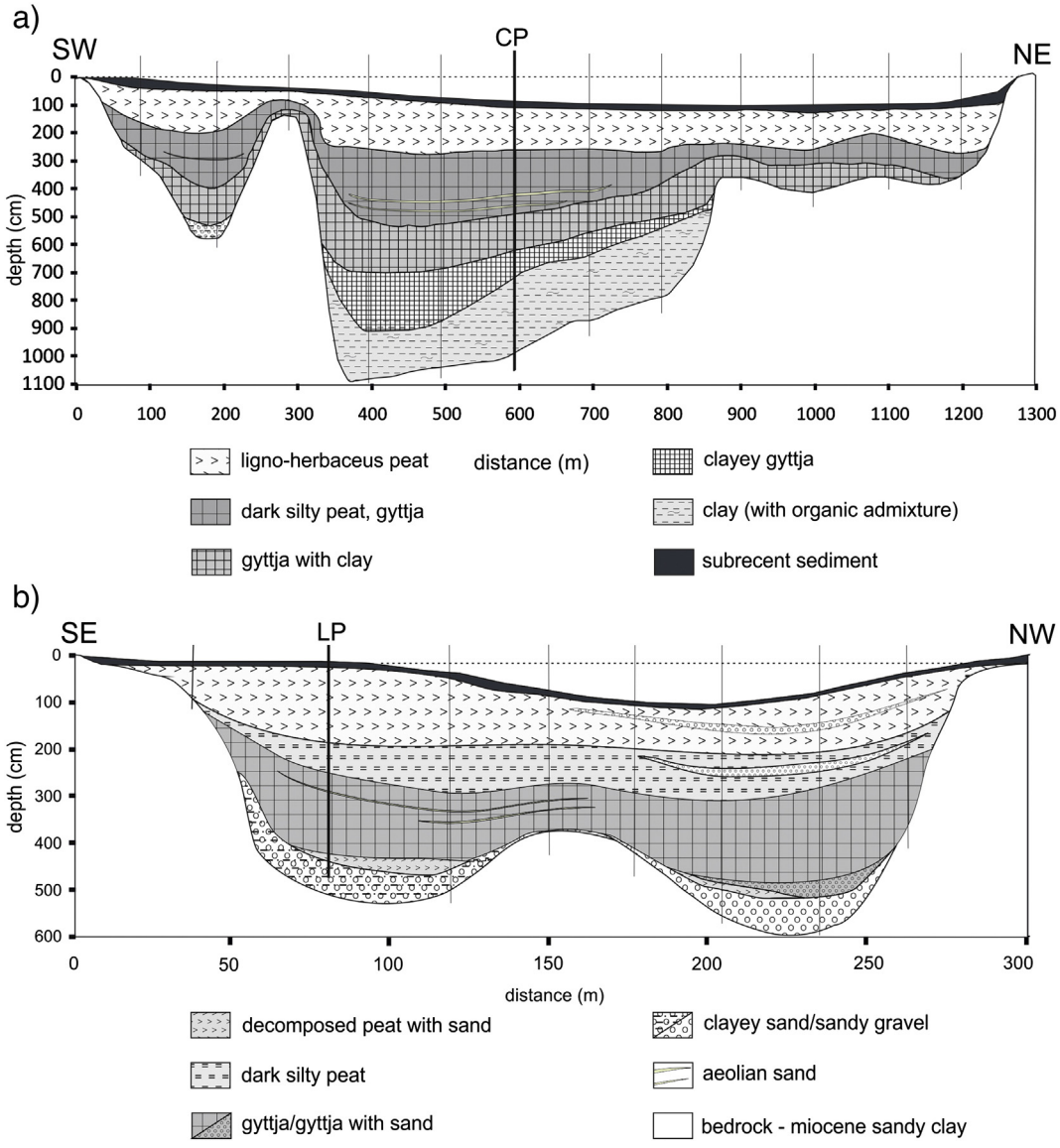

Fig. 3. Two stratigraphical cross section with positions of the cores LP and CP (see also Fig. 1).

extracted microfossils were lightly stained with 0.3% safranin and mounted in a liquid glycerol–water (1:1) mixture. For pollen identification, the following keys were used besides a reference collection: Faegri and Iversen (1989), Moore et al. (1991), Punt (1976–1996) and Beug (2004). Pollen nomenclature follows the local pollen database PALYCZ (http://botany.natur.cuni.cz/palycz/). Algae and other microfossils were identified with the help of publications of Van Geel et al. (1981, 1983, 1989), Jankovská (1983), and Jankovská and Komárek (2001, 1982).

The lowermost Late Glacial sediments contained lots of reworked Tertiary pollen. Fortunately, its state of preservation was relatively poor, giving reworked pollen grains a 'ghosty' appearance. It has been assumed that different degrees of fossilization resulted in different chemical composition and physical properties of the exine. Considering this assumption, a simple method was developed to test the Tertiary origin of pollen grains: pollen samples, already stained by 0.3% safranin, were bleached in 40% ethanol for one minute. They were then

Table 1
Radiocarbon dating from Švarcenberk Lake sediments (all AMS).

Lab. code	Profile, depth	Type of material	Conventional ^{14}C age	Cal BP
LuA-4588	CP, 150–153 cm	Woody stem fragment	4650 ± 100 BP	5170 (68%); 5512
LuA-4589	CP, 324–327 cm	*Trapa natans* nut	6350 ± 100 BP	7172 (68%); 7384
LuA-4590	CP, 390–393 cm	Woody stem fragment	9640 ± 115 BP	10,801 (68%); 11,147
LuA-4591	CP, 520–523 cm	Bulk gyttja sample	10,780 ± 115 BP	12,654 (68%); 12,877
LuA-4738	CP, 680–683 cm	Alkali-soluble fraction from gyttja	11,750 ± 120 BP	13,464 (68%); 13,813
LuA-4737	CP, 985–995 cm	*Salix* twigs	12,800 ± 120 BP	14,943 (68%); 15,617
Poz-29404	LP, 190–191 cm	*Trapa natans* nut	6360 ± 40 BP	7266 (68%); 7367
Poz-34211	LP, 268–270 cm	Twigs	9040 ± 50 BP	10,191 (68%); 10,238
Poz-29405	LP, 307–309 cm	Seeds of water plants	10,870 ± 50 BP	12,755 (68%); 12,920
Poz-29406	LP, 437–438 cm	Twigs	11,820 ± 60 BP	13,599 (68%); 13,860

centrifuged and transferred to glycerol–water mounting medium again. As the result of this procedure, all pollen grains were bleached to a different degree, but the Tertiary ones became almost completely transparent and hence easily separable from Quaternary ones.

In pollen diagrams, percentage values were calculated on the basis of the AP + NAP pollen sum, excluding all aquatic and wetland taxa. The concentration of reworked Tertiary pollen grains was established relative to the above-described Quaternary upland pollen sum. Pollen diagrams were first zoned visually, on the basis of both presence and abundance of taxa. Precise zone boundaries were identified using cluster analysis with CONISS (Grimm, 1987).

4.4. Plant macrofossils

After subsampling the littoral core (LP) for all other analyses, the remaining material was used for macrofossil analysis. Contiguous samples 10 cm long were cut, and the volume of each was determined. Macrofossils were wet-sieved with running water. Sieves with mesh sizes of 200, 300 and 700 μm were used. The residues were examined under a dissecting stereomicroscope. The absolute number of individuals was recalculated to a standard volume of 65 cm^3 of fresh sediment (i.e. the minimum volume encountered among samples). For determination of the seeds/fruits a reference collection (Faculty of Science, Charles University in Prague, CZ) was used.

4.5. Chironomid stratigraphy

Chironomid data used in this study include 25 samples from the central core CP. Sediment samples were deflocculated for 1–2 h in H_2O (70 °C), then passed through 233 μm and 85 μm sieves. The Chironomid remains were hand sorted under a stereomicroscope. The head capsules were slide-mounted ventral side up in Berlese solution, and identified with reference to Brooks et al. (2007), Kowalyk (1985) and Rieradevall and Brooks (2001).

Specimens that consisted of a right half, or more than half, of the mentum were enumerated as one head capsule. Fragments that consisted of the left half or of less than a half of the mentum were excluded. The majority of identifications were made to the genus level, and in rare cases to the species level. After separation, the sediments were dried to a constant weight at 120 °C, and the number of Chironomid remains was calculated per 10 g of dry sediment. Zones, defined by major changes in chironomid assemblage composition, were identified using cluster analysis with CONISS (Grimm, 1987). Correspondence analysis (CA) was used to assess the trajectory of chironomid community development. All ordinations were performed using the program C2 (Juggins, 2007) with $\log_{10}(x + 1)$-transformation of species data. Only taxa that were found at ≥25% samples were included in the analysis.

Selected Chironomid taxa were divided into three ecological categories: according to temperature (cold-, temperate-, and warm-optimal), trophic status (oligotrophic, oligo-mesotrophic, mesotrophic, meso-eutrophic, eutrophic), and bathymetric distribution (profundal, littoral) according to Brooks et al., 2007.

Pollen, plant macrofossil and Chironomid diagrams were drawn using the TGView 2.0.2 program (Grimm, 2004).

4.6. Mineral magnetic measurements

Rock-magnetic investigations were carried out to characterize changes in the erosion and weathering processes in the lake catchment. These processes are recorded as changes in the concentration, mineralogy and grain size of remanence-carrying minerals of the alochtonous components of the lake sediment.

The LP core (464 cm length) was subsampled continuously using plastic cubes with an inner volume of 6.7 cm^3. The distance between each box was less than 0.5 cm. All magnetic measurements were carried out in the Paleomagnetic laboratory of the Institute of Geology, Academy of Sciences of the Czech Republic, v.v.i. All the samples were measured for magnetic susceptibility (MS), while remanent magnetism (RM) measurements were carried out on every second sample of the section 464–180 cm of the core. MS was measured with a kappabridge KLY-3 (AGICO s.r.o.), in a weak magnetic field with frequency 875 kHz and was given as normalized as mass specific susceptibility — χ (m^3/kg^{-1}). The low-field magnetic susceptibility depends on the concentration of magnetic (especially ferromagnetic s.l.) minerals, and their grain-size. The signal can be reduced by the presence of diamagnetic material (e.g. organic matter, SiO_2, $CaCO_3$).

Anhysteretic remanent magnetisation (ARM) was measured using a demagnetizer LDA-3 with AMU 1A. The samples were imparted in a DC field 0.05 mT, superimposed on an alternating field of 100 mT. Higher ARM values indicate the presence of fine grained single-domain (SD) grains in the sediment. Natural remanent magnetization (NRM) was measured on a Superconducting Rock Magnetometer (2G Enterprises). This parameter indicates the presence of ferrimagnetic (e.g. magnetite) and antiferrimagnetic minerals (e.g. hematite, goethite). NRM is not influenced by the presence of diamagnetic material. Values of saturated isothermal remanent magnetization (SIRM) were imparted with a MMPM 10 pulse magnetizer using a field of 1 T and then back field remanence measurements at 300 mT. The SIRM mainly reflects the presence of smaller (<10 μm) magnetite grains.

The S-ratio was calculated as SIRM 300 mT/SIRM. The S-ratio reflects the proportion of low-to-high-coercivity minerals in a sample. Values close to 1 denote the dominance of low-coercivity minerals like magnetite while higher values denote the presence of high-coercivity minerals (e.g. hematite, goethite).

Magnetic values are presented without units in the text. For MS the units are 10^{-9} m^3/kg, for ARM and NRM 10^{-6} A/m, and in the case of SIRM it is 10^{-3} A/m.

4.7. LOI and TOC

The percentage of organic material in the sediment of the LP core was determined by Loss on Ignition (LOI). Material from magnetic boxes of the interval 464–213 cm was used for measurements. LOI was calculated as the difference in weight between the sediment dried at 60 °C and the ash created following ignition at 550 °C within a high temperature muffle furnace (Heiri et al., 2001). The CP core was sampled each 10 cm for measurement of total organic carbon (TOC), following standard techniques (after Hammarlund and Buchardt, 1996). TOC content was calculated from the difference between total carbon and carbonate carbon. Results of organic matter content bring us information about the biomass of the lake, extent of vegetation cover and degree of soil development in the lake catchments.

4.8. Rb content and grain size analyses

After removing organic matter, the core CP was analyzed by X-ray fluorescence (XRF), sampling interval of 10 cm, and the core LP by inductively-coupled plasma mass spectroscopy (ICP-MS); sampling interval the same as that for LOI measurements. The detection limit of both methods is approximately 4 ppm and the results are calculated in mg/kg. The Rb concentration in the sediment was used for the reconstruction of weathering and erosion intensity (see Section 6).

The same samples as for the LOI and Rb measurement were used for grain size analyses in the core LP. Particle size was analyzed with a laser size analyzer CILAS 1190 LD, after standard preparation procedures (Syvitski, 1991).

5. Results

5.1. Instrumental analysis of the LP core

5.1.1. Magneto-mineralogical analysis, grain size and LOI

The results of instrumental analyses of the LP core are summarized in Figs. 5 and 6. In general, the magnetic characteristics show a distinct correlation to the lithological characteristics of the respective horizon. The highest values correspond with sandy silt sediment (464–438 cm) and with coarse organic detritus gyttja (302–320 cm). Minimal values (negative susceptibility) were measured in the layer with clayey peat and in the lingo-herbaceous peat above 180 cm.

The dominant magnetic mineral in the sediment was magnetite, as suggested by the SIRM and S-ratio results. The S-ratio (mostly ≥ 0.9) suggests only small variations, which was interpreted to indicate a uniform magnetite assemblage (Maher, 1988; Peters and Dekkers, 2003). For the S-ratio 0.4 (sample 354 cm) are likely to be dominated by a high coercivity (antiferromagnetic) fraction. A positive correlation of susceptibility with SIRM suggests a dominance of magnetite in the profile too. A higher content of organic matter, and eventually a presence of sand grains (diamagnetic quartz and feldspar grains) could cause lower values of MS.

On the basis of MS and RM fluctuation it is possible to identify four major units in the core, corresponding with the core's regional pollen zones (see Fig. 5). As pollen zones were determined based on upland pollen taxa only (i.e. based on vegetation events in the catchment outside the lacustrine environment), these close correlations confirm the high interpretative meaning of instrumental analyses in respect to events in the catchment.

In the following text magnetic results are described together with LOI results, macro- (micro-) petrographic characteristics of the sediment and the laser grain-size record (percentage of clay–silt–sand fraction).

5.1.1.1. Unit 1 (464–438 cm). In this section, a relatively high content of the fine-grained (sub-angular) sand is typical (clay ~ 9%, silt 80–88%, sand 5–13%). Mineral components consist mainly of well-worked quartz and feldspars and accessory mica. Porifera SiO_2 sclerites are present. Organic detritus is represented by 3%. This unit is generally characterized by high values of MS and RM, χ gradually increasing from the bottom of the unit (37.1) to 438 cm (50.1). Values of remanent magnetization are more than an order of magnitude higher in comparison with the overlying unit. ARM increases relatively linear from 53.6 to 256.2 (maximum value of the core), NRM from 12.8 to 37.9 and SIRM from 9.2 to 72.5

5.1.1.2. Unit 2 (440–345 cm). The relatively high content of organic matter is typical for this unit. In the sand fraction, subangular grains of quartz and elongated reworked clasts of feldspars prevail. The highest sand concentration is at the bottom of the unit (~4%) where a silty/clayey peat with sand and wooden pieces (437–405 cm) is recorded. The content of sclerites is relatively high (~1%, 200–400 μm long). This layer has probably accumulated after erosion during a low water level. It suggests a high organic matter content (LOI up to 60%) and relatively high amount (up to 2%) of coarser quartz grains (>500 μm). The presence of organic matter and quartz grains significantly degreases the magnetic susceptibility and marks a sharp border with the underlying unit. χ decreases to negative values of about −4. ARM as well as NRM values are close to 0 A/m. In the overlying part (402–392 cm) a sharp decrease in organic matter content (35–42%) is apparent and a relatively rapid increase in χ (from −2.7 up to 14.2) and RM values. The part 390–353 cm is characterized by a continuous increase in magnetic values and higher content of organic matter (LOI about 40%). The increase is better seen on the values of NRM and SIRM which are not affected by the presence of diamagnetic organic material such as MS.

5.1.1.3. Unit 3 (353–270 cm). A relatively rapid increase in all magnetic values (more than twice as high in comparison with Unit 2) and a rapid decrease of organic matter content (LOI about 20–25%) is characteristic for this unit. Maximum magnetic values are concentrated in the part where gyttja with coarse detritus had accumulated (326–305 cm with maxima at 310 cm). χ increases from 19.8 to 56.1, ARM from 31.8 to $145.3 * 10^{-6}$ A/m, NRM from 22.3 to 51 (maximum at 315 cm) and SIRM from 12.7 to 80.9. A relatively higher content of organic matter is apparent in this layer (about 35%). The decrease in magnetic values and organic matter content in the overlying part could be caused by the high content of the sand fraction (up to 10%). In the coarse fraction sub-angular quartz grains prevail, 125–700 μm in diameter. On the top of Unit 3 (270 cm) is a 2-cm thick layer of very fine perfectly-sorted sand accumulated (fraction ~ 200 μm). On the basis of a microscope study this layer was correlated with material from CP where 5 similar layers accumulated during YD (see Fig. 4). Pokorný and Růžičková (2000) interpreted this material as aeolian sand. This layer has a relatively high magnetic signal.

5.1.1.4. Unit 4 (270–0 cm). In the sediment from the upper part a gradual decrease in magnetic susceptibility and SIRM values begins. χ falls from 29.2 to −8, and SIRM from 30.2 to 0.3in the horizon 270–185 cm. This could be caused by a decline in the amount of magnetite together with an increased presence of larger quartz grains (125–1100 μm in diameter, up to 9%) and a rapid increase in the content of organic detritus, mainly in the dark silty peat (from 20 to 60%). ARM and NRM have relatively stable values of about 18, and 8, respectively. Nevertheless, several events of short-term increases in magnetic signal disturb these trends. The most significant event is recorded in the horizon 215–186 cm. In the part above this unit, lingo-herbaceus peat is recorded. Due to the presence of a high organic matter content very low (negative) magnetic susceptibility values were measured from this part.

5.1.2. Rubidium concentrations

Rubidium concentration results are shown in Fig. 6. The variation in pattern in the content of rubidium throughout core LP corresponds to magnetic units and PAZ pollen zones (Fig. 6.). The highest values were measured in Unit 1 (up to 135 ppm). The overlaying unit (2) is generally characterized by low values (20–50 ppm). Nevertheless, a significant increase is recorded in this unit in the horizon 405–388 cm (up to 105 ppm). A further increase is also apparent in Unit 3 where the respective Rb values vary around 120 ppm (decreasing to 90 ppm in the horizon 315–308 cm). The upper part of the sediment (Unit 4) is characterized by a significant and rapid decrease in Rb content down to a minimum of 4 ppm (at 224 cm). A relatively higher content was measured in the horizon 265–258 cm (about 50 ppm). Rb concentration closely correlates negatively with the organic matter content throughout the whole core.

A comparison of the Rb content from the LP core and the CP core is given in Fig. 11. A very similar trend between the LP and CP cores is apparent. The results of the Rb content were used for the correlation of both profiles (LP and CP; Fig. 11) and for drawing up paleoclimatic implications (see Section 6).

5.2. Pollen and plant macrofossils

5.2.1. The littoral core (LP; Figs. 7 and 8)

An analysis of macrofossils always leads to a more precise taxonomic identification of plants compared with pollen analysis. Of course, information obtained in this way has a different interpretative value as the macrofossil content of lake sediment is highly local in character. Thus independent zonation for pollen (LP) and plant macrofossils (mLP) was made.

In the pollen zone LP-1 (425–355 cm), high pollen values are reached among plants indicative of steppe–tundra vegetation (*Alnus viridis*, *Betula nana*, *Dryas octopetela*, *Artemisia*, Chenopodiaceae,

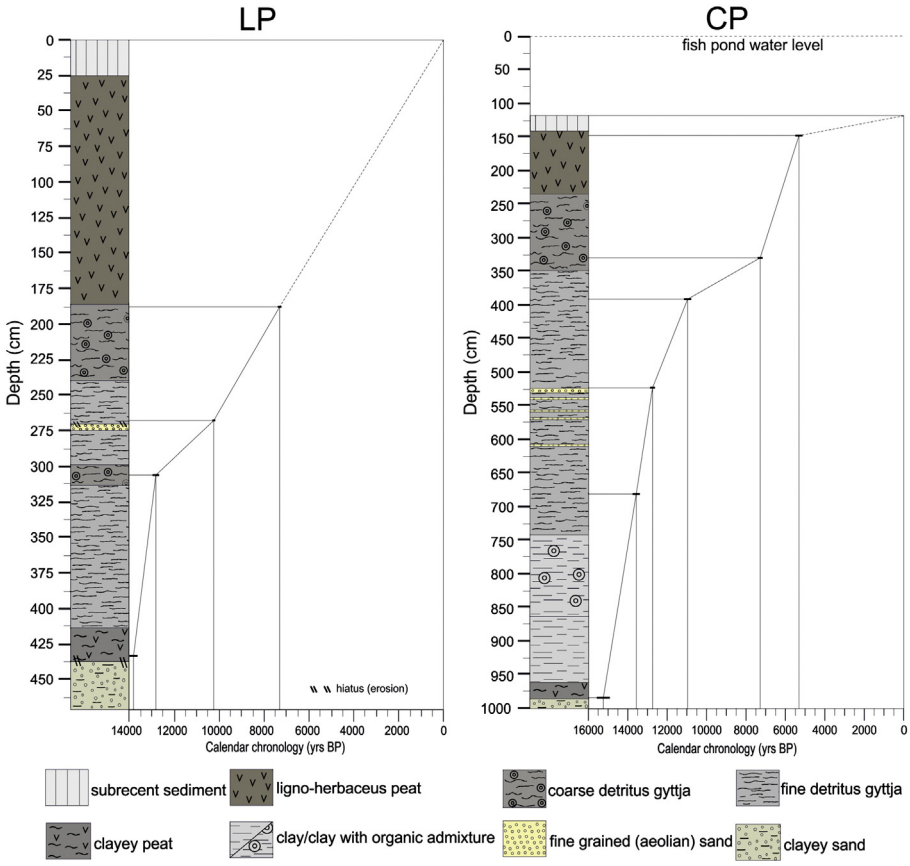

Fig. 4. Age–depth model and litostratigraphy of the cores LP and CP.

Helianthemum). The presence of *Betula nana* and *Betula humilis* in the macrofossil record has been confirmed for the oldest period of accumulation (radiocarbon-dated to 11,820 ± 60 BP; see also high *Betula alba*-type and *B. nana* pollen maxima). These results point to severe climatic conditions, the absence of well-developed soils, and an open, mostly treeless vegetation, steppe- and tundra-like in character. The local presence of scattered pine and birch trees is likely. In the same period, most of the finds point to a relatively low water level status; macrofossils of aquatic taxa are virtually absent in the LP-1 zone. That is suggested also by the plant macrofossil record (mLP-1; 450–410 cm) where the presence of shoreline heliophilous plants (*Lemna* sp., *Hippuris vulgaris* and *Ranunculus flammula*) indicate a muddy substrate near the margin of water-body.

The change towards a relatively higher water level came with the start of the macrofossil subzone mLP-2a (410–320 cm). That is indicated by the presence of diverse aquatic flora e.g. *Ceratophyllum demersum*, *Myriophyllum spicatum*, *Potamogeton filiformis*. Also fish remains — scales of perch (*Perca fluviatilis*) are present in this level. Macrofossil subzone mLP-2b (320–300 cm) is characterized by the presence of tall sedges and reed vegetation (*Carex acutiformis*, *Typha*, *Poaceae*) that points to a sudden decline of the water level. This clearly corresponds with the lithological change (from fine- to coarse-detritus *gyttja*). In the overlying zone mLP-2c (300–280 cm) the occurrence of Charophytes (*Chara* sp. and *Nitella* sp.) deserves a special mention as they indicate some change in conditions, connected most probably with the increase in the input of eroded inorganic material (sand and silt) to the lake and with a carbonaceous environment. This last find is in sharp contrast with present-day conditions in the area under study, for most soils are leached, highly acidic, and almost completely lacking calcium carbonate.

In the pollen zone LP-2 (355–280 cm) *Betula alba*-type pollen declines while *Juniperus* and *Artemisia* reach their maxima. The occurrence of Tertiary palynomorphs as indicators of erosion is also highest in this zone. A strong change in the aquatic environment took place: *Ranunculus* Subgen. *Batrachium* and *Myriophyllum spicatum* became dominant among macrophytes. Among planctonic algae, a prominent change from *Tetraedron*- and *Pediastrum*-dominated communities to *Scenedesmus*-dominated ones took place at the lower boundary of the zone. All the aforementioned changes point to climatically less-favorable conditions when compared with the adjoining zones lying above and below.

The extremely sharp (compared with the CP core pollen record; see below) LP-2 to LP-3 transition at the depth 280 cm is probably caused by the presence of a long sedimentary hiatus. Most prominent in this zone boundary is a sharp decline in most herbs and shrubs, often to zero values. In the aquatic environment the change in the taxa represented is also extremely sudden. The occurrence of *Pediastrum simplex* var. *simplex* points to warm water conditions (Komárek and Jankovská, 2001) during the time of LP-3 zone sedimentation. The decline in *Pinus* and rise in *Picea abies* and broadleaf thermophylous trees is the main feature of the LP-3 zone. Its upper boundary has been delimited by the disappearance of open water indicators. Within the LP-3 zone (280–180 cm) climatically-demanding aquatic macrophytes developed (most prominently *Trapa natans*). The position of the studied section in close proximity to the lake shore is reflected in the common occurrence of many marsh plant taxa, including several eutrophic ones. The common presence of *Urtica dioica* seeds in this zone deserves special note as its occurrence is correlated with an increased presence of charcoal particles and with archeological evidence of local Mesolithic occupation (Pokorný et al., 2010). In macrofossil subzone mLP-3a (280–250) *Chara* was dominant. This was related to the deposition of sand in the sediment. In depths of 250–180 cm (subzone mLP-3b) the presence of aquatic plants (e.g. *Trapa natans*, *Nymphaea alba*) and littoral plants (e.g. *Carex pseoudocyperus*, *Typha* sp., *Poaceae*) indicates terrestralization of the lake. That clearly corresponds with a change in lithology (coarse *gyttja* deposition).

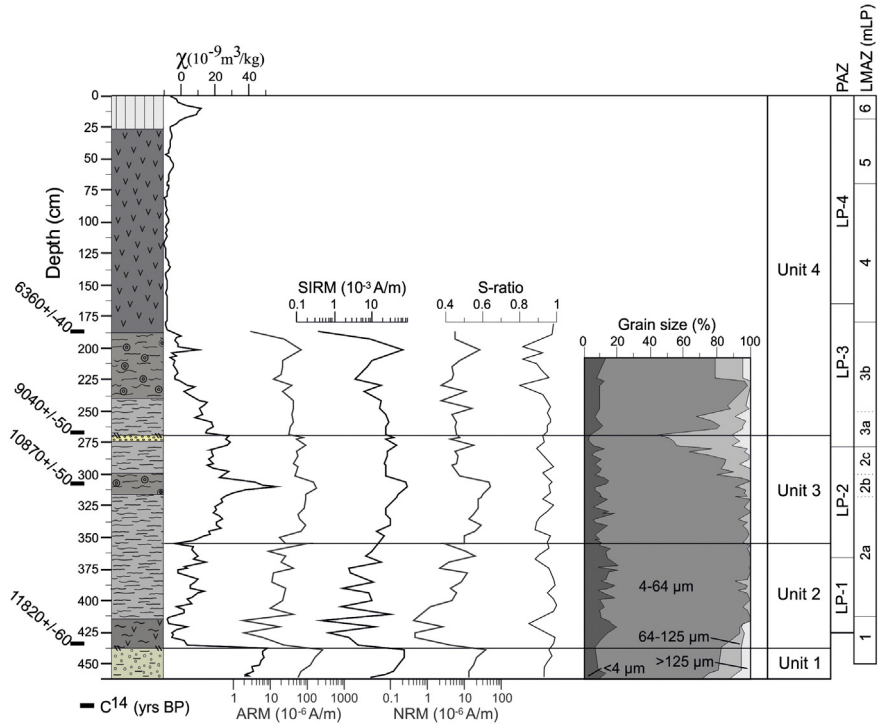

Fig. 5. Results of the mineral-magnetic and grain size analyses of the core LP together with local pollen and macrofossils assemblage zones.

The transition from LP-3 to LP-4 pollen zones at the depth of 180 cm roughly corresponds with macrofossil zones mLP-3 to mLP-4. That is marked by the disappearance of aquatic taxa and the development of alder carr (see the occurrence of *Alnus glutinosa* macrofossils).

The low frequency of macrofossils in the zone mLP-5 (70–20 cm) probably relates to the decomposition that took place after peat extraction that was documented for the turn of the 17th and 18thcenturies. Macrofossil zone mLP-6 at depths of 0–20 cm was distinguished due to the occurrence of water (*Chara* sp., *Nitella* sp., Cladocera) and wetland taxa (e.g. *Juncus* cf. *bulbosus*, *Ranunculus flammula*). This way, the existence of the fishpond (known historically to be constructed in the turn of 17th and 18th centuries) is indicated.

5.2.2. The central core (CP; Fig. 9)

The results of the pollen analyses from both profiles (LP and CP) show many similarities. Nevertheless in comparison with the pollen record of LP, the central profile CP record is more complex, reaches deeper (in terms of chronology) and is more likely to be complete (i.e. lacks the evidence for sedimentation hiatuses). The results of pollen analyses from CP has been described in Pokorný (2002), therefore we only very briefly recapitulate the most important features of the pollen record here, using integrative pollen zonation.

5.2.2.1. Zone CP-1. Absolute pollen concentrations in the deepest sediments of the lake-basin center are relatively low – if compared with the above-lying ones – suggesting high accumulation rates. The

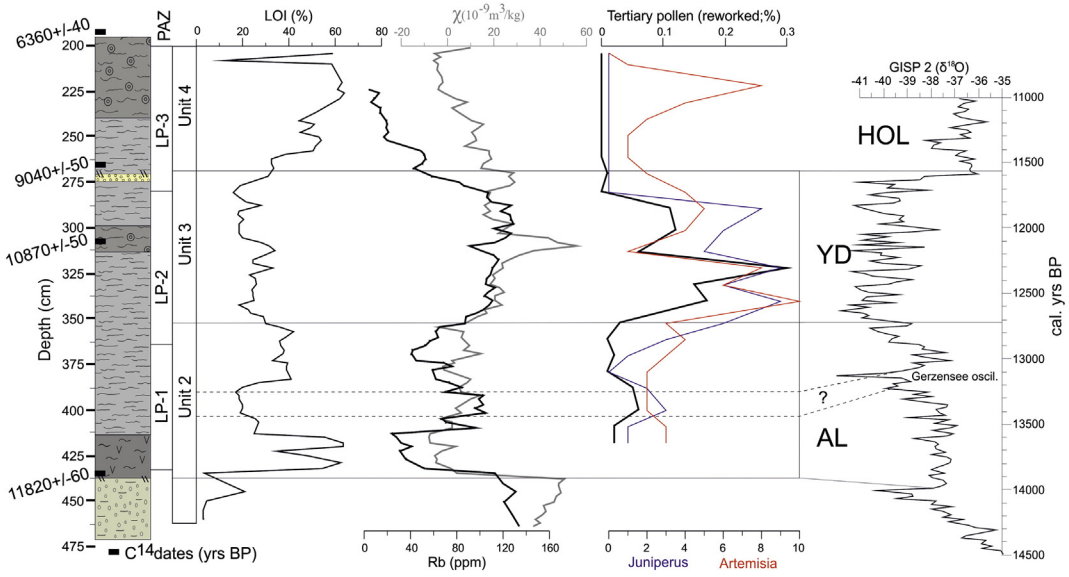

Fig. 6. LOI, Rb content, magnetic susceptibility and concentration of Tertiary pollen and heliophilous vegetation from the core LP correlated with the GISP2 oxygen isotope record (Stuiver et al., 1995).

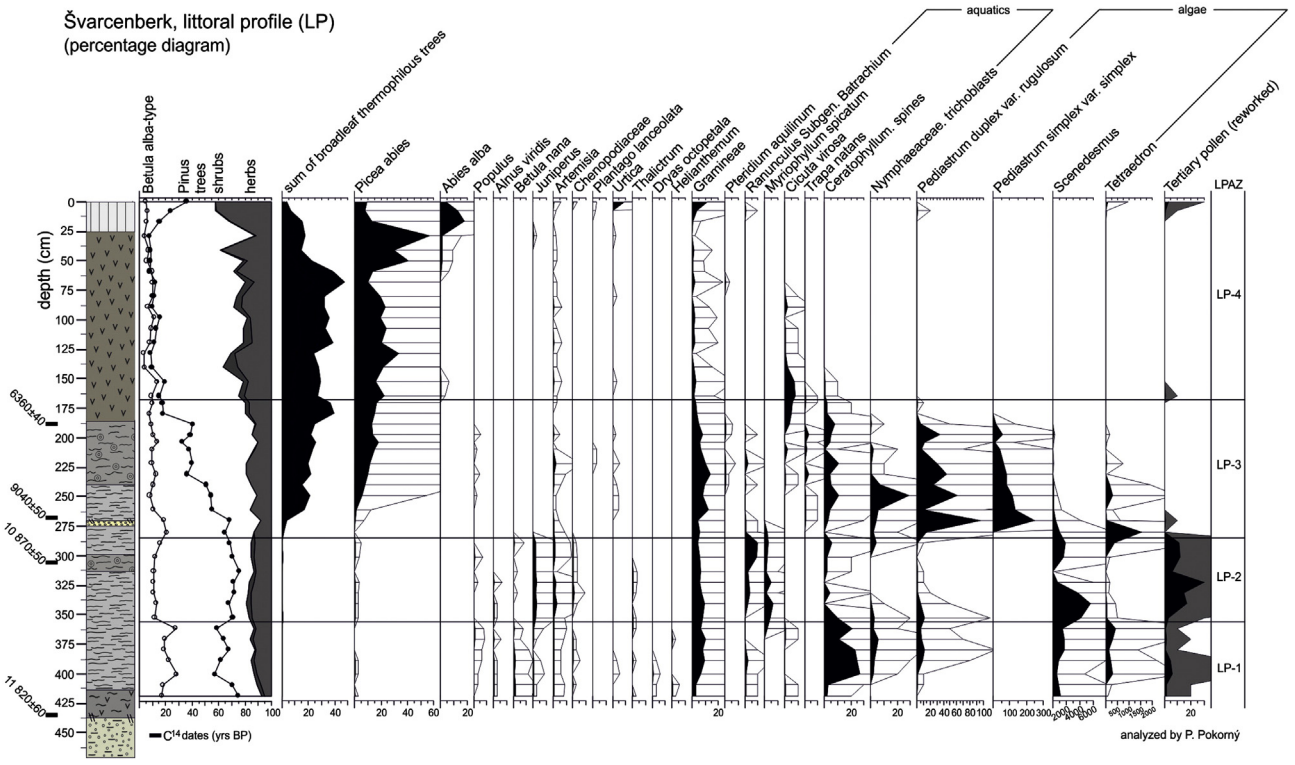

Fig. 7. Percentage pollen diagram of the LP core. Selected taxa of trees, shrubs, herbs and aquatic plants are presented. LPAZ — local pollen assemblage zones.

zone is characterized by high (but gradually decreasing) NAP values, suggesting open herbaceous vegetation. Gramineae, Chenopodiaceae, *Betula nana*, *Alnus viridis*, *Salix*, *Thalictrum*, and *Artemisia* formed steppe–tundra vegetation. *Pinus* values rise from 35 to 55%, while *Betula alba*-type values do not exceed 5%. *Helianthemum* is indicative of a bare, calcareous substratum (Hoek, 1997). The pollen of submerged water plants is virtually absent.

5.2.2.2. Zone CP-2. This zone is characterized by a local *Pinus* maximum and a relative decrease in some heliophylous dwarf shrubs and herbs (*Alnus viridis*, *Salix*, *Artemisia*, *Thalictrum*, *Helianthemum*). Apparently, pine became a successful competitor for light with the heliophylous vegetation (the local presence of pine is confirmed also by the finding of *Pinus* stomata.) Nevertheless, Gramineae, Chenopodiaceae, *Alnus viridis*, *Salix*, *Thalictrum*, *Artemisia*, and *Betula nana* were still important components in the vegetation. The *Betula alba*-type pollen curve is continuous during the entire zone, but still too low (under 5%) to suggest the local occurrence of birch trees. Absolute pollen concentrations in the sediment are still low during this zone. The increased content of reworked Tertiary palynomorphs point to increased erosion of Tertiary bedrock.

5.2.2.3. Zone CP-3. The decline of pine and new expansion of heliophyllous herbs in this zone can be interpreted as indication of some strong, but brief, cooling. In the upper half of the CP-3 zone, a new pine expansion predates the transition to CP-4.

5.2.2.4. Zone CP-4. This prominent zone starts with a rise in *Salix* pollen percentages, followed by a clear *Betula alba*-type increase. *Salix* probably formed the shrub belt in front of the expanding birch forest-line (similar to that observed by Gaillard, 1985; Hoek, 1997), so high values of *Salix* are observed in advance of a *Betula alba*-type expansion. In the second half of the zone, birch trees became dominant in the pollen spectra instead of *Pinus*. This assemblage reflects the development of open boreal birch woodland with some dispersed pine trees. The lower limit for a mean July temperature needed for tree birch colonization is usually taken as 10 °C, but 12 °C is the optimum for the development of *birch* woodlands (Birks, 1993). The open character of the forest can be inferred from the pollen diagram, for most of the heliophylous herbs typical for steppe and tundra communities are still abundant. In the aquatic environment, an abrupt warming period caused the expansion of submerged macrophytes, including the relatively-demanding (thermophylous) *Ceratophyllum demersum*, which appears for the first time in this zone. The amount of reworked Tertiary palynomorphs decreases, thus indicating a diminished rate of erosion.

5.2.2.5. Zone CP-5. The basal pollen spectrum of this zone coincides with a strong decrease in the *Betula alba*-type from 40% to about 20% and a new increase in *Pinus* up to values of about 60%. The forest cover became still more closed, as reflected by a decrease in all open-communities indicators (and AP around 90%, i.e. similar to values in the Holocene). *Helianthemum* and the *Plantago maritima*-type disappeared completely. The presence of *Nuphar* points to minimum July temperatures of at least 12 °C (Huizer and Izarin, 1997). *Ceratophyllum demersum* became the dominant submerged aquatic (The decline of other aquatic macrophytes is probably the result of competition with the two aquatic taxa just mentioned.). The virtual absence of reworked Tertiary palynomorphs points to only minimum erosion.

5.2.2.6. Zone CP-6. The values of the *Betula alba*-type remain low (around 20%), whereas *Pinus* percentages are generally the same compared to those of the preceding zone. *Alnus viridis*, *Salix*, *Betula nana*, Chenopodiaceae, and *Artemisia* values increase again, suggesting a new cooling period and an opening up of forest cover. An even more prominent increase is recorded in the *Juniperus* curve. Vegetation change reflecting cooling period is also recorded within the lake: values for *Ceratophyllum* basal nut spines decrease and *Nuphar* pollen is even completely lacking in favor of a massive occurrence of *Myriophyllum verticillatum* and *Ranunculus* subgen. *Batrachium*. Increased erosion is indicated by an increased content of reworked Tertiary palynomorphs.

5.2.2.7. Zone CP-7. This zone is characterized by a gradual decrease in all NAP taxa, especially *Alnus viridis*, *Betula nana*, Chenopodiaceae, and

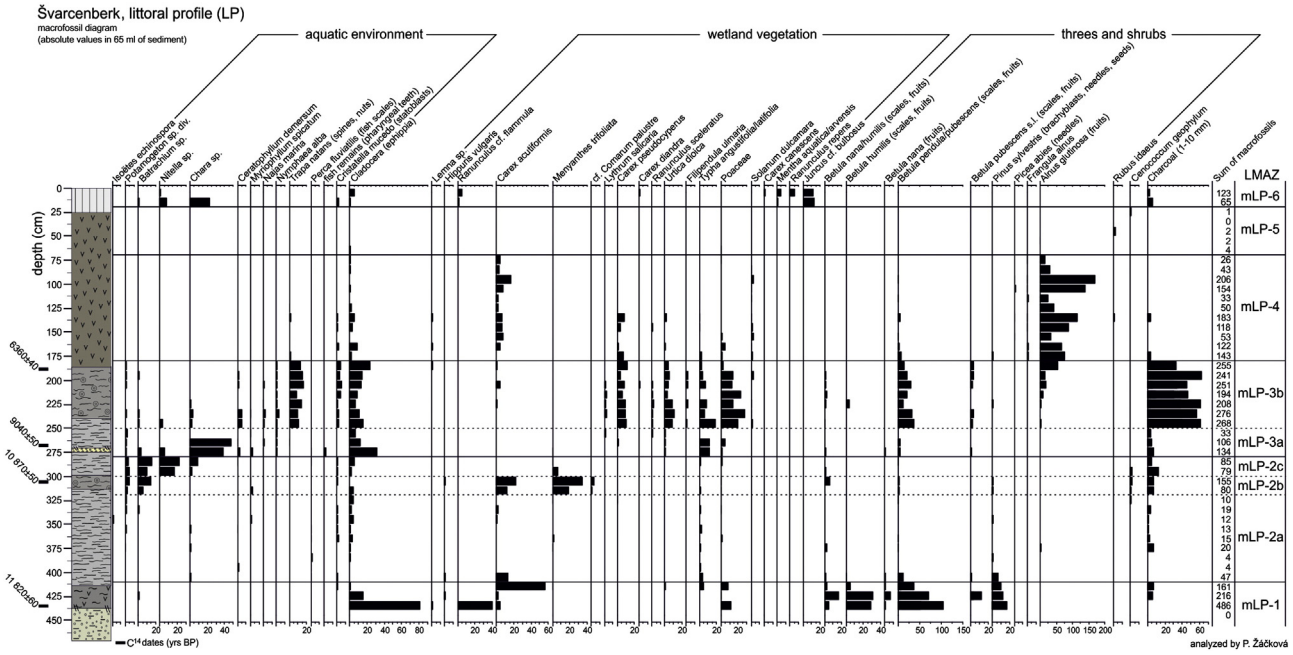

Fig. 8. Late-Glacial and Early-Holocene macrofossil diagram of the LP profile. LMAZ — local macrofossils assemblage zones.

Artemisia among the most important. At the same time, *Betula* and *Populus* percentages rise (*Populus tremula* may have been favored as a pioneer tree in areas that were left open during the preceding period; Ammann et al., 1994). *Alnus viridis* and *Betula nana*, the most characteristic tundra elements surviving from the preceding zone, were gradually outcompeted by expanding forests, and their pollen values fall finally to zero. As in the preceding period, pine was still dominant in the regional forest cover.

5.2.2.8. Zone CP-8. Boreal forest dominated by birch trees was gradually replaced by mixed deciduous forest during this zone. The pollen curve of *Pinus*, hitherto very high, started to decrease as a result of competition with deciduous trees even on poor substrates, where soils had developed since the beginning of the Holocene. *Picea* expansion took place in the same period. Afforestation reached its maximum by the upper limit of the zone. Terrestrialization of the lake culminated at the same point (The disappearance of aquatic

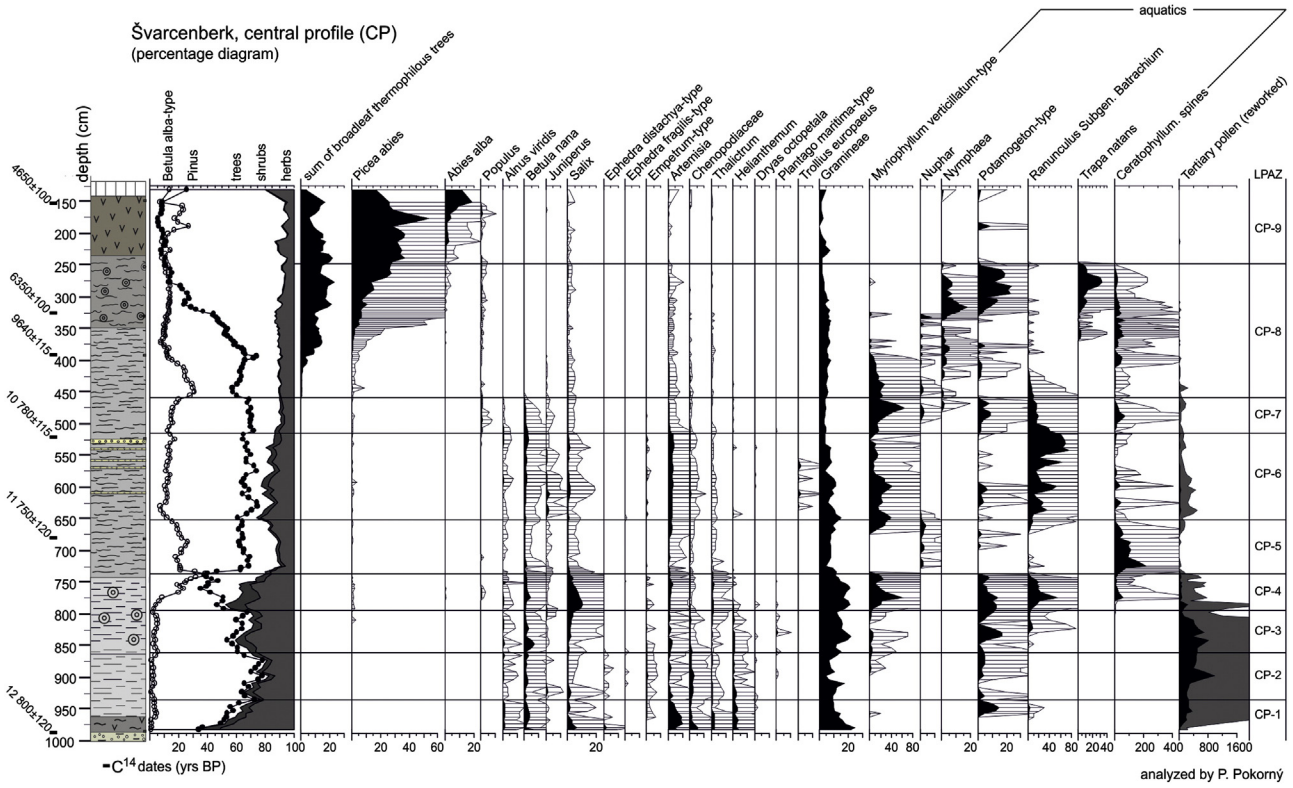

Fig. 9. Late-Glacial and Early-Holocene percentage pollen diagram of the CP. Selected taxa of trees, shrubs, herbs and aquatic plants are presented. LPAZ — local pollen assemblage zones.

taxa has been used here as a criterion for delimitation of the upper zone boundary.)

5.2.2.9. Zones CP-9. Mixed deciduous forest has been partially replaced by coniferous stands, first by *Picea*, then also by *Abies*. Afforestation of the region was almost absolute (see AP values higher than 90% and curves of most herbs falling to zero). Lake terrestrialization has been completed in this zone as indicated by the sudden decline in all aquatic taxa.

5.3. Chironomid stratigraphy (Fig. 10)

Among the 6246 counted specimens, 68 chironomid genus or species morphotype were identified. Three major zones and two subzones were distinguished by cluster analysis of the assemblages. In Fig. 10 only the chironomid taxa discussed in Section 6 are shown.

5.3.1. Zone CP Ch-1

The first colonizers of the lake include mainly *Procladius*, Chironomus anthracinus, *C. plumosus*, *Corynocera oliveri*, *Paratanytarsus* and *Tanytarsus lugens*. The relative abundance of *Microtendipes pedellus* increased and peaked at 30% around 920 cm, while in the upper part it declined. Other taxa were found only sporadically. The zone ended with the disappearance of *Corynocera oliveri*, *Stictochironomus* and *Protanypus*. This chironomid zone roughly corresponds with pollen zones CP-1, CP-2 and CP-3.

5.3.2. Zone CP Ch-2

The zone is dominated by *Polypedilum* and *Corynocera ambigua*. Subzone Ch2a was marked by a rise of *Polypedilum* (14–25%) and a continuous increase of *C. ambigua* (10–65%). *Chironomus anthracinus* and *Chironomus plumosus* were also common. This chironomid subzone corresponds with pollen zones CP-4 and CP-5. The start of subzone Ch2b was characterized by a temporary sharp fall in the relative abundance of *Corynocera ambigua*. Nevertheless, this taxon rose towards of the rest of the subzone. The subzone was also defined by slight declines in *Polypedilum* and *Chironomus* species. *Microtendipes pedellus* increased with the peak around 590 cm (42%). However, at the upper part of the subzone this taxon finally disappeared. *Dicrotendipes*, *Polypedilum* and *Corynocera ambigua* made a brief rise at the end of the zone. Orthocladiinae were also present in low numbers. Relative abundance in littoral taxa was present at the highest percentages (up to nearly 80%). This chironomid subzone corresponds with pollen zone CP-6.

5.3.3. Zone CP Ch-3

The major change in the fauna was represented by the increase in Chironomini (50–>90%) and the decrease of Tanytarsini (40–7%). Oligotrophic taxa were absent in this zone and cold-adapted taxa, and temperate-adapted taxa and mesotrophic taxa were present only sporadically. The zone was dominated by *Chironomus plumosus*, but *Einfeldia*, *Glyptotendipes* and *Tanytarsus* were also common. Other taxa were found in very low percentages. This Chironomid zone corresponds with pollen zones CP-7 and CP-8.

5.4. Correlation between central (CP) and littoral (LP) cores

Pollen analyses of the littoral core (LP; Fig. 7) show a much less complex picture when compared with the central core (CP). This is due to less temporal resolution and due to its less continuous sedimentation caused by its position near the lake basin margin that makes the littoral record sensitive to lake level fluctuations (This last mentioned fact can be taken as an advantage in certain respects, as shown in the discussion below). To be more specific, the LP record shows indications of a possible sedimentary hiatus (or sharply decreased sedimentation rate) that is inferred to be the level of transition between the LP-2 and LP-3 zones.

An attempt to find correlation between both cores was made on a palynostratigraphic basis, in combination with rubidium concentration curves and the results of the organic matter content analyses. We also used the relative concentration of reworked Tertiary pollen in the sediment as an index of erosion intensity in the lake catchment. The result of this correlation is shown in Fig. 11. This correlation is a very important step in our heuristic procedure, as many analyses were performed only on material recovered in the LP core. This is the case with regard to the instrumental sedimentological and magnetic analyses which are a main matter for discussion. Biotic results from the central core CP are used in this paper mostly as an important source of information about the regional paleoecological background of the site.

6. Discussion

6.1. Structure of the record, comparing proxy resolutions

Previous studies from the Švarcenberk Lake have been focused on biotic proxies and have already brought much information about Late Glacial–Holocene paleoecological development in the study area (Pokorný and Jankovská, 2000; Pokorný, 2002; Pokorný et al., 2008, 2010). Our main focus in this paper is a confrontation of the abiotic processes with the biotic ones.

In general we found a good correspondence between erosion-weathering processes in the lake catchment (mineral-magnetic enhancement, rubidium content), organic production within the lake (LOI, TOC, Chironomids record) and density of vegetation cover in the lake's surroundings (concentration of non-arboreal pollen such as

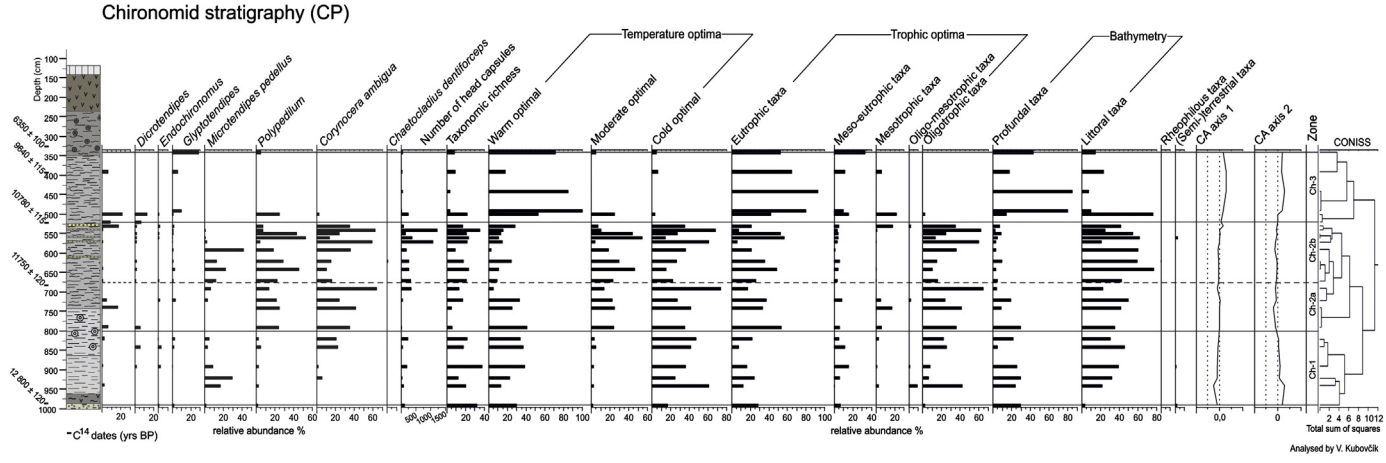

Fig. 10. Chironomid assemblage diagram from the CP core showing relative abundances and assemblage diversity.

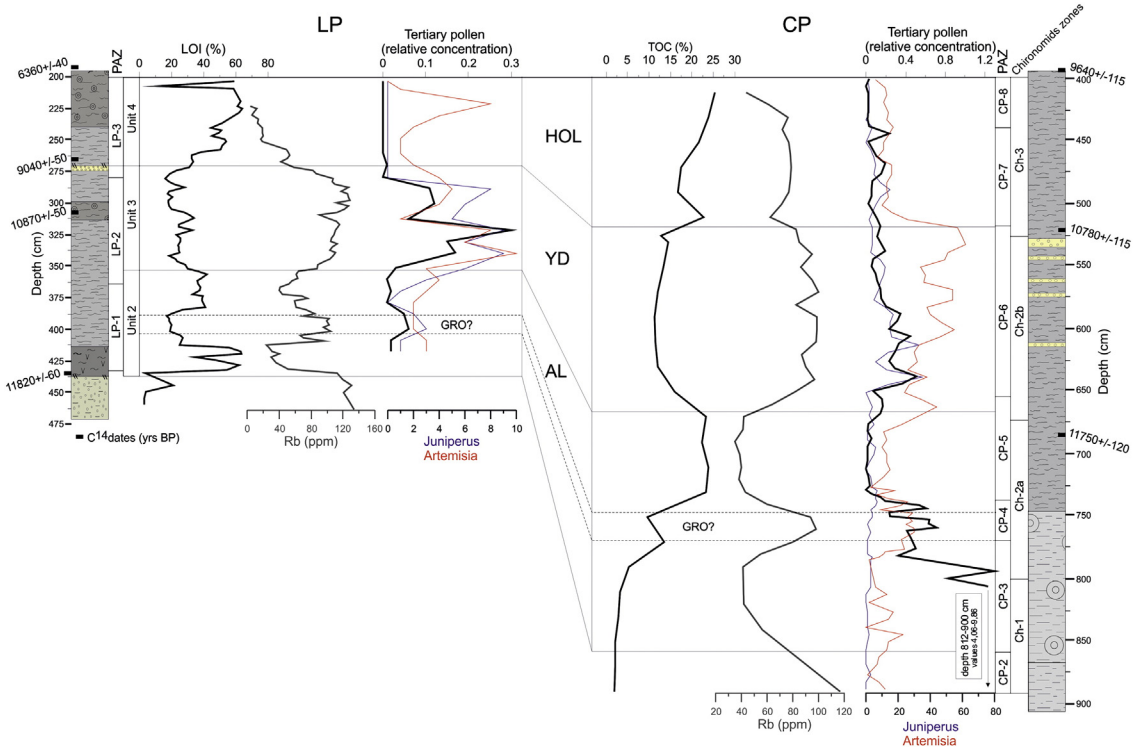

Fig. 11. Correlation of the Alleröd and Younger Dryas chronozones in the core LP and CP based on organic matter, Rb content, Juniperus–Artemisia pollen and relative concentration of Tertiary pollen.

Juniperus and *Artemisia*, plant macrofosils). The various reasons for this are discussed below and summarized in Figs. 6 and 11.

The difference between the magnetic susceptibility (MS) of the bedrock in the catchment (χ ~ 10) and lake sediments (χ up to 55; Fig. 5) suggests a mineral magnetic enhancement of lake sediment by another detrital component from the catchment, probably by eroded soils from the lake catchment.

During pedogenesis, iron-reducing bacteria produces mainly ultrafine (superparamagnetic — SP) fractions of magnetite (<0.1 μm). MS is sensitive to changes in the concentration of coarse-grained as well as fine-grained magnetic minerals, while ARM values are more responsive to changes in fine-grained magnetic minerals (mostly magnetite), but less sensitive to variations in coarse-grained (King et al., 1982). The high similarity of the MS and ARM record therefore indicates an increase in the influx of fine-grained mineral assemblages typical for soil horizons.

A positive correlation of MS with the heliophilous vegetation (such as *Artemisia* and *Juniperus*) (Fig. 6) supports the interpretation of the magnetic record as a proxy for the flux of detrital material from the catchment: weathering and soil development are linked with more favorable climatic conditions, while cooling leads to defragmentation of the vegetation cover, increased erosion and limited pedogenesis processes.

A number of papers have already shown that MS maxima may reflect intense detrital inputs in response to climate cooling and changes in vegetation cover during the Late Glacial and the Holocene (Dearing and Flower, 1982; Thouveny et al., 1994) or forest clearings and land use history (Zolitschka et al., 2003), while warmer climates with a higher surface cohesion have led to decreasing trends in erosional processes, causing less minerogenic deposition. Additionally, higher organic production within a lake during warmer periods leads to low magnetic susceptibilities, because the organic matter is diamagnetic. On the basis of this syllogism, it is possible to use magnetic results as good proxy indicator of environmental changes and to interpret the units of the LP core as individual climatostratigraphic substages of the period. In this sense, the magnetic signal record from the LP core corresponds with the records from several other Late Glacial lacustrine sites in Europe (e.g. Day, 1996; Nolan et al., 1999; Stockhausen and Zolitschka, 1999) and these have proved to be a useful tool for the detection of environmental changes in the catchment.

The high similarity between magnetic parameters and Rb concentration (Fig. 6) demonstrates that these parameters recorded similar environmental changes. This may be caused by the fact that both parameters are sensitive to the erosion-weathering processes in the catchment. Rubidium generally coexists with K in K-rich minerals, such as K-feldspar. This element is unaffected by sediment diagenesis and by concentrations of Fe and Mn oxi-hydroxides. Even in highly organic sediments, the minuscule mineral fraction may be responsible for most of the Rb fixation. This is consistent with the aluminosilicate affiliation of elements. Rb is strongly retained in the weathering zone due to adsorption or exchange onto clay minerals (e.g. vermiculite) and may not be removed until extensive K-feldspar alteration occurs (Nesbitt et al., 1980). Rubidium fixation in soil is a tracer of the transformation process affecting the 2:1 clay minerals in the acid brown earth-pods weathering sequence: kaolinite, illite, chlorite, vermiculite and smectite (Herbauts, 1982; Ross et al., 1989). During warmer periods, the surface weathering zone (including soils and weathered bedrock) is more widespread and mobility of Rb in the lake catchment is decreased. Therefore Rb content in lake sediments will be low due to the bonding of Rb to more strongly-weathered clay-like minerals in the catchment. As the climate deteriorates and the landscape begins to be more unstable, erosion intensity increases and the surface weathering zone is removed into the lake basin. As a result, during cold periods, lake sediments are more or less depleted in Rb depending on the erosion rate and on the relative intensity and duration of weathering of the previous warmer period. The variations of Rb concentration observed in the lake sediment are therefore, as with MS, related to climatic parameters through pedogenesis (weathering) and erosion rate. Our hypothesis of the climatic control of Rb content in the Švarcenberk Lake record is further supported, similarly to that of the magnetic parameters, by a correlation with NAP and LOI. In addition, there exists good agreement with the record of $\delta^{18}O$ GISP 2 during the Alleröd and Younger Dryas periods (Fig. 6).

Rb content in sediment has been used for determination of in-situ weathering of loess/paleosol sequences (Chen et al., 2000; Buggle et al., 2009). For lacustrine deposits it has been demonstrated, for example, by Jin et al. (2006) in mineral and organic-rich Holocene lake sediment.

A good correlation of abiotic proxies with a regional pollen record (Figs. 5, 6 and 7) implies some sensitivity of the vegetation cover of the catchment to climatic changes. A strong biotic response could be related to the position of a site being close to an ecological boundary, where a critical threshold has been crossed: cooling led to weaker chemical weathering and in particular deforestation, which caused an increase in soil erosion dynamics and lower lake productivity.

Nevertheless, while a strong relationship between biotic and abiotic proxies was found in both cores and correlations between particular records could be found (Fig. 11), the radiocarbon dates do not support this cross-core correlation so evidently — the date 11,750 +/− 120 corresponds with the upper part of the Alleröd in the CP core, whilst in the LP core a very similar date (11,820 +/− 60) was obtained from the beginning of this period (see Fig. 4). The reason for this shift may be related with the inwash of older organic carbon detritus, i.e. the same process as described, for example, by Andrée et al. (1986). The inwash could be caused by some relatively strong artesian springs that were found in the study area and also directly in the lake basin (close to the CP core, see Fig. 1). Considering that the age determination was made on a bulk sample of the alkali-soluble fraction from gyttja in core CP, such a means of contamination is possible. From this point of view, the sample for dating in the LP core should be more reliable, because it was taken from a macroremain (twig). Furthermore, radiocarbon dating of the Late Glacial period is a common problem in many lacustrine sites (Andrée et al., 1986; Lowe and Walker, 2000; Litt et al., 2001; Pilcher, 2003). Calendar age assessment in the Late Glacial may be hindered by the existence of periods of constant ^{14}C age, the so-called 'radiocarbon plateaus' that have been identified at around 12.7, 10 and 9.6 kyr ^{14}C BP (Ammann and Lotter, 1989), coinciding with ocean ventilation/thermohaline circulation changes (Andersen et al., 2000).

6.2. Late Glacial paleoenvironmental changes in the study area

The complete series of the fine-scaled primary record obtained by the respective analytical techniques were separately subdivided into particular units based on the degree of similarity among compared horizons. In the following text we interpret these units as (inter)stadial units of the Late Glacial. This interpretation is further supported by palynostratigraphy and, to a certain degree, by ^{14}C dates.

6.2.1. Pre-Alleröd period (Unit 1 — CP3? Ch1?)

The high magnetic mineral concentrations could be caused by the high intensity of erosion in the catchment and by the inflow of weathered surface horizons into the lake basin. High ARM and SIRM values suggest that the unit is rich in ultra-fine, single-domain, magnetic grains of magnetite. An increased erosion of rock detritus is also suggested by high Rb values. With respect to radiocarbon measurements from the upper layer (437 cm, 11820 +/− 60 BP, i.e. 13835–13452 cal. yrs. BP), we date this period before the Alleröd. The results denote the presence of well-developed soils in the catchment during the Bölling interstadial. A significant enrichment of the colluvial sediment by pedogenetic magnetite is probable, because the MS signal of bedrock sediment is very low (5–12) in comparison with this unit. The same process of soil development is also recorded in lowland loess plateaus of Central Europe. Loess formation, which is characteristic of the late Pleniglacial, generally terminates during the Bölling phase, and initial pedogenesis takes place during that time (Ložek and Cílek, 1995).

This unit is sharply separated from the upper one. This could be the result of an erosion of the upper part of this unit, causing some sedimentary hiatus. This event is recorded in the decreasing magnetic values and Rb concentrations.

6.2.2. Alleröd (Unit 2-LP1-CP4,5 — Ch2a)

The basal layer of this unit – a clayey peat with wooden pieces (437–405 cm) – probably started to accumulate after the exposure of the littoral and the following erosion event. The sediment has accumulated close to the lake shore under lower water level conditions. This is suggested by the lithological record (clayey peat) and by the presence of tree and shrub macrofossils (especially *Betula nana* and *Betula humilis*). On the basis of the radiocarbon date 11,820 +/− 60 yrs BP obtained from the bottom of this layer, it is possible to assign the unit into the Alleröd chronozone. Fine-grain gyttja, deposited above the layer, indicates the lake level rising and increasing humidity during the second part of the Alleröd interstadial.

That is supported also by macrofossil records (Fig. 8) where aquatic flora (e.g. *Ceratophyllum demersum*, *Myriophyllum spicatum*, *Potamogeton filiformis*) is present. The slightly increasing trend in magnetic values during the Alleröd (Fig. 5) could be caused by an acceleration of pedogenetic processes in the catchment. A stratigraphic investigation of the "Vlkovský přesyp" aeolian sand dune (situated some 3 km NW from the coring site; see Fig. 1) has revealed fossil soil buried under more than 5 m of aeolian sands. A distinctive layer of pine charcoal fragments buried with this soil has been dated to 11,260 +/− 120 BP (Pokorný and Jankovská, 2000). This find resembles conditions in the Netherlands, where the "Usselo soil layer" formed during the Alleröd period with an average date around 11,000 BP (Hoek, 1997). Early soil formation during the Late Glacial Interstadials is supposed also e.g. for the Swiss Plateau (Ammann et al., 1994, 2013).

The formation of soils during the Alleröd period required stable climatic conditions with less aeolian activity and relatively dense vegetation cover. The catchment of the Švarcenberk Lake was covered by *Pinus* dominated forest, which then became more closed, as is reflected by a decrease in all open-community indicators in the pollen spectra (Figs. 7, 8 and 9). Woodland cover helped prevent surface washes and slope processes. Considering this, it is no surprise that during the Alleröd a low erosion intensity and chemical weathering dominated in the lake catchment and Rb was fixed in the weathering horizons, leading to a diminished Rb content of mineral material prior to its erosive removal and sedimentation in the lake basin (Fig. 6). The topsoil with SP and SD magnetic grains was washed to the lake basin, but the intensity and depth of erosion was generally weak, and the magnetic values of the sediment are not high (Fig. 5). Also the Chironomid assemblage from core CP indicates that conditions in the lake remained relatively warm and mesotrophic during this period (Fig. 10). The climatic amelioration caused a population increase of *Polypedilum* and *Corynocera ambigua* as indicators of the temperate conditions. Nowadays, these taxa are broadly distributed along a temperature gradient (mean July air temperature ranging from 8.1 °C to >14 °C) in northern Sweden, Finland and Canada (Walker and MacDonald, 1995; Simola et al., 1996; Larocque et al., 2001). At the same time, *Cladopelma* appears in the record, indicating a July temperature ranging from 12.1 to >14 °C (Larocque et al., 2001). The relative high abundance of *Chironomus* spp. may also suggest an increase in temperature and higher content of nutrients.

6.2.3. Gerzensee oscillation

If the Alleröd period seems to be climatically favorable, in the horizon 402–392 cm of LP, a significant increase in Rb content, together with a higher magnetic susceptibility and reworked Tertiary pollen concentration are recorded (Figs. 5 and 6). Simultaneously, aquatic production decreased considerably (Fig. 7), possibly the effect of colder water temperatures and shorter summer seasons. These proxies indicate some short-term, but pronounced, cooling. The stratigraphic position of the layer suggests that this event may be attributed to the Gerzensee oscillation. This centennial-scale cooling event is recorded mainly in the decline of δ^{18}O during the second part of the Alleröd (13,100–13,200 yrs BP) in the Greenland ice-cores — the GI-1b event (Dansgaard et al., 1993; Björck et al., 1998) and foraminifera record

of marine sediments (Lehman and Keigwin, 1992). From land sites, it was first documented in the $\delta^{18}O$ and $\delta^{13}C$ isotopic record of the Swiss lake Gerzensee (Eicher and Siegenthaler, 1976; Schwander et al., 2000; Lowe et al., 2008; van Raden et al., 2013; dated 13,274–12,989 and 13,261–12,909 yrs BP, respectively) and later from other sites of the Atlantic rim of Europe (e.g. Litt and Stebich, 1999). From lakes in Denmark, the onset of the oscillation is dated between 11,400 and 11,300 ^{14}C BP (Andersen et al., 2000). It has been found also in Atlantic Canada, where it is called the Killarney oscillation (Levesque et al., 1993).

The radiocarbon date 11,820 ± 60 ^{14}C (13,599–13,860 cal. yrs BP) obtained from the depth of 437 cm supports this correlation. The pollen record of LP is marked by an increase of *Juniperus* and *Dryas octopetala* and suggests an opening up of the forest during this period. That is supported also by the low sum of macrofossils in this horizon (Fig. 8). This intra-Alleröd climatic oscillation had a perceptible impact on both the terrestrial and limnic ecosystems of Lake Švarcenberk and caused vegetation changes, increased soil erosion and lowered aquatic production in the study area. Climatic deterioration is also supported by aeolian activity at "Vlkovský přesyp" (see above) shortly after 11,260 +/− 120 ^{14}C BP (13,239–12,985 cal. yrs BP). After this event, a centennial-scale warming period occurred, followed by gradual cooling at the end of the Alleröd period.

Similarly, an Rb concentration increase was found in the Alleröd part of core CP in the horizon 730–755 cm, i.e. in the upper part of the pollen zone CP-4 (Fig. 11). Proxies from this layer also denote sparse vegetation cover and higher erosion dynamics: the content of organic carbon shows a short-term, but significant, decline, whereas Rb and reworked Tertiary pollen concentration together with open community pollen indicators (see Gramineae, *Artemisia* and *Juniperus* pollen; Fig. 9) increase. Nevertheless, radiocarbon dates obtained from the above layer don't suggest this cross-core correlation. Possible reasons for this were already discussed in Section 6.1.

6.2.4. Younger Dryas (Unit 3-LP2-CP6 — Ch2b)

All proxies from this horizon indicate a relatively rapid cooling. The high magnetic values (Fig. 5) are caused by the intensive soil erosion in the catchment, connected with the inwash of topsoil horizons into the lake basin. The increased intensity of erosion is related to the less dense forest cover. This is demonstrated by the increase in Gramineae, *Artemisia* and *Juniperus* pollen (Figs. 7, 9 and 11). The significant increase in reworked Tertiary pollen in the first half of the sediment record in both cores also has to be linked with the increased erosion of the Tertiary bedrock (Fig. 11). In the Chironomid record, warm- and moderate-adapted taxa slightly decrease in relative abundance (Fig. 10). The rise in *Microtendipes pedellus* indicates an increase in minerogenic sedimentation (Hofmann, 1984; Brodersen and Lindegaard, 1999). The Rb concentration (Fig. 11) in the sediment is high due to unweathered horizons not retaining it in the catchment.

Correlation of this unit with the Younger Dryas chronozone is confirmed by the ^{14}C date 10 870 +/− 50 BP (12,755–12,920 cal. yrs BP) obtained from the depth 307 cm of core LP and 10,780 +/− 120 ^{14}C yrs (12,654–12,877 cal. yrs BP) from the depth 520 cm of core CP. The radiocarbon dates are slightly higher than the Al/YD boundary derived from European varved lake sediments, where absolute dates from 12,600 to 12,700 BP have been obtained (Alley et al., 1993;Goslar et al., 1995; Wohlfarth, 1996; Brauer et al., 1999; Litt et al., 2001). Nevertheless, precise radiocarbon dating of YD is relatively problematic due to the extensive radiocarbon plateau (Ammann and Lotter, 1989), a problem discussed already above.

We suppose that the magnetic oscillation in Unit 3 (Fig. 5) could also be indirectly linked to climatic changes, through lake level fluctuations — lower water levels exposing the shoreline zone. The unconsolidated sediment profile was then removed to the lake basin together with surface runoff, causing an enhanced contribution to the sediment by (pedogenetic) ultra-fine magnetic minerals.

In the YD part of core LP there exists a good negative correlation between a major peak of magnetic susceptibility (about 310 cm) and a minimum content of aquatic vegetation and algae, namely *Scenedesmus* (see Fig. 7). This abyssal alga is sensitive to the water level status and its increased content in the sediment generally points to higher water levels. These dates, together with lithological and sedimentological changes in the core (fine/coarse detritus, coarse-grain sand; see Fig. 5), suggest a higher lake level in the first part of the YD and fall in the in the second part. The high relative abundance of Chironomideae littoral taxa such as *Dicrotendipes*, *Endochironomus*, *Glyptotendipes*, *Polypedilu or*, *Chaetocladius* (Fig. 10) suggests the prevalence of shallow water and reflect a well-developed macrophyte vegetation in the littoral zone during the Younger Dryas.

A significant lake level lowering in the second part of YD is marked by the input of coarse sand that diminishes the MS signal (Fig. 5). Plant macrofossils (namely Charophyta) also denote the increased input of mineral material (Fig. 8). Shortly before the onset of the Holocene warming (during the transition between the YD and PB) a drop in the lake level has led to the complete exposure of the littoral. As a result of this a short-term stratigraphical hiatus is indicated in the sedimentary record. This hiatus is apparent from the littoral core pollen stratigraphy as a sharp decline of most herbs and shrubs (Fig. 7).

Due to the small lake catchment and its weak tributaries, hydrological changes on the site are likely to be related mostly with the paleoprecipitation distribution and its influence on the lake level — this situation has been described from many recent lakes (see Cohen, 2003). A lake level oscillation derived from biotic and abiotic proxies suggest a relatively wet first half of YD and a markedly drier second half. These hydrological conditions are in accordance with most western and northwestern Europe sites (Walker, 1995; Magny, 2001; Magny et al., 2006; Neugebauer et al., 2012). In contrast to this, sites located in areas of a stronger continental climatic regime, as is eastern and northeastern Europe, show that the first part of the YD was certainly drier and cooler, whereas in the second part a warming period occurred (Goslar et al., 1993; Velichko et al., 1997, 2002; Kulesza et al., 2011).

In the studied region, the drier climate of the YD/PB transition was probably accompanied by increased wind activity. This is marked by a thin 2-cm sand layer from the top of the YD unit. The sand grains show features typical for aeolian sands: a rounded shape and matte surface. The grains are mixed with more angular grains in a ratio of 3:1. That could be transported to the basin by aeolian and/or colluvial processes, though the uniform size fraction (150–200 μm) suggests rather an aeolian origin for the layer. The top soil horizons with magnetic grains were also transported to the basin, causing a mineral magnetic enhancement of the respective layer. Several similar layers are preserved in core CP in the YD record; these aeolian sand layers had already been correlated with the formation of the nearby "Vlkovský přesyp" sand dune and with the opening up of forest cover (Pokorný and Růžičková, 2000).

The cooling period connected with the YD/PB transition is also recorded at several western and central European sites. It is marked as a short-term decline of $\delta^{18}O$ before the Holocene increase (Goslar et al., 1993; von Grafenstein et al., 1999) or as a mixing of surface sediments caused by unstable environmental conditions due to increased wind activity (Brauer et al., 1999).

6.2.5. Holocene (Unit 4 — LP3,4 — CP7,8,9 — Ch3)

Sedimentation in the SE littoral was restored at the beginning of the Preboreal, as suggested by the 9040 ± 50 BP radiocarbon date obtained from a position just above the layer of aeolian sand (273 cm). Both pollen and Chironomideae records show a rapid warming. A short-term cooling period at the beginning of the Holocene (layer 265–258 cm) signaled by abiotic proxies could be caused by the Preboreal oscillation. Nevertheless, after this event, the MS and Rb content rapidly decline and the organic matter content simultaneously increases (Figs. 5 and 6) as the result of warming period. Since that time, the erosion intensity

remained weak and weathering processes retained Rb in the catchment. The higher autochtonous organic production of the lake caused an increase in the organic matter content of the sediment. This change has finally led to the complete infilling of the lake basin.

Nevertheless, both MS and RM values rise in some horizons (especially 258–230 and 215–186 cm; Fig. 5). These events may not be linked with the climate; erosion processes but could be influenced by human activity. Along the shores of Švarcenberk Lake, archeological excavations so-far have revealed an intensive Mesolithic occupation during the Early Holocene (Šída et al., 2007; Pokorný et al., 2010). The resulting anthropogenic disturbances along the fringes of the shoreline could have caused soil and bedrock erosion that have been transferred to the lake basin. Therefore a significant increase in magnetic values and reworked Tertiary pollen occurs in this horizon (Fig. 6). The above interpretation is supported by the fact that a period of the respective higher magnetic values correlates with increasing synatrophic pollen indicators (e.g. *Plantago lanceolata*, *Pteridium aqulinum*, *Utrica*) in the pollen diagram of core LP, as well as an increased content of charcoal particles in the sediment (Figs. 7 and 8). The impact of human activity on the magnetic properties of lake sediment has already been well documented from many sites (e.g. Wessels, 1998; Dearing and Zolitschka, 1999).

6.3. Comparison with other European lacustrine records

In general, the course and major events of the Late Glacial climatic developments are well pronounced around the Northern Hemisphere and have been repeatedly identified and described. Yet, their duration and intensity have obviously exhibited considerable geographic variation accompanied by regionally-specific minor oscillations depending both on the geographic position and orographic specifics of the region (Davis et al., 2003). In Europe, particularly valuable information has been obtained during the last decade thanks to the application of a multi-proxy approach on well-stratified, precisely-dated (and sometimes varved) lake sediments such as Eifel Maars, or the lakes in the Swiss Alpine foreland, Germany and central Poland (e.g. Eicher and Siegenthaler, 1976; Goslar et al., 1993; von Grafenstein et al., 1999; Ammann et al., 2000; von Grafenstein et al., 2000; Marshall et al., 2002; Ammann et al., 2013; van Raden et al., 2013). Unfortunately, large-scale analyses of geographic variation are limited by the fact that the geographic distribution of lake sediments is not evenly distributed and a considerable part of central Europe lacks lacustrine deposits for various hydrological and geomorphological reasons. This applies wholly to the interior of the Czech Republic, where a representative sedimentary archive has been so far missing. The presented record from Švarcenberk Lake partly fills the gap and the results given in this paper can be directly compared to the situation in other parts of Europe. The sensitivity of the applied instrumental sedimentological methods to climatically-driven processes allows trans-regional comparisons and thus enables us to discuss the pattern of geographic variation in these processes.

In general, the period of the Pleistocene/Holocene transition documented in Švarcenberk Lake corresponds quite well to the course of the transition at other sites. As in western Europe, the Alleröd is here characterized by birch woodland development, stabilization of catchment soils and a decline in detrital sedimentation, whereas during the Younger Dryas a cooling period occurs, which sees the return of an open, dwarf shrub and herb, tundra-like vegetation, and minerogenic sedimentation. The warming period of the Early Holocene saw the return of woodland vegetation and a shift to a more organic sedimentary regime (Ralska-Jasiewiczowa et al., 1999; Ammann et al., 2000; Davis et al., 2003).

The fine scale comparisons, mentioned in the previous section, suggest that the interior of the Bohemian Massif (situated as it is on the border between west-oceanic and east-continental climatic conditions) shows a better agreement in the course of the Pleistocene/Holocene transition with the North Atlantic region than with the eastern part of the European continent. The main differences between the former and latter part of Europe are in their hydrological balance (Mol et al., 2000; Velichko et al., 2002; Magny et al., 2007). The records in the western part of Europe show more pronounced reactions to North Atlantic oscillations in paleoclimatological (paleohydrological) currents (as recorded in the marine sediment and Greenland Ice Cores) than do those from eastern Europe (including the Carpathian basin or the northeastern part of central Europe).

The cool event of the later part of the Alleröd interstadial, here co-identified with the Gerzensee oscillation, can serve as a good example. This oscillation has been observed in various climatic proxies over a wide North Atlantic region (see Section 6.2.); nevertheless, further inland, it has only been recorded exceptionally and as an event of only very low intensity (Björck et al., 1996; Velichko et al., 2002; Battarbee et al., 2004). In records from northern and western Europe, the event has been indicated by a distinct fall in $\delta^{18}O$ (von Grafenstein et al., 1999; Lowe et al., 2008; van Raden et al., 2013), corresponding to changes in magnetic susceptibility (Nolan et al., 1999) and the pollen record: a temporary decline in arboreal pollen with an increase in open-habitat herbaceous taxa (especially those characteristic of immature soils), and in the sedimentary dynamics characterized by increased soil erosion (Walker, 1995). In the corresponding strata of the present study site all these phenomena can be well observed.

In addition, the hydrological changes accompanying the climatic oscillations suggest a good agreement between Bohemia and the North Atlantic region. Here it should be remembered that due to its small catchment and weak tributaries the level of the lake studied was directly dependent upon paleoprecipitation – a situation that been described from many recent lakes (see Cohen, 2003) – and hence the record of oscillations in the lake's level derived from biotic and abiotic proxies can be looked upon as a record of paleoprecipitation dynamics. This then clearly suggests (a) a quite humid condition during the Alleröd, (b) that continued even during the first half of YD, but (c) was markedly drier during the second half of YD. Identical dynamics of hydrological conditions has been reported from sites from western and northwestern Europe (Magny and Rufaldi, 1995; Walker, 1995; Magny, 2001; Neugebauer et al., 2012). Further, the rapid drop in the lake level at the time of the YD/Preboreal transition, through which the lake sediment in the littoral core of the study site was temporarily exposed to terrestrial development, corresponds to a similar event reported from sites in the Swiss plateau and Jura mountains (Magny et al., 2006). In contrast to this, in the lacustrine series located in an area of stronger continental climatic regime, i.e. east and northeast Europe, the first part of the YD was certainly drier and cooler, whereas a climatic warming, including an increase in humidity, occurred here in the second half of YD (Goslar et al., 1993; Velichko et al., 1997, 2002; Makhnach et al., 2004; Kulesza et al., 2011).

7. Conclusions

Sedimentary deposits of Švarcenberk Lake have provided a great archive for the detailed study of the Late Glacial paleoenvironmental changes in eastern-central Europe — a transition zone between the realms of the Atlantic and continental climatic regimes, the zone from where, until now, no similar record had been available. Using a multi-proxy approach, that combined sedimentological, palynological, paleozoological, geochemical and geophysical methods, we have demonstrated that:

- The biotic and abiotic components of the land/lake ecosystem reacted quasi-synchronously and sensitively to both short- and long-term climate-induced environmental changes during the Alleröd and Younger Dryas and show distinct differences between the Late Glacial

and Holocene environmental conditions; the short-term intra-Alleröd cool event was correlated with Gerzensee oscillation.
- Proxy evidence suggests that the earlier lower part of the Younger Dryas was more humid, whereas the later upper part was relatively dry with a significant fall in the lake level at the YD/Preboreal transition.
- The erosion and weathering processes in the lake catchment are connected with the vegetation cover and lake productivity; there is a clear relationship between sparse vegetation cover and higher erosion intensity and vice versa.
- The magnetic properties are a good indicator of the flux of eroded soils into the lake basin, and magnetic enhancement of the lake sediment should also relate with oscillations in lake levels; variations in Rb content in the lake sediment reflect erosion and chemical weathering intensity in the surroundings of the lake and should be used as a suitable tool for the reconstruction of past climatic changes on a superregional scale.
- Interpretations of several proxies imply a climatic connection of the study area with the circum-Atlantic region during the Alleröd and Younger Dryas.
- Variations in the intensity of erosion in the Švarcenberk Lake catchment during the Upper Holocene could have been influenced by the activities of Mesolithic human populations (archeologically documented).

The interregional comparisons suggest considerable differences between the north Atlantic-western European region and that of continental eastern Europe (including northeastern central Europe and the Carpathian basin) in the course of the major climatic events during the Alleröd, Young Dryas and along the YD/Preboreal transition. In all these respects, the record from this study site, situated in the center of the Bohemian Massif, clearly shows the development corresponding to the former region. Indirectly this may indicate that the boundary between the two climatic regions and/or the two different modes of the Pleistocene/Holocene transition in central Europe could be quite narrow. Yet, to confirm this hypothesis, further new sites are urgently needed.

Acknowledgments

This research was possible thanks to Project no. 13-08169S of the Grant Agency of the Czech Republic (GAČR). Steve Ridgill is acknowledged for improving our English. We greatly appreciated the detailed reviews and constructive comments of two anonymous reviewers, who helped to improve the manuscript enormously.

References

Alley, R.B., Meese, D.A., Shuman, C.A., Grow, A.J., Taylor, K.C., Grootes, P.M., White, J.W.C., Ram, M., Waddington, E.D., Mayewski, P.A., Zielinski, G.A., 1993. Abrupt increase in Greenland snow accumulation at the end of the Younger Dryas event. Nature 362, 527–529.

Ammann, B., Lotter, A.F., 1989. Late-glacial radiocarbon stratigraphy and palynostratigraphy on the Swiss plateau. Boreas 18 (2), 109–126.

Ammann, B., Lotter, A.F., Eicher, U., Gaillard, M.J., Wohlfarth, B., Haeberli, W., Lister, G., Maisch, M., Niessen, F., Schlüchter, C., 1994. The Würmian Late-glacial in lowland Switzerland. J. Quat. Sci. 9 (2), 119–125.

Ammann, B., Birks, H.J.B., Brooks, S.J., Eicher, U., von Grafenstein, U., Hofmann, W., Lemdahl, G., Schwander, J., Tobolski, K., Wick, L., 2000. Quantification of biotic responses to rapid climatic changes around the Younger Dryas — a synthesis. Palaeogeogr. Palaeoclimatol. Palaeoecol. 159, 313–347.

Ammann, B., van Raden, U.J., Schwander, J., Eicher, U., Gilli, A., Bernasconi, S.M., van Leeuwen, J.F.N., Lischke, H., Brooks, S.J., Heiri, O., Nováková, K., van Hardenbroek, M., Colombaroli, D., Nielsen, E., Tinner, W., Wright, H.E., 2013. Responses to rapid warming at Termination 1a at Gerzensee (Central Europe): primary succession, albedo, soils, lake development, and ecological interactions. Palaeogeogr. Palaeoclimatol. Palaeoecol. http://dx.doi.org/10.1016/j.palaeo.2013.11.009.

Andersen, C.S., Björck, S., Bennike, O., Heinemeier, J., Kromer, B., 2000. What do D 14C changes across the Gerzensee oscillation/GI-1b event imply for deglacialoscillation? J. Quat. Sci. 15, 203–214.

Andrée, M., Oeschger, H., Siegenthaler, U., Riesen, T., Moell, M., Ammann, B., Tobolski, K., 1986. ^{14}C dating of plant macrofossils in lake sediment. Radiocarbon 28, 411–416.

Battarbee, R.W., Gasse, F., Stickley, C.E., 2004. Past climate variability through Europe and Africa. In: Smol, J.P. (Ed.), Developments in Paleoenvironmental Research. Springer, New York, pp. 339–371.

Bergsten, H., 1994. Recent benthic foraminifera of a transect from the North Pole to the Yermak Plateau, eastern central Arctic Ocean. Mar. Geol. 119 (3–4), 251–267.

Beug, H.J., 2004. Leitfaden der Pollenbestimmung: für Mitteleuropa und angrenzende Gebiete. Pfeil, München.

Birks, H.H., 1993. The importance of plant macrofossils in Late-Glacial climatic reconstructions: an example from western Norway. Quat. Sci. Rev. 12, 719–726.

Birks, H.H., Wright, H.E., 2000. Introduction to the reconstruction of the late-glacial and early-Holocene aquatic ecosystems at Kråkenes Lake, Norway. J. Paleolimnol. 23, 1–5.

Björck, S., Kromer, B., Johnsen, S., Bennike, O., Hammarlund, D., Lemdahl, G., Possnert, G., Rasmussen, T.L., Wohlfarth, B., Hammer, C.U., Spurk, M., 1996. Synchronised terrestrial–atmospheric deglacial records around the North Atlantic. Science 274, 1155–1160.

Björck, S., Walker, M.J.C., Cwynar, L.C., Johnsen, S., Knudsen, K.-L., Lowe, J.J., Wohlfarth, B., 1998. An event stratigraphy for the Last Termination in the North Atlantic region based on the Greenland ice-core record: a proposal by the INTIMATE group. J. Quat. Sci. 13 (4), 283–292.

Brauer, A., Endres, C., Gunter, C., Litt, T., Stebich, M., Negendank, J.F.W., 1999. High resolution sediment and vegetation responses to Younger Dryas climate change in varved lake sediments from Meerfelder Maar, Germany. Quat. Sci. Rev. 18 (3), 321–329.

Brodersen, K.P., Lindegaard, C., 1999. Classification, assessment and trophic reconstruction of Danish lakes using chironomids. Freshw. Biol. 42, 143–157.

Brooks, S.J., Langdon, P.G., Heiri, O., 2007. The identification and use of Palaearctic Chironomidae larvae in palaeoecology. QRA Technical Guide No. 10. Quaternary Research Association, London.

Buggle, B., Glasera, B., Hambach, U., Markovič, S., 2009. An evaluation of geochemical weathering indices in loess–paleosol studies. Quat. Int. 29, 1–10.

Chen, J., Ji, J., Chen, Y., An, Z., Dearing, J.A., Wang, Y., 2000. Use of rubidium top date loess and paleosols of the Luochuan sequence, central China. Quat. Res. 54, 198–205.

Clark, P.U., Marshall, S.J., Clarke, G.K.C., Hostetler, S.W., Licciardi, J.M., Teller, J.T., 2001. Freshwater forcing of abrupt climate change during the last glaciation. Science 293, 283–287.

Cohen, A.S., 2003. Paleolimnology: The History and Evolution of Lake Systems. Oxford University Press, US.

Dansgaard, W., Johnen, S.J., Clausen, H.B., Dahl-Jensen, D., Gundestrup, N.S., Hammer, C.V., Hvidberg, C.S., Stephensen, J.P., Sveinbjornsduttir, A.E., Jouzel, J., Bond, G., 1993. Evidence of general instability of past climate from a 250-kyr ice-core record. Nature 364, 218–220.

Davis, B.A.S., Brewer, S., Stevenson, A.C., Guiot, J., Contributors, D., 2003. The temperature of Europe during the Holocene reconstructed from pollen data. Quat. Sci. Rev. 22, 1701–1716.

Day, P., 1996. Devensian Late-Glacial and Early Flandrian environmental history of the Vale of Pickering, Yorkshire, England. J. Quat. Sci. 11 (1), 9–24.

Dearing, J.A., Flower, R.J., 1982. The magnetic susceptibility of sedimenting material trapped in Lough Neagh, Northern Ireland, and its erosional significance. Limnol. Oceanogr. 27, 969–975.

Dearing, J.A., Zolitschka, B., 1999. System dynamics and environmental change: an exploratory study of Holocene lake sediments at Holzmaar, Germany. The Holocene 9, 531–540.

Eicher, U., Siegenthaler, U., 1976. Palynological and oxygen isotope investigation on Late-Glacial sediment cores from Swiss lakes. Boreas 5, 109–117.

Engel, Z., Treml, V., Křížek, M., Jankovská, V., 2004. Lateglacial/holocene sedimentary record from the Labe source area, the Krkonoše Mts., Acta Universitatis Carolinae 2004. Geogr. 95–105.

Faegri, K., Iversen, J., 1989. Textbook of Pollen Analysis. Wiley, Chichester.

Gaillard, M.J., 1985. Late glacial and Holocene environments of some antient lakes in western Swiss Plateau. Diss. Bot. 87, 236–273.

Goslar, T., Kuc, T., Ralska-Jasiewiczowa, M., Rozanski, K., Arnold, M., Bard, E., Van Geel, B., Pazdur, M.F., Szeroczynska, K., Wici, B., Wieckowski, K., Walanus, A., 1993. High-resolution lacustrine record of the Late Glacial/Holocene transition in Central Europe. Quat. Sci. Rev. 12, 295–305.

Goslar, T., Arnold, M., Bard, E., Kuc, T., Pazdur, M.F., Ralska-Jasiewiczowa, M., Rozanski, K., Tisnerat, N., Walanus, A., Wicik, B., Wickowski, K., 1995. High concentration of atmospheric ^{14}C during the Younger Dryas cold episode. Nature 377, 414–417.

Grimm, E.C., 1987. CONISS: a fortran 77 program for stratigraphically constrained cluster analysis by the method of incremental sum of squares. Comput. Geosci. 13, 13–35.

Grimm, E.C., 2004. TGVIEW 2.0.2 (Computer Software). IllinoisState Museum, Research and Collections Center, Springfield, Il.

Hammarlund, D., Buchardt, B., 1996. Composite stable isotope records froma Late Weichselian lacustrine sequence at Graenge, Lolland, Denmark: evidence of Alleröd and Younger Dryas environments. Boreas 25, 8–22.

Heiri, O., Lotter, A.F., Lemcke, G., 2001. Loss on ignition as a method for estimating organic and carbonate content in sediments: reproducibility and comparability of results. J. Paleolimnol. 25, 101–110.

Herbauts, J., 1982. Chemical and mineralogical properties of sandy and loamy–sandy ochreous brown earths in relation to incipient podzolization in a brown-podzol evolutive sequence. J. Soil Sci. 33, 743–762.

Hoek, W., 1997. Palaeogeography of Lateglacial vegetations. Aspects of Late Glacial and Early Holocene vegetation, abiotic landscape, and climate in The Netherlands. Neth. Geogr. Stud. 230, 1–147.
Hofmann, W., 1984. Stratigraphie subfossiler Cladocera (Crustacea) und Chironomidae (Diptera) in zwei Sedimentprofilen des Meerfelder Maares. Cour. Forsch. Inst. Senckenberg. 65, 67–80.
Huizer, A.S., Izarin, R.F.B., 1997. The reconstruction of past climates using multi-proxy evidence: an example of the Wichselian Pleniglacial in northwest and central Europe. Quat. Sci. Rev. 16, 513–533.
Jankovská, V., 1983. Palynologische Forschung amehem aligen Komořany-See (Spetglazial bis Subatlanticum). Věst. Ústř. Úst. Geol. 58 (2), 99–107.
Jankovská, V., 2006. Late Glacial and Holocene history of Plešné Lake and its surrounding landscape based on pollen and palaeoalgological analyses. Biologia (Bratislava) 61, 371–385.
Jankovská, V., Komárek, J., 2001. Review of the green algal genus *Pediastrum*; implication for pollen-analytical research. Bibl. Phycol. 108, 119–127.
Jin, Z.D., Cao, J.J., Wu, J.L., Wang, S.M., 2006. A Rb/Sr record of catchment weathering response to Holocene climate change in Inner Mongolia. Earth Surf. Process. Landf. 31, 285–291.
Johnsen, S.J., Clausen, H.B., Dansgaard, W., Fuhrer, K., Gundestrup, N., Hammer, C.U., Iversen, P., Jouzel, J., Stauffer, B., Steffensen, J.P., 1992. Irregular glacial interstandials recorded in a new Greenland ice core. Nature 259, 311–313.
Juggins, S., 2007. C^2 Version 1.5 User guide. Software for Ecological and Palaeoecological Data Analysis and Visualisation.University of Newcastle, Newcastle upon Tyne, UK.
King, J., Banarjee, S.K., Marvin, J., Özdemir, Ö., 1982. A comparison of different magnetic methods for determining the relative grain size of magnetite in natural materials: some results from lake sediments. Earth Planet. Sci. Lett. 59, 404–419.
Komárek, J., 1982. Das Vorkommen einiger Chlorokokalalgen in Bömischen Spätglazial und Postglazial. Folia Geobot. Phytotax. 17, 165–195.
Komárek, J., Jankovská, V., 2001. Review of the green algae genus Pediastrum; Implication forpollen-analytical research. Bibl. Phycol., Cramer J. Berlin-Stuttgart.
Kowalyk, H.E., 1985. The larval cephalic setae in the Tanypodinae (Diptera: Chironomidae) and their importance in generic determinations. Can. Entomol. 117, 67–106.
Kulesza, P., Suchora, M., Pidek, I.A., Dobrowolski, R., Alexandrowicz, W.P., 2011. Chronology and directions of Late Glacial paleoenvironmental changes: a multi-proxy study on sediments of Lake S1one (SE Poland). Quat. Int. 238, 89–106.
Larocque, I., Hall, R.I., Grahn, E., 2001. Chironomids as indicators of climate change: a 100-lake training set from a subarctic region of northern Sweden (Lapland). J. Paleolimnol. 26, 307–322.
Lehman, S.J., Keigwin, L.D., 1992. Sudden changes in North Atlantic circulation during the last deglaciation. Nature 356, 757–762.
Levesque, A.J., Mayle, F.E., Walker, I.R., Cwynar, L.C., 1993. A previously unrecognized late-glacial cold event in eastern North America. Nature 361, 623–626.
Litt, T., Stebich, M., 1999. Bio- and chronostratigraphy of the lateglacial in the Eifel region, Germany. Quat. Int. 61 (1), 5–16.
Litt, T., Brauer, A., Goslar, T., Merkt, J., Balaga, K., Muller, H., Ralska-Jasiewiczowa, M., Stebich, M., Negendank, J.F.W., 2001. Correlation and synchronisation of Lateglacial continental sequences in northern central Europe based on annually laminated lacustrine sediments. Quart. Sci. Rev. 20, 1233–1249.
Lowe, J.J., Walker, M.J.C., 2000. Radiocarbon dating the Last Glacial–Interglacial transition (ca. 14–9 ^{14}C ka BP) in terrestrial and marine records: the need for new quality assurance protocols. Radiocarbon 42 (1), 53–68.
Lowe, J.J., Ammann, B., Birks, H.H., Björck, S., Coope, G.R., Cwynar, L., De Beaulieu, J.-L., Mott, R.J., Peteet, D.M., Walker, M.J.C., 1994. Climatic changes in areas adjacent to the North Atlantic during the last glacial–interglacial transition 14–9 ka BP: a contribution to IGCP-253. J. Quat. Sci. 9, 185–198.
Lowe, J.J., Rasmussen, S.O., Björck, S., Hoek, W.Z., Steffensen, J.P., Walker, M.J.C., Yu, Z.C., Grp, I., 2008. Synchronisation of palaeoenvironmental events in the North Atlantic region during the Last Termination: a revised protocol recommended by the INTIMATE group. Quat. Sci. Rev. 27 (1–2), 6–17.
Ložek, V., Cílek, V., 1995. Late Weichselian–Holocene sediments and soils in mid-European calcareous areas. Anthropozoikum 22, 87–112.
Magny, M., 2001. Palaeohydrological changes as reflected by lake-level fluctuations in the Swiss Plateau, the Jura mountains and the northern French Pre-Alps during the Last Glacial–Holocene transition: a regional synthesis. Glob. Planet. Chang. 30, 85–101.
Magny, M., Vannière, B., de Beaulieu, J.-L., Bégeot, C., Heiri, O., Millet, L., Peyron, O., Walter-Simonnet, A., 2007. Early-Holocene climatic oscillations recorded by lake-level fluctuations in west central Europe and in central Italy. Quat. Sc. Rev. 26, 1951–1964.
Magny, M., Rufaldi, P., 1995. Younger Dryas and early Holocene lake-level fluctuations in the Jura mountains, France. Boreas 24, 155–172.
Magny, M., Aalbersberg, G., Begeot, C., Benoit-Ruffaldi, P., Bossuet, G., Disnar, J.R., Heiri, O., Laggoun-Defarge, F., Mazier, F., Millet, L., Peyron, O., Vanniere, B., Walter-Simonnet, A.V., 2006. Environmental and climatic changes in the Jura mountains (eastern France) during the Late glacial–Holocene transition: a multi-proxy record from Lake Lautrey. Quat. Sci. Rev. 25, 414–445.
Maher, B.A., 1988. Magnetic properties of some synthetic sub-micron magnetites. Geophys. J. Int. 94, 83–96.
Makhnach, N., Zernitskaya, V., Kolosov, I., Simakova, G., 2004. Stable oxygen and carbon isotopes in Late Glacial–Holocene freshwater carbonates from Belarus and their palaeoclimatic implications. Palaeogeogr. Palaeoclimatol. Palaeoecol. 209, 73–101.
Marshall, J.D., Jones, R.T., Crowley, S.F., Nash, S., Bedford, A., 2002. A high resolution late glacial isotopic record from Hawes Water NW England: climatic oscillations-calibration and comparison of palaeotemperature proxies. Palaeogeogr. Palaeoclimatol. Palaeoecol. 185 (1–2), 25–40.
Mol, J., Vandenberghe, J., Kasse, C., 2000. River response to variations of periglacial climate in mid-latitude Europe. Geomorphology 33, 131–148.
Moore, P.D., Webb, J.A., Collinson, M.E., 1991. Pollen Analysis. Blackwell, Oxford.
Nesbitt, H.W., Markovics, G., Price, R.C., 1980. Chemical processes affecting alkalis and alkaline earths during continental weathering. Geochim. Cosmochim. Acta 44, 1659–1666.
Neugebauer, I., Brauer, A., Dräger, N., Dulski, P., Wulf, S., Plessen, B., Mingram, J., Herzschuh, U., Brande, A., 2012. A Younger Dryas varve chronology from the Rehwiese palaeolake record in NE-Germany. Quat. Sci. Rev. 36, 91–102.
Nolan, S.R., Bloemendal, J., Boyle, J.F., Jones, R.T., Oldfield, F., Whitney, M., 1999. Mineral magnetic and geochemical records of late Glacial climatic change from two northwest European carbonate lakes. J. Paleolimnol. 22 (1), 97–107.
Peters, C., Dekkers, M.J., 2003. Selected room temperature magnetic parameters as a function of mineralogy, concentration and grain size. Phys. Chem. Earth 28, 659–667.
Pilcher, J.R., 2003. Radiocarbon dating and environmental radiocarbon studies. In: MacKay, A., Battarbee, R., Birks, J., Oldfield, F. (Eds.), Global Change in the Holocene. Arnold Publishers, London, pp. 63–74.
Pokorný, P., 2002. A high-resolution record of Late-Glacial and Early-Holocene climatic and environmental change in Czech Republic. Quat. Int. 91, 101–122.
Pokorný, P., Jankovská, V., 2000. Long-term vegetation dynamics and the infilling process of a former lake (Švarcenberk, Czech Republic). Folia Geogr. 35, 433–457.
Pokorný, P., Růžičková, E., 2000. Changing environments during the younger dryas climatic deterioration: correlation of aeolian deposits in Southern Czech Republic. Geol. 11, 89–92.
Pokorný, P., Šída, P., Kuneš, P., Chvojka, O., 2008. Výzkum mezolitického osídlení v okolí bývalého jezera Švarcenberk v jižních Čechách. In: Beneš, J., Pokorný, P. (Eds.), Bioarcheologie v České republice. (Bioarchaeology in the Czech Republic). AÚ AVČR, Praha, pp. 145–176.
Pokorný, P., Šída, P., Chvojka, O., Žáčková, P., Kuneš, P., Světlík, I., Veselý, J., 2010. Palaeoenvironmental research of the Schwarzenberg Lake, southern Bohemia, and exploratory excavations of this key Mesolithic archaeological area. Pamatky Archeol. 101, 5–38.
Punt, W. (Ed.), 1976–1996. The Northwest European Pollen Flora. Elsevier, Amsterdam, pp. 1–7.
Ralska-Jasiewiczowa, M., Goslar, T., Bałaga, K., 1999. Biostratigraphy of the Lateglacial in the Lowland of Poland based on the calendar time scale. Terra Nostra 99 (10), 66–71.
Rieradevall, M., Brooks, S.J., 2001. An identification guide to subfossil Tanypodinae larvae (Insecta: Diptera: Chironomidae) based on cephalic setation. J. Paleolimnol. 25, 81–99.
Ross, G.J., Schuppli, P.A., Wang, C., 1989. Quantitative determination of vermiculite by a rubidium fixation method. Soil Sci. Soc. Am. J. 53, 1588–1589.
Ruddiman, W.F., McIntyre, A., 1981. The North Atlantic during the last deglaciation. Palaeogeogr. Palaeoclimatol. Palaeoecol. 35, 145–214.
Schwander, J., Eicher, U., Ammann, B., 2000. Isotope signature of the Younger Dryas and two minor oscillations at Gerzensee (Switzerland): palaeoclimatic and palaeolimnologic interpretation based on bulk and biogenic carbonates. Palaeogeogr. Palaeoclimatol. Palaeoecol. 159 (3–4), 215–229.
Šída, P., Pokorný, P., Kuneš, P., 2007. Dřevěné artefakty raně holocenního stáří z litorálu zaniklého jezera Švarcenberk. Přehled Výzkumů 48, 55–64.
Simola, H., Meriläinen, J.J., Sandman, O., Marttila, V., Karjalainen, H., Kukkonen, M., Julkunen-Tiitto, R., Hakulinen, J., 1996. Palaeolimnological analyses as information source for large lake biomonitoring. Hydrobiologia 322, 283–292.
Stockhausen, I., Zolitschka, B., 1999. Environmental changes since 13,000 cal. BP reflected in magnetic and sedimentological properties of sediments from Lake Holzmaar (Germany). Quat. Sci. Rev. 18, 913–925.
Stuiver, M., Grootes, P.M., Braziunas, T.F., 1995. The GISP2 δ^{18}O climate record of the past 16,500 years and the role of sun, ocean, and volcanoes. Quat. Res. 44, 341–354.
Syvitski, J.P.M. (Ed.), 1991. Principles, Methods, and Application of Particle Size Analysis. Cambridge University Press, Cambridge.
Thouveny, N., De Beaulieu, J.L., Bonifay, E., Creer, K.M., Guiot, J., Icole, M., Johnsen, S., Jouzel, J., Reille, M., Williams, T., Williamson, D., 1994. Climate variations in Europe over the last 140-kyr deduced from rock magnetism. Nature 371 (6497), 503–506.
van Geel, B., Bohncke, S.J.P., Dee, H., 1981. A palaeoecological study of an upper Lateglacial and Holocene sequence from"De Borchert", The Netherlands. Rev. Palaeobot. Palynol. 31, 367–448.
van Geel, B., Hallewas, D.P., Pals, J.P., 1983. A Late Holocene deposit under the Westfriese dijk near Enkhuizen (Prov. of Noord-Holland, The Netherlands) palaeoecological and archaeological aspects. Rev. Palaeobot. Palynol. 38, 269–335.
van Geel, B., Coope, G.R., van der Hammen, Th., 1989. Palaeoecology and stratigraphy of the Lateglacial type section at Usselo (The Netherlands). Rev. Palaeobot. Palynol. 39, 25–129.
van Raden, U.J., Colombaroli, D., Gilli, A., Schwander, J., Bernasconi, S.M., van Leeuwen, J.F.N., Leuenberger, M., Eicher, U., 2013. High-resolution late-glacial chronology for the Gerzensee lake record (Switzerland): δ^{18}O correlation between a Gerzensee-

stack and NGRIP. Palaeogeogr. Palaeoclimatol. Palaeoecol. http://dx.doi.org/10.1016/j.palaeo.2012.1005.1007.
Velichko, A.A., Andreev, A.A., Klimanov, V.A., 1997. Climate and vegetationdynamics in the tundra and forest zone during the Late Glacial and Holocene. Quat. Int. 41, 71–96.
Velichko, A.A., Catto, N., Drenova, A.N., Klimanov, V.A., Kremenetski, K.V., Nechaev, V.P., 2002. Climate changes in East Europe and Siberia at the late glacial-Holocene transition. Quat. Int. 91, 75–99.
von Grafenstein, U., Erlenkeuser, H., Brauer, A., Jouzel, J., Johnsen, S.J., 1999. A mid-European decadal isotope-climate record from 15,500 to 5000 years BP. Science 284 (5420), 1654–1657.
von Grafenstein, U., Eicher, U., Erlenkeuser, H., Ruch, P., Schwander, J., Ammann, B., 2000. Isotope signature of the Younger Dryas and two minor oscillations at Gerzensee (Switzerland): palaeoclimatic and palaeolimnologic interpretation based on bulk and biogenic carbonates. Palaeogeogr. Palaeoclimatol. Palaeoecol. 159 (3–4), 215–229.
Walker, M.J.C., 1995. Climatic changes in Europe during the last glacial/interglacial transition. Quat. Int. 28, 63–76.
Walker, I.R., MacDonald, G.M., 1995. Distribution of Chironomidae (Insecta: Diptera) and other freshwater midges with respect to treeline, Northwest Territories, Canada. Arct. Alp. Res. 3, 258–263.
Wessels, M., 1998. Late-glacial and postglacial sediments in Lake Constance (Germany) and their palaeolimnological implications. Arch. Hydrobiol. 53, 411–414.
Wohlfarth, B., 1996. The chronology of the last termination: a review of radiocarbon-dated, high resolution terrestrial stratigraphies. Quat. Sci. Rev. 15, 267–284.
Zolitschka, B., Behre, K.-E., Schneider, J., 2003. Human and climatic impact on the environment as derived from colluvial, fluvial and lacustrine archives — examples from the Bronze Age to 20 the Migration period, Germany. Quat. Sci. Rev. 22, 81–100.